(a) **Nuclear Energy levels**—Similar to the discrete energy states of the electrons in an atom, the nucleons comprising a nucleus have possible energy states given by Heisenberg principle.

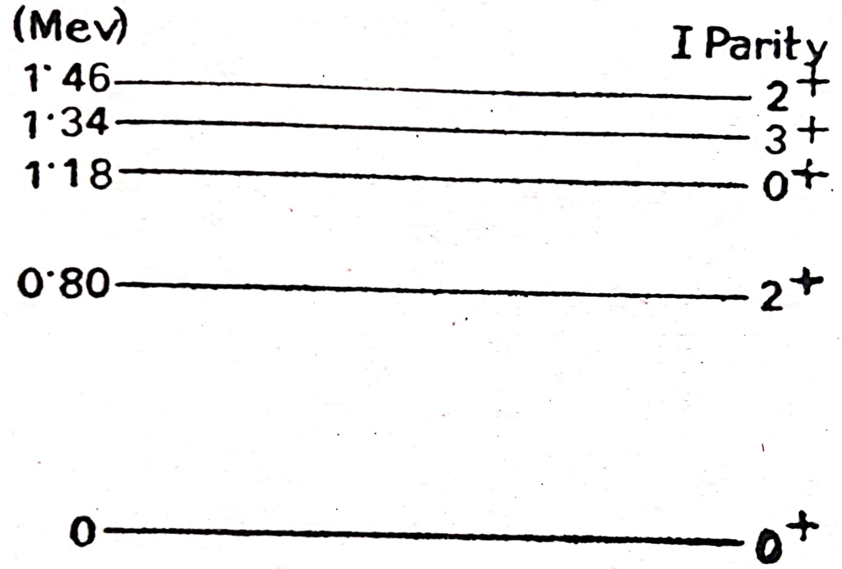

Fig. 1.24. Level Scheme of Pb-206.

$$H_n\psi_n = E_n\psi_n.$$

Here Schrodinger wave function ψ_n depends upon spatial coordinates and also spin and isospin quantum numbers. The ground state possesses latent energy, in the form of potential energy which is normalized to zero. Excitation energies of the higher levels are referred to the zero energy of the ground level. γ-rays of discrete values are emitted by the de-excitation of the nucleus to its ground state. The energy level diagram represents excitation energy, nuclear spin I, parity π, lifetime τ and isospin T.

(b) Nuclear Angular Momentum. In 1924, W. Pauli, while explaining hyperfine structure of spectral lines, suggested that certain atomic nuclei may possess an intrinsic angular momentum as well as a magnetic moment. The nuclear angular momentum can be deduced from the measurement of multiplicity and relative spacing of the spectral lines.

It has been found that the neutron and the proton possess an intrinsic angular momentum, commonly referred to as its spin, of magnitude $\frac{1}{2}\hbar$ just as the electron does. Since nuclei are built up of neutrons and protons, each possesses an angular momentum, which consists of both orbital angular momentum due to the motion about the centre of the nucleus and intrinsic spin angular momentum of $\frac{1}{2}\hbar$ per nucleon. The total angular momentum of a particular nuclear state is the resultant of the individual momenta of the constituent nucleons. Corresponding to total angular momentum quantum number I, the absolute magnitude of total angular momentum is $\hbar[I(I+1)]^{1/2}$. The value of I depends on the type of interaction between the nucleons.

LS-Coupling—In this case the spin-orbit interaction is negligible and there is a collective interaction of orbital and intrinsic momenta, *i.e.*.

$$\mathbf{I}=\mathbf{L}+\mathbf{S}, \quad \text{where } \mathbf{L}=\sum_i l_i \text{ and } \quad \mathbf{S}=\sum_i s_i.$$

For $L=0, 1, 2, 3...,$ we have levels $S, P, D, F....$ For each value of L there are $(2S+1)$ possible separated energy levels. The multiplicity $(2S+1)$ is written as a superscript before the letter representing L and the value of I as subscript. Hence for $L=1$ and $S=1/2$, we have levels $^2P_{1/2}$ and $^2P_{1/2}$, the spin doublet.

j.j-Coupling—In this case the orbital and spin momenta of each individual nucleon are strongly coupled. I is the vector sum of the individual j values. Hence

$$I=\sum_i \mathbf{j} \quad \text{where} \quad \mathbf{j}_i=\mathbf{l}_i+\mathbf{s}_i.$$

This type of coupling is called strong spin-orbit coupling. If s-nucleon $(l=0, j=1/2)$ couples with p-nucleon $(l=1. \; j=3/2, \; 1/2)$, we have $I=0, 1, 1$ or 2.

These two coupling schemes are the extreme forms. One can employ intermediate coupling schemes of varying degrees of complexity. The total angular momentum of a nucleus is usually called as *nuclear spin*. It is an unfortunate terminology for the angular momentum, because spin is generally used for intrinsic angular momentum of elementary particles. Experimentally it is found that all nuclei have relatively low spin in their ground states. The spins of the excited states may differ from the spin of the ground state by integral multiplies of $\hbar$. The term "spin of the nucleus", without any specification, always refers to the ground state. It has been found that all even-even nuclei have a spin $I=0$ in the ground state. Odd-odd nuclei all have integral nuclear spin, other than zero. All odd-even nuclei have half integral nuclear spins lying between $\hbar/2$ to $9\ \hbar/2$.

Total angular momentum vector I can be oriented in space with respect to a given axis in $(2I+1)$ directions. The component along the axis in any of the states has the magnitude $m\hbar$, where m is the magnetic quantum number, having values from I to $-I$, as I, $(I-1)$, $(I-2)$......, $-(I-2)$, $-(I-1)$, $-I$. Thus the largest value of m is I.

(c) **Parity**—Nuclear parity is the product of the parities of nuclear constituents. As will be discussed in the chapter of nuclear models, for even Z-even N nuclei, ground states have positive parity ($I^{\pi}=0^{+}$). The parity of odd A nuclei is given by $(-1)^{l}$, where l is the orbital angular momentum of the unpaired nucleon. Odd-odd nuclei have a parity $(-1)^{l_n+l_p}$. Few exceptions to this rule requre explanation. In general the parity of the system of n particles is given by Σl_n. Parity is even if this sum is +ve and is odd if the sum is −ve.

(d) **Isospin**—For a given nucleus, the value of T_z is just the minus one half of the neutron excess.

$$T_z=\tfrac{1}{2}(Z-N)=-\tfrac{1}{2}(N-Z).$$

In a set of isobars of given A, a member X will have an isospin $T_{z,\,max}$ largest among the set. For this $T=T_{z,\,max}=\tfrac{1}{2}(Z_x-N_x)$, having $(2T+1)$ states. These states are corresponding to different T_3 and hence to different charges $(Z=A/2\pm T)$. The isobars C^{14}, N^{14}, O^{14} have $T_z=-1$, 0 and +1 respectively. The mirror nuclei H^3 and He^3 have $T=\tfrac{1}{2}$ in their ground state. Isospin assignments to excited nuclear levels can be established through reaction or scattering studies.

(e) **Statistics**—It can be seen experimentally that H^1, Li^7, F^{19}, Na^{23}, P^{31}, Cl^{35} obey the Fermi Dirac statistics. In general, all nuclei of odd mass numbers obey the Fermi-Dirac statistics. H^2, He^4, C^{12}, N^{14}, O^{16}, S^{32} are known to obey Einstein-Bose statistics. In general, the photons and all nuclei of even mass number follow Einstein-Bose statistics.

1.11. NUCLEAR MAGNETIC DIPOLE MOMENT

Any charged particle moving in a closed path produces a magnetic field, which at large distances acts as due to magnetic dipole located at the current loop. The protons inside the nucleus are in orbital motion and therefore produce electric currents which produce extra nuclear magnetic fields. Each nucleon possesses an intrinsic magnetic moment which is parallel to its spin and is probably caused by the spinning of the nucleon. A spinning positive charge produces a magnetic field whose N-pole direction is parallel to the direction of spin. The magnetic moment is defined as +ve in this case.

If a particle having a charge q and mass m circulates about a force centre with a frequency ν, the equivalent current $i=q\nu$. From Kepler's law of areas area swept dA in time dt by the particle is related with its angular momentum **l** as

$$dA/dt=\tfrac{1}{2}\,\mathbf{l}/m=\text{constant.}$$

On integration over one period T,

$$A=\tfrac{1}{2}T\,\mathbf{l}/m. \qquad \ldots(80)$$

Hence magnetic moment of a ring of current around an area of magnitude A is given by

$$\vec{\mu}_l=\mu_0\, i\vec{A}=\mu_0\,(q\nu)\left(\frac{1}{2}\frac{T\vec{l}}{m}\right)=\frac{q}{2m}\,\mu_0\vec{l}. \qquad \ldots(81)$$

Thus $\vec{\mu}_l$ and $\vec{l}$ are proportional. This relation is also valid in quantum mechanics. However, since the particles (electron, proton and neutron) possess a spin in addition to orbital angular momentum, experimentally it is found that the spin is also the source of a magnetic moment. Using $q=e$ and a dimensionless correction factor g_s, we can write eqn (81) as

$$\vec{\mu}_s=g_s\,(\mu_0 e/2m)\,\vec{s}. \qquad \ldots(82)$$

The factor g_s is different for the electron, proton and neutron. Similarly, we introduce a factor g_l and have

$$\vec{\mu}_l=g_l(\mu_0 e/2m)\,\vec{l}. \qquad \ldots(83)$$

The total magnetic dipole moment μ is given as :

$$\vec{\mu}=\vec{\mu}_s+\vec{\mu}_l=(\mu_0 e/2m)\,[g_s\,\vec{s}+g_l\,\vec{l}]. \qquad \ldots(84)$$

For the nucleus of mass number A, magnetic dipole moment

$$\vec{\mu}=\frac{\mu_0 e}{2m}\left[\sum_{k=1}^{A} g_s\,\vec{s}_k+\sum_{k=1}^{Z} g_l\,\vec{l}_k\right]. \qquad \ldots(85)$$

Since total angular momentum of the nucleus

$$\vec{I}=\sum_{k=1}^{Z}\vec{l}_k+\sum_{k=1}^{A}\vec{s}_k. \qquad \ldots(86)$$

$$\therefore\ \vec{\mu}=g(\mu_0 e/2m)\,\vec{I}=g\,(\mu_0 e\hbar/2m)\,\vec{I}/\hbar, \qquad \ldots(87)$$

where g is the *gyromagnetic ratio* (g-factor) of the nucleus. It is the dimensionless ratio of the magnetic moment μ in terms of $\mu_0 e\hbar/2m$ to the angular momentum in terms of $\hbar$. Using quantum mechanics, we have $[l\,(l+1)]^{1/2}$ and $[s\,(s+1)]^{1/2}$ instead of l and s respectively, we get

$$g=\tfrac{1}{2}\,(g_l+g_s)+\tfrac{1}{2}\,(g_l-g_s)\frac{l\,(l+1)-s\,(s+1)}{I(I+1)}\,. \qquad \ldots(88)$$

The magnetic dipole moment is measured in terms of nuclear magneton, defined as

$$\mu_N=\mu_0 e\hbar/2m_p=\mu_0 e\,\hbar/2m_n$$
$$=3.152\times 10^{-8}\ eV\text{-}m^2/\text{weber}.$$

The magnetic moment of even-odd and odd-even nuclei is due to only a single (unpaired) nucleon. If the odd nucleon is a proton $g_l=1$, $g_s=g_p$, and if it is a neutron $g_l=0$, $g_s=g_n$. In this case $s=1/2$ and $I=l+1/2$ or $l-1/2$.

clear charge distribution along the angular momentum axis and to a flattened distribution respectively.

1.12. ELECTRIC QUADRUPOLE MOMENT

We now consider how the internal distribution of nuclear charge contributes to the effective moments. We place a nucleus having a charge density $\rho(x, y, z)$ with its charge center at the origin. As the nucleus is surrounded by its orbital electrons hence an electrostatic potential ϕ which originates from these electrons produces an electrostatic interaction energy, resulting from the interaction between ϕ and ρ. This energy is defined as

$$U=\int_v \rho(x, y, z)\, \phi(x, y, z)\, dv. \qquad ...(97)$$

To express this energy in terms of the electric moments of the distribution, we expand the potential in a Taylor's series about the origin as

$$\phi(x, y, z)=\phi_0+\left[\left(\frac{\partial\phi}{\partial x}\right)_0 x+\left(\frac{\partial\phi}{\partial y}\right)_0 y+\left(\frac{\partial\phi}{\partial z}\right)_0 z\right]+$$
$$\left[\frac{1}{2}\left(\frac{\partial^2\phi}{\partial x^2}\right)_0 x^2+\frac{1}{2}\left(\frac{\partial^2\phi}{\partial y^2}\right)_0 y^2+\frac{1}{2}\left(\frac{\partial^2\phi}{\partial z^2}\right)_0^2 z^2\right]+$$
$$\left[\left(\frac{\partial^2\phi}{\partial x\partial y}\right)_0 xy+\left(\frac{\partial^2\phi}{\partial x\partial z}\right)_0 xz+\left(\frac{\partial^2\phi}{\partial y\partial z}\right)_0 yz\right]+\ldots,$$

where the subscript means that the quantity is evaluated at the origin. Inserting this value in eqn. (97) with the idea that each of the derivatives is constant with respect to the variables of integration, we get

$$U=\phi_0\int\rho\, dv+\left[\left(\frac{\partial\phi}{\partial x}\right)_0\int x\rho\, dv+\left(\frac{\partial\phi}{\partial y}\right)_0\int y\rho\, dv+\left(\frac{\partial\phi}{\partial z}\right)_0\int z\rho\, dv\right]$$
$$+\left[\frac{1}{2}\left(\frac{\partial^2\phi}{\partial x^2}\right)_0\int x^2\rho\, dv+\frac{1}{2}\left(\frac{\partial^2\phi}{\partial y^2}\right)_0\int y^2\rho\, dv+\right.$$
$$\frac{1}{2}\left(\frac{\partial^2\phi}{\partial z^2}\right)_0\int z^2\rho\, dv+\left(\frac{\partial^2\phi}{\partial x\partial y}\right)_0\int xy\,\rho\, dv+$$
$$\left.\left(\frac{\partial^2\phi}{\partial x\partial z}\right)_0\int xz\,\rho\, dv+\left(\frac{\partial^2\phi}{\partial y\partial z}\right)_0\int yz\,\rho\, dv+\ldots\right]$$
$$+\ldots\text{high order terms}, \qquad ...(98)$$

The first term gives simply the interaction energy of a point charge (monopole). The terms in first bracket give the energy of a dipole. The six terms in the second bracket are the quadrupole energy terms. The above relation can be written in tensor form as

$$U=\phi_0\int\rho\, dv+\left(\frac{\partial\phi}{\partial x_i}\right)_0\int x_i\,\rho\, dv+\frac{1}{2}\left(\frac{\partial^2\phi}{\partial x_i\partial x_j}\right)_0\int x_i x_j\,\rho\, dv+\ldots(99)$$

Here integrals are the various moments of the distribution.

Let us now discuss quadrupole energy terms. For an ellipsoid of rotation, because of symmetry, the three integrals involving the cross products xy, yz and xz vanish. When the z-axis is the symmetry axis the integral over y^2 gives the same result as the integral over x^2. We can therefore write the quadrupole interaction energy

$$\Delta U_2=\frac{1}{2}\left(\frac{\partial^2\phi}{\partial z^2}\right)_0\int z^2\,\rho\, dv+\frac{1}{2}\left(\frac{\partial^2\phi}{\partial x^2}+\frac{\partial^2\phi}{\partial y^2}\right)\int\frac{x^2+y^2}{2}\,\rho\, dv. \qquad ...(100)$$

From Laplace's equation, we have $\partial^2\phi/\partial x^2+\partial^2\phi/\partial y^2+\partial^2\phi/\partial z^2=0$. By substituting this and $r^2=x^2+y^2+z^2$, we get

$$\Delta U_2=\frac{1}{4}\left(\frac{\partial^2\phi}{\partial z^2}\right)_0\int(3z^2-r^2)\,\rho\, dv=\frac{1}{4}\, eQ\left(\frac{\partial^2\phi}{\partial z^2}\right)_0, \qquad ...(101)$$

where the quadrupole moment Q is defined as

$$Q=\frac{1}{e}\int(3z^2-r^2)\,\rho\, dv\,. \qquad ...(102)$$

This relation shows that $Q=0$ for a spherically symmetric charge distribution ($\langle x^2\rangle=\langle y^2\rangle=\langle z^2\rangle=\frac{1}{3}r^2$). The Q is $+ve$ when $3z^2>r^2$ and the charge distribution is stretched in the z-direction (*prolate*). In an *oblate* distribution $3z^2<r^2$ and Q is $-ve$. Since the expression is divided by the electronic charge, the dimension of the quadrupole moment is that of an area. As it is very small, hence in nuclear physics it is measured in *barns* (1 barn$=10^{-28}$ m^2).

In semi-classical calculations, one must consider the fact that the nuclear symmetry axis is not the *space fixed z-axis* but *I*-axis can be regarded as a symmetry axis. According to quantum mechanics the angular momentum vector I^* can never line up in any given direction say that of an external field, but always precess around it at some angle. The magnitude of I^* is $[I(I+1)]^{1/2}\hbar$ and the maximum

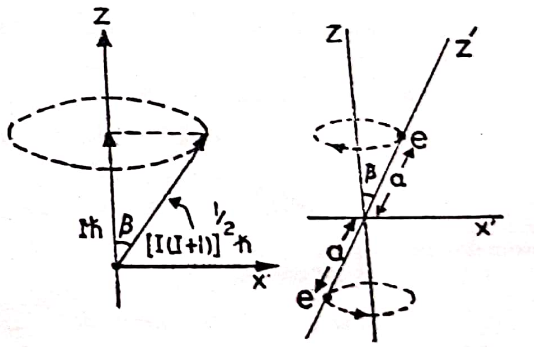

Fig. 1.28

projected value is $I\hbar$. Thus the smallest possible value of β is given by (assuring $I>0$) the relation

$$\cos\beta = I/\sqrt{[I(I+1)]}, \qquad \ldots(103)$$

Nuclear quadrupole moments are defined not to the body axis of the charge distribution (z'-direction) but to the precession axis (z-direction). The I^* is along z'-direction and $I\hbar$ is along z-direction.

For the charge distribution of fig. 1.28 the result of applying eqn. (102) to the z'-axis is

$$Q' = (3a^2 - a^2)e + (3a^2 - a^2)e = 4e\, a^2.$$

Applying it to the z-axis yields

$$Q = 2e\, a^2\,(3\cos^2\beta - 1) = \tfrac{1}{2}\, Q'\,(3\cos^2\beta - 1)$$

$$\therefore\; Q = \tfrac{1}{2}\,\frac{2I-1}{I+1}\,Q' = \tfrac{1}{2}\,\frac{2I-1}{I+1}\int (3z'^2 - r^2)\,\rho\, dv. \qquad \ldots(104)$$

Thus nuclei which have $I=0$ and $1/2$ can exhibit no quadrupole moment Q and hence smallest value of angular momentum I for which Q does not vanish is one.

Let us assume that the nuclei are uniformaly charged ellipsoids of rotation with the semi-axis a along the axis of symmetry and the semi axis b ⊥ to the symmetry axis. Let us further suppose that $a = R(1+\epsilon)$ and $b = R(1-\tfrac{1}{2}\epsilon)$, where ϵ is a distortion parameter. These assumptions ensure that the volume of the distorted sphere is equal to the undistorted sphere. Thus for such an ellipsoid, with charge Ze, we have

$$Q = Z(3z^2 - r^2)_{av} = \tfrac{2}{5} Z(a^2 - b^2) = \tfrac{6}{5} Z R^2 \epsilon. \qquad \ldots(105)$$

From observations of Q, we see that the distortions of nuclei from the perfect sphere are relatively small.

In a quantum mechanical definition, the charge density ρ is replaced by the probability density $|\psi|^2$ and the eqn. (104) thus reduces to

$$Q = \tfrac{1}{2}\,\frac{2I-1}{I+1}\int \psi(r)\,(3z'^2 - r^2)\,\psi^*(r)\, dv. \qquad \ldots(106)$$

From the compilation-by Klinkenberg, the largest positive quadrupole moment is 7×10^{-28} m^2 for Lu^{176} and the largest negative quadrupole moment is -1.2×10^{-28} m^2 for Sb^{123}. The fact that the deuteron possesses a small quadrupole moment (2.73×10^{-31} m^2) is an important to the basic nature of nuclear forces. The study of quadrupole moment gives an idea about nuclear closed shells and helps in the study of nuclear models.

The quadrupole moments of nuclear ground states may be detected through their interaction with electric field gradients. Observations of various effects due to the interaction result in values of the *quadrupole coupling*, which is the product of the Q and the electric field gradient. The coupling measurements have been made from optical hyperfine spectra, microwave spectroscopy and para-

parameters are taken to be the strength V_0 (the value of potential at the origin and the range α (the distance beyond which potential goes to zero rapidly). It is less than nuclear dimensions.

We use the principles of wave mechanics on nuclear problems and then by comparison with experimental data, find a consistent description of the nuclear forces acting between two nucleons (*two body problem*). There are two general methods of investigation, the study of *n p* and *p-p* scattering events over a wide range of energy and the study of deuteron (only bound state of two nucleons).

8.2. DEUTERON

Let us first consider deuteron in order to exhibit some of the concepts involved in discussing nuclear potentials and the quantum states of nuclei. The deuteron does possess measurable properties which might serve as a guide in the search for the correct nuclear interaction. These properties are :

1. The extraordinary stability of the alpha particle shows that the most stable nuclei are those in which number of neutrons and photons are equal. The deuteron consists of two particles of roughly equal masses M, so that the reduced mass of the system is $\frac{1}{2}M$.

2. The binding energy of the deuteron is very small. Its experimental value is 2.225 ± 0.002 *MeV*. Since the energy needed to pull a nucleon out of a medium mass nucleus is about 8 *MeV*, we must regard the deuteron as loosely bound.

3. The angular momentum quantum number, often called the nuclear spin, of the ground state of the deuteron determined by a number of optical, radiofrequency and micro-wave methods is one. It suggests that the spins are parallel (triplet state) and the orbital angular momentum of the deuteron about their common center of mass is zero. Thus the ground state is ^3S state.

4. The parity of deuteron as measured, indirectly, by studies of nuclear disintegrations and reactions for which certain rules of parity changes exist, is even.

5. The sum of the magnetic dipole moments of the proton ($2.79275\mu_N$) and neutron ($-1.91315\mu_N$), do not exactly equal to magnetic moment of the deuteron ($0.85735\mu_N$) measured by magnetic resonance absorption method.

6. A radiofrequency molecular beam method has been employed to determine the quadrupole moment of the deuteron as $Q = 0.00282 \times 10^{-28}$ m^2. This shows the departure from spherical symmetry of a charge distribution. The +ve sign indicates that this distribution is prolate rather than oblate.

The electric quadrupole moment and the magnetic moment discrepancy can be explained if the ground state is a mixture of the triplet states $^3S_1$ and $^3D_1$ having even parity. The percentage probability of finding the deuteron in *D*-state is $4 \pm 2\%$. As deuteron spends

most of the time in the spherically symmetrical state (*S*-state), we will for the moment ignore the *D*-state contribution to the deuteron wavefunction.

7. Since the neutron has no charge, the force between the neutron and proton can not be electrical. This force can not be magnetic as magnetic moments are very small. It can not be gravitational force, as the masses are very small. So we must accept the nuclear force as a new type of force. This force is short range, attractive and along the line joining the two particles (central force). Since a central force can not account for the quadrupole moment of the deuteron. As a quadrupole moment is small, the assumption will be approximately correct.

8. The force depends only on the separation of the nucleons not on the relative velocity or orientation of the nucleon spins with respect to the line. This force can be derived from a potential. Since the force is attractive, $V(r)$ is negative and decreases with decreasing r. Since it is short range, $V(r)$ vanishes for $r > b$, where $b \sim 3$ fermi.

The Schrodinger wave equation for the two body problem is

$$\nabla^2\psi + (2m/\hbar^2)(E-V)\psi = 0, \quad ...(1)$$

where m is the reduced mass, E the total energy of the system equal to the binding energy of deuteron and V the potential energy describing the forces acting between the two bodies.

In the terms of spherical polar coordinates, eqn (1) becomes

$$\left[\frac{1}{r^2}\frac{\partial}{\partial r}\left(r^2\frac{\partial\psi}{\partial r}\right) + \frac{1}{r^2\sin\theta}\frac{\partial\theta}{\partial}\left(\sin\theta\frac{\partial\psi}{\partial\theta}\right) + \frac{1}{r^2\sin^2\theta}\frac{\partial^2\psi}{\partial^2\phi}\right]$$

$$+ (2m/\hbar^2)\,[E - V(r, \theta, \phi)]\psi = 0 \quad ...(2)$$

Let us assume that $V(r, \theta, \phi)$ actually depends on r only and not on θ and ϕ. The solution of the above equation can be written as a product of a function of r only and one of θ and ϕ only as $\psi(r, \theta, \phi) = \psi(r)\,\psi(\theta, \phi)$. Substituting it into equation (2) we have

$$\frac{1}{\psi(r)}\frac{d}{dr}\left(r^2\frac{d\psi(r)}{dr}\right) + \frac{2mr^2}{\hbar^2}\left[E - V(r)\right] = -\frac{1}{\psi(\theta,\phi)}$$

$$\left[\frac{1}{\sin\theta}\frac{\partial}{\partial\theta}\left(\sin\theta\frac{\partial\psi(\theta,\phi)}{\partial\theta}\right) + \frac{1}{\sin^2\theta}\frac{\partial^2\psi(\theta,\phi)}{\partial\phi^2}\right] \quad ..(3)$$

The left hand side of this equation depends only on r, the right hand side depends only on θ and ϕ. For all values of the variables, each side of this must separately equal to the some constant, which comes out to be $l(l+1)$. Thus we have

$$\frac{1}{r^2}\frac{d}{dr}\left(r^2\frac{d\psi(r)}{dr}\right) + \frac{2m}{\hbar^2}\left[E - V(r) - \frac{l(l+1)\hbar^2}{2mr^2}\right]\psi(r) = 0, \quad ...(4)$$

where l is the angular momentum quantum number of the system.

The last term in the bracket appears as a straight addition to the actual potential $V(r)$ and is known as centrifugal potential.

The Schrodinger equation for ^3S state ($l=0$) of the deuteron is

$$\frac{1}{r^2}\frac{d}{dr}\left(r^2\frac{d\psi(r)}{dr}\right)+\frac{2m}{\hbar^2}[E-V(r)]\,\psi(r)=0. \qquad ...(5)$$

In this case reduced mass $m=\frac{1}{2}M$. We expect the ground state to be spherically symmetric (*S*-state), so that $\psi(r)$ depends only or r. Substituting $\psi(r)=u(r)/r$ in equation (5), where $u(r)$ is called the radial wavefunction, we have

$$(d^2u/dr^2)+(M/\hbar^2)[E-V(r)]\,u=0. \qquad ....(6)$$

The wavefunction of the bound state of the deuteron is not markedly dependent on the exact shape of the potential $V(r)$ between a proton and neutron provided that a potential of short range is chosen. For simplicity, we represent $V(r)$ by a *square well* of depth V_0 and radius b, where b is the range of the nuclear force. In it $V(r)$ has a constant negative value$-V_0$ for separations less than a certain value b and the value zero for all greater separations. The other central force potentials may be of

Gaussian well type $V(r)=-V_0e^{-(r/\alpha)^2}$

Exponential well type $V(r)=-V_0e^{-r/\alpha}$

Yukawa well type $V(r)=-\dfrac{V_0e^{-r/\alpha}}{(r/\alpha)}$

For the ground state of the deuteron, the total energy E is negative and equal to$-B$, where B is the binding energy of deuteron. Thus equation (6) can be written as

$$\frac{d^2u}{dr^2}+\frac{M}{\hbar^2}[V_0-B]u=0 \quad \text{for } r<b \qquad ..(7)$$

and
$$\frac{d^2u}{dr^2}+\frac{M}{\hbar^2}(-B)u=0 \quad \text{for } r>b. \qquad ...(8)$$

These equations can be written as

$d^2u/dr^2+K^2u=0,\ r<b$ ...(9)

and $d^2u/dr^2-\alpha^2u=0,\ r>b,$ ...(10)

where $K^2=M(V_0-B)/\hbar^2$

and $\alpha^2=MB/\hbar^2$.

General solutions of eqns (9) and (10) are

$u=A_1\sin Kr+B_1\cos Kr$ ...(11)

$u=A_2e^{\alpha r}+B_2e^{-\alpha r}$ ...(12)

The following boundary conditions must be imposed :

(1) $u\ (r\to 0)=0$, to keep wave function ψ finite.

(2) $u\ (r\to\infty)=0$, u must not diverge faster than r as $r\to\infty$.

To satisfy the conditions at zero and infinity, the solutions reduce to

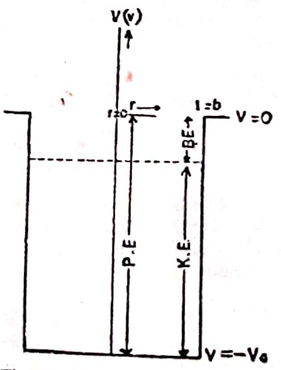

Fig. 8.1. Square well potential of deuteron.

$u=A_1\sin Kr$ for $r<b$ ...(13)

$u=B_2e^{-\alpha r}$ for $r>b$. ...(14)

Since these two solutions join smoothly at $r=b$. Hence equating the values and first derivatives of u at $r=b$, we have

$A_1\sin Kb=B_2e^{-\alpha b}$ ...(15)

and $A_1K\cos Kb=-B_2\alpha e^{-\alpha b}$. ...(16)

$\therefore$ $K\cot Kb=-\alpha$. ...(17)

The constants A_1 and B_2 are obtained from the requirement that the integral of $|\psi|^2$ over all space must be equal to unity.

$$4\pi\int_0^\infty|\psi|^2r^2dr=4\pi\int_0^\infty u^2dr=1$$

or
$$4\pi\int_0^b A_1^2\sin^2 Kr\,dr+4\pi\int_b^\infty B_2^2e^{-2\alpha r}\,dr=1$$

$$A_1^2[b-(1/2K)\sin 2Kb]+(B_2^2/\alpha)\,e^{-2\alpha b}=1/2\pi. \qquad ...(18)$$

Thus A_1 and B_2 can be obtained from this equation with the help of eqns (13) and (14). With the values of b and α as given above, the second term is about twice as large as the first. Hence the *nucleons in the deuteron spend only one third of the time within the range of nuclear force and thus the deuteron is loosely bound.* This can be seen from fig. 8.2, where $u(r)$ is plotted against r.

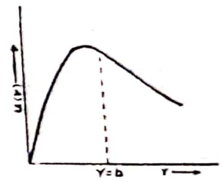

Fig. 8.2. Ground state deuteron wave function

No excited S-states—Equation (17) can be written as

$$x\cot x=-\alpha b, \qquad ...(19)$$

where $x=Kb$. Using $B=2.225\pm0.002$ MeV and $b\leqslant 3f$ we find that $\alpha=0.232$ and $\alpha b\leqslant 0.7$. If we draw now curves $y=\cot x$ and $y=-\alpha b/x$, the intersections give the roots of eqn (19). From fig. 8.3 it is clear that roots are slightly greater than $\pi/2$, $3\pi/2$, $5\pi/2$,...... The correct solution is $x=Kb\approx\frac{1}{2}\pi$, since if Kb were greater than π, the wave function would have a node at $Kb=\pi$ and thus $u(r)$ and hence $\psi(r)$ would not be the wave function of the ground state—*a contradiction of our hypothesis.* We may thus put $Kb=\frac{1}{2}\pi+\epsilon$ in eqn (19) and get

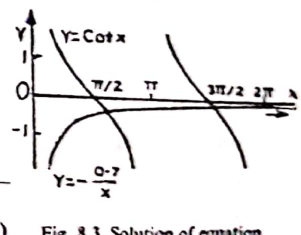

Fig. 8.3. Solution of equation $x\cot x=-0.7$

$$(\tfrac{1}{2}\pi+\epsilon)\cot(\tfrac{1}{2}\pi+\epsilon)=-\alpha b. \qquad ...(20)$$

As ϵ is small, hence $\cot(\frac{1}{2}\pi+\epsilon)\simeq-\epsilon$, and $\epsilon\simeq 2\alpha b/\pi$.

Thus $Kb=\pi/2+2\alpha b/\pi$. ...(21)

This shows that *there can not be any excited S-states.*

Range and Depth of Potential—Using $Kb=\pi/2$ and again neglecting B in the expression for K [as the depth of potential is very much greater than the binding energy *i.e.*, $K^2 >> \alpha^2$ which can be obtained from eqn (21)], we get

$$MV_0 b^2/\hbar^2=\pi^2/4 \quad \text{or} \quad V_0 b^2=\pi^2\hbar^2/4M. \qquad ...(22)$$

It is the relation between range b and potential depth V_0. Actually $V_0 b^2$ is slightly greater than $\pi^2\hbar^2/4M$, as Kb is slightly greater than $\pi/2$. By accepting the aproximate value of range $b=2$ fermi, the value of potential depth is $V_0=36$ Mev. Other types of short range potential function give about the same results at the square well.

Another result which does not depend on the form of potential is the wavefunction outside the range of nuclear forces. In this region function $u(r)$ decreases exponentially with r and reduces to zero at infinity. The radial distance where the amplitude decreases to $1/e$ of its maximum amplitude is often called the *radius* of the deuteron.

$$\therefore \quad \text{Radius } R=1/\alpha=\hbar/\sqrt{(MB)}=4.31\times10^{-15}\ m. \qquad ...(23)$$

It is about twice that of the range b. This explains that the *deuteron is a loosely bound system.* As $b<R$, hence the nuclear forces can be said to be *short range.*

In the zero range approximation the potential acts within a short distance and must be deep, and the wave function is exponential everywhere. As the range becomes larger compared to nuclear radius, the depth of the potential decreases and the sinusoidal part becomes more and more predominant.

Excited States of the Deuteron—To see that there cannot be any bound states with higher angular momenta we first write the radial part of the Schrodinger equation for any angular momentum as

$$\frac{d^2u_l(r)}{dr^2}+\left[K^2-\frac{l(l+1)}{r}\right]u_l(r)=0. \qquad r\leqslant b \qquad ...(24)$$

and

$$\frac{d^2u_l(r)}{dr^2}-\left[\alpha^2+\frac{l(l+1)}{r}\right]u_l(r)=0. \qquad r>b, \qquad ...(25)$$

where K^2 and α^2 are having their usual values.

The general solution of these equations involve spherical Bessel functions j_l and spherical Neumann functions n_l. As the latter approaches $-\infty$ as $r\to0$, thus the solution of eqn (24) is

$$u_l(r)=A\,j_l(Kr), \qquad r\leqslant b \qquad ...(26)$$

where

$$j_l(Kr)=(\pi/2Kr)^{1/2}\,J_{l+1/2}(Kr). \qquad ...(27)$$

The solution of eqn (25) is

$$u_l(r)=B\,h_l(i\alpha r)=B[j_l(i\alpha r)+in_l(i\alpha r))] \qquad ...(28)$$

where $$m(i\alpha r)=(-1)^{l+1}\,(\pi/2i\alpha r)^{1/2}\,J_{-l-1/2}(i\alpha r). \qquad \ldots(29)$$

Using boundary conditions that the function and its first derivative are continuous at the edge of the well, we get

$$\left[\frac{1}{u_l}\,\frac{du_l(r)}{dr}\right]_{inside}=\left[\frac{1}{u_l}\,\frac{du_l(r)}{dr}\right]_{outside}, \quad (r=b) \qquad \ldots(30)$$

Using the relation $\dfrac{dj_l(\rho)}{d\rho}=j_{l-1}(\rho)-\dfrac{l+1}{\rho}j_l(\rho)$, we get

$$K\left[\frac{j_{l-1}(Kb)}{j_l(Kb)}-\frac{l+1}{Kb}\right]=i\alpha\left[\frac{h_{l-1}(i\alpha b)}{h_l(i\alpha b)}-\frac{l+1}{i\alpha b}\right]$$

or

$$j_{l-1}(Kb)/j_l(Kb)=(\alpha/K)[ih_{l-1}(i\alpha b)/h_l(i\alpha b)] \qquad \ldots(31)$$

For $b<1.43\times10^{-15}m, \alpha b<1$ and since $\alpha<<K$ the expression in the bracket on R H S is less than one, and is approximately zero. Thus

$$j_{l-1}(Kb)\approx 0. \qquad \ldots(32)$$

This condition holds for all angular momenta except $l=0$. We have already discussed the case $l=0$. For $l=1$, we get $j_0(Kb)\approx 0=\sin(Kr)/Kr$. Hence $Kb\simeq\pm\pi, \pm2\pi, \pm3\pi, \ldots$ ...Thus the minimum well depth is

$$V_0\simeq\pi^2\hbar^2/Mb^2. \qquad \ldots(33)$$

If we choose $b=2\times10^{-15}m$, we get $V_0=144$ MeV, which is almost four times as large as the actual well depth in the ground state. Repeating this procedure for larger and larger values of l, we find that a deeper and deeper well depth is required to produce a bound state. Thus we conclude that no bound state exists for $l>0$. This also confirms experimental results.

8.6 NEUTRON-PROTON SCATTERING AT

of odd parity are pure ...

(d) The ground state of the deuteron : *Magnetic moment.* We know that the small discrepancy between the sum of the magnetic moment of proton and neutron and the measured value for the deuteron can be interpreted as a contribution of the orbital motion of the proton in the *D*-state in the deuteron ground state. If nuclear forces are supposed to be central forces, the difference will be zero. This contribution can appear only with the non-central forces. The operator describing the magnetic moment of deuteron is

$$\vec{\mu}=\vec{\mu}_p \times \vec{\sigma}_p+\vec{\mu}_n \times \vec{\sigma}_n+\vec{\mathbf{L}}_p, \qquad \ldots(78)$$

where $\vec{\mu}_n$ and $\vec{\mu}_p$ are the magnetic moments of neutron and proton measured in nuclear magnetons, $\vec{\sigma}_n$ and $\vec{\sigma}_p$ their unitary spin operators and $\mathbf{L}_p$ is the orbital angular momentum of the proton. The uncharged neutron cannot contribute any magnetic moment by orbital motion alone. In the centre of mass system the orbital angular momentum of the proton is half of the combined orbital angular momentum *L*. Thus the above equation can be written as :

$$\mu=(\mu_n+\mu_p)\,\tfrac{1}{2}\,(\sigma_n+\sigma_p)+\tfrac{1}{2}\,(\mu_n-\mu_p)\,(\sigma_n-\sigma_p)+\tfrac{1}{2}L.$$

Since the operator $(\sigma_n-\sigma_p)$ in the second term vanishes for a triplet state, and $\mathbf{I}=\mathbf{L}+\mathbf{S}$, hence the magnetic moment operator becomes

$$\vec{\mu}=(\mu_n+\mu_p)\,\mathbf{I}-(\mu_n+\mu_p-\tfrac{1}{2})\,\mathbf{L}. \qquad \ldots(79)$$

The observed value of μ is the expectation value of this expression in the state with $I_z=I$. We, therefore, can replace L by L_z.

$$\therefore \quad \mathbf{L}\rightarrow L_z=\frac{\mathbf{L.I}}{I^2}I_z=\frac{I(I+1)+L(L+1)-S(S+1)}{2I(I+1)}I_z \quad ...(80)$$

For the deuteron, $I(I+1)=S(S+1)=2$ and in a mixture of S and D states, $[L(L+1)]_{av}=0\times p_S+6\times p_D=6p_D$. Here p_D and p_S represent the D-and S-state probabilities respectively. For the deuteron $I=1$, the value of I_z in the state with $I_z=I$ is unity.

$$\therefore \quad \mu \text{ of deuteron}=\mu_n+\mu_p-\tfrac{3}{2}(\mu_n+\mu_p-\tfrac{1}{2})\,p_D. \quad ...(81)$$

The last term gives a direct measure of the D-state probability. The experimental results imply a D-state probability of about 4%. The above relation does not give accurate results. There are various other causes which can give corrections, especially of relativistic effects. Hence the measured magnetic moment gives only a rough estimate of the D-state probability. One may expect that p_D is really between 2 and 8%.

Quadrupole moment. In chapter 1, the quadrupole moment Q was defined as the average value of $(3z^2-r^2)$ in the state with $m=I$. When evaluating the quadrupole moment of the deuteron we must remember that only the proton contributes to the quadrupole moment and its distance from the centre of gravity is half of the proton neutron separation r.

$$\therefore \quad Q=\tfrac{1}{4}(3z^2-r^2)=\tfrac{1}{4}r^2(3\cos^2\theta-1). \quad ...(82)$$

Since the quadrupole moment is estimated from the S and D waves beyond the potential well, hence the expectation value of this operator Q is given by

$$(\psi, Q\psi)=(\psi_S, Q\psi_S)+(\psi_D, Q\psi_D)+2(\psi_S, Q\psi_D). \quad ...(83)$$

The first term is zero because the S state is spherically symmetrical and cannot have a quadrupole moment. The second term is a pure D-state term and is smaller than the cross term (as $p_S>>p_D$), hence only the cross term contributes. The measured quadrupole moment Q is, therefore, be written as

$$Q=\frac{1}{\sqrt{(50)}}\int_0^\infty r^2\,u(r)\,\omega(r)\,dr, \quad ...(84)$$

where the constant comes from the spin sum and angular integration. $u(r)$ is the deuteron ground state S-wave function outside the range of nuclear forces and can be written as $u(r)=N_S\,e^{-kr}$. $\omega(r)$ is the deuteron D-wave function at distances beyond the range of the specific potentials and can be written as

$$\omega(r)=N_D\,e^{-kr}\,(1+3/kr+3/k^2r^2).$$

Here N_S and N_D are normalization constants and $k=\sqrt{(MB)}/\hbar^2$.

The rough estimate of N_S can be obtained by neglecting the small D-state probability compared to unity by substituting

$$p_s=\int^\infty u^2dr=1 \qquad N_S=\sqrt{(2k)}. \quad ...(85)$$

Since the weighing factor r^2 favours the contribution of the outside wave function, hence we can estimate the quadrupole moment by substituting the values of $u(r)$ and $\omega(r)$ into the equation (84). The result will be

$$Q = N_S N_D/\sqrt{8}k^3. \qquad \text{...(86)}$$

This relation can be used for a good estimate of N_D. If value of N_S is taken from eqn. (85), we have

$$Q = N_D/2k^{5/2} \quad \text{or} \quad N_D = 2Qk^{5/2}. \qquad \text{...(87)}$$

Thus we see that the function $\omega(r)$ outside the range of the forces is determined completely by the quadrupole moment. This result implies that the D-state probability p_D depends strongly on the tensor force range R_T and increases rapidly as R_T is made shorter. The integral of ω^2 from the radius R_T on out is given by

$$\int_{R_T}^{\infty} \omega^2 \, dr = \frac{3N_D^2}{R_T^3 k^4} \qquad \text{...(88)}$$

To take into account the contribution from $r < R_T$ we can roughly double this and thus get the physically important quantity

$$p_D = \int_0^{\infty} \omega^2 \, dr = 2\int_{R_T}^{\infty} \omega^2 \, dr = \frac{6N_D^2}{R_T^3 k^4} = \frac{24Q^2 k}{R_T^3}. \qquad \text{...(89)}$$

This equation implies that the tensor force cannot have an arbitrarily small range otherwise the ground state would become a predominantly D state rather than predominantly S state. The experimental value of Q is $+2{\cdot}73\ (e \times 10^{-31}\ \text{m}^2)$.

A rough measurment of p_D is obtained from the deuteron magnetic moment (eqn. 81). This value of p_D leads to a fair estimate of R_T, since it is in the cube of R_T which occurs in eqn (89). This gives that the tensor force range R_T falls near 3×10^{-15} m, which is almost independent of the range of the central force and is slightly larger than the range of central forces.

... confirms experimental results.

8.3. NEUTRON-PROTON SCATTERING AT LOW ENERGIES

The fact that the deuteron is a bound system, shows that attractive forces exist between neutrons and protons. Further information on the inter-nucleon forces can be obtained from a study of the scattering of free neutrons by protons. In such experiments a parallel beam of neutrons is allowed to impinge upon a target containing hydrogen atoms and the number of neutrons deflected through various angles is determined as a function of neutron energy. Since neutrons have no charge, they are uneffected by the electrostatic field and their scattering will directly reflect the operation of the nuclear forces.

Two kinds of the reactions can be involved in neutron proton interaction : One scattering and other radiative capture. The latter has low probability and cross section for high energy neutrons, as the cross section for the competing radiative capture reaction decreases with $1/v$, where v is the neutron velocity. In practice protons are bound in molecules. The chemical binding energy of the proton in a molecule is about 0.1 eV. Thus for neutron energies

> 1eV the proton can be assumed as free. *This sets a lower limit to the neutron energy.* If the neutron energy is less than 10 MeV, only the S-wave overlaps with the nuclear potential and is scattered.

In the centre of mass system, the Schrodinger equation for the two body (*n*-p system) problem is

$$\nabla^2\psi+\frac{M}{\hbar^2}[E-V(r)]\psi=0, \qquad ...(34)$$

where M=Proton or neutron mass=2×Reduced mass of the system.

E=Incident kinetic energy in *C-M* system=½ (incident K. E. in *L*-co-ordinates)

and $V(r)$=Inter-nucleon potential energy.

At large distances from the centre of scattering the solution of this equation is expected to be of the form

$$\psi=e^{ikz}+\frac{e^{ikr}}{r}f(\theta). \qquad ...(35)$$

The term e^{ikz} represents a plane wave describing a beam of particles moving in the *z*-direction towards the origin (scattering centre). The second term represents the scattered wave. The complex quantity $f(\theta)$ is the scattering amplitude in the direction θ and is to be evaluated in terms of k. In the case of a spherically symmetric potential the entire arrangement is axially symmetric about the incident direction and hence does not depend on the azimuthal angle ϕ. The $1/r$ dependence is necessary for the conservation of particles in the outgoing wave. The volume of a spherical shell, between r and $r+dr$ is $4\pi r^2\,dr$ and hence the density of particles in it or the probability of finding one particle in the spherical shell must vary with $1/r^2$ which is proportional to the square of the amplitude of the scattered wave in the shell. Hence the amplitude of the scattered wave must vary with $1/r$.

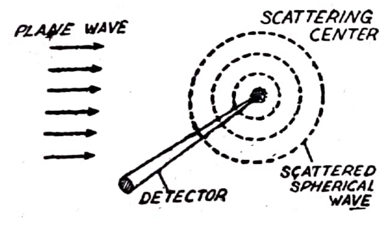

Fig. 8.4. Scattering Process.

To compute the differential scattering cross section, we must find the number of particles dN scattered in unit time by one target nucleus into a solid angle $d\Omega$ and the incident flux F. If v is the speed of an incoming particle with respect to the scatterer, then

Incoming flux of particles $F=\psi_{in}^*\,\psi_{in}v=v$.

Similarly dN is equal to the flux of scattered particles $\psi_{sc}^*\,\psi_{sc}v$

multiplied by the area $r^2d\Omega$ cut out by $d\Omega$ on a spherical surface of radius r and is given by

$$dN=\psi_{sc}^*\psi_{sc}\,vr^2d\Omega=|f(\theta)|^2\,vd\Omega.$$

∴ The differential cross section $d\sigma=|f(\theta)|^2vd\Omega/v=|f(\theta)|^2d\Omega$

or

$$\sigma=\int|f(\theta)|^2d\Omega=2\pi\int|f(\theta)|^2\sin\theta\,d\theta. \qquad ...(36)$$

First of all let us consider the wave equation (34) in the absence of a scattering centre [$V(r)=0$ for all values of r].

$$\nabla^2\psi+(ME/\hbar^2)\psi=0. \qquad ...(37)$$

This has the solution $\psi=e^{ikz}$, (38)

where

$$k=1/\lambda\!\!\!^{-}=\sqrt{(ME)}/\hbar.$$

Lord Rayleigh proposed that this type of wavefunction can be expanded into a series in terms of spherical harmonic functions. Thus equation (38) can be written as an infinite series

$$\psi=e^{ikz}=e^{ikr\cos\theta}=\sum_{l=0}^{\infty}R_l(r)\,Y_{l,0}(\theta),$$

where l is the integer representing the number of the partial waves. It, as usual, signifies the orbital angular momentum of the system. The radial functions $R_l(r)$ are solutions of the radial part of equation (37).

$$\frac{1}{r^2}\frac{d}{dr}\left(r^2\frac{dR}{dr}\right)+\left(k^2-\frac{l(l+1)}{r^2}\right)R=0 \qquad ...(40)$$

This equation has two solutions, one is not finite at the origin and cannot represent the plane wave. The other is finite at origin and can be represented in terms of spherical Bessel functions as

$$R_l(r)=i^l\sqrt{[4\pi(2l+1)]}\,j_l(kr). \qquad ...(41)$$

The square of this gives the r-dependence of the probability density for each partial wave in expression (39). The values of first few spherical Bessel functions are

$$j_0(kr)=\frac{\sin kr}{kr},\; j_1(kr)=\frac{\sin kr}{(kr)^2}-\frac{\cos kr}{kr},$$

$$j_2(kr)=\left(\frac{3}{(kr)^3}-\frac{1}{kr}\right)\sin kr-\frac{3\cos kr}{(kr)^2},$$

The spherical harmonic function

$$Y_{l,0}(\theta)=\frac{(2l+1)^{1/2}}{(4\pi)^{1/2}}P_l(\cos\theta), \qquad ...(42)$$

where $P_l(\cos\theta)$ is the Legendre polynominal of order l. The square of the spherical harmonic function gives the angular dependence of the probability density. The values of the first few Legendre polynomials are

$P_0(\cos\theta)=1$, $P_1(\cos\theta)=\cos\theta$, $P_2(\cos\theta)=\frac{1}{2}(3\cos^2\theta-1)$.

For incident neutrons kinetic energy less than 10 MeV (in the lab-system), the only partial wave involved in scattering is the $l=0$ or S-wave. The scattering is then spherically symmetric in the centre of mass system. The higher the l-value, the larger the impact parameter has to be for a particle with given linear momentum. In the absence of a scattering potential equation (39) can be written as

$$\psi=R_0(r)\,Y_{0,0}(\theta)+\sum_{l=1}^{\infty}R_l(r)\,Y_{l,0}(r)=\frac{\sin kr}{kr}+\left(e^{ikz}-\frac{\sin kr}{kr}\right) \qquad ...(43)$$

The averaged value of the quantity within the brackets over all directions in space is zero. The first term corresponds to the spherically symmetric partial wave (S-wave). For S-wave scattering, only the first term is affected and can therefore be written as ψ_s in the presence of the scattering potential $V(r)$. We can write it as $\psi_s=u(r)/r$. Outside the range of the scattering potential, the amplitude of the outgoing wave is unchanged. The only possible change in the wave is therefore a change of phase.

Thus as $r\to\infty$, the solution $u(r)$ assumes the form $c\sin(kr+\delta_0)$, where c is an arbitrary constant and δ_0 is some phase angle. Thus the complete wave function ouiside the scattering potential is

$$\psi=\frac{c\sin(kr+\delta_0)}{r}+\left(e^{ikz}-\frac{\sin kr}{kr}\right)$$

$$=e^{ikz}+\frac{c}{r}\,\frac{e^{ikr}e^{i\delta_0}-e^{-ikr}e^{i\delta_0}}{2i}-\frac{1}{kr}\,\frac{e^{ikr}-e^{-ikr}}{2i}$$

$$=e^{ikr}+\frac{e^{ikr}}{r}\left(\frac{ce^{i\delta_0}-1/k}{2i}\right)-\frac{e^{-ikr}}{r}\left(\frac{ce^{-i\delta_0}-1/k}{2i}\right)$$

This scattered wave must contain no incoming wave. Therefore we can write the coefficient of e^{-ikr} as zero. Thus we have

$$ce^{-i\delta_0}-1/k=0 \quad\text{or}\quad c=(1/k)\,e^{i\delta_0},$$

hence $$\psi=e^{ikz}+\frac{e^{ikr}}{r}\,\frac{e^{2i\delta_0}-1}{2ik}. \qquad ...(44)$$

Comparing this with the standard solution (35), we have

$$f(\theta)=\frac{e^{2i\delta_0}-1}{2ik}=\frac{e^{i\delta_0}}{k}\cdot\frac{e^{i\delta_0}-e^{-i\delta_0}}{2i}=\frac{e^{i\delta_0}}{k}\sin\delta_0, \qquad ...(45)$$

The total elastic scattering cross section is

$$\sigma_0=2\pi\int_0^{\pi}\frac{\sin^2\delta_0}{k^2}\sin\theta\,d\theta=\frac{4\pi}{k^2}\sin^2\delta_0$$

$$=4\pi\bar{\lambda}^2\sin^2\delta_0. \qquad ...(46)$$

The analysis here is carried through only for $l=0$ scattering. Higher orbital angular momentum waves also have to be considered at higher energies. The total cross-section can be written as a sum of partial cross-sections, one for each l-wave. The partial cross-sections are

$$\sigma_l=4\pi\bar{\lambda}^2(2l+1)\sin^2\delta_l. \qquad ...(47)$$

Scattering length. For neutrons of very low energy scattered by free protons, $\bar{\lambda}$ is very large and hence k is very small. It can be seen from eqn. (45) that as $k\to 0$, δ_0 must also approach zero, otherwise $f(\theta)$ would become infinite. Thus for low energy neutrons $f(\theta)$ can be written as

$$f_0=\lim_{\delta_0\to 0}\frac{e^{i\delta_0}\sin\delta_0}{k}=\frac{\delta_0}{k}=-a, \qquad ...(48)$$

where the quantity $+a$ is called the *scattering length* in the convention of Fermi and Marshall. Hence for low energy neutrons

$$u(r)=c\,(kr+\delta_0)=ck\,(r-a). \qquad ...(49)$$

This is the equation of a straight line intersceting the r-axis at $r=a$, and is obtained by extrapolating the radial wave function $u(r)$ from the point just beyond the range of the nuclear force. Scattering from a potential giving a bound state produces a positive a. If the potential gives only a virtual state, the slope of the inner wave function at $r=b$ is positive and a is negative.

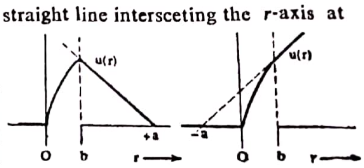

Fig. 8·5. (left) Positive scattering length (bound state) ; (right) Negative scattering length (unbound state).

From eqns (46) and (48) the zero energy scattering cross-section becomes

$$\sigma_0=4\pi a^2. \qquad ...(50)$$

This is identical with the scattering cross-section of an impenetrable sphere of radius a, in the limit of zero energy. The measurement of σ_0 *determines the magnitude of the scattering length a but not its sign.*

Determination of the phase shift δ_0—We shall now attempt to determine the phase shift δ_0 for low energy neutron-proton scattering by solving also the Schrodinger's equation in the region where the interaction between the two particles takes place. For this we make the simple assumption of a square well for the nuclear potential. Inside the well of depth V_0 and radius b the radial wave equation for particles whose total energy has the positive value E is

$$\frac{d^2u}{dr^2}+\frac{M}{\hbar^2}[E+V_0]\,u(r)=0. \qquad ...(51)$$

Inside the square well this equation has the simple solution

$$u(r)=A \sin k_1 r, \text{ where } k_1=\sqrt{[M(E+V_0)]}/\hbar. \qquad ...(52)$$

Outside the square well, the solution can be written as

$$u(r)=B \sin (kr+\delta_0). \qquad ...(53)$$

At the edge of the rectangular well ($r=b$), the two solutions and their derivatives with respect to r must be continuous.

$$\therefore \quad A \sin k_1 b=B \sin (kb+\delta_0)$$

and

$$k_1 A \cos k_1 b=Bk \cos (kb+\delta_0).$$

Hence

$$k_1 \cot k_1 b=k \cot (kb+\delta_0). \qquad ...(54)$$

This relationship is analogous in form to equation

$$K \cot Kb=-\alpha, \qquad ...(17)$$

which describes the binding energy B of the deuteron in terms of the same rectangular well (V_0, b).

Here $K=\sqrt{[M(V_0-B)]}/\hbar$ and $\alpha=\sqrt{(MB)}/\hbar$.

For low energy neutrons ($E \ll V_0$), we may assume $K=k_1$ (as $V_0 \gg B$), hence *the wavefunction u(r) inside the well is nearly the same for the deuteron and the n-p-scattering system.* Thus for approximation we can write

$$\frac{\sqrt{(ME)}}{\hbar} \cot \left(\frac{\sqrt{(ME)}}{\hbar} b+\delta_0 \right)=-\frac{\sqrt{(MB)}}{\hbar}.$$

As the scattering length a is much larger than the range b of the potential, thus for very low energy neutrons kb can be neglected in comparison to δ_0.

$$\therefore \quad \cot \delta_0=-\sqrt{\left(\frac{B}{E}\right)} \text{ or } \sin \delta_0=\frac{E}{E+|B|} \qquad ...(55)$$

Substituting this value of $\sin^2 \delta_0$ in equation (46) we obtain the approximate value of total scattering cross-section as

$$\sigma=4\pi\hbar^2 \frac{E}{E+|B|}=\frac{4\pi\hbar^2}{M} \cdot \frac{1}{E+|B|} \qquad ...(56)$$

The Spin Dependence of Nuclear Forces. At very low energies the situation is very different. Numerical substitution of $B=2.22$ MeV in equation (56) gives a predicted value for zero energy neutrons ($E=0$), $\sigma_0 \simeq 2.3$ barns. Which is in violent disagreement with the measured value $\sigma_0=20.36 \pm 0.10$ barns. This disagreement is a sign of some fundamental error in our assumptions. This point was cleared up by E. P. Wigner in 1935. He suggested that the scattering occurs not only in the triplet state (^3S), but in the singlet state (^1S) as well.

Experimentally the total angular momentum of the deuteron nucleus is unity. The spins are, therefore, correlated in the ground state of the deuteron. The situation is different in n-p scattering

experiment. When unpolarized neutrons strike randomly oriented protons, their uncorrelated spins add up to unity in three fourths of the collisions and to zero in one fourth of the collisions. In other words we can say that the triplet state ($S=1$) has three times the statistical weight ($2S+1$) of a singlet ($S=0$) state. The total n-p scattering cross-section will then be

$$\sigma=\tfrac{3}{4}\sigma_t+\tfrac{1}{4}\sigma_s,$$

where σ_t and σ_s indicate the cross-sections in triplet and singlet states respectively.

One test of Wigner's hypothesis is by measurement of the cross-section over the range 0 to 5 MeV, where the theoretical expression for σ_0 should hold. We can use the calculated value $\sigma_t=2.3$ barns and the experimental information on σ_0 (zero energy cross-section) to calculate σ_s. To fit the experimental data, we must have (in barns)

$$20.36=\tfrac{3}{4}(2.3)+\tfrac{1}{4}\sigma_s$$

$$\therefore \quad \sigma_s=74 \text{ barns}. \qquad ...(57)$$

Introducing the singlet and triplet scatterring lengths a_s and a_t, where $\sigma_s=4\pi a_s^2$ and $\sigma_t=4\pi a_t^2$, we obtain the rough estimates $a_t \sim 4.3$ fermi and $a_s \sim 24.3$ fermi.

Coherent Scattering of Slow Neutrons. Equation (50) shows that we can find the magnitude, but not the sign, of the scattering length a. The most important evidence is the scattering of neutrons by *ortho and para hydrogen*. An experimental comparison of the coherent scattering from ortho and para hydrogen was first suggested by Teller in 1936 to test the spin dependence of the neutron proton interaction. Not only we are able to verify that the scattering is spin dependent but also will be able to show that singlet state scattering length is negative. In para-hydrogen molecules the proton spins are anti-parallel. The molecules can rotate with energies given by

$$E_J=J(J+1)\,\hbar/2\mathscr{I}, \qquad (J=0, 2, 4, ...),$$

where $\mathscr{I}$ is the moment of inertia. In ortho hydrogen proton spins are parallel. The rotational states are given by $J=1, 3, 5.....$ If temperature is low enough practically all the para hydrogen will be in the state $J=0$ and all the ortho hydrogen will be in state $J=1$.

We shall now derive an expression for the scattered intensity from a molecule of ortho or para hydrogen when the incident neutron energy is so small that $\lambda\!\!\!^{-}_n$ is much greater than $0.78 \times 10^{-10} m$, the distance between the atoms in hydrogen molecule. The theoretical expressions for total cross-section for the special case of neutron energy of 0.001463 eV and a gas temperature of 19·5°K, as derived by Schwinger and Teller in 1937, are

$$\sigma_{para}=6.69\,(3a_t+a_s)^2 \qquad ..(58)$$

$$\sigma_{ortho}=6.69\,[(3a_t+a_s)^2+2(a_t-a_s)^2]+1.74\,(a_t-a_s)^2 \qquad ...(59)$$

where a_t and a_s are triplet and singlet scattering lengths. The last term in σ_{ortho} was added to take into account inelastic scattering by conversion of ortho to para. This process is energetically possible but its cross-section is small. It is clear from above relations that σ_{para} and σ_{ortho} become identical if $a_t = a_s$. In this case the total nuclear forces are said to be spin independent.

According to the experimental results of Sutton (1947), $\sigma_{para} = 4.0$ barns and $\sigma_{ortho} = 125$ barns. This great difference between these cross-sections indicates that the *n-p* force is strongly spin dependent.

$|3a_t + a_s|$ is very much smaller than $|a_t - a_s|$ when $a_s < 0$ but very much larger when $a_s > 0$. Since $\sigma_{para} < \sigma_{ortho}$, hence $|3a_t + a_s|$ is smaller than $|a_t - a_s|$ or $a_s < 0$. This —ve value of a_s indicates that the *singlet state of the deuteron is virtual or unbound.* We can now solve equations (58) and (59) for a_t and a_s. There are four possible pairs of a_t and a_s values. Two can be discarded because they have —ve a_t values. A third pair can be shown to be inconsistent with *n-p* scattering data. The remaining solution is $a_t = 0.52 \times 10^{-14}$ m. and $a_s = -2.3 \times 10^{-14}$ m. Therefore, the total cross-section will be

$$\sigma_0 = \tfrac{3}{4}\sigma_t + \tfrac{1}{4}\sigma_s = \tfrac{3}{4} \times 4\pi a_t^2 + \tfrac{1}{4} \times 4\pi a_s^2 = 19.8 \text{ barns},$$

which is in fair agreement with experimental value 20.36 barns.

Spin of neutron. The large observed value of $\sigma_{ortho}/\sigma_{para}$ relates to the spin of the neutron. The ground state of the deuteron has $I=0$ and $I=1$, if

$$S_n + S_p = \tfrac{1}{2} + \tfrac{1}{2} = 1 \qquad \text{(spin parallel)}$$

$$S_n + S_p = \tfrac{3}{2} - \tfrac{1}{2} = 1 \qquad \text{(spin anti-parallel).}$$

In the second case the relative statistical weights for *n-p* collisions with free protons would change from their values of 3/4 and 1/4 to values of 5/8 and 3/8. This will change the scattering cross-sections.

$$\sigma_{ortho}/\sigma_{para} \simeq 2.$$

This is against experimental results, hence the neutron has spin 1/2 not 3/2.

1.15 Nuclear forces

According to Coulomb's law, the positively charged protons, closely spaced within the nucleus, should repel each other strongly and they should fly apart. It is therefore difficult to explain the stability of nucleus unless one assumes that nucleons are under the influence of some *very strong attractive type forces*. The forces inside the nucleus, binding neutron to neutrons, protons to protons and neutrons to protons, are classified as *strong interactions* and are represented as $n-n$, $p-p$ and $n-p$ forces respectively. These forces are essentially equal in magnitude as warranted by *experimental* evidence and were studied extensively over a long period by the Japanese scientist Hideki Yukawa. In 1935, he described the chief characteristics of *nuclear forces* and postulated a particle, a *pion* with a rest mass 270 m_e, that played an integral part in the explanation of nuclear forces. Yukawa was awarded Nobel Prize in physics in 1949 for his contributions to the understanding of nuclear forces.

According to Yukawa, the following are the ***characteristics*** of nuclear forces :

1. They are *short range* forces, i.e. effective only at short ranges.
2. They are *charge-independent,* i.e. they do not seem to depend on the charge of the particle.
3. They are the *strongest* known forces in nature.
4. They get readily *saturated* by the surrounding nucleons, and
5. They are *spin-dependent.*

We shall now discuss the above characteristics of nuclear forces in somewhat more details.

Short range — The results of scattering experiments : *pp* scattering, *np* scattering etc. show that nuclear forces operate over extremely short distances inside the nucleus. Between two nucleons, the distance is of the order of 1 *Fermi* ($1F=10^{-15}$ m) or less. They are *not* like the inverse square law forces such as Coulomb force between electric charges. If a nucleus is bombarded with protons and if the range of nuclear force be of the same order of magnitude as Coulomb repulsion, they would be affected by both type of forces. But the scattering of protons will be different from the one corresponding to a pure Coulomb scattering.

The protons that pass not too close to the nucleus are scattered by electric repulsive forces. But if the energy of the incident protons be large enough to overcome Coulomb repulsion, they may pass very close to nucleus, within a distance r_0 from the centre of the nucleus, and fall in the range of attractive nuclear forces. They would then be captured and fall, as it were, into the *potential well* of the nucleus. The scattering of protons in this case is mainly due to strong and attractive nuclear forces and the distribution is distinctly different from Coulomb scattering.

There is however some evidence to suggest that at extremely short distances (0.5 F), the *attractive force turns into a repulsion* so that in a stable nucleus, the nucleons do not get too close together.

Charge independence — *Experimental* evidence indicates that the interaction between any two nucleons is ***independent of the charge***. Also the interactions among the nuclear forces between $n-n$, $p-p$ and $p-n$, exclusive of Coulomb forces, have been found to be the same to a high degree of accuracy.

Strong forces — The ***strong interactions,*** the forces between the nucleons, are the strongest forces found in nature. The gravitational and the electromagnetic interaction were known to us long before the nuclear forces, as they were associated with macroscopic bodies, e.g. the gravitational forces between the planets and the sun and the electrical forces between charged bodies. But they are far weaker compared to the nuclear force. For instance, the gravitational force is only $\sim 10^{-40}$ of the strong interaction.

Saturation — Nuclear forces are the only ones in nature that show saturation effect. The ability of nuclear forces to act upon other particles attain a point of saturation when a nucleon gets completely surrounded by other nucleons. Those nucleons that are located outside the surrounding nucleons do not 'feel' the interaction of the surrounded nucleon.

Summarising : (i) the forces between nucleons are attractive in nature when they are 0.5 – 25 F apart; (ii) these forces are of short range having maximum value at about 2×10^{-15} m and fall off sharply with distance, becoming negligible beyond this range; (iii) they are charge-independent so that the nuclear force between a proton and a neutron or between a neutron and a neutron are almost the same; (iv) they have the property of saturation – a particular nucleon interacts with a limited number of nucleons around it and the other surrounding ones remain unaffected. So they become saturated over short distances; (v) the nuclear forces depend on the ***mutual orientation of spins of various nucleons*** and are *different in parallel and antiparallel spins*.

• In addition to the strong nuclear force which is far stronger than Coulomb interaction, there is, as indicated by *experimental evidence*, a third type of force which is also a short range force but much weaker than the nuclear force. This is termed ***weak interaction***. It may be as small as 10^{-14} of strong nuclear force. It is also not of gravitational type.

Interestingly, the weaker the force, the larger must be the system in order that it might be of importance. For example, the strong interactions hold the nucleons, the electromagnetic force holds the larger systems of atoms and molecules, while the gravitational force becomes important only in astral systems.

The chief forces of nature are thus of the following four types : (i) the *strong nuclear force*, (ii) the *electromagnetic force*, (iii) the *weak interaction force* and (iv) the *gravitational force*.

• According to Yukawa's theory, protons and neutrons do not exist independently within a nucleus but constantly exchange charges by emission and absorption of π-mesons (pions) in themselves. This constant emission and absorption result in an exchange of virtual mesons by nucleons, within the nucleus, in ultra short intervals $\sim 10^{-23}$ to 10^{-24} s. As the exchange occurs in a very short time, the uncertainty principle requires that no visible change in nucleonic mass would be observed. This gives rise to rapid meson exchange or *meson field* between protons and neutrons in which meson acts as a quantum of nuclear force. The process is analogous to exchange of photons between charged particles in electromagnetic interactions.

• Read also the Chapter 9 : *Nuclear force*, for more details.

(A) **Exchange Forces.** In 1932, Heisenberg proposed, in order to explain the saturation of nuclear forces, that nuclear forces were *exchange forces* which would depend explicitly on the symmetry of the wave function. At the time of Heisenberg's idea of exchange forces, mesons were known and it was known that π-meson was being exchanged between nucleons, by any of the following processes:

$$
\begin{array}{llll}
n, p \,; p, n & ; \; p, p & ; \; n, n \\
p+\pi^-, p \,; n+\pi^+, n & ; \; p+\pi^\circ, p & ; \; n+\pi^\circ, n \\
p, \pi^- + p \,; n, \pi^+ + n & ; \; p, p+\pi^\circ & ; \; n, n+\pi^\circ \\
p, n \,; \quad n, p & ; \; p, p & ; \; n, n.
\end{array}
$$

The exchange of a pion is thus equivalent to charge exchange. We can think of the nucleons as exchanging their space and spin co-ordinates. The wave equation of the two body system for an ordinary central force is

$$[(\hbar^2/M)\nabla^2+E]\Psi(\mathbf{r}_1\mathbf{r}_2\,\sigma_1\,\sigma_2)=V(\mathbf{r})\Psi(\mathbf{r}_2\,\mathbf{r}_2\,\sigma_1\,\sigma_2). \qquad \text{...(92)}$$

The force is known as *no exchange, ordinary or Wigner* force. The interaction does not cause any exchange.

Exchange forces are classified as :

1. *Majorana Forces.* The Majorana interaction is that in which it is assumed that two particles attract one another if the wave function describing the entire system does not change sign when the special co-ordinates of the two particles are interchanged and that they repel if the wave function changes sign, *i.e.*,

$$[(\hbar^2/M)\nabla^2+E]\,\psi(\mathbf{r}_1,\mathbf{r}_2,\sigma_1,\sigma_2)=V(r)\psi(\mathbf{r}_2,\mathbf{r}_1,\sigma_1,\sigma_2). \qquad \text{...(93)}$$

This interaction reflects the coordinates and replaces $\mathbf{r}$ by $-\mathbf{r}$ in the wave-function. Hence eqn (93) may be written as

$$[(\hbar^2/M)\nabla^2+E]\psi(\mathbf{r})=(-1)^l\,V(\mathbf{r})\psi(\mathbf{r}). \qquad \text{...(94)}$$

This eqn indicates that the force is always attractive for states of even $l(S, D, G,...)$ and always repulsive for states of odd l.

2. *Bartlett Forces.* This involves the exchange of the spin but not the position coordinates of the two interacting nucleons. For such an interaction, the Schrodinger eqn is

$$[(\hbar^2/M)\nabla^2+E]\psi(\mathbf{r}_1,\mathbf{r}_2,\sigma_1,\sigma_2)=V(\mathbf{r})\psi(\mathbf{r}_1,\mathbf{r}_2\,\sigma_2,\sigma_1). \qquad \text{...(95)}$$

The wave function of two particles is symmetric if the total spin $S=1$ and anti-symmetric if $S=0$. Thus eqn (95) gives

$$[(\hbar^2/M)\nabla^2+E]\psi(\mathbf{r})=(-1)^{s+1}\, V(\mathbf{r})\psi(\mathbf{r}). \quad \ldots(96)$$

This relation is equivalent to an ordinary potential which changes sign between $S=0$ and $S=1$. The nuclear force can not be totally of the Bartlett type because it is clear from neutron proton scattering data that both the ^3S and ^1S potentials are attractive.

3. *Heisenberg Forces*. In the type of interaction there is an exchange of both the position and the spin co-ordinates of the two nucleons. For such an interaction, the Schrodinger eqn is

$$[(\hbar^2/M)\nabla^2+E]\psi(\mathbf{r}_1, \mathbf{r}_2, \sigma_1, \sigma_2)=V(\mathbf{r})\psi(\mathbf{r}_2, \mathbf{r}_1, \sigma_2, \sigma_1)\,. \quad \ldots(97)$$

Since the wave function of two particles is symmetric for $(l+S)$ even and anti-symmetric for $(l+S)$ odd, hence eqn (97) may be written as

$$[(\hbar^2/M)\nabla^2+E]\psi(\mathbf{r})=(-1)^{l+s+1}V(\mathbf{r})\psi(\mathbf{r}). \quad \ldots(98)$$

This relation indicates that sign of ordinary potential is positive if $(l+S)$ is odd and is negative if $(l+S)$ is even. This gives that the force is attractive for even l triplet states and odd l singlet states, but is repulsive in odd l triplet and even l singlet states.

The three types of exchange operators P^M, P^B and P^H are used to construct these three types of exchanged forces. The reversal of sign between ^3S and ^1S states indicates that the nuclear force cannot be wholly of the Heisenberg type. The difference between the $n-p$ interactions in these states can be explained by assuming that the interaction is roughly 25 per cent Heisenberg or Bartlett and 75 per cent Wigner or Majorana.

The three types of exchange operators can be related as

$$P^H=P^M P^B \text{ and } (P^M)^2=(P^B)^2=(P^H)^2=1. \quad \ldots(99)$$

This shows that each operator has only two eigenstates $+1$ and -1. The Majorana exchange operator is $+1$ for the states of even l and -1 for the states in odd l. The Bartlett exchange operator gives $+1$ in triplet states and -1 in singlet states, independent of l In the various states of the two particle systems, the exchange operators have the values given below

Operator	Even parity states Triplet	Even parity states Singlet	Odd parity states Triplet	Odd parity states Singlet
P^H	1	-1	-1	1
P^M	1	1	-1	-1
P^B	1	-1	1	-1

The most general potential of the exchange type is written in the form

$$V=V_W(\mathbf{r})+V_M(\mathbf{r})P^M+V_B(\mathbf{r})P^B+V_H(\mathbf{r})P^H. \quad \ldots(100)$$

This potential also has tensor operator S_{12} term for mixtures of Wigner and Majorana forces.

(B) Isotopic Spin Formalism. In this formalism we are considering the proton and the neutron as different quantum states of the same particle, the nucleon. The total wave-function is written as a product of the space part, a spin part and an isospin part. The nucleus must obey Fermi-statistics in order to the consistent with the ordinary theory. Thus the total wave-function for the two or more particles

$$\psi=\psi\text{ (space) }\psi\text{ (spin) }\psi\text{ (isotopic spin)} \qquad ...(101)$$

must be anti-symmetric with respect to interchange of all co-ordinates of two nucleons. In the ground state of the deuteron, for example, ψ (space) is symmetric, as it a mixturé of an S-state and a D-state, ψ (spin) is symmetric (the two spins are parallel), so that the ψ (isotopic spin) must be anti-symmetric and thus $T=0$ (the two isotopic spins are oppositely oriented). The lowest state of deuteron in which the two nucleon spins are opposed, ψ (spin) is then anti-symmetric, is the lowest one in which $T=1$.

The concept of the T multiplet has been applied to β-decay, γ-decay and to nuclear reactions. *The success of these applications supplies additional support for the hypothesis of the charge independence of nuclear forces.*

In order to confirm with isospin conservation, the Hamiltonian describing the interaction between two nucleons must be rotationally invariant in isospace. Thus it must contain scalar quantities formed with the isospins $\vec{\tau}_1$ and $\vec{\tau}_2$. The product of operators $\vec{\tau}_1.\vec{\tau}_2$ gives $+1$ when applied to isotopic spin triplet states and -3 when applied to isotopic spin singlet states. We can use $\vec{\tau}_1.\vec{\tau}_2$ to define an isotopic spin operator P^τ analogous to spin operator σ.

$$P^\tau=\tfrac{1}{2}(1+\vec{\tau}_1 \,.\, \vec{\tau}_2). \qquad ...(102)$$

The operator gives $+1$ when applied to the (symmetric) isotopic spin triplet states, -1 when applied to the (anti-symmetric) isotopic spin singlet states. Hence it is equivalent to simple exchange of the isotopic spin co-ordinates η_1 and η_2 of the two particles. Thus we can write

$$P^\tau\psi(\mathbf{r}_1, \zeta_1, \eta_1\,;\,\mathbf{r}_2, \zeta_2, \eta_2)=\psi(\mathbf{r}_1, \zeta_1, \eta_2\,;\,\mathbf{r}_2, \zeta_2, \eta_1), \qquad ...(103)$$

where $\mathbf{r}_1$ denotes the position of the one particle and ζ_1 its spin direction.

We have required complete anti-symmetry under the full exchange of all the co-ordinates of the two particles. Since Heisenberg exchange operator P^H exchanges position and mechanical spin and the isotopic spin operator P^τ exchanges the isotopic spin co-ordinates, hence we can write

$$P^H P^\tau\psi=-\psi. \qquad ...(104)$$

This is a condition on ψ, not an operator identity. We multiply equation (104) by P^{τ} on both sides and have

$$P^{H}\psi=-P^{\tau}\psi \qquad ...(105)$$

because equation (103) shows that $(P^{\tau})^2=1$.

It is clear from equation (105) that we can replace the Heisenberg exchange operator by the isotopic spin operator $-P^{\tau}$. As the Bartlett exchange operator P^{B} can be written as

$$P^{B}=\tfrac{1}{2}(1+\vec{\sigma}_1 \cdot \vec{\sigma}_2). \qquad ...(106)$$

Thus we can replace the Majorana exchange operator by the combination

$$P^{M}=-\tfrac{1}{4}(1+\vec{\sigma}_1 \cdot \vec{\sigma}_2)(1+\vec{\tau}_1 \cdot \vec{\tau}_2) \qquad ..(107)$$

Equations (105), (106) and (107) show the expressions for the three linearly independent exchange operators in terms of the mechanical and isotopic spin operators. From the point of view of the isotopic spin formalism it is more convenient to use three other linearly independent operators $(\vec{\sigma}_1 \cdot \vec{\sigma}_2)$, $(\vec{\tau}_1 \cdot \vec{\tau}_2)$ and $(\vec{\sigma}_1 \cdot \vec{\sigma}_2)(\vec{\tau}_1 \cdot \vec{\tau}_2)$. The values of these products in states of the two particle system are listed below :

Spin product	Even parity state		Odd parity state	
	triplet	*singlet*	*triplet*	*singlet*
$\vec{\sigma}_1 \cdot \vec{\sigma}_2$	1	−3	1	−3
$\vec{\tau}_1 \cdot \vec{\tau}_2$	−3	1	1	−3
$(\vec{\sigma}_1 \cdot \vec{\sigma}_2)(\vec{\tau}_1 \cdot \vec{\tau}_2)$	−3	−3	1	9

8.10. MESON THEORY OF NUCLEAR FORCES

Any attractive force between two particles is regarded as the exchange of an attractive property. The exchanged attractive property between two protons is an electron for an $(H_2)^+$ molecule and is the surrounding electric field for the Coulomb force between two charges. We may introduce similarly a new nuclear field surrounding each nucleon. The application of quantum mechanics to the electromagnetic field surrounding a charged particle leads to the conclusion that the electrical force is exerted by the transfer of a photon, which is referred to as *the field particle of the electro-magnetic field,* from one charged body to another. Yukawa (1935) thought that *the strong interaction between nucleons might be accounted for in a similar manner by postulating an appropriate field particle of rest mass different from zero. This virtual particle has been given the name meson.* To show that the range of force is related to the mass of exchanged particle, assume that the π°-meson is contained virtually in a proton. A temporary dissociation would be allowable if it does not take a time longer than Δt, given by uncertainty principle

$$\Delta t \approx \hbar / \Delta E. \quad \text{...(112)}$$

Here $\Delta E = (M_p + m_\pi)\, c^2 - M_p c^2 = m_\pi c^2$.

If this virtual particle travels with the velocity of light, as might be expected for a field particle, then the greatest distance the meson could travel in this time, also known as *range of the pion exchange force*

$$R \simeq c \Delta t \approx \hbar / m_\pi c. \quad \text{...(113)}$$

Based on known nuclear dimensions, Yukawa assumed that the range of the nucleon force and of the field particle would be about 2×10^{-15} m and this led to a value of m_π roughly 200 times the mass of an electron. About two years after Yukawa's theory, particles of mass about 200 m_e were discovered in cosmic radiation. These virtual particles are now known as mesons which were thought to be Yukawa field particles for more than ten years. Several different mesons with different charges and rest masses have been discovered. It was found that the Yukawa particle was not the

μ-meson but its parent, the shorter lived π-meson. The pion, which occurs in positive, negative and neutral forms has a mass about 270 times that of the electron and interacts very rapidly with matter. It has other properties spin and parity, which qualify it to be the field particle for nucleon forces.

The attraction between any two nucleons could arise from the transfer of a π^0-meson from one nucleon to the other. The force between a proton and a neutron could result from the transfer of a π^+-meson from the former to the latter or of a π^--meson in the opposite direction. To interpret the nucleon-nucleon scattering data in terms of a potential function, let us compare the meson theory with the quantum theory of electro-magnetic interactions. To obtain a pion wave-equation we express the total energy E of a pion in terms of the pion rest mass energy $m_\pi c^2$ and momentum p as

$$E^2=c^2p^2+m_\pi^2c^4. \qquad ...(114)$$

The energy E and momentum component p are represented by the operators

$$E=i\hbar\,\partial/\partial t,\ p_x=-i\hbar\,\partial/\partial x,\ p_y=-i\hbar\,\partial/\partial y \text{ and } p_z=-i\hbar\,\partial/\partial z.$$

Introducing a pion wavefunction ϕ (a scalar), we obtain the Klein Gordon equation for a free particle of spin 0.

$$-\hbar^2\partial^2\phi/\partial t^2=-c^2\hbar^2\nabla^2\phi+m_\pi^2c^4\phi$$

or

$$\nabla^2\phi-\frac{1}{c^2}\frac{\partial^2\phi}{\partial t^2}-\frac{m_\pi^2c^2}{\hbar^2}\phi=0. \qquad ...(115)$$

From $m_\pi=0$, it reduces to the well known wave-equation

$$\left(\nabla^2-\frac{1}{c^2}\frac{\partial^2}{\partial t^2}\right)\phi=0 \qquad ...(116)$$

for the quanta of the electromagnetic field. The simplest type of electromagnetic field is the electrostatic field, where $\partial\phi/\partial t=0$. The corresponding static pion field is the analogue of Laplace's equation in the absence of electric charges. The presence of charge requires the analogue of Poisson's equation $\nabla^2\phi=e\rho/\epsilon_0$, where e is the magnitude of the electronic charge and ρ is the electron particle density. In our present case we have nucleon charges interacting with the pion field. For a static pion potential due to a single point nucleon charge g at the origin, we have an equation

$$\nabla^2\phi-(m_\pi^2c^2/\hbar^2)\,\phi=4\pi g\,\delta(r). \qquad ...(117)$$

The solution of this eqn which vanishes at infinity is

$$\phi(\mathbf{r})=-\int\frac{e^{-\mu|\mathbf{r}-\mathbf{r}'|}}{|\mathbf{r}-\mathbf{r}'|}g\delta(\mathbf{r}')\,\delta\tau \qquad ...(118)$$

Here $\mu\approx m_\pi c/\hbar$ and $d\tau'$ is the volume element. If we have a point soure of strength g at $\mathbf{r}_1$, then we have,

$$\phi(\mathbf{r})=-g\frac{e^{-\mu|\mathbf{r}-\mathbf{r}_1|}}{|\mathbf{r}-\mathbf{r}_1|}$$

$\therefore$ Potential energy of a source g at $\mathbf{r}_2$ in this field is given by $V=g\phi(\mathbf{r}_2)$. If the potential ϕ is due to another source g at $\mathbf{r}_1$, then the interaction energy between two sources

$$V=-g^2\frac{e^{-\mu|\mathbf{r}_1-\mathbf{r}_2|}}{|\mathbf{r}_1-\mathbf{r}_2|}=-\frac{g^2e^{-\mu r}}{r} \qquad ...(119)$$

Comparing with the relation for Coulomb potential, we see that this nuclear potential decreases more rapidly with distance from the source than the Coulomb potential by an exponential factor. At separations small compared to μ^{-1}, this potential energy varies with r just as the Coulomb energy loss. Yukawa noted that this interaction energy may account for the fact that nuclear forces act only over a short range and that the range

$$R=1/\mu=\hbar/m_\pi c. \qquad ...(120)$$

Substitution of the value of m_π as 270 m_e, gives $R=1.4$ fermi.

Since in this theory the nuclear particle does not change its charge, we find that according to the theory n-n, n-p and p-p forces are equal. However the theory does not explain the exchange nature of nuclear forces, which is established from high energy scattering experiments and is able to explain saturation of nuclear forces. The theory in its simple form cannot explain the spin dependence or the presence of non-central forces. The theory is modified by several theoretical physicists taking into account, (1) the tensoral character of the meson field wave funtions, (2) the isobaric-spin character of the meson field wave functions, (3) the intrinsic nature of the source field coupling and (4) the strength of the source-coupling constant.

The interaction potential between two nucleons so calculated gives approximately $g^2/\hbar c=17$. It may be compared with the fine structure constant $e^2/4\pi\epsilon_0\hbar c=1/137$. The large dimensionless coupling constant $g^2/\hbar c$ suggests that more than one meson is transferred simultaneously between two nucleons. For small distances, we have strong repulsive core arising from the δ function. This core prevents the nucleons from coming close together. When two nucleons collide at very high energy ($\sim$BeV), the nucleons can penetrate or disturb each other's core. Thus we see that only the exchange of a relatively small number of mesons can have an appreciable effect on the nuclear force at low and medium energies. On the one hand, we see that the meson theory is qualitatively correct, but on the other hand, not a single quantity has been calculated and measured which confirms quantitative correctness.

EXERCISES

Example 1. *Recall that $b\sim\lambda/4\sim\pi/2K$ for the ground level of the deuteron. From this, show that the radius of the deuteron, in the rectangular well model is approximately given by*

$$R=2b\,V_0^{1/2}/\pi B^{1/2}.$$

The radioactive radiations can be distinguished by their different penetrating powers and by different responses to the effect of strong magnetic and electric fields. Alpha radiations can be deflected by strong magnetic and electric fields, which proves that they must be rapidly moving charged particles. Using semi-empirical mass formula, it is easy to find that the energy liberated in α-decay is positive for heavy nuclei ($A \geqslant 150$), which are, therefore, α-unstable.

The α-particles can be detected by the following devices—(*a*) Nuclear emulsions, (*b*) Cloud chambers, (*c*) Ionization chambers, proportional counters and Geiger Müller counters, (*d*) Scintillation counters. The energy of the particles can be measured by the above detectors, magnetic spectrographs, electrostatic deflection method range measurements and calorimetric measurements.

5.1. DETERMINATION OF q/M FOR THE α-PARTICLE

The principle of the method, first used by Rutherford and Robinson, is identical with the employed in making the determination of e/m for cathode rays by J.J. Thomson. The beam of α-particles is deflected by magnetic and electric fields and from the displacements produced the value of q/M can be calculated.

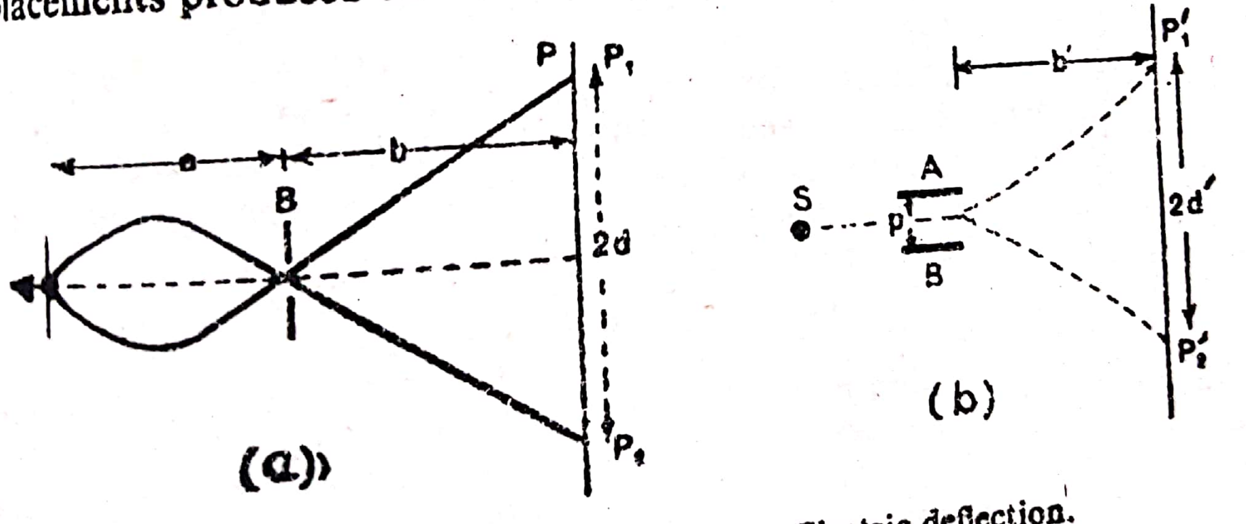

Fig. 5.1. (a) Magnetic deflection (b) Electric deflection.

The apparatus used for the magnetic deflection experiment is shown in fig. 5.1 (a). The source of α-particles, S, is set, parallel to the slit *B* at a distance *a* from it. The α-particles emanating from the source are limited by this slit *B* and are incident on a photographic plate P which is at a distance b from slit B. The chamber is placed in a strong uniform magnetic field with the lines of force parallel to the slit, *i.e.* perpendicular to the plane of the figure. Under the action of the magnetic field, the α-particle will describe an arc of a circle of radius r and there is only one angle of emission for which the path is through the narrow slit to the photographic plate. On reversing the magnetic field the path of the particle is reversed. The α-particles, with velocity v, thus reach the points P_1 and P_2 respectively before and after reversing the magnetic field. If q and M respectively be the charge and mass of the α-particle moving in a magnetic field B, then we can write

$$Mv^2/r = Bqv. \quad \ldots(1)$$

From geometry of the figure it can be shown that for a small deflection

$$2dr = b(a+b). \quad \ldots(2)$$

$$q/Mv = 2d/b\,(a+b)B. \quad \ldots(3)$$

Thus to get the value of q/M, v is to be determined. For this, α-particles are allowed to pass between two vertical parallel metallic A and B plates 35 cms long, separated by a small distance p (about 4 mm), and oppositely charged. The whole apparatus is evacuated and a potential V (2000 volts) is applied between the plates A and B. The particles have a parabolic path between the plates, the deflection being proportional to $1/v^2$. Let $2d'$ be the distance between the two points on the photographic plate, at which the α-particles impinge, before and after reversal of the electric field and b' be the distance between photographic plate P and the end of parallel plates nearer to it. Similar to the calculation of electrostatic deflection of cathode rays we have

$$\frac{q}{Mv^2} = \frac{(d'-p)^2}{8Vb'^2} \quad \ldots(4)$$

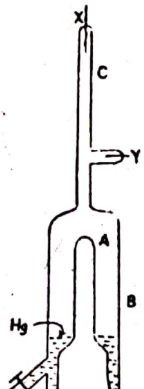

Fig. 5.2

From eqns (3) and (4) q/M and v can be easily determined. The value of specific charge q/M found by Rutherford and Robinson for all α-particles, irrespective of the source was 4.82×10^7 coul/kg. This was very close to the value of q/M calculated for doubly ionised helium. This identity was proved in 1909, by Rutherford and Royds using the following method. Radon gas emitting α-particles was placed in a thin walled glass tube A, surrounded by a wider tube B which had been evacuated. The α-particles passed through the thin walls into outer bulb B. After a week the gas, which had collected in B, was compressed by the mercury into the fine capillary C. On applying a high potential difference between X and Y its spectrum could be examined. The spectrum was identified as that of helium gas. This could only have come from α-particles by picking up two electrons. Thus it must be regarded that *α-particles were the doubly charged helium ions.*

5.2. RANGE OF α-PARTICLES

W.H. Bragg in England had produced evidence that α particles had a definite range. The

apparatus used by Bragg and Kleeman in 1904 is shown in fig. 5.3. Here the α-particles from the source X, in a lead shield, traverse the distance D to the ionization chamber. The ionization chamber consists of a metallic gauze G and a plate P, parallel and close to each

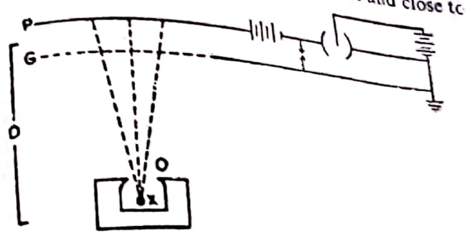

Fig. 5.3. Apparatus for measuring the range of α-particles.

other, maintained at a constant potential difference by a battery. The upper plate is connected to an electrometer. The ionization produced by the α-particles at any given distance from the source is measured by means of the electrometer. Bragg found that the curve relating the specific ionization (*the number of ions produced by*

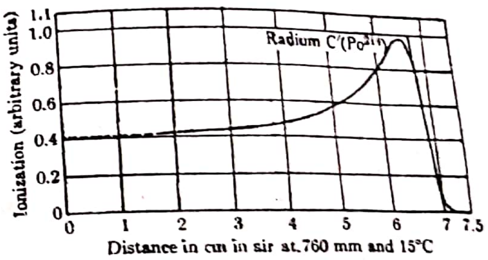

Fig. 5.4. Bragg curve.

a particles per unit length of the path) with the distance from the source was shown in fig. 5.4. This curve is known as *Bragg curve*. This curve shows that the specific ionization along the path of a particle climbs steadily to a maximum and then falls with great rapidity to zero, making a slight ankle in the curve just before the zero line is reached. As the α-particle moves more slowly, it spends more time in the vicinity of each of the molecules of the air which it encounters in its path and so the probability of removing an electron, and producing an ion pair, increases. The specific ionization thus increases steadily at first as the α-particle moves away from its source. Ultimately a point of specific ionization reaches when electrons attach themselves to the particle and convert it into a neutral atom. The tail end ankle of the curve (*the straggle effect*) arises from the fact that the α-particles do not all lose exactly the same amount of energy in their encounters with the molecules in their path. It is also partly due to the formation of He^+ ions, by the attachment of one electron to some of the α-particles. These ions still possess ionizing power, and hence cause a slight extension of the range before become neutral atoms. This method is not well suited to weak sources.

For week sources simple method has been devised by Geiger and Nuttall, illustrated by fig. 5.5. The source of α-particle is placed on a rod at the centre of a glass bulb which is silvered on the inside, and a high voltage is applied between the bulb and the metallic holder of the source. The radius of the spherical bulb is greater than the maximum range at atmospheric pressure. Since the *range varies directly as the absolute temperature and inversely as the pressure of the gas* through which the rays pass, hence by reducing the pressure in bulb, the α-particles are able to reach its wall. The saturation current for different gas pressures is measured, giving ionization curves as shown in fig. 5.6. The ionization current as measured by the electroscope is fairly constant as the pressure is decreased, until after the particles have begun hitting the wall. It then falls off since the particles are not producing as many ions as they are capable of doing. At the sharp turn-over point in the curve, the α-particles just reach the silvered wall of the bulb, so that the bulb radius is the range. Two kinks in the fig. 5.6 indicate two sets of α-particles of different ranges coming from two radioactive substances. The range for a particular gas pressure has thus been measured. Since the range in the gas is inversely proportional to the pressure, the range at atmospheric pressure is deduced simply.

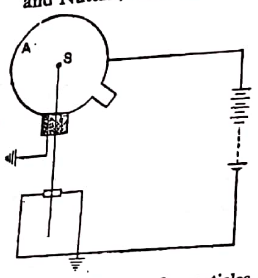

Fig. 5.5. Range of α-particles from weak sources.

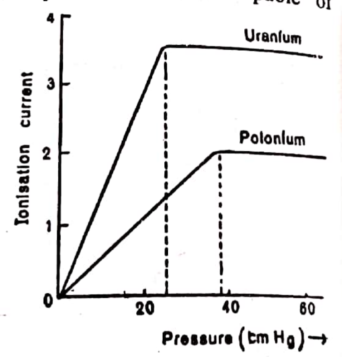

Fig. 5.6. Saturation ionization current for different gas pressures.

Alpha-particles are unable to penetrate a few sheets of paper or a thin aluminium foil, yet they can travel through several centimetres of air. This indicates that the range of an α-particle depends on the medium through which it travels. It was observed by Bragg that for most elements the atomic stopping power varied directly as the square root of the atomic weight.

5.3. RANGE-VELOCITY-ENERGY-LIFE RELATIONS

In 1910, H. Geiger made some measurements of the relative speeds of the α-particles from radium-*C*, after they had passed through various thicknesses of mica of known stopping power, relative to air. From these results Geiger gave a law known after his name as the *Gelger law*.

$$R = av_0^3, \quad \ldots(5)$$

where R is the extrapolated range in metres, v_0 the initial velocity in m/sec. at the source and a the constant numerically equal to 9.6×10^{-24}.

The energy E_0 of an alpha particle, in MeV, is related to the velocity by $E_0 = 2.08 \times 10^{-14} v^2$. Hence the relation between energy and range is given by

$$R = 9.6 \times 10^{-24} (E_0/2.08 \times 10^{-14})^{3/2} = 0.0038 \, E_0^{3/2}, \quad \ldots(6)$$

where E_0 is the initial energy of the α-particle in MeV and R the range in metres in air.

Actually these relations are applicable only for medium range. At lower ranges R is approximately proportional to $v_0^{3/2}$ and $E_0^{3/4}$ and at higher ranges for v_0^4 and E_0^2.

In 1911, Geiger and Nuttall arrived at an interesting conclusion relating the half-life of an α-emitter and the range of its α-particles.

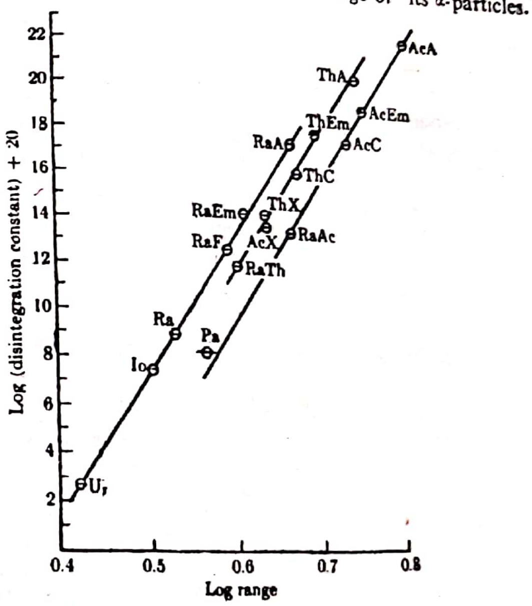

Fig. 5.7. Geiger Nuttall law.

They showed that if the logarithm of the range in air of the α-particle is plotted against the corresponding value of the logarithm of the distintegration constant, for a number of radioelements, an *approximately straight line* is obtained for each radioactive series. This is known as Geiger Nuttall rule, represented by the relation

$$\log \lambda = A \log R + B, \quad \ldots(7)$$

where A is a constant which has practically the same value for each of the three radioactive series and B is a constant which has a different value for each series. The Geiger-Nuttall law is illustrated by fig. 5.7. This rule has proved useful in determining the disintegration constant λ of some of the products of disintegration which could not be easily determined by direct measurements. It can be used to check up the validity of any theory of alpha particle decay.

The Geiger-Nuttall law can be derived from eqn (7) in the alternative form by utilizing the relationship between the range and energy of the alpha particles. Thus we have

$$\log \lambda = \frac{3}{2} A \log E_0 + B', \quad \ldots(8)$$

where A has the same value as in eqn (7) and B' is a constant for each radioactive series.

5.4. ALPHA ENERGY-MASS NUMBER

If the α-decay energy (for ground to ground transitions) is measured and is plotted against mass number A and nuclear charge Z. The points of equal Z are connected by straight lines. It is clear from this figure that E_α decreases as A increases for constant Z.

Corresponding to $N=126$ and $Z=82$, the shell effect is sufficiently strong to reduce the available α-decay energy. Just above a closed shell, a maximum in α-decay energy is observed.

When shell effects are excluded, the variation of E_α with A can be obtained by semi-empirical formula as

$$\frac{\partial E_\alpha}{\partial A} = -\frac{8}{9}\frac{a_s}{A^{4/3}} - \frac{4}{3} a_c \frac{Z}{A^{4/3}}\left(1 - \frac{4Z}{3A}\right) - 16 a_a \frac{Z}{A^2}\left(1 - \frac{2Z}{A}\right) \quad \ldots(9)$$

It shows the negative slope because every term is negative.

5.6 GAMOW'S THEORY OF ALPHA DECAY

Since an α-particle is emitted from a heavy nucleu as as discrete particle, one might infer that the some tightly bound assembly of two neutrons and two protons pre-existed in the nucleus, or a heavy nucleus might have a sub-structure of α-particles as shown in fig. 5.10. Light nuclei do exhibit periodic properties, can be shown by binding energy curve, which indicate the existence of α clustors within them. According to Frankel, for heavy nuclei, the formation of an α-particle in nuclear α-decay occurs in the course of decay.

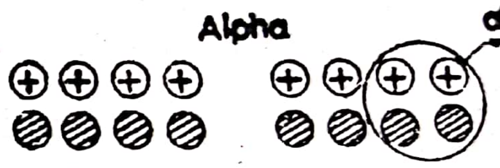

Fig. 5·10. α-particle decay.

In experiments on the scattering of α-particles, it was found that even the fastest of such particles from radioactive sources, having an energy of 10 MeV, are repelled by atomic nuclei. However, the more energetic the particle the more closely it can approach the nucleus before it is turned back. Although we do not know the exact nature of the forces acting on the α-particle, but know that there are repulsive forces due to the charges and some strong attractive nuclear short range forces. Due to the rapid decline of nuclear forces with distance, a positively charged particle will experience diminishing attraction near the surface of the nucleus when receding from the latter and at a certain distance, equal to the nuclear radius R, the forces of attraction will be balanced by the Coulomb force of repulsion. From this it follows that the internal part of the nucleus is separated from the outer space by a certain potential barrier, which prevents penetration of an

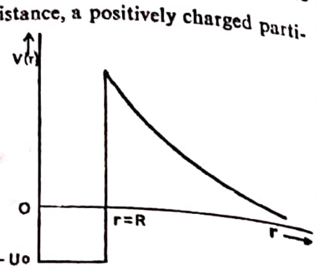

Fig. 5.11. Potential Energy Curve.

α-particle into the nucleus. The height of this barrier is the potential energy of an α-particle at $r=R$. The potential energy $V(r)$ of an alpha-particle outside the nucleus at a distance r from the centre of the nucleus is given by

$$V(r)=2(Z-2)\, e^2/4\pi\epsilon_0 r, \text{ for } r>R \qquad \text{...(13)}$$

where $(Z-2)$ is the atomic number of the daughter nucleus. In the case of U^{238}, the height of the potential barrier for an alpha-particle is given by

$$V(R)=\frac{2\,(Z-2)\,e^2}{4\pi\epsilon_0 R}=\frac{2\times 90\times(1.6\times10^{-19})^2}{10^{-14}}\times 8.99\times10^9$$

$$\simeq 26 \text{ MeV}$$

The interaction in the nucleus may be represented by a constant attractive potential U_0, exerted over a distance R. It is spoken of as a potential well of depth U_0 and of width R. Hence the potential energy

$$V(r)=-U_0 \quad \text{for } r<R. \qquad \text{...(14)}$$

The Coulomb potential and the constant potential energy U_0 are joined, for the sake of simplicity, by a straight line at $r=R$. The radial dependence of the net nuclear potential is indicated in fig. 5.11. It only shows the shape. The actual potential is generated by a rotation about the V-axis.

If the potential barrier prevents the entrance of α-particles from outside the nucleus, the same should prevent the emission of particles from the interior. Thus 26 MeV is the minimum energy that an alpha-particle must have, according to classical ideas, in order to escape from the nucleus of U^{238}. But the energies carried out by alpha particles, emitted by radio-active nuclei, are much lower than the heights of the potential barriers of the respective nuclei. Thus it is very difficult to understand how the particles contained inside the nucleus can go over a potential barrier which is more than twice as high as their total energy.

Classical mechanics, provided no explanation of this state of affairs, but in 1928 the English Physicist R. W. Gurney in collaboration with E. U. Condon of the United States and the Russian-born G. Gamow independently explained this paradox by means of the wave mechanics. If the motion of a particle in the neighbourhood of a potential barrier is treated wave mechanically, it is found that there is a finite probability that the particle can leak through the barrier even though its kinetic energy is less than the height of the barrier. The probability that an α-particle can leak through the barrier (*the "tunnel effect"*) can be calculated as under.

To avoid mathematical complexity we shall proceed in several steps. First, we shall use semi-classical treatment and second, we shall apply quantum mechanical ideas. Let us, for simplicity of the treatment, consider one dimensional Coulombs potential barrier of rectangular shape with width a, and height V, which is greater than the kinetic energy of an alpha-particle. There are three regions of interest.

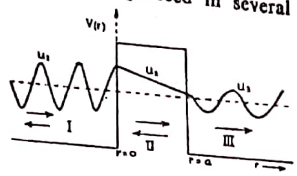

Fig. 5.12 Tunnel Effect

The Schrodinger equation in regions I and III is

$$\frac{d^2u}{dr^2}+\frac{2m}{\hbar^2}Eu=0, \qquad \text{...(15)}$$

where $m=M_\alpha M_D(M_\alpha+M_D)$, the reduced mass of the alpha-particle and the residual nucleus.

The equation in region II is

$$\frac{d^2u}{dr^2}+\frac{2m}{\hbar^2}(E-V)\,u=0. \qquad \text{...(16)}$$

Since the region I has both incident and reflected alpha-waves, hence the solution of equation (15) in this region is

$$u_1=A_1e^{ik_1r}+B_1e^{-ik_1r},$$

where

$$k_1=\sqrt{(2mE)}/\hbar. \qquad \text{...(17)}$$

$$\text{...(18)}$$

Since the region II has both foward moving transmitted wave and reflected from the other side of the barrier, hence the solution of equation (16) is

$$u_2=A_2e^{k_2r}+B_2e^{-k_2r},$$

where

$$k_2=\sqrt{[2m(V-E)]}/\hbar. \qquad \text{...(19)}$$

$$\text{...(20)}$$

Since region III has only forward moving transmitted wave hence the solution of eqn. (15) in this region is

$$u_3=A_3e^{ik_1r} \qquad \text{...(21)}$$

The constants A_1, A_2, A_3, B_1 and B_2 are to be determined by using following boundary conditions :

(I) $u_1=u_2$ and $\partial u_1/\partial r=\partial u_2/\partial r$ at $r=0$

(II) $u_2=u_3$ and $\partial u_2/\partial r=\partial u_3/\partial r$ at $r=a$ . ...(22)

By substituting the values of u_1, u_2 and u_3 in the above relations, we have

$$A_1+B_1=A_2+B_2 \quad \text{...(23)}$$

$$ik_1A_1-ik_1B_1=k_2A_2-k_2B_2 \quad \text{...(24)}$$

$$A_2e^{k_2a}+B_2e^{-k_2a}=A_3e^{ik_1a} \quad \text{...(25)}$$

$$A_2k_2e^{k_2a}-B_2k_2e^{-k_2a}=ik_1A_3e^{ik_1a} \quad \text{...(26)}$$

From eqns (25) and (26), we have

$$A_2=\tfrac{1}{2}A_3(1+ik_1/k_2)e^{(ik_1-k_2)a} \quad \text{...(27)}$$

and

$$B_2=\tfrac{1}{2}A_3(1-ik_1/k_2)e^{(ik_1+k_2)a} \quad \text{...(28)}$$

From eqns (23) and (24), we have

$$A_1=\tfrac{1}{2}A_2(1+k_2/ik_1)+\tfrac{1}{2}B_2(1-k_2/ik_1),$$

Substituting the values of A_2 and B_2, we have

$$A_1=\tfrac{1}{4}A_3(1+ik_1/k_2)(1+k_2/ik_1)e^{(ik_1-k_2)a}+\tfrac{1}{4}A_3(1-ik_1/k_2)(1-k_2/ik_1)e^{(ik_1+k_2)a} \quad \text{...(29)}$$

As velocity of alpha particle in I region is same as in III region. Hence transmistion probability of incident α-particle

$$T=\frac{\text{Transmitted flux}}{\text{Incident flux}}=\frac{|A_3|^2\times v}{|A_1|^2\times v}=\frac{|A_3|^2}{|A_1|^2} \quad \text{...(30)}$$

Since in practice $k_2a \gg 1$, hence first term of eqn (29) can be neglected in comparison to the second. Hence we have

$$\frac{|A_1|^2}{|A_3|^2}=\left(\frac{A_1}{A_3}\right)\left(\frac{A_1}{A_3}\right)^*=\frac{1}{16}\left(1-\frac{ik_1}{k_2}\right)\left(1+\frac{ik_1}{k_2}\right)\left(1-\frac{k_2}{ik_1}\right)\left(1+\frac{k_2}{ik_1}\right)e^{2k_2a}=\frac{(k_1^2+k_2^2)^2}{16\,k_1^2k_2^2}e^{+2k_2a}.$$

$$\therefore \text{ Transmissivity of the barrier } T=\frac{16\,k_1^2k_2^2}{(k_1^2+k_2^2)^2}e^{-2k_2a} \quad \text{...(31)}$$

When $2k_2a \gg 1$, the most important factor in this equation obviously is the exponential, which then will be extremely small. The factor in front of the exponential part is usually of the order of magnitude of unity (maximum value is four). For order of magnitude calculations we can, therefore, write

$$T=e^{-2k_2a}. \quad \text{...(32)}$$

This equation represents the fraction of the α-particles that will penetrate the barrier of width a and of height V ($>E$). If the potential is not constant in the region $0<r<a$, we can always approximate it with a series of small steps, each with a constant potential. As the total probability is the product of individual probabilities, hence we get a sum in exponent of the exponential. By making the intervals smaller and smaller, the sum goes over into an integral, so that we end up with

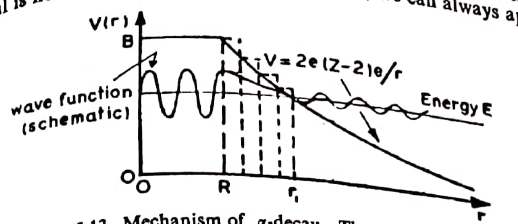

Fig. 5.13. Mechanism of α-decay. The wave function is large inside the well.

$$T=e^{-2\int k_2dr}. \quad \text{...(33)}$$

The integral is taken through the whole region between R and r_1, where the Coulomb repulsion $V(r)$ is greater than the energy E of an alpha particle. Substituting the value of k_2 in the above relation, we have

$$T=\exp.\left[-\frac{2\sqrt{(2m)}}{\hbar}\int_R^{r_1}[V(r)-E]^{1/2}\,dr\right]. \quad \text{...(34)}$$

Let us assume that an alpha particle moves inside the potential well with a certain velocity v_0 and hence hits the wall $v_0/2R$ times per second. Alpha-particle has the probability T of leaking out at each hit. Hence multiplication of frequency, with which the α-particle strikes the barrier, with escape probability T will give us decay constant λ, in $\sec^{-1}$ units.

$$\therefore\ \lambda=\frac{v_0}{2R}\exp.\left[-\frac{2\sqrt{(2m)}}{\hbar}\int_R^{r_1}[V(r)-E]^{1/2}\,dr\right]. \quad \text{...(35)}$$

Since the speed of an α-particle is of the order of 10^6 m/sec. and radius of the nucleus is about 10^{-14} m, hence the α-particle will find itself at the exterior surface of the nucleus 10^{20} times per sec. The actual values of λ vary from roughly $10^7\ \sec^{-1}$ for ThC′ to $10^{-18}\ \sec^{-1}$ for thorium. Hence the probabilityof escape ranges from 10^{-13} to 10^{-38}. Taking logarithm of eqn (35), we have

$$\log_e \lambda=\log_e \frac{v_0}{2R}-\frac{2\sqrt{(2m)}}{\hbar}\int_R^{r_1}[V(r)-E]^{1/2}\,dr$$

$$\log_e \lambda = \log_e \frac{v_0}{2R} - \frac{2\sqrt{(2mE)}}{\hbar} \int_R^{r_1} \left[\frac{2(Z-2)e^2}{4\pi\epsilon_0 r E} - 1 \right]^{1/2} dr \quad \ldots(36)$$

Since $E=2(Z-2)\, e^2/4\pi\epsilon_0 r_1$, hence upper limit of the integral $r_1=2(Z-2)\, e^2/4\pi\epsilon_0 E$. The integral may be simply determined by means of substitution

$$r=r_1 \cos^2 \psi \text{ and } R=r_1 \cos^2 \psi_0$$

we have

$$\log_e \lambda=\log_e \frac{v_0}{2R}+\frac{4\sqrt{(2mE)}}{\hbar} r_1 \int_{\psi_0}^{0} \sin^2 \psi d\psi$$

$$=\log_e \frac{v_0}{2R}+2\frac{\sqrt{(2mE)}}{\hbar} r_1[-\psi_0+\sin \psi_0 \cos \psi_0]$$

$$=\log_e \frac{v_0}{2R}-\frac{2\sqrt{(2mE)}}{\hbar} r_1 \left[\cos^{-1}\left(\frac{R}{r_1}\right)^{1/2} - \left(\frac{R}{r_1}\right)^{1/2}\left(1-\frac{R}{r_1}\right)^{1/2} \right]$$

Since $R \ll r_1$, hence we may write

$$\cos^{-1} (R/r_1)^{1/2} \approx \tfrac{1}{2}\pi-(R/r_1)^{1/2} \text{ and } (1-R/r)^{1/2}\approx 1.$$

$$\therefore \log_e \lambda=\log_e \frac{v_0}{2R}-\frac{2\sqrt{(2mE)}}{\hbar} r_1 \left[\frac{\pi}{2}-2\left(\frac{R}{r_1}\right)^{1/2}\right]$$

$$=\log_e \frac{v_0}{2R}+\frac{4e}{\hbar}\left(\frac{m}{\pi\epsilon_0}\right)^{1/2}(Z-2)^{1/2}\, R^{1/2}-\frac{e^2}{\hbar\epsilon_0}\left(\frac{m}{2}\right)^{1/2}(Z-2)\, E^{-1/2}$$

$$=\log_e \frac{v_0}{2R}+2.97 Z_D^{1/2}\, R^{1/2}-3.95 Z_D\, E^{-1/2}, \quad \ldots(37)$$

where E is in MeV, R is in units of 10^{-15} m, and Z_D $(=Z-2)$ is the atomic number of the residual nucleus. To compare the theory with observations more easily, we may take logarithms to the base 10 as

$$\log_{10} \lambda=\log_{10} (v_0/2R)+1.28(Z_D)^{1/2}\, R^{1/2}-1.71\, Z_D\, E^{-1/2}. \quad \ldots(38)$$

This is the theoretical expression of a phenomenon which Geiger-Nuttall had already demonstrated empirically. This may conveniently be compared with experiment. It can be done in two ways. One way is to substitute radii calculated from $R=R_0 A^{1/3}$ into the theory and make a theoretical plot, for various Z values, of log λ or log T against E. For various alpha emitters the experimental values of λ and E can then be entered on the graph and a comparison is made. The agreement for even-even nuclei is remarkably good. Because of the logarithmic nature of the scale, an error of a factor of 2 in frequency would only move the curve up or down by about 1 mm in this figure.

Another way to check the theory is to substitute experimental values of disintegration constant and energy into the theory and cal-

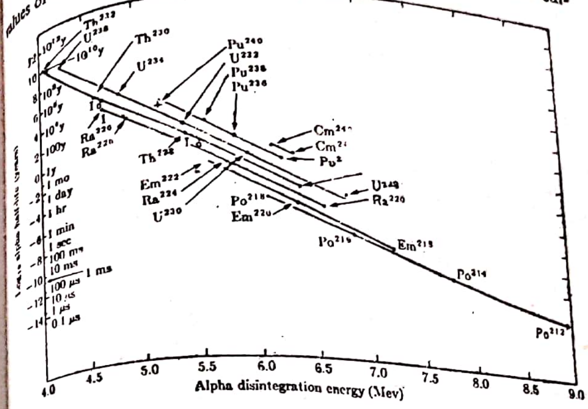

Fig. 5.14. Relationship between half life and α-disintegration energy for even-even alpha emitters.

culate the value of R_0, the effective radius of the nucleus for α-emission. Table 5.1 shows Kaplan's result for some even-even alpha emitters. Here we see that Po^{210} and Po^{208} exhibit smaller radii than normal. One may suspect here a failure of the hypothesis that the α-particle is performed before emission. Any lack of performability would tend to slow the decay process.

Table 5.1

Parent Nucleus	Disintegration energy MeV	$\log_{10} \lambda$	$r_0 \times 10^{-15}$ m
Cm^{242}	6.18	−7.282	1.55
Pu^{240}	5.20	−11.437	1.60
Pu^{236}	5.85	−8.090	1.56
U^{238}	4.25	−17.312	1.59
U^{232}	5.40	−9.504	1.57
U^{228}	6.83	−3.017	1.53
Th^{226}	6.41	−3.426	1.58
Po^{218}	6.12	−2.421	1.56
Po^{214}	7.83	−3.666	1.56
Po^{210}	5.40	−8.765	1.43
Po^{208}	5.24	−9.867	1.43

Hindrance Factors. The theory as presented above applies only to ground state decays between even-even nuclei, where α-particles have no internal angular momenta. If the decay takes place from an excited state of the parent or to an excited state of the daughter, an angular momentum change will generally be involved, and the

α-particle is emitted in a higher orbital angular momentum state ($l>0$). In this case, the centrifugal barrier term $l(l+1)\hbar/2mr^2$ must be added with the Coulomb barrier. The transition probability thus decreases due to this term.

The probability equation (34) thus can be written as

$$T_l = \exp\left[\frac{-2\sqrt{(2m)}}{\hbar}\int_R^{r_1}\left[\frac{2(Z-2)}{4\pi\epsilon_0 r}\frac{e^2}{} + \frac{l(l+1)\hbar^2}{2mr^2} - E\right]^{1/2} dr\right. \quad ...(39)$$

For large Z the influence of the centrifugal term is small compared to the Coulomb term, then the decay probability does not depend strongly on the quantum number l. Ratio of the α-emission probability of an α-particle with an angular momentum l to the emission probability with $l=0$, calculated for $Z_D=86$, $\frac{1}{2}M_\alpha v^2=4.88$ MeV and $R=9.87\times10^{-15}$ m is listed as :

l	0	1	2	3	4	5	6
λ_l/λ_0	1	0.7	0.37	0.137	0.037	0.0071	0.0011

The ratios of calculated (for even-even transitions) to observed transition probabilities are called *hindrance factors* and are larger than can be accounted for by inclusion of angular momentum effects in the theory.

Most probable even-even α-emissions go from ground state to ground state. In this type of transition, both the parent and the daughter nucleus will have zero angular momentum, the angular momentum of the ejected α-particle is zero and the parity does not change. In transitions to states other than the ground and first excited states (mostly $4^+, 6^+, 8^+$ states and few odd parity states) have hindrance factors ranging from unity to about 12000. Our striking feature is that the ground state transitions, specially for strongly deformed odd-A nuclei, are highly hindered even when there is no spin change involved, whereas some transitions to an excited state is usually almost unhindered. For example Am^{241} ($\frac{5}{2}^-$) to the ground and first excited states of Np^{237} ($\frac{5}{2}^+$ and $\frac{7}{2}^+$) have hindrance factors of the order of 500. Similarly, the transitions of the even-odd U^{235} to the ground and first excited states of Th^{231} are hindered by factors of about 1000.

The possible values of l for the outgoing α-particles are determined by the conservation laws of angular momentum and parity. The minimum value of l of the α-particle in the transition $C\to X+\alpha$ is determined by classifying transitions as :

Parity favoured $\Pi_C\,\Pi_X=(-1)^{I_C-I_X}$, $l_{min}=|I_C-I_X|$

Parity unfavoured $\Pi_C\,\Pi_X=(-1)^{I_C-I_X+1}$, $l_{min}=|I_C-I_X|+1$

provided I_C or $I_X\neq0$.

Alpha decays involving the ground states of even-even nuclei are presumably parity favoured with $I_C=I_X=0$. These decays

would be completely forbidden if $\Pi_C=-\Pi_X$. No such case has been found in the natural α-emitters. This suggests that *all even-even nuclei have not merely zero angular momentum but also have the same parity*.

Spontaneous Nuclear Disintegration. Spontaneous disintegration of a nucleus by α-decay is repressed by a low Gamow factor G ($=e^{-\gamma}$). The large values of Z and a for heavy nuclei tend to make γ so large that α-decay is prohibited. Let us take the example

$$Pb^{200}\to Hg^{196}+\alpha+3.3 \text{ MeV}. \quad ...(40)$$

Assuming the kinetic energy of the α-particle as equal to the Q-value of the reaction. We get, the thickness of the barrier a as

$$Q=2(Z-2)\,e^2/4\pi\epsilon_0 a.$$

$$\therefore \quad a = 69.8 \text{ fermi}.$$

This is very large in comparison to the nuclear radius $R=r_0A^{1/3}=8.13$ fermi. This large value of a corresponds to low transparency and high mean lifetime.

EXERCISES

Example 1. *Polonium-212 emits an α-particle of 8.776 MeV energy. Calculate the disintegration energy that corresponds to it and compare the α-particle energy inside the polonium nucleus to the barrier height for the α-particle.*

We know that the disintegration energy E is related with-particle energy E_α as :

$$E=E_\alpha\,[1+M_\alpha/M_R].$$

To a very close approximation we can replace the ratio of masses by the ratio of the mass numbers.

$$\therefore \quad E=E_\alpha\,[1+4/(A-4)]=E_\alpha\,A/(A-4)$$

$$=8.776\times212/208=8.945 \text{ MeV}.$$

Barrier height for an α-particle within the nucleus

$$=2Z_De^2/4\pi E_0R_0A^{1/3}$$

$$=\frac{2\times82\times(1.6021\times10^{-19})^2\times9\times10^9}{1.3\times10^{-15}\times(212)^{1/3}}$$

$$=30.51 \text{ MeV}.$$

Example 2. *What energy must be imparted to an α-particle to force it into the nucleus of bismuth? What energy will be required to obtain proton penetration to the same radius?*

The energy required to force an α-particle into the nucleus $=$Maximum height of the potential barrier$=Zze^2/4\pi\epsilon_0 r$. In our problem $Z=$Atomic number of target nucleus$=83$, z the atomic number very carefully oriented so that the magnetic field has cylindrical symmetry about the line joining the source and detector. The approximate expression for the focal length of a short magnetic lens for electrons of momentum *BRe* as obtained from elementary electron optics is given by

$$f=8(BR)^2/aB_0^2\pi, \qquad ...(15)$$

where B_0 is the axial field at the centre of the lens coil and a is the half width of the axial distribution.

6.3. THE NEUTRINO HYPOTHESIS

The continuous energy distribution of electrons in β-decay proved to be a great puzzle, although the maximum energy of the distribution corresponds to that expected from the mass difference of the parent and the daughter. There is also an apparent failure to conserve linear and angular momentum in β-decay. The emitted electron does not usually travel in a direction opposite to that of the product nucleus. In the process $C^{14} \rightarrow N^{14} + \beta^-$ the nuclear angular momenta of C^{14} and N^{14} are found to be 0 and 1 respectively. As the electron has an intrinsic spin of $\frac{1}{2}$, therefore, the angular momentum cannot be conserved during this transition. As far as the statistics are concerned, $N^{14}+\beta^-$ is a fermion and C^{14} is a boson.

All these difficulties were eliminated by Pauli in 1933 by assuming the existence of an additional particle. This hypothetical particle is called a *neutrino* (little neutral one). To preserve not only the principle of energy conservation but also the principle of conservation of electric charge and of angular momentum and the rules governing statistics, we must ascribe certain properties to the neutrino. Charge is already conserved by the disintegration electron in β decay hence *the neutrino has zero charge.* In β-decay the parent and daughter nuclei always have the same mass number. This requires that both have the same statistics and that their nuclear angular momenta may differ only by zero or an integer multiple of $h/2\pi$. As the β ray electron has Fermi-Dirac statistics and a spin of $\frac{1}{2}\hbar$, the neutrino *must also have Fermi-Dirac statistics* and an intrinsic spin of $\frac{1}{2}\hbar$ in order to conserve statistics and angular momentum. Since the neutrino has a spin $\frac{1}{2}$, it is expected to obey the Dirac theory. In addition to a neutrino, an *anti-particle*, called *anti-neutrino*, should also exist. Just as electron is a generic term used for positrons and negative electrons, *neutrino is a term often used generically for a neutrino or an antineutrino.* The neutrino and antineutrino are represented as ν and $\bar{\nu}$ respectively. The particle anti-particle relation assigns to the antineutrino the same mass, spin, charge and magnitude of magnetic moment as those of the neutrino. In all processes where a neutrino is emitted, an antineutrino can be absorbed with the same result and vice versa. As neutrinos have zero charge. Now question arises whether there are in fact two different neutrinos. A positive answer to this question seems to have been given by the requirements of a *doubly beta particle decay.* If ν and $\bar{\nu}$ are not identical, the double beta decay must be accompanied by the emission of two antineutrinos. The two particles in the neutrino pair cannot differ in charge, but it appears that they do differ in the relative directions of their spin vectors. *In the neutrino the spin and angular momentum vector are oppositely directed and in the antineutrino these vectors are aligned together.*

Since, a matter-antimatter pair is formed whenever energy is converted into mass, hence in a conversion of a nuclear neutron to a proton, the negative electron (a member of the matter) should accompany antineutrino (antimatter). Similarly neutrino is emitted with β^+ emission and orbita electron capture. Thus three types of β-decay are :

$$n \rightarrow p + e^- + \bar{\nu}$$
$$p \rightarrow n + e^+ + \nu$$
$$p + e^- \rightarrow n + \nu . \qquad \ldots(16)$$

The electron, neutrino and product nucleus share among them the energy, momentum and angular momentum available from the nuclear transitions. The β-particle gets maximum energy when the neutrino is emitted with zero momentum.

Two general procedures have been used to provide positive evidence for the supposition that neutrinos accompany beta-decay.

Indirect Method—In this method the neutrino energy can be determined in two ways. First by measuring the electron energy and subtracting it from the total energy available and second by measuring the momentum of an electron and of recoiling residual nucleus and using conservation of momentum to obtain the neutrino momentum and energy. Unfortunately this method requires measurement of both the nuclear recoil energy and its direction with respect to the electron momentum. Because of the small recoil energy both of these are very difficult measurements. In 1952, a more satisfactory method has been employed in which the recoil nucleus from *K*-electron capture is observed. Since the *K*-electron has negligible momentum, the momentum of the recoil nucleus will be equal to that of the neutrino

$$p_{re} = p_\nu (= E_\nu / c).$$

Hence the recoil energy $\qquad E_{re} = p_{re}^2/2M = (E_\nu/c)^2/2M, \qquad \ldots(17)$

where E_ν is the neutrino energy, c is the velocity of light and of neutrino, and M is the mass of recoiling nucleus.

Direct Method—It is based on the possibility of observing the results of its interaction with a proton. In this interaction mass, charge and spin are conserved as they are in the normal beta decay. However, theoretical calculations indicate that the probability of the interaction of neturino with a proton is very small. Thus for the detection of this rare interaction, number of neutrinos is expected to be extremely large. Experiments were performed at several places in United States, near the nuclear reactors. The idea of the experiment wasthat a neutrino entering the water would occasionally interact with a proton, producing a positron and a neutron $[p+\nu \rightarrow n+e^+]$. Within an extremely short time ($\sim 10^{-9}$ sec.) the positron will encounter an electron and then positron electron annihilation will occur. Thus two photons each carrying 0.51 MeV are emitted in opposite directions and so they should be detected by scintillations in coincidence in the detector tanks on each side of the target tanks. Neutron is captured by cadmium nucleus, 8 MeV of energy is released. This energy is divided among three or four gamma ray photons, which also produce scintillations. The electronic counting system associated with the photomultipliers is, therefore, designed, so that it will record only the production of scintillations separated by the appropriate time interval. The results showed that the delayed coincidences were due to neutrinos, the uncharged particles with probably no mass, but having a definite spin and capable of carrying off energy.

6.4. ENERGY HALF-LIFE RELATIONSHIPS

In 1933, B.W. Sargent found that when log λ was plotted against log E_{max} for the naturally occurring β-emitters, most of the points fell on or near two straight lines, as depicted in fig. 6.8. These lines, called *Sargent diagram* (or *curves*), represent empirical rules,

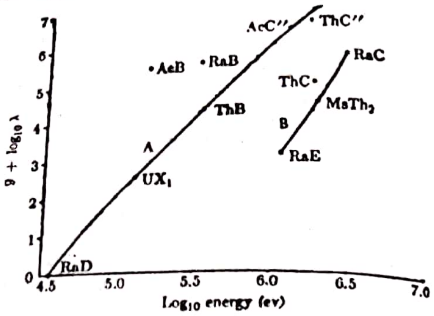

Fig. 6.8. Sargent curves.

analogous to the Geiger-Nuttall law in α-decay. The two curves do not correspond each to one radioactive series. For a given value of E_{max}, the upper curve gives a value of λ, which is about 100 times greater than corresponding value on the lower curve. The transitions in the short lived group are said to be *allowed*, the longer half-lives come from *forbidden transitions*, hence the *upper curve represents allowed transitions and the lower curve the forbidden transitions*. The transitions, are now said to be first, second,...or *n*-forbidden. As in α-decay, hindered would be a better term than forbidden, but the latter is now firmly established.

The degree of forbiddenness affects the shape of the β-particle spectrum as well as the half-life of the transitions. The forbidden transitions show a greater number of low energy particles than are seen in an allowed transitions, but in many cases the differences are not great.

Most of the beta decay cases obey the Gamow-Teller rules and some follow the Fermi rules. A few nuclei appear to require a mixture of two sets of rules. Favoured transitions are found only in light nuclei, $A < 44$. In most of these cases, parent and daughter are *mirror nuclei*. Favoured transitions occur in a very small group of three member isobars, each case consisting of a parent made up of two nucleons more than a core of even N=even Z. For example

$$_{9}F^{18} \rightarrow {}_{8}O^{18} + \beta^{+}. \qquad ...(18)$$

6. 5. FERMI THEORY OF BETA DECAY

In 1934, Fermi made a successful theory of beta decay based on Pauli's neutrino hypothesis. This theory is based on the following assumptions :

(1) The light particles, the electron and neutrino are created by the transformation of a neutron into a proton in a nucleus, or *vice versa*.

(2) The energy remains conserved in the decay process, the available energy being shared among the electron and the neutrino. Due to the larger mass product nucleus does not receive K.E.

(3) The neutrino has rest mass zero, or very small compared to that of the electron.

(4) The β-decay process is analogous to the emission of electromagnetic radiation by an atom, with the electron neutrino field acting in place of the electromagnetic field.

(5) Electron-neutrino field is weak in contrast to the short range strong interaction which exist between the nucleons bound in the nucleus.

(6) Time dependent perturbation theory is a very good approximation because of the smallness of coupling constants.

(7) No nuclear parity change occurs and higher order terms in R/λ can be neglected.

(8) As nucleons move with velocities of only $\sim c/10$ in nuclei, calculations can be made with non-relativistic nuclear wave functions.

Using Dirac's expression for the transition probability per unit time of an atomic system to emit photon, using time dependent perturbation theory, the probability that an electron of momentum between p_e and $p_e + dp_e$ is emitted per unit time may be written as

$$P(p_e)\, dp_e = \frac{2\pi}{\hbar} \left| H_{if} \right|^2 \frac{dN}{dE_0}, \qquad ...(19)$$

where dN/dE_0 is the number of quantum mechanical states of the final system per unit energy interval and H_{if} the *matrix element of the interaction* for the initial and final states.

Interaction Matrix Element—It is defined as

$$H_{if} = \int \Psi_f{}^* H \Psi_i \, d\tau, \qquad ...(20)$$

where Ψ_f and Ψ_i respectively are the wave functions of the system in its final state and in its initial state. H is the Hamiltonian operator that describes the weak interaction between the two states and $d\tau$ is the volume element.

For the negatron decay $n \rightarrow p + {}_{-1}e^0 + \bar{\nu}$, we have

$$\Psi_i = \psi \text{ (parent nucleus)} = \psi_i$$

$$\Psi'_f = \psi \text{ (daughter nucleus) } \psi \text{ (electron) } \psi \text{ (antineutrino)}$$

and

$$= \psi_f \, \psi_e \psi_{\bar{\nu}}.$$

We do not know the form of interaction operator H, but Fermi suggested a new constant, called as *Fermi coupling constant denoted by* g, which determines the strength of the interaction. This universal constant g has the value 0.9×10^{-4} *MeV* fm^3 and is analogous to the electron charge e in the photon decay theory. Moreover, the emission of a neutrino and the absorption of an anti-neutrino of opposite momentum are equivalent and we may replace $\psi_{\bar{\nu}}{}^*$ by ψ_ν to make the equations more symmetrical. Thus the matrix element is written as

$$H_{if} = g \int \left[\psi_f{}^* \psi_e{}^* \psi_\nu \right] M \psi_i d\tau. \qquad \text{...(21)}$$

where M is a dimensionless matrix element, which is an operator.

Since the neutrino interact weakly with nucleons, it is reasonable to use for the neutrinos a time independent wave function, which characterizes a free particle with the propagation constant $k = p_\nu/\hbar$, as

$$\psi_\nu = V^{-1/2} \exp. \left[-(i/\hbar) \, \mathbf{p}_\nu . \mathbf{r} \right]. \qquad \text{...(22)}$$

For high velocity electrons one may ignore the electrostatic effect of the nucleus upon the ejected electron and use the wave-function

$$\psi_e{}^* = V^{-1/2} \exp. \left[-(i/\hbar) \, \mathbf{p}_e . \mathbf{r} \right] \qquad \text{...(23)}$$

Here V is the whole volume in which we enclose the system for normalization purposes. $\mathbf{p}_\nu$ and $\mathbf{p}_e$ are the momenta of the neutrino and electron respectively and r is the position co-ordinate. Here we have neglected the spins, as the magnitudes of wave functions ψ_ν and ψ_e at the position of the nucleus are certainly much larger for S-wave neutrinos and electrons than for these particles with larger orbital angular momenta. By assuming the plane waveform for the wave function of the electron and neutrino, we have neglected their possible interactions with the nucleus.

Thus matrix element becomes

$$H_{if} = g \int \psi_f{}^* \frac{1}{V} \left\{ \exp. \left[-\frac{i}{\hbar} (\mathbf{p}_e + \mathbf{p}_\nu) . \mathbf{r} \right] \right\} M \psi_i d\tau. \qquad \text{...(24)}$$

The exponential factor can be written as

$$\exp. \left[-\frac{i}{\hbar} (\mathbf{p}_e + \mathbf{p}_\nu) . \mathbf{r} \right] = 1 - \frac{i}{\hbar} (\mathbf{p}_e + \mathbf{p}_\nu) . \mathbf{r} - \frac{1}{2\hbar^2} [(\mathbf{p}_e + \mathbf{p}_\nu) . \mathbf{r}]^2 + \qquad \text{...(25)}$$

Since the nuclear wave functions have appreciable values only in regions of the order of nuclear dimensions, the significant values of r are no greater than the nuclear radius R. If p_e and p_ν are both of the order of magnitude mc, as is usually the case, the exponent will be of the order of $2mcR/\hbar \simeq 1/50$. This small value suggests that we need to retain only the highest term, unity, in the power series. When this term is inserted into eqn (24) the matrix element is non-vanishing and is no longer dependent upon the energies or momenta of the light particles. This gives us the allowed transitions. Matrix elements of forbidden transitions will be energy dependent as they contain terms of the form $(\mathbf{p}_e + \mathbf{p}_\nu).\mathbf{r}$. Thus for allowed transitions eqn (24) can be written as

$$H_{if} = \frac{g}{V} \int \psi_f{}^* M \psi_i d\tau = \frac{g}{V} \left| M_{if} \right|. \qquad \text{...(26)}$$

where $|M_{if}|$ is the overlap integral or the nuclear matrix element of the final and initial wave functions of the nucleus. This can only be computed in a few cases where the structure of the nuclei is reasonably well known.

Statistical Factor (*Final State Density*) dN/dE_0— The position and momentum of electron or neutrino can be represented by a point in phase space, *the space containing three spatial and three momentum dimensions.* We now assert that the uncertainty principle prevents us from representing a moving particle by a single vector. This is because such a representation would amount to specifying both the position and the momentum exactly. Thus phase space must be divided into cells of volume

$$\Delta x . \Delta y . \Delta z . \Delta p_x . \Delta p_y . \Delta p_z \approx h^3.$$

The state of a system cannot be specified more closely than by saying that the tip of the vector representing it lies in one of these cells. The states available to a free particle are distributed uniformly in phase space with a density h^{-3}. Thus the number of states of a particle restricted to a volume V in actual space and whose momentum lies between the limits p and $p+dp$ is given by

$$dN = V \times 4\pi p^2 \, dp / h^3. \qquad \text{...(27)}$$

The number of states corresponding to the appearance in volume V of the electron with the momentum in the range p_e to $p_e + dp_e$ is

$$dN_e = 4\pi V p_e{}^2 \, dp_e / h^3.$$

Similarly $\quad dN_\nu = 4\pi V p_\nu{}^2 \, dp_\nu / h^3.$

As electron and neutrino are independent of one another, hence the number of states available to them jointly is given by

$$dN = (4\pi V p_e{}^2 \, dp_e / h^3)(4\pi V p_\nu{}^2 \, dp_\nu / h^3). \qquad \text{...(28)}$$

The number of states per unit energy of the electron is

$$\frac{dN}{dE_0} = \frac{16\pi^2 V^2}{h^6} \, p_e{}^2 p_\nu{}^2 \, dp_e \, \frac{dp_\nu}{dE_0}. \qquad \text{...(29)}$$

The total available energy

$$E_0 = E_\nu + E_e. \qquad \text{...(30)}$$

For a fixed electron energy E_e, we have

$$dE_0 = dE_\nu. \qquad \ldots(31)$$

The momenta p_e and p_ν are related to the electron and neutrino energy respectively by the equations

$$E_e^2 = p_e^2c^2 + m^2c^4 \text{ and } E_\nu = cp_\nu \text{ (Assuming zero rest mass)} \qquad \ldots(32)$$

$$dE_\nu = c\, dp_\nu. \qquad \ldots(33)$$

Using eqns (30), (31), (32) and (33) in eqn (29), we have

$$\frac{dN}{dE_0} = \frac{16\pi^2V^2}{h^6}\, p_e^2 \left(\frac{E_0 - E_e}{c}\right)^2 dp_e \cdot \frac{1}{c}.$$

Inserting this statistical factor and H_{if} from equation (25) into equation (19) we get the probability

$$P(p_e)\, dp_e = \frac{2\pi}{\hbar}\frac{g^2}{V^2}\, |M_{if}|^2 \cdot \frac{16\pi^2V^2}{c^3h^6}\, p_e^2 (E_0 - E_e)^2\, dp_e$$

$$= \frac{g^2 |M_{if}|^2}{2\pi^3c^3\hbar^7} (E_0 - E_e)^2\, p_e^2\, dp_e. \qquad \ldots(34)$$

This equation can also be written as

$$P(W_e)dW_e = \frac{G^2}{2\pi^3} \mid M_{if}|^2 p_e\, W_e (W_0 - W_e)^2\, dW_e, \qquad \ldots(35)$$

where W_e and W_0 are the energies in units of m_ec^2 and are defined as

$$W_e = E_e/m_ec^2 \text{ and } W_0 = E_0/m_ec^2 \qquad \ldots(36)$$

and

$$G^2 = (m_e^5c^4/\hbar^7)g^2. \qquad \ldots(37)$$

Coulomb Correction. In the derivation of above relation no account has been taken of the coulomb interaction which can be neglected only for the lightest nuclei ($Z < 10$) and sufficiently high electron energies. If this restriction is relaxed the plane wave for the emitted electrons must be replaced by a distorted coulomb wave function. This can be taken into account by multiplying $|\psi_e|^2$ with a factor sometimes called *coulomb factor*, $F(Z, E_e)$, also called *Fermi function*. It is thus the ratio of the electron density at the daughter nucleus to the density at infinity, *i.e.*

$$F(Z, E_e) = |\psi_e(0)|^2_{coulomb} / |\psi_e(0)|^2_{free}. \qquad \ldots(38)$$

In a non-relativistic approximation, it has the value

$$F(Z, E_e) = 2\pi\eta/(1 - e^{-2\pi\eta}), \qquad \ldots(39)$$

where $\eta = Ze^2/4\pi\epsilon_0\hbar\nu$ for electrons, $\eta = -Ze^2/4\pi\epsilon_0\hbar\nu$ for positrons, Z the atomic number of the *product* nucleus and ν being the velocity of electron at a great distance from the nucleus. When consideration is given to this effect, equation (34) becomes

$$P(p_e)\, dp_e = \frac{g^2|M_{if}|^2}{2\pi^3c^3\hbar^7} F(Z, E_e)(E_0 - E_e)^2 p_e^2\, dp_e$$

$$= C^2F(Z, E_e)(E_0 - E_e)^2 p_e^2\, dp_e, \qquad \ldots(40)$$

where

$$C = g \mid M_{if} \mid (2\pi^3c^3\hbar^7)^{-1/2}. \qquad \ldots(41)$$

The behaviour of β-spectrum at very low electron or positron energies can be obtained directly from above relation. The coulomb correction enhances the probability of electron emission and decreases the probability of positron emission, especially at low energies. The Coulomb force loses its effect on the spectrum shape at high energies and spectrum approaches that computed without the Coulomb correction. This can be explained in the following way : The Coulomb field accelerates the positive electron and decelerates the negative electron. Hence the positron spectrum has fewer slow particles and electron spectrum more slow particles, than they would have in the absence of the Coulomb correction.

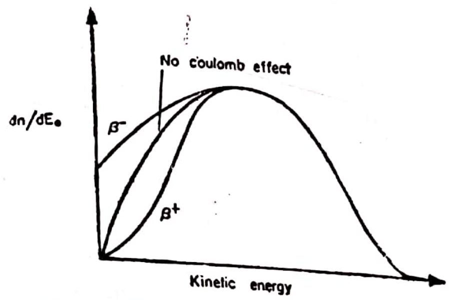

Fig. 6.9. Theoretical β-energy spectrum (Fermi theory)

Classically, no positron would be expected to emerge below the barrier energy $Ze^2/4\pi\epsilon_0R$. The actual spectrum does contain some low energy positrons, as a result of the tunnel effect. The relation is identical to that for α-decay, as for low energy β^+-emission.

$$F(Z, E_e) = -\frac{2\pi Ze^2}{4\pi\epsilon_0\hbar\nu}\, \frac{1}{1 - e^{2\pi Ze^2/4\pi\epsilon_0\hbar\nu}}$$

$$\simeq \frac{Ze^2}{2\epsilon_0\hbar\nu}\, e^{-Ze^2/2\epsilon_0\hbar\nu}. \qquad \ldots(42)$$

Screening by Atomic Electrons. In addition to the nuclear coulomb effect the electrostatic potential of the atomic electrons affects the shape of the β-spectra. Reitz has tabulated and found corrections from 1.5 to 400 keV. This effect reduces the probability of β^--emission by about 2% for a 50 keV β^--ray at $Z \sim 50$. The correction increases as Z increases or as β^--ray energy decreases. This effect is more important for β^+-ray as it reduces the height and thickness of the potential barrier. The probability of β^+-emission is increased by about 37% at $Z \sim 50$ for a 50 keV β^+-rays. Thus the atomic electrons exert very little effect on β^--spectra but affect considerably the emission of low energy (<100 keV) β^+-rays, especially in heavy elements.

Allowed Spectra, β^+/β^- Ratio. Assuming the screening by atomic electrons as negligible, the ratio of positron to electron decay can be obtained by eqn. (40) for the same momentum interval p_e and $p_e + dp_e$, as

$$\frac{P_+(p_e)\,dp_e}{P_-(p_e)\,dp_e} = \frac{|M_{if}|^2_+ F_+(Z, E_e)(E_0 - E_e)^2_+}{|M_{if}|^2_- F_-(Z, E_e)(E_0 - E_e)^2_-}$$

This ratio is dominated by the exponential term in $F(Z, E_e)$ while all other energy dependent terms nearly cancel, hence

$$\frac{P_+(p_e)}{P_-(p_e)} \simeq \frac{e^{-(Z-1)e^2/2\epsilon_0\hbar v}}{e^{(Z+1)e^2/2\epsilon_0\hbar v}}$$

$$\simeq e^{-2Ze^2/2\epsilon_0\hbar v}.$$

Wu and Albert, using Cu^{64} source, found that the experimental and theoretical curves between log $[P_+(p_e)/P_-(p_e)$ and $2Ze^2/2\epsilon_0\hbar v$ were in excellent agreement. This was the best test for the Fermi theory in the light of β-ray spectra.

Kurie Plots. A more convenient way of plotting the experimental results and checking with the theory was suggested in 1936 by Kurie. Equation (40) can be written as

$$\sqrt{[P(p_e)/F(Z, E_e)\, p_e^2]} = C(E_0 - E_e) = C(T_0 - T_e), \qquad \ldots(43)$$

where T_0 and T_e are kinetic energies. A plot of the function on the left hand side of above equation against T_e should be a straight line intersecting the energy axis at T_0. This graph is known as *Kurie plot*. This provides a good means of determining the maximum energy of the β-spectrum. Maximum energies of electron and positron, obtained by Kurie plots are 571 and 657 keV respectively for β-rays emitted from Cu^{64}.

Many of the early Kurie plots were non-linear at low electron energies. The deviations at the low energy side are probably instrumental, caused by electron scattering and source due to the energy loss in the source material. If we take into account a relativistic mass correction term for the neutrino, then we see that Fermi plot near the end point energy is not a straight line but turns sharply to intersect the energy axis at a point smaller than the value for zero mass neutrino.

Mass of the Neutrino. The rest mass of neutrino can be measured with the help of Fermi-theory. Taking into account a relativistic mass correction term for the neutrino, the momentum distribution can be written as

$$P(p_e)\,dp_e = C^2 F(Z, E_e)\, p_e^2\,(E_0 - E_e + m_\nu)\,[(E_0 - E_e + m_\nu)^2 - m_\nu^2]^{1/2} \left[1 \mp \frac{m_\nu}{E_e(E_0 - E_e + m_\nu)}\right] dp_e \qquad \ldots(44)$$

This reduces to equation (40) for $m_\nu = 0$. A great many experiments have been carried on the β-spectrum of H^3. Langer and Moffat obtained a Fermi plot that is linear down to about 4 keV. Fig. 6.10 shows four curves, theoretical plots of eqn (44) for assumed neutrino rest energies of 0, 250, 500 and 1000 eV. Comparing

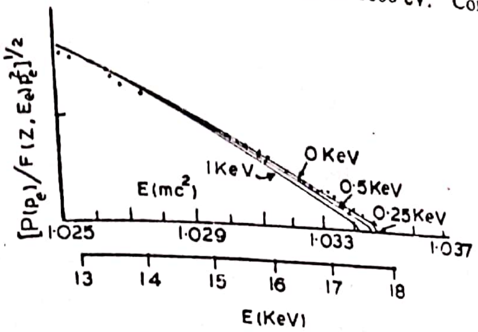

Fig. 6.10. Fermi plot of H^3.

with experimental curve, they proposed a possible upper limit of 250 eV for the rest mass of neutrino. It is about 0.05% of the electron rest mass and can thus be assumed as zero.

Life time of β-decay. Equation (40) gives the probability per second for the emission of an electron with the momentum p_e and $p_e + dp_e$. The total probability per second, λ, for beta disintegration can be computed from this by integrating over all values of the electron momentum from 0 to p_{max}.

$$\lambda = \frac{\log_e 2}{t_{1/2}} = \int_0^{p_{max}} P(p_e)\,dp_e$$

$$= \frac{g^2|M_{if}|^2 m^5c^4}{2\pi^3\hbar^7} \int_0^{p_{max}/mc} F(Z, E_e)\,\frac{p_e^2}{m^2c^2}\,\frac{(E_0 - E_e)^2}{m^2c^4}\,\frac{dp_e}{mc}$$

$$= \frac{g^2|M_{if}|^2 m^5c^4}{2\pi^3\hbar^7}\, f. \qquad \ldots(45)$$

If $E_0 \gg mc^2$ or $p_{max} \gg mc$ and $F(Z, E_e) \sim 1$, f varies roughly as E_0^5. This E_0^5 dependence connecting λ and E_0 was first noticed by Sargent in 1933, and is known as the *fifth power law* and is obeyed in some cases, particularly by the positron spectra of light nuclei. For heavy nuclei the distortion due to the coulomb field is more effective and there is no simple analytical expression for f. The *comparative half life* of a beta unstable nuclide is defined as $ft_{1/2}$, usually written as ft. The product ft depends solely upon the nuclear matrix element, as

$$ft=\frac{2\pi^3\hbar^7 \log_e 2}{g^2 m^5 c^4 \mid M_{if} \mid^2}=\frac{0.693\ \tau_0}{\mid M_{if} \mid^2}, \qquad \ldots(46)$$

where τ_0 is a new natural constant, known as *universal time constant*. This equation shows that the comparative half-life is proportional to the inverse square of the matrix element, which depends on the nuclear structure. Since it is usually a large number, it has been found more convenient to use its logarithm, *i.e.*, *log ft*. The greater the value of *ft*, the longer is the comparative half-life and smaller the probability of the radioactive change.

The beta-decay of O^{14} is of special interest as it involves a $0 \to 0$ transition. Knowing the parameters

$t_{1/2}=72.5$ sec, $E_0=T_0+mc^2=1.81$ MeV$+mc^2$, $f(Z, E_0)=42.8$,

we get,

$$g=1.410\times 10^{-62} \text{ joule m}^3=0.9\times 10^{-4} \text{ MeV } fm^3.$$

Selection Rules. The above theory is applicable when the electron and neutrino carry away no orbital angular momentum while leaving nucleus. In fact, if electron and neutrino are emitted with their intrinsic spins antiparallel (*singlet state*), the change in nuclear spin ΔI must be strictly zero, if these are emitted with their spins parallel (*triplet state*), ΔI may be $+1$, 0, or -1 (but no $I_i=0$ to $I_f=0$). The former selection rule was one originally proposed by *Fermi*, the latter was subsequently suggested by *Gamow and Teller*. In both types of allowed transitions orbital angular momentum and parity are left unchanged. The interactions that give rise to Fermi and Gamow Teller selection rules are different. Experiment shows that the allowed transitions of the type $\Delta I=1$, obeying $G-T$ selection rule, are forbidden by *F*-selection rule, as in the decay

$$He^6 \to Li^6 + e^- + \bar{\nu} \qquad (0^+ \to 1^+)$$

There are also allowed transitions of the $0 \to 0$ type that are allowed by *F*-selection rules but forbidden by *G-T* selection rules, as in the decay

$$O^{14} \to N^{14*} + e^+ + \nu. \qquad (0^+ \to 0^+)$$

The ground state of N^{14} has a spin 1, however 2.31 MeV excited state N^{14*} has a spin *O*.

However, many transitions are allowed by both selection rules. This is always possible in the allowed decays in which $I_i=I_f\neq 0$, where subscripts *i* and *f* refer to the initial and final nuclear states. The examples are

$$n \to p + e^- + \bar{\nu} \qquad (\tfrac{1}{2}^+ \to \tfrac{1}{2}^+)$$
$$H^3 \to He^3 + e^- + \bar{\nu} \qquad (\tfrac{1}{2}^+ \to \tfrac{1}{2}^+)$$
$$S^{35} \to Cl^{35} + e^- + \bar{\nu} \qquad (\tfrac{3}{2}^+ \to \tfrac{3}{2}^+)$$

These allowed transitions are further classified as *favoured super allowed) and unfavoured transitions.* The allowed transition is

said to be favoured if the nucleon which changes its charge remains in the same level, it is unfavoured if the nucleon changes its level. Most of the allowed β-transitions are unfavoured. For the β^--decay, the change of a neutron into a proton without the change of level would increase the total energy of the nucleus and would, therefore, not lead to a spontaneous decay. For the β^+-decay, the surplus of neutrons makes the allowed transitions unfavoured. There are few exceptions, *e.g.*,

$$He^6 \to Li^6,\ H^3 \to He^3,\ C^{11} \to B^{11} \text{ and } F^{18} \to O^{18}.$$

The conditions for super-allowed transitions are same as that for allowed transitions. The matrix element is also energy independent. The main difference between the two cases is that the allowed transitions are not between mirror nuclei.

Let us now consider what happens when the transition from initial to final nucleus does not take place by the emission of *S*-wave electron and neutrino. Because of the finite size of the nucleus, the electron and neutrino emission with orbital angular momenta other than zero is also possible. The magnitudes of the wave functions ψ_e & ψ_ν for *p*-wave, *d*-wave, etc., over the nuclear volume decrease rapidly with increasing orbital angular momentum. β-transitions with angular momentum, carried off by the two light particles together, $l_\beta=1$, 2, 3, etc., are classified as first, second, third, etc., *forbidden transitions.*

If l_β is odd, initial and final nucleus must have opposite parities (*parity changes in this transitions*) ; for even l_β values the initial and final nucleus must have same parity (*no change in parity*). Furthermore, as in allowed transitions, the emission of leptons (electron and neutrino) in the singlet state (Fermi-selection rule) requires $\Delta I \leqslant l_\beta$, whereas triplet-state (*G-T* selection rule) emission requires $\Delta I \leqslant l_\beta+1$. Thus selection rules for forbidden transitions are :

First forbidden—For these transitions $l_\beta=1$ and parity changes.

Fermi-selection rules : $\Delta I=\pm 1, 0$ (except $0 \to 0$).

Gamow Teller rules : $\Delta I=\pm 2, \pm 1, 0$ (except $0\to 0$, $\tfrac{1}{2}\to\tfrac{1}{2}$, $0 \longleftrightarrow 1$)

The examples are :

$Kr^{87} \to Rb^{87} + \beta^-$	$(5/2 \to 3/2)$
$Ag^{111} \to Cd^{111} + \beta^-$	$(1/2 \to 1/2)$
$Ce^{141} \to Pr^{141} + \beta^-$	$(7/2 \to 5/2)$
$S^{37} \to Cl^{37} + \beta^-$	$(7/2 \to 3/2)$
$Kr^{85} \to Rb^{85} + \beta^-$	$(9/2 \to 5/2)$
$Cs^{137} \to Ba^{137*} + \beta^-$	$(7/2 \to 11/2)$

Second forbidden. For these transitions $l_\beta=2$ and no change in parity.

Fermi-selection rules : $\Delta I=\pm 2, \pm 1$ (except $0 \longleftrightarrow 1$)

Gamow Teller rules : $\Delta I=\pm 3, \pm 2, 0 \to 0$ (except $0 \longleftrightarrow 2$)

The examples are :

$Cs^{135} \to Ba^{135} + \beta^-$	$(7/2 \to 3/2)$
$Be^{10} \to B^{10} + \beta^-$	$(0 \to 3)$
$Na^{22} \to Ne^{22} + \beta^+.$	$(3 \to 0)$

Similarly for third, fourth and so on forbidden we have :

Third forbidden: $Rb^{87} \rightarrow Sr^{87} + \beta^{-}$ (3/2 → 9/2) change in parity

Fourth forbidden: $In^{115} \rightarrow Sn^{115} + \beta^{-}$(9/2→1/2) no change in parity

n^{th} *forbidden* : Fermi-selection rule $\Delta I = \pm n, \pm(n-1)$

Parity changes for n odd

G.T. selection rules $\Delta I = \pm n, \pm(n+1)$

Parity does not change for n even.

The allowed and forbidden nature of the transitions is often determined from the ft value, which depends upon the atomic number, the end point energy and half-life period. ft values threw light on nuclear matrix elements. as it varies inversely as the squaor of the matrix element.

The smallest values of ft are found for a group of light nuclei for which $\log ft = 2.7$ to 3.7. The transformations of this group are described as *favoured allowed transitions.* Another group of nuclides is found for which $\log ft = 4$ to 5.8. The transformations are described as *normal (or unfavoured) allowed transitions.* The first forbidden transitions have ft about 1000 times bigger. The rough classification into categories according to ft value is shown in Table 6·1.

Table 6·1. Classification of β-Transitions,

$\log_{10} ft = 2.7 \sim 3.7$	Super-allowed
$\log_{10} ft = 4 \sim 5.8$	allowed
$\log_{10} ft = 6 \sim 10$	for first forbidden
$\log_{10} ft = 10 \sim 14$	,, second ,,
$\log_{10} ft = 14 \sim 17$	,, third ,,
$\log_{10} ft = 17 \sim 24$	,, fourth ,,

To explain forbidden transitions the use is made of Hamiltonian as sum of five terms,

$$H = H_S + H_V + H_T + H_A + H_P,$$

where S, V, T, A and P stand for scalar, vector, tensor, axial-vector and pseudoscalar. These involve characteristic coupling constants g_S, g_V, g_T, g_A and g_P respectively. In Fermi-transitions the two possible modes of decay go via the scalar and vector interactions. In Gamow-Teller transitions the interactions are tensor and axial vector. There is no support of any pseudoscalar transitions. The difference in the effects of the four types of interaction is predicted by angular correlation between the directions of β^{-} and ν. The angular correlation coefficient a can be obtained by using relativistic quantum mechanics. For a pure Fermi-transition

$$a = \frac{|g_V|^2 + |g'_V|^2 - |g_S|^2 - |g'_S|^2}{|g_V|^2 + |g'_V|^2 + |g_S|^2 + |g'_S|^2} \qquad \text{...(47)}$$

and for a pure G-T transition

$$a = \frac{1}{3} \frac{|g_T|^2 + |g'_T|^2 - |g_A|^2 - |g'_A|^2}{|g_T|^2 + |g'_T|^2 + |g_A|^2 + |g'_A|^2}, \qquad \text{...(48)}$$

where primed and unprimed constants respectively represent the relative strengths of the parity non-conserving and the parity conserving interactions. For allowed transitions, parity conservation is valid, hence primed constants are zero and therefore,

$$a_S = -1,\ a_V = 1,\ a_T = \frac{1}{3} \text{ and } a_A = -\frac{1}{3}.$$

$$|M_{if}|^2 = \tfrac{1}{2}\{|g_S|^2 + |g'_S|^2 + |g_V|^2 + |g'_V|^2\}|M_F|^2 + \tfrac{1}{2}\{+|g_T|^2 + |g'_T|^2 + |g_A|^2 + |g'_A|^2\}|M_{GT}|^2 .$$

The nucleus matrix element for the allowed transitions can be written as

$$|M_{if}|^2 = |C_F|^2 |M_F|^2 + |C_{GT}|^2 |M_{GT}|^2, \qquad \text{...(49)}$$

where M_F and M_{GT} are integrals over nuclear wave functions for Fermi and Gamow-Teller interactions. Thus eqn (46) can be written as

$$ft = \frac{B}{(1-x)|M_F|^2 + x|M_{GT}|^2}, \qquad \text{...(50)}$$

where $$B = \frac{2\pi^3 \hbar^7 \log_e 2}{g^2 m^5 c^4} \cdot \frac{1}{|C_F|^2 + |C_{GT}|^2},$$

and $$x = \frac{|C_{GT}|^2}{|C_F|^2 + |C_{GT}|^2}.$$

The constants in eqn (50) can be obtained from experimental results on nuclei such as n, H^3, He^6, O^{14}, for which M_F and M_{GT} are known because of the simple nuclear structure. These results give the value of g and the ratio C_{GT}/C_F.

Corrected matrix element is given by

$$a|M_{if}|^2 = \tfrac{1}{2}\{|g_V|^2 + |g'_V|^2 - |g_S|^2 - |g'_S|^2\}|M_F|^2 + \tfrac{1}{6}\{|g_T|^2 + |g'_T|^2 - |g_A|^2 - |g'_A|^2\}|M_{GT}|^2$$

For a pure Fermi Transition, a is found unity experimentally. $|g_S| = |g'_S| = 0$ and $g_V = g'_V$. Knowing the matrix element and determining ft, Bardin found for $0^+ \rightarrow 0^+$ transition $g_V = (1.4025 \pm 0.0022) \times 10^{-62}$ joule m^3.

Since the transition probability is proportional to $|H_{if}|^2 \sim |\psi_e \psi_\nu|^2$ and $\psi_e \psi_\nu \propto \exp[-i(\mathbf{k}_e + \mathbf{k}_\nu).\mathbf{r}]$. The power expansion shows that the first term generates the allowed transition matrix element and the successive terms refer to forbidden transitions of increasing order. As $kR \simeq 1/10$, hence the probability of p-wave emission is reduced by a factor of $(KR)^2 \simeq 1/100$ in comparison with s-wave emission. The term $(k_e + k_\nu)$ gives rise to a momentum or energy dependence $|k_e + k_\nu|^2 \sim k_e^2 + k_\nu^2$. Hence the correction to eqn (43) for first forbidden transition is

$$a_1 = [p_e^2 + p_\nu^2]/(mc)^2. \qquad \text{...(51)}$$

For second forbidden transition, exponential term is $(kR)^2$, hence $(kR)^4 \simeq 10^{-4}$ and the energy dependent contribution

$$|(k_e+k_\nu)^2|^2 \simeq |k_e+k_\nu|^4 \sim k_e^4+k_\nu^4+\tfrac{10}{3}k_e^2k_\nu^2$$

and the correction to eqn (43) for second forbidden transition is

$$a_2=[p_e^4+p_\nu^4+\tfrac{10}{3}\,p_e^2p_\nu^2]/(mc)^4. \qquad \ldots(52)$$

Similarly for third forbidden transitions the correction term is

$$a_3=[p_e^6+p_\nu^6+7p_e^2p_\nu^2(p_e^2+p_\nu^2)]/(mc)^6. \qquad \ldots(53)$$

To obtain ft values from measured decay energies and half-lives, it is convenient to use either the extensive graphs of log f verses E_0 and Z published by Feenberg and Trigg or the monograph of ft, half-life and E given by Moszkowski. One can use approximate expressions.

$$\log_{10} f_{\beta^-}=4.0\log_{10} E_0+0.78+0.02Z-0.005\,(Z-1)\log_{10} E_0$$

$$\log_{10} f_{\beta^+}=4.0\log_{10} E_0+0.79+0.007Z-0.009\,(Z+1)\,(\log_{10} E_0/3)^2,$$

where E_0 is the K.E. in MeV and Z is the atomic number of the product nuclide.

7

Gamma Radiation

7.1. INTRODUCTION

A third type of radiation which could not be deflected in a magnetic field, but which nevertheless had considerable penetrating power and a marked effect on a photographic plate, was discovered in 1900 by P. Villard in France. These radiations are now called γ-rays. Gamma rays, like X-rays and light rays, are electromagnetic radiations, but of shorter wavelengths. Actually it is difficult to distinguish between the longest gamma rays and the shortest X-rays. Main difference in their behaviour is that the X-rays result from transitions between electronic energy levels while gamma rays are associated with transitions between nuclear energy levels.

The transition from one nuclear state to another of lower energy state by virtue of the electromagnetic field may proceed by one of the three distinct processes ; *gamma ray emission*, *internal conversion and internal pair creation*. Electromagnetic radiation also appears in other nuclear transitions, especially those in which charged particles are emitted. The information concerning nuclear properties, obtained from observations of electromagnetic transitions, fall into three main categories :

(*a*) The gamma ray energies or the energies of internal conversion electrons determine the energies of the transitions, which give the energy differences between nuclear levels.

(*b*) The geometrical properties of the electromagnetic transition field, *i.e.*, the angular and radial distribution of its intensity and polarization with respect to a nuclear axis give information concerning the spins and parities of the nuclear states involved.

(*c*) The results, especially, for magnetic multipoles support the view that the radiation is due to the charge and magnetic moments of protons and neutrons in the nucleus rather than due to the quanta of the nuclear force field. Except in some isolated instances, there is little evidence of the predominance of a single "radiating particle". In some cases of electric quardrupole transitions, the large transition rates indicate that many particles must contribute to the radiating system.

There are two categories of gamma sources, useful in nuclear spectroscopy :

(*a*) Gamma rays produced by electrons in targets of X-ray tubes, betatrons, linear accelerators, synchrotrons, etc. Gamma-rays, produced in this way, appear in a continuous energy spectrum.

(*b*) Gamma rays from excited nuclear states, either prompt in (n, γ), (p, γ), etc., reactions or delayed by belonging to an isometric transition or appearing as prompt radiation following beta or alpha decay of relatively long half-life.

Intense sources of gamma rays or higher energies are available from machine production. Gamma ray energies from few keV upto 20 MeV can be found among the prompt decay and upto 5 MeV in the case of delayed emission.

A very large variety of effects has been used for the quantitative detection of gamma radiation, *e.g.*, *conductivity of gases, liquids and solids, fluorescence and phosphorescence, blackening of photographic emulsions, discolouration of transparent solids, changes in elastic constants of piezoelectric crystals, formation of tracks in cloud chambers by secondary electrons, etc.* The proportional counters, G.M. Counters and scintillation counters are used in most of the experiments. In all these counters gamma rays are detected by the secondary electrons they produce. We have discussed these counters in chapter 4.

to the strength of the sources and boundary conditions.

Selection Rules. The selection rules for emission of electric or magnetic multipole radiation may be obtained from the angular momentum and parity of the field. Since one quantum in the mode L, M carries an angular momentum $\sqrt{[L(L+1)]}$ and z-component M (both measured in units of $\hbar$), radiation of multipolarity L, M must remove from the nucleus a total angular momentum exactly equal to $\sqrt{[L(L+1)]}$ with z-component M. If this quantum is emitted by a nucleus in going from the state Ψ_a to state Ψ_b, the vector difference between the angular momenta $\mathbf{J}_a$ of the initial state and $\mathbf{J}_b$ of the final state must be $\sqrt{[L(L+1)]}$ and the z-component must change by $\Delta m_J = -M$. Thus we see that transitions by emission of single multipole quantum are possible only between states of total angular momentum J_a and J_b if

$$\mathbf{J}_a - \mathbf{J}_b = \mathbf{L} \quad \text{or} \quad |J_a - J_b| \leqslant L \leqslant J_a + J_b \qquad \text{...(24)}$$

and

$$m_{J_a} - m_{J_b} = M. \qquad \text{...(25)}$$

For even values of L, the spherical harmonic function is even, therefore, the product of Ψ_b and Ψ_a must be even. For odd values of L, the product of Ψ_b and Ψ_a must be odd. The multipole order is expressed through the rank L, *e.g.*, radiation represented by the rank L has multipolarity 2^L. Thus $L=1$ is called dipole radiation, $L=2$ is quadrupole, etc. For each multipole order both *electric* and *magnetic* waves are possible. For each value of L, the electric and magnetic radiations have the same angular momentum but differing parity. The parity of an electric multipole is the same as that of a material particle having the same L, *i.e.*, it is even when L is even and is odd if L is odd. Magnetic multipole radiation has the opposite parity, *i e.* odd when L is even and even when L is odd. We, therefore, get the following rules for the combination of parities of the initial and final states.

$$\Pi_a\Pi_b=(-1)^L \text{ (in electric multipole transition)} \qquad ...(26)$$

$$\Pi_a\Pi_b=-(-1)^L \text{ (in magnetic multipole transition).} \qquad ...(27)$$

Since there does not exist any multipole radiation with $L=0$, relation (24) shows that *radiative transitions between two states with* $J_a=J_b=0$ *are completely forbidden by single quantum emission.* The emission of electric dipole radiation ($L=1$) is connected with a change of parity of the nucleus, while the emission of magnetic dipole radiation is possible only if the parity does not change. The rules given above for the angular momentum and parity changes resulting from a transition of a given multipolarity are summarized in Table 7.1.

Table 7.1. Selection Rules for γ-radiation

Type	Symbol	Change in Angular momentum	Parity change
Electric dipole	E_1	1	Yes
Magnetic dipole	M_1	1	No
Electric quadrupole	E_2	2	No
Magnetic quadrupole	M_2	2	Yes
Electric octupole	E_3	3	Yes
Magnetic octupole	M_3	3	No
Electric 2^L—pole	E_L	L	No for L even Yes for L odd
Magnetic $2L$—pole	M_L	L	Yes for L even No for L odd

In general more than one type of multipole transition is possible between two states. For instance, if the angular momenta and parities of the initial and final states are $J_a=1^+$ and $J_b=2^-$, the

possible L-values are 1, 2 and 3. Since the parity changes, the possible transitions are E_1, M_2 and E_3. The scheme of selection rules is illustrated in Table 7.2.

Table 7.2.

	$\Delta J=0$			$\Delta J=1$		
$\Pi_a\Pi_b=-1$ $\Pi_a\Pi_b=+1$ Forbidden	E_1 M_1 $0\to0$	M_2 E_2 $0\to0$ $\frac{1}{2}\to\frac{1}{2}$	E_3... M_3... $0\to0$... $\frac{1}{2}\to\frac{1}{2}$... $1\to1$...	E_1 M_1	M_2 E_2 $0\rightleftharpoons1$	E_3... M_3... $0\rightleftharpoons1$... $\frac{1}{2}\rightleftharpoons\frac{3}{2}$...
	$\Delta J=2$			$\Delta J=3$		
$\Pi_a\Pi_b=-1$ $\Pi_a\Pi_b=+1$ Forbidden	M_2 E_2	E_3 M_3 $0\rightleftharpoons2$	M_4... E_4... $0\rightleftharpoons2$... $\frac{1}{2}\rightleftharpoons\frac{5}{2}$...	E_3 M_3	M_4 E_4 $0\rightleftharpoons3$	E_5... M_5... $0\rightleftharpoons3$... $\frac{1}{4}\rightleftharpoons\frac{7}{2}$...
	$\Delta J=4$			$\Delta J=5$		
$\Pi_a\Pi_b=-1$ $\Pi_a\Pi_b=+1$ Forbidden	M_4 E_4	E_5 M_5 $0\rightleftharpoons4$	M_6... E_6 ... $0\rightleftharpoons4$... $\frac{1}{2}\rightleftharpoons\frac{9}{2}$...	E_5 M_5	M_6 E_6 $0\rightleftharpoons5$	E_7... M_7... $0\rightleftharpoons5$... $\frac{1}{2}\rightleftharpoons\frac{11}{2}$...

Decay Constants. To calculate decay constants, we shall follow the method used by Blatt and Weisskopf. Let us first consider the source a classical system of currents, which varies periodically as

$$\mathbf{j}(\mathbf{r},t)=\mathbf{j}(\mathbf{r})e^{-i\omega t}+\mathbf{j}^*(\mathbf{r})e^{i\omega t} \qquad ...(28)$$

The charge density associated with this current is

$$\rho(\mathbf{r},t)=\rho(\mathbf{r})e^{-i\omega t}+\rho^*(\mathbf{r})e^{i\omega t} \qquad ...(29)$$

We define the electric multipole moment of order L, M as

$$Q_{L,M}=\int r^L\, Y^*_{L,M}(\theta,\phi)\,\rho(\mathbf{r})\,d\tau. \qquad ...(30)$$

The amplitude of the electric radiation of order L, M is given by

$$a_e(L,M)=-\frac{4\pi}{(2L+1)!!}\left(\frac{L+1}{L}\right)^{1/2}\left(\frac{\omega}{c}\right)^{L+2} Q_{L,M}. \qquad ...(31)$$

Here ω is the frequency of the radiation and $(2L+1)!!=1\times3\times5\times\ldots(2L+1)$.

The magnetic multipole moment of order L, M can be defined in a manner similar to that of electric multipole moment, as

$$M_{L,M}=-\int r^L Y^*_{L,M}(\theta,\phi)\,\frac{div(\mathbf{r}\times\mathbf{J})}{(L+1)}\,d\tau. \quad \ldots(32)$$

The amplitude of the magnetic radiation of order L, M is given by

$$a_m(L,M)=\frac{4\pi}{(2L+1)!!}\left(\frac{L+1}{L}\right)^{1/2}\left(\frac{\omega}{c}\right)^{L+2} M_{L,M}. \quad \ldots(33)$$

The energy $U_e(L, M, \Omega)\,d\Omega$ in a pure electric multipole radiation of order L, M with amplitude $a_e(L, M)$, emitted per second into the solid angle element $d\Omega$ can be written as

$$U_e(L,M,\Omega)=\frac{1}{4\pi\epsilon_0}\,\frac{c}{2\pi k^2}\,Z_{L,M}(\theta,\phi)\,|a_e(L,M)|^2$$

and the total energy emitted per sec

$$U_e(L,M)=\frac{1}{4\pi\epsilon_0}\,\frac{c}{2\pi k^2}\int|a_e(L,M)|^2 Z_{L,M}(\theta,\phi)\,d\Omega$$

$$=\frac{1}{4\pi\epsilon_0}\,\frac{c}{2\pi k^2}\,|a_e(L,M)|^2$$

$$=\frac{2(L+1)c}{\epsilon_0 L[(2L+1)!!]^2}\left(\frac{\omega}{c}\right)^{2L+2}|Q_{L,M}|^2 \quad \ldots(34)$$

Here we have used the integral of the angular distribution function $Z_{L,M}(\theta,\phi)$ over the full solid angle as unity.

Similarly the energy emitted per sec. by a magnetic multipole radiation is given by

$$U_m(L,M)=\frac{\mu_0}{4\pi}\,\frac{c}{2\pi k^2}\int|a_m(L,M)|^2 Z_{L,M}(\theta,\phi)\,d\Omega$$

$$=\frac{\mu_0}{4\pi}\,\frac{c}{2\pi k^2}\,|a_m(L,M)|^2$$

$$=\frac{2(L+1)c\,\mu_0}{L[(2L+1)!!]^2}\left(\frac{\omega}{c}\right)^{2L+2}|M_{L,M}|^2. \quad \ldots(35)$$

The decay constant λ, which is the probability for emission of a quantum $(\hbar\omega)$ per unit time can be obtained from above equations as

$$\lambda_e(L,M)=\frac{U_e(L,M)}{\hbar\omega}=\frac{2(L+1)}{\hbar\epsilon_0 L[(2L+1)!!]^2}\left(\frac{\omega}{c}\right)^{2L+1}|Q_{L,M}+Q'_{L,M}|^2$$

$$\lambda_m(L,M)=\frac{U_m(L,M)}{\hbar\omega}=\frac{2(L+1)\mu_0}{\hbar L[(2L+1)!!]^2}\left(\frac{\omega}{c}\right)^{2L+1}|M_{L,M}+M'_{L,M}|^2. \quad \ldots(36)$$

Here $Q'_{L,M}$ and $M'_{L,M}$ correspond to the intrinsic magnetic moments associated with the spins of the nucleons.

Reduced transition probability. For a given transition $J_a\to J_b$, the reduced transition rate for electric transitions of order L is defined as

$$B(EL, J_a\to J_b)=\frac{1}{2J_a+1}\sum_{m_a}\sum_{m_b} Q^2_{L,M}(a,b) \quad \ldots(37)$$

The double sum is taken as $|m|=|m_a-m_b|\leq L$. For magnetic transitions, we replace $Q_{L,M}(a,b)$ with $M_{L,M}(a,b)$. We can thus write decay constants as

$$\lambda_e(L, J_a\to J_b)=\frac{2(L+1)}{\hbar\epsilon_0 L[(2L+1)!!]^2}\left(\frac{\omega}{c}\right)^{2L+1} B(EL, J_a\to J_b)$$

$$\lambda_m(L, J_a\to J_b)=\frac{2(L+1)\mu_0}{\hbar L[(2L+1)!!]^2}\left(\frac{\omega}{c}\right)^{2L+1} B(ML, J_a\to J_b). \quad \ldots(38)$$

The reduced transition probability B_{ge} for the upward excitation process is related to the downward probability B_{eg} as

$$B_{ge}(L)=[(2I_e+1)/(2I_g+1)]\;B_{eg}(L). \quad \ldots(39)$$

In the single particle shell model, the radiation may be regarded as a result of the transition of a single nucleon from one state to another. With the rough estimate for the case of zero orbital angular momentum in the final state, Weisskopf found that

$$B(EL)=\frac{e^2}{4\pi}\left(\frac{3R^L}{L+3}\right)^2$$

and
$$B(ML)=10\left(\frac{\hbar}{m_p cR}\right)^2 B(EL), \quad \ldots(40)$$

where R is the nuclear radius and m_p the mass of the nucleon.

Using the relation $R=R_0A^{1/3}$ and gamma decay width $\Gamma=\hbar\times$ transition probability λ. Hence for different transitions, the single particle radiative widths are given directly as

$$\Gamma_\gamma(E1)=0.068\;A^{2/3}\;E_\gamma^3$$

$$\Gamma_\gamma(M1)=0.021\;E_\gamma^3$$

$$\Gamma_\gamma(E2)=4.9\times10^{-8}\;A^{4/3}\;E_\gamma^5$$

$$\Gamma_\gamma(M2)=1.5\times10^{-8}\;A^{2/3}\;E_\gamma^5, \quad \ldots(41)$$

where Γ_γ is in eV and E_γ in MeV.

Since transition probability drops very quickly with increasing L, hence the chief contributions are corresponding to $L=\Delta J$. A weak admixture of transitions or multipole order $\Delta J+1$ is to be expected mainly when the chief contribution ($L=\Delta T$) comes from a magnetic multipole. Experimentally $M1+E2$ is found. The admixture of $L'=L+1$ electric multipolarity in a mixed transition ($ML+EL'$) is expressed by the mixing ratio, whose square is defined as

$$\delta^2=I(L')/I(L). \qquad ...(42)$$

It is zero for pure L-radiation and infinity for pure L'-radiation. The percentage of ML intensity is $(1+\delta^2)^{-1}$ and of EL' is $\delta^2(1+\delta^2)^{-1}$

From the half life measurement, the multipole order of the γ-radiation can be determined, and thus statements about ΔJ and relative parities in the transition may be made. If we know the spin and parity of final state we can obtain the values for the spin and parity of the initial state.

7.6. NUCLEAR ISOMERISM

The occurrence of long lived, low-lying excited states is rather common among nuclei of intermediate and large mass. Observed life times vary over wide limits, from 10^{-10} sec to 10^{8} years. These delayed transitions are called *isomeric transitions* and the states from which they originate are called *isomeric states* or *isomeric levels*. Nuclear species which have the same atomic and mass numbers, but have different radioactive properties, are called *nuclear isomers* and their existence is referred to as nuclear *isomerism*. Nuclides that are isomeric states of a given isotope differ from each other in energy and in angular momentum.

The phenomenon of nuclear isomerism was discovered by O. Hahn, in 1921. He found that UX_2 and UZ, both have the same atomic number and the same mass number but have different half lives and emit different radiations. Both grow out of UX_1 by β^-decay. UX_2 has a half life of 1.18 minutes and emits three groups of electrons with end point energies of 2.31 MeV (90%), 1.50 MeV (9%) and 0.58 MeV (1%). On the other hand, UZ has a half life of 6.7 hours and emits four groups of electrons with end point energies of 0.16 MeV (28%), 0.32 MeV (32%), 0.53 MeV (27%) and 1.13 MeV (13%).

After the discovery of artificial radioactivity, indications came from several different directions that other nuclides exist in isomeric forms. When a sample containing bromine was bombarded with slow neutrons, the product was found to show three different half lives for beta decay: 18 min, 4.5 hr and 34 hr. Chemical tests showed that the radioactive elements were isotopes of bromine. This result was surprising because the reactions with slow neutrons are invariably of the (n, γ) type and since ordinary bromine consists of two isotopes only, Br^{79} and Br^{81}, not more than two radioactive products Br^{80} and Br^{82} [Br^{79} (n, γ) Br^{80} and Br^{81} (n, γ) Br^{82}] were to be expected. When bromine was bombarded with gamma ray photons, two products Br^{78} and Br^{80} [Br^{79} (γ, n) Br^{78}, Br^{81} (γ, n) Br^{80}], with three decay periods, 6.4 min, 18 min, 4.4 hr were obtained. Two of these periods (4.4 hr. and 18 min) are common to both sets of reactions and must, therefore, be assigned to the isotope that is common to both sets of reactions namely, Br^{80}. The two half lives were attributed to two isomeric states of Br^{80}. The difference between the nuclear isomers is attributed to a difference of nuclear energy states, one isomer represents the nucleus in its ground state, whereas the other is the same nucleus in an excited state of higher energy, or the *metastable state* and the letter *m* is sometimes written following the mass number to designate it.

Half period of isomeric transition. Most known γ-decay rates have been determined by the direct measurement of the life-times of the exited states.

Total decay rate $\lambda = \lambda_\gamma + \lambda_e = \lambda_\gamma\,(1+\alpha)$

$$\therefore \quad T_{1/2} = (\log_e 2)/\lambda = 0.693\ \tau_\gamma/(1+\alpha). \qquad (\ldots 54)$$

Since the internal conversion coefficient α can be measured or can be calculated theoretically and half life $T_{1/2}$ can be measured hence τ_γ the average life or λ_γ the rate of photon emission can be calculated.

Classification of nuclear Isomers. Nuclear isomers may be classified as:

(*a*) *Isomers with independent decay*—In this type, each isomer decays independently of the other with its own particular half life. The transition from the *metastable to the ground state is highly forbidden*. The transitions are shown in fig. 7.8 with T_1 and T_2 representing the different half-lives. One or other or both may also yield an excited state of the decay product, which will then emit the excess energy as gamma radiation. The examples of this type of nuclear isomers, together with the type of activity and half-lives are given below:

Mn^{52} (β^+, 5.7 days ; β^+, 21 min.) ; Zn^{71} (β^-, 4.1 hr ; β^-, 2.4 min.) ;
Ag^{106} (*EC*, 8.3 days ; β^+, 24 min.) ; Cd^{115} (β^-, 43 days ; β^-, 2.3 days).

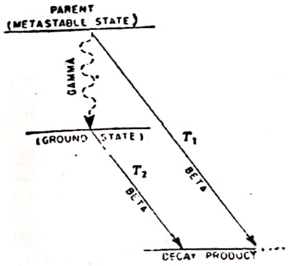

Fig. 7.8. Nuclear isomerism with independent decay.

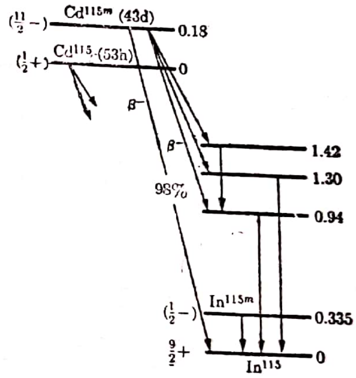

Fig. 7.9. Decay scheme of nuclear isomer Cd^{115}.

(*b*) *Genetically related Isomers*—In this type, the meta stable state decays to the ground state with a definite half-life T_1. Mostly, the gamma radiation is internally converted and produces line spectrum of electrons together with characteristic X-rays. The ground state decays to form the product with a half-life of T_2, different from T_1. The product is not necessarily formed in its ground state and so gamma radiation may accompany the radioactive change. Broken line of fig. 7.10 shows the possibility of direct independent decay of the excited metastable state of the parent nucleus. Some examples of genetically related isomers are given below.

Sc^{44} (IT, 2 44 days ; β^+, 3.91 hr) ; Zn^{69} (IT, 13.8 hr ; β^-, 55 min) ;
Br^{80} (IT, 4 5 hr. β^-, 17.6 min) ; Se^{81} (IT, 57 min ; β^- min) ;
In^{114} (IT, 50 days ; β^-, 72 sec) ; Te^{131} (IT, 1.2 days ; β^-, 25 min).

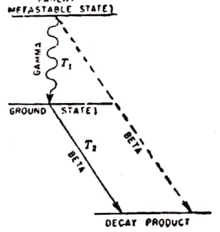

Fig. 7.10. Genetically related isomers.

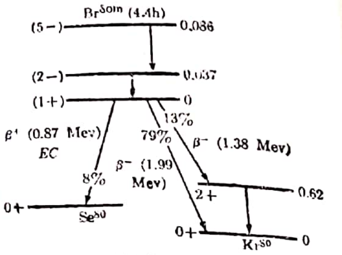

Fig. 7.11. Decay scheme of nuclear isomer Br^{80}.

Here symbol IT implies to *isomeric transition*. From these examples it will be observed that the half-life of the internal transition process is often longer than that of the beta decay of the ground state. As a result, two groups of beta particles, corresponding to two distinct half-lives, are emitted. Sometimes isomeric transition is accompanied by the breaking of a chemical bond, which may make possible a separation of the isomeric nuclei.

(*c*) *Isomers of Stable nuclei*—In this type of isomers, the decay process involves an isomeric transition from the metastable state to the ground state of a stable nucllde, accompanied by the emission of gamma radiation. If gamma radiation is converted internally, the line spectrum of electrons, together with characteristic X-rays, is observed. More than 30 stable species are found in nature. Among them Kr^{83}, Sr^{87}, Rh^{103}, Ag^{107}, Sn^{117}, Ba^{137} and Au^{197} form metastable states of appreciable life. Other number of stable nuclides form isomers of short life, *e g*, a millionth of a sec. or less.

Isomerism and Nuclear Spin. In 1936, C.F. von Weizsacker, a German physicist, proposed an explanation for the existence of metastable states of both stable and unstable nuclides. The probability of the transition between two excited states or an excited state and the ground state of the nucleus is dependent partly on the energy difference between these states but mainly on the multipole character of the radiation. This is determined by the spins and parities of the nuclear states involved in the transition. Goldhaber and co-workers could classify the nuclear properties of 77 isomers, for which half-life time is between 1 sec and 8 months. About half of these are $M4$ transitions ($\triangle I=4$, yes) and the remainder are $M3$,

$E3$ and E_4. The transitions accompanied by $E5$ radiations are not common. The correlation of nuclear angular momentum values with the *single particle shell model* is excellent. The shorter lived group (life times between 10^{-5} and 10^{-9} sec) is made up of $M1$, $M2$ and $E2$ transitions.

$E2$ transitions in heavy nuclei are 100 times faster than predicted by the single particle model. The properties of these fast $E2$ transitions are best accounted for by the *collective model*. This model predicts bands of rotational states for these spherically deformed nuclei.

7.7. ANGULAR CORRELATION IN GAMMA EMISSION

The photons emitted by a sample in which a large number of nuclei are undergoing identical gamma ray transitions will be isotropic in the lab co-ordinates. As the atoms and nuclei are randomly oriented, there is no preferred direction of emission for the gamma ray photon from the individual transition. When two gamma rays are emitted in rapid succession by the same nucleus, their directions and planes of polarization are not entirely independent, but there is often angular correlation between the directions of emission of these two successive γ-rays. There are similar angular correlations for other pairs of successive radiations, such as α-γ, β-γ, β-e^{-1}, γ-e^{-1},... The measurements of angular distribution of γ-radiation or of the angular correlation between two radiations can yield valuable information on multipole mixing ratios or nuclear level spins.

Let us examine briefly the directional correlation between two successive γ-rays in the sequence shown in fig. 7.12. The nuclear excited state (spin I_a) de-excites by a cascade of γ-rays γ_1 and γ_2 through an intermediate state (spin I_b) to the final state (spin I_c). The multipolarity of the γ-rays γ_1 and γ_2 is L_1 and L_2 respectively.

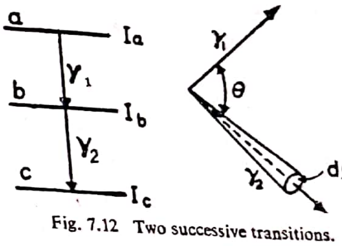

Fig. 7.12 Two successive transitions.

If the intermediate state is sufficiently short-lived, coincidences between counts in the two counters (to accept signals γ_1 and γ_2) yield the angular correlation between the two radiations. The counting (coincidence) rate between γ_1 and γ_2 is measured as a function of the angle θ between the direction of emission of γ_1 and γ_2. The *directional correlation*, $W(\theta)\,d\Omega$, is defined as the relative probability that γ-ray 2 is emitted into the solid angle $d\Omega$ at an angle θ with respect to γ-ray 1 and can be expressed as

$$W(\theta)=1+A_2P_2(\cos\theta)+A_4P_4(\cos\theta)+\ldots=\sum_{i=0}^{L} A_{2i}P_{2i}(\cos\theta), \quad ..(5$$

7.10. MOSSBAUER EFFECT

R. L. Mossbauer had discovered in 1957 that some of the low energy gamma radiations ($\sim 10^4$ eV) emitted by long lived 'isomeric' states of nuclei, with life times of the order of 10^{-7} to 10^{-8} sec., were practically recoil free. The reason for this is that the mass M is now comparable to the mass of a microcrystal of the solid. The mass to which the recoil momentum is transferred can be considered infinite in comparison with that of an atom, so that velocity of recoil is zero. This recoil free emission and resonant absorption of gamma radiation is known as the *Mossbauer effect*, in honour of its discoverer.

In his original experiment, Mossbauer measured the emission of 129 keV gamma radiations from radioactive Ir^{191}. They were passed through a metallic iridium absorber (39% of Ir^{191}) and then on to a detector. Gamma source Ir^{191} was formed in an isomeric state in the beta decay of Os^{191}. The natural width and life time of the 129 keV level of Ir^{191} are 5×10^{-6} eV and 1.3×10^{-10} seconds respectively. After Mossbauer's discovery a search was made for the other substances which could be used and many more have since been found. The substance which has been used most extensively is Fe^{57}. The excited state, with an energy of only 14.4 keV above the ground state, is produced by

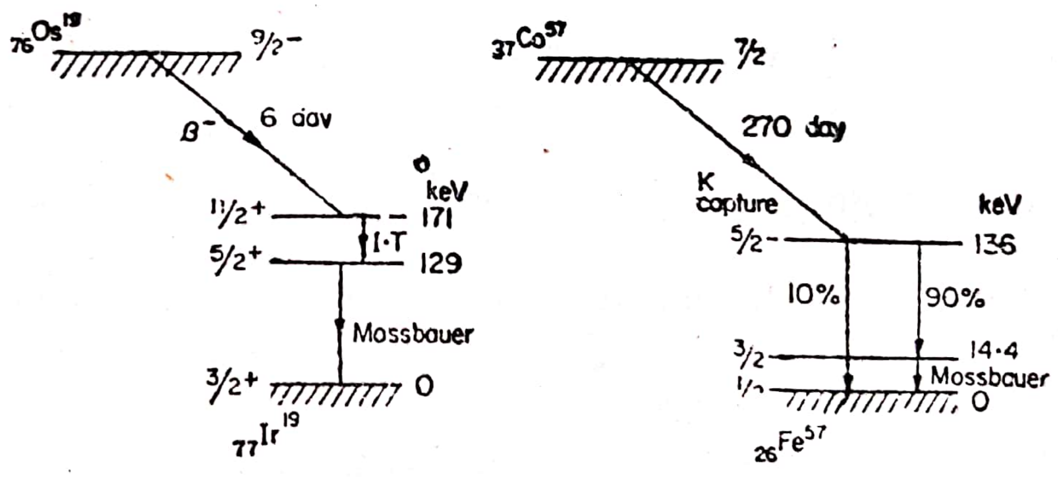

Fig. 7.17. The Mossbauer transitions of 129 keV Ir^{191} and 14.4 keV Fe^{57}.

the process of orbital electron capture in Co^{57}, which has a half-life of 270 days and is generally prepared by deuteron bombardment of an iron target in the form of a strip. Decay schemes of Osmium and Cobalt are given in fig. 7.17. The positive and negative signs after the quantum numbers refer to the parity of the states.

The 14.4 keV level in Fe^{57} has a mean life of 1.4×10^{-7} sec and the corresponding line width is 4.6×10^{-9} eV. This life time is long enough for the excited Fe^{57} ions to occupy suitable sites in the iron crystal lattice before the decay. The 14.4 keV gamma rays can be passed through an iron absorber which can be enriched in Fe^{57} so as to increase the probability of recoilless absorption. The gamma rays can be detected by a proportional counter or scintillation counter.

After Fe^{57}, the substance employed most frequently is probably tin 119 and a fair amount of work has also been done with some rare earth elements. The theory of recoilless emission shows that the effect is greater when : (*a*) the gamma ray energy E is small (The best example is the 14.4 keV transition of Fe^{57}) ; (*b*) the temperature of the crystal source is small ; (*c*) the Debye temperature of the crystal lattice is high.

About one per cent of the Ir^{191} transitions at 80°K are recoilless, in contrast to 70 per cent for the 14.4 keV Fe^{57} transitions at room temperature.

The Doppler energy shift Ev/c sufficient to destroy the resonance condition. A relative velocity of 0·1 mm. per sec is sufficient to produce a marked reduction in the resonant absorption of the 14.4 keV Fe^{57} ; Mossbauer radiation by an Fe^{57} absorber. The energy change may be induced by temperature change, by change in the magnetic field at the nucleus and by change in the gravitational field.

The theoretical analysis, following Lamb's treatment, used Debye continuous theory to describe lattice vibration behaviour. The lattice system is assumed to have independent linear oscillations with a continuous frequency distribution upto a maximum ω_D. It is related with Debye temp Θ as

$$\hbar\omega_D = k\Theta, \qquad \ldots(68)$$

where k is the Boltzmann constant. The fraction of recolless γ-transition, also known as Lamb Mossbauer factor, is given as

$$f \simeq \exp\left[\frac{-3E_R}{2k\Theta}\left\{1+\frac{2}{3}\left(\frac{\pi T}{\Theta}\right)^2\right\}\right]. \qquad \ldots(69)$$

In order to utilize the Mossbauer effect, one has to consider transitions in which —

(*a*) f is adequately large ;

(*b*) E_0 must be fairly large for a good precision ;

(*c*) there must be small livelihood of internal conversion ;

(*d*) fine structure splitting should not occur, if possible.

When these requirements are satisfied, precautions should be made against :

(*a*) the changes in nuclear mass on emission and absorption of γ-rays, which cause the γ-ray to change ;

(*b*) the differences in the average isotopic mass number ;

(*c*) the differences in the Debye and the absolute temperatures between source and absorber ;

(*d*) the differences in chemical constitution of presence or lattice defects ;

(*e*) relative velocity between emitter and absorber.

Applications of Mossbauer Effect : (*a*) *Isomer Shift or Chemical Shift*—Different chemical states of an atom are associated with differences in the electron distribution around the nucleus and contribute to the energy of transition.

$$E_\gamma = \Delta E_{nuc} + \Delta E_{elec},$$

where ΔE_{nuc} is the change in nuclear binding energy and ΔE_{elec} is the change in B.E. of the atomic electrons. If the emitting nucleus (excited state) and the absorbing nucleus (ground state) are in different chemical compounds, the distributions in atomic electrons will be different, which will cause differences in ΔE_{elec} and thus in E_γ. The change in E_γ is called the *isomer* shift or *chemical shift* (as it is related to the chemical environment of the atom).

(*b*) *Magnetic Hyperfine Splitting*—If either the emitting or the absorbing nucleus has a spin $I \geqslant \frac{1}{2}$, it will also have a magnetic moment. In the presence of magnetic field, the energy of the nucleus will depend on its orientation with respect to that magnetic field. The projection of spin I may take $2I+1$ values. The absorption spectrum obtained by the Mossbauer technique will thus show a hyperfine splitting into $2I+1$ parts fig (7.18). Thus $2I+1=5$ and nuclear spin is 2. The energy difference between adjacent absorption maxima, as determined from the source velocity differences, is related to the product of the field strength and the nuclear magnetic moment ($\Delta E = g\mu_N B$). If field strength is known, magnetic moment of the excited state of nucleuscan be evaluated. If both the absorber and source are *ferromagnetic*, there will

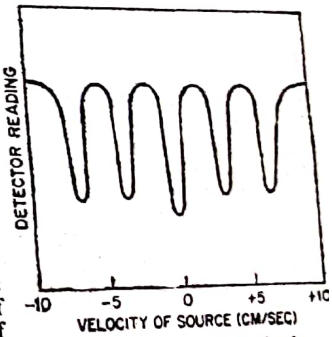

Fig. 7·18. Nuclear spin determination.

be some velocities for which the energy change will be equal to the separations of some of the energy levels, so that the several components may overlap. Thus a non-ferromagnetic material, such as stainless steel, should be used as either the source or the absorber. Mössbauer effect is also applicable to study internal magnetic compounds and alloys, which have magnetic properties.

(*c*) *Quadrupole hyperfine splitting*—If either the emitting or the absorbing nucleus has a spin $I > 1$ and is in an inhomogeneous electric field energy may split, in several lines. It is because the interaction between the nuclear quadrupole moment and the inhomogeneous electric field causes the energy of the nucleus to depend on its orientation.

(*d*) *Lifetime measurement*—Mössbauer technique is best for the measurement of fairly short lifetimes, since when the lifetime exceeds about 10^{-10} sec, extra nuclear fields can cause line broadening. Basically the range 10^{-13} sec $\leq \tau \leq 10^{-10}$ sec seems best suited to such determinations.

(*e*) *Gravitational shift*—On the basis of the principle of equivalence, Schiff has given a simple derivation of the gravitational Doppler shift. We shall give an even more elementary derivation which is directly applicable to nuclear fluorescence experiments.

We know that the intensity I of the earth gravitational field at a distance R from an earth of mass M is the acceleration due to gravity. Hence

$$I = GM/R^2 = g. \qquad ...(70)$$

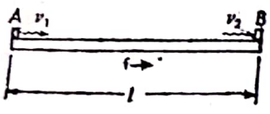

Fig. 7.19. Table PQ has constant acceleration f in inertial frame.

Similarly the gravitational potential ϕ at the point R due to earth is

$$\phi = -GM/R = -gR \qquad ...(71)$$

Let us place a source nucleus A and an observer nucleus B on a horizontal table PQ, distance l apart. Suppose that at some particular instant when the velocity of table is V_1, the nucleus A at one end emits a gamma ray photon of frequency ν_1 in the direction of its motion. The frequency of this radiation as measured by a stationary observer will be

$$\nu_{ob} = \nu_1(1 + V_1/c). \qquad (72)$$

This photon moves towards B with a constant velocity c. It will reach an identical absorber nucleus B at a time $t(=l/c)$, where velocity of table $V_2 = V_1 + ft$. The apparent frequency of radiation, which can be absorbed by observer nucleus B, will be ν_2. The

frequency of this radiation as measured by a stationary observer will be

$$\nu_{ob} = \nu_2(1 + V_2/c). \qquad ...(71)$$

Clearly if the gamma ray absorbed by nucleus at B is to be that one which has been emitted by nucleus A, we must have

$$\nu_1(1 + V_1/c) = \nu_2(1 + V_2/c). \qquad ...(72)$$

This relation indicates that absorption would take place for identical recoilless nuclei, only if $V_1 = V_2$.

If we assume that $\nu_1 - \nu_2 = \Delta\nu$ and $\nu_1 = \nu_2 = \nu$, then we have

$$\Delta\nu = \frac{\nu}{c}(V_2 - V_1) = \frac{\nu}{c} \cdot f \cdot \frac{l}{c} \quad \text{or} \quad \frac{\Delta\nu}{\nu} = \frac{fl}{c^2}. \qquad ...(73)$$

The principle of equivalence of an accelerated system tells us that the system having an acceleration f produces an effect equivalent to that of a gravitational acceleration $-f\,(=g)$. If $\Delta\phi$ is the potential difference between two points in a gravitational field, the difference in frequency of identical clocks at these points will be

$$\Delta\nu = \nu\,\Delta\phi/c^2. \qquad ...(74)$$

Thus for resonance absorption, the frequency of emission ν_1 must be larger than the frequency of absorption ν_2 by an amount $\nu\Delta\phi/c^2$. Hence the frequency of radiation coming from a source located below the absorber will be sifted towards the red.

Until 1960, the gravitational red shift could only be observed with light coming from stars, as $\Delta\phi$ is very large in that case. The discovery of Mössbauer technique makes it possible, for the first time to carry out a gravitational Doppler effect experiment. A series of experiments was performed independently by R. V. Pound and G. A. Rebka Jr. at Harvard and by T. E. Cranshaw and others at Harwell in 1960, using Fe^{57} as the emitter and absorber. The Harwell group electro-deposited a Co^{57} source on an iron disc, mounted about 40′ above a 5″ diameter foil containing 4 mg/cm² of iron enriched in Fe^{57}. A proportional counter filled with krypton to about 20 cm of mercury pressure is placed underneath the absorbing iron foil to detect the transmitted 14.4 keV gamma rays. A simplified schematic diagram of their apparatus is sketched in fig. 7.20.

The source is mounted on a transducer device and vibrated to and fro at 50 c/s. When the Doppler shift produced by moving the source exactly compensates the gravitational shift maximum resonance will occur. The transmitted gamma rays are recorded by two scalars for alternate halves of the vibrating cycle. The mean counting rate is slightly different due to the asymmetry introduced by the gravitational shift. It was found that the observed red shift was (0.96±0.45) times the expected shift. This source of error has to do with the Doppler shift due to the motion of the nuclei in the lattice. The emitting and absorbing nuclei are vibrating with fairly high speeds, given by the temperature of the solid. Therefore it might be expected that vibration would impart a Doppler shift.

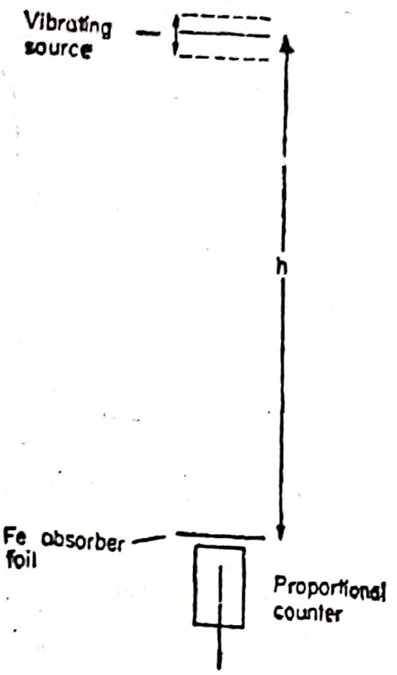

Fig. 7.20 Gravitational Shift experiment.

EXERCISES

Example 1. *In a bent crystal spectrometer, the quartz crystal has an interplaner spacing of 1.18×10^{-8} cm. The radius of the focal circle is 2 meters. The source emits gamma rays of energies 1.33 and 1.16 MeV. Assuming that the source is in a position where it gives first order Bragg reflection for the 1.33 MeV gamma-ray, calculate the distance it has to be moved to obtain first order reflection for the 1.16 MeV gamma ray.*

For the first order Bragg reflection, we have $2d \sin\theta=\lambda$.

If f is the focal length and $BR=x_1$ (fig. 7.1), then we have

$$2d\,(x_1/f)=hc/E_1.$$

If x_1 and x_2 are the distances for energies E_1 and E_2 then

$$(2d/f)\,(x_1-x_2)=hc(1/E_1-1/E_2),$$

or
$$x_1-x_2=\frac{hcf}{2d}\left(\frac{1}{E_1}-\frac{1}{E_2}\right)$$

$$=\frac{6.6256\times10^{-34}\times3\times10^{8}\times2}{2\times1.18\times10^{-10}}\times\frac{0.17}{1.33\times1.16\times1.6\times10^{-13}}$$

$$=1.16\times10^{-3}\text{ meter.}$$

3.2 Ionisation chamber

An extensive class of *particle detectors* exists that depends for their performance on the electric *pulse of current* produced when ions are formed by the passage of a *charged particle* between two electrodes maintained at a sufficient potential difference. These detectors are usually called *gas-filled detectors*, the simplest of which is the *ionisation chamber* described below.

Construction and action — An *ionisation* chamber essentially consists of a *closed vessel* having a *suitable gas e.g. argon* in which ions have rather long life-time and *two electrodes* maintained at a *moderate* (~ few hundred to few thousands) voltage. Commonly used chambers possess either *parallel-plate geometry* or *cylindrical* geometry. While in the former class, two parallel plates are separated by a distance, in the latter a cylindrical conducting shell with a coaxial insulated metallic wire (dia ~ 1 cm) acts as electrodes.

In Fig. 3.5 where a typical ionisation chamber is shown schematically, one of the electrodes is the *outer metal cylinder* connected to the *negative terminal* of a dc-power supply and the other electrode is the *central straight wire* connected in series to a resistor R, to the *positive* of the power supply (220 V). The gas inside is maintained under some pressure to enhance the sensitivity of the instrument by providing more targets for the incoming colliding particles. A thin mica *window* W, provided in the chamber, allows photons or charged particles to enter the chamber and ionise the gas inside. The ions produced are attracted towards the respective electrodes due to the electric field maintained between them. A *voltage pulse* is thereby developed between A and B and is then amplified and registered.

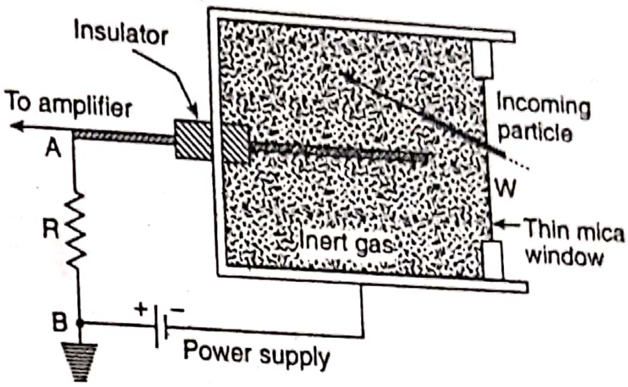

Fig. 3.5 Ionisation chamber

Fig. 3.6 gives the **voltage pulse vs. applied voltage** between the electrodes. The region AB, from a few volts to about 200 V, typically corresponds to ionisation chamber. In this region, all the ions produced by the incident particles or incoming photons are collected by the electrodes. Note that the *pulse height* between A and B is practically *independent* of the applied *voltage*. So the chamber *does not measure* the *energy* of the incoming particles. The *energy* deposition however is *proportional* to the *number of ions* produced and is a measure of the *charge* and the *velocity* of the particle. These then are the quantities an ionisation chamber measures.

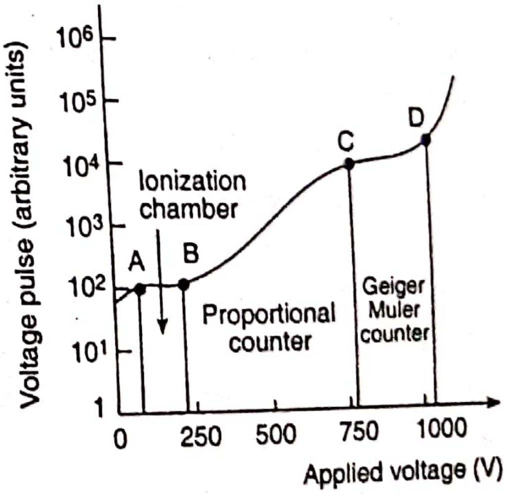

Fig. 3.6 Voltage pulse vs. Applied voltage

The energy required to make an ion-pair is about, 35 eV for air; but the ionisation produced by a single charged particle is very small. The chamber therefore detects *bursts of particles* rather than individual particles. It is however capable of distinguishing between bursts of α-particles and bursts of β-particles. Since x-rays and γ-rays readily ionise gases, they are also easily detected by an ionisation chamber.

• An ionisation chamber is said to be, for a particular ionising radiation, *deep* or *shallow* according as it can completely absorb or not, the ionising radiation.

3.3 Proportional counter

A second type of *gas-filled* detector, derived in a sense from ionisation chamber, is the *proportional counter*. Low energy ionising particles cannot be detected by an ionisation chamber since the voltage pulses they produce have very small amplitude. If the field between the electrodes be increased, it is possible to produce pulses of higher amplitude with such particles, utilising *gas multiplication*. This is done in a proportional counter.

Construction and action — It consists (Fig. 3.7) essentially of a metal chamber filled with a gas and having a thin wire of dia ~ 0.1 mm running *axially* along the centre. The *wire* acts as the *anode* and the *metal case* as the *cathode*, being connected to a power supply as shown. A voltage of 250–800 V which causes no discharge is applied

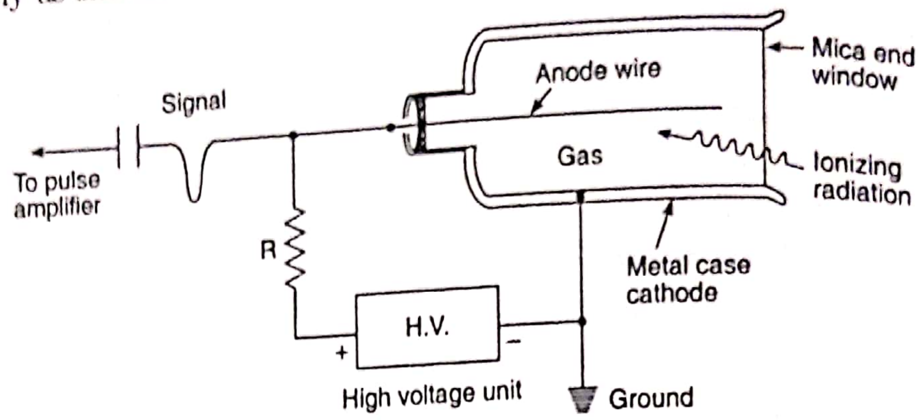

Fig. 3.7 "End window" type proportional counter

between the electrodes. Let now an ionising particle enter into the counter through the thin mica 'end window'. The electrons produced are attracted toward the central wire. In its vicinity, the electric field is very high compared to other regions. So, an electron near the anode-wire acquires sufficient kinetic energy between two successive collisions with gas atoms to ionise them to produce additional ion-pairs (*secondary ions*). The process is known as *gas multiplication* and the number of ions may increase by a factor of about 10^4.

The total amount of charge collected is thus greater than the original charge produced. The output pulse of the current is *proportional* to the number of ion-pairs formed by the ionising particle. The counter thus used is therefore termed *proportional counter*. By the IR-drop across the resistance R, the current pulse forms a *voltage pulse* which is amplified and recorded.

In Fig. 3.6, BC corresponds to the proportional counter region. In this region, the pulse height is practically proportional to the energy of the incident particle.

If the pulses are fed into an oscilloscope, the *pulse heights* could measure the *energies* of the ionising radiation. *Such information is of great importance* in the study of nuclear disintegration. The proportional counters may be accurately calibrated to give *distinctive voltage pulses characteristic of different particles* or they may be set to completely ignore some types of particles. With the help of such a counter, therefore, it is easy to distinguish α-particles from β and the protons by the larger voltage pulses they produce due to greater electric charge.

- If the radius of the wire (anode) be a and that of the counter (cathode) be b, then the radial field E at any point distant r from the centre will be given by

$$E = \frac{V}{r \ln (b/a)} = \frac{k}{r} \tag{3.3.1}$$

where V is the p.d. between the anode and the cathode, $k = V/\ln(b/a)$ = constant.

The field is thus very strong near the anode wire and the *avalanche production* (a very rapid increase in the number of ions) thus takes place near the central wire.

The potential difference V across the tube is given by

$$V = k \ln (b/a) = 2.3\, k \log_{10}(b/a) \tag{3.3.2}$$

The potential gradient, dV/dr, can thus be calculated using (3.3.1), for different values of r.

- This counter not only counts the incoming particles, but is also capable of measuring the energy of the particles.

3.4 Geiger-Muller counter (GM-counter)

The chief among the gas-filled counters is the *Geiger-Muller counter* which is one of the *most versatile* instruments for *detecting* the ionising radiations *and measuring* their *energies.*

If the electrodes of a gas-filled counter are so shaped that there exists a high field near one of them even when a moderately high dc-voltage is applied to it, then the amplification of an ionic charge reaches, in the region of high voltage, an *avalanche condition.* Practically, all of the gas present in the local volume of the electrode gets ionised. This results in a *much larger voltage pulse* on the electrode. The pulse height is independent of the amount of ionisation originally produced by the particle. It depends only on the counter potential and increases with it. Only a single ion reaching the vicinity of high voltage electrode may trigger the process. This counter is *very simple to construct* and is *extremely sensitive* to the passage of charged particles.

Apparatus — It is similar in construction to proportional counters and consists of a *cylindrical metallic tube TT* inside which is fitted a *fine tungsten wire CW*, stretched *along its axis* and is mounted inside a *glass tube GC*.

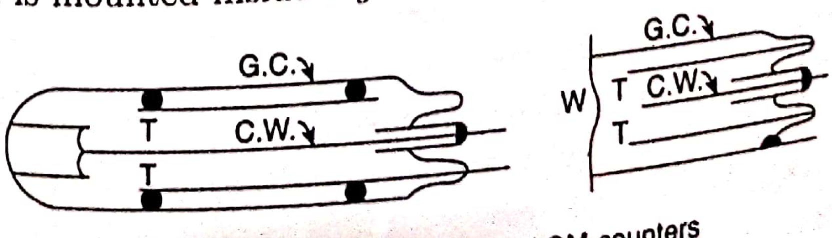

Fig. 3.8 Two common types of GM-counters

Two common types of GM-counters are shown in Fig. 3.8. In the first, the particle enters the counter through the glass envelope, while in the second type, called *end-window GM-counter,* the tube has a thin mica sheet *W* at one end to serve as a *window.* The former is used for counting penetrating particles, the latter for less penetrating ones. In the window-type, the central wire *CW* does *not* extend throughout the length of the tube, but terminates at a point.

The counter is filled with an *inert gas* (e.g. monatomic argon which is transparent to UV-light), at a pressure of *few cm* (2-10) of mercury, together with a *trace of polyatomic organic vapour* (e.g. alcohol) acting as a *quenching agent* that quenches the initial discharge soon after it is initiated. The diameter of the tube varies, depending on the purpose of its use, from 1-5 cm and its length from 2-100 cm.

Action — The central wire *CW* acts as the anode and is mounted at so high a positive potential (*H.T.*), about 1000 V, with respect to the metallic cylinder *TT* (Fig. 3.9a) that acts as the cathode, that a discharge *just not* sets in. Then even a single ion-pair formed by a single incident particle can produce an electric discharge. The important fact is that the electric pulse produced in this discharge is the *same,* no mater what is the energy of the incident particle. The central wire is *very thin,* the electrical field in its vicinity is *very high.*

Let an ionising particle enter the GM-tube and produce one single ion-pair in the volume enclosed by the outer cylinder. The resulting electron would be rapidly accelerated towards the central wire and reach a relatively high velocity producing rapidly a large number of additional ion-pairs by *repeated collisions.* The new electrons are also accelerated and may in turn produce more ion-pairs. The process is cumulative and an *avalanche* occurs. A very large number of electrons reaches the anode which gets surrounded by the massive slow-moving positive ion sheath. The initial formation of a single ion-pair thus results in a *very large pulse of current* to the anode.

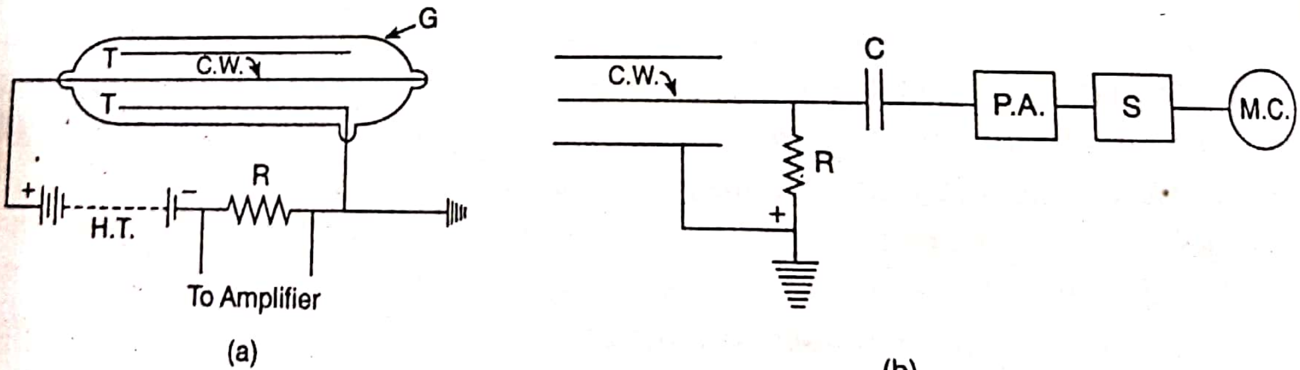

Fig. 3.9 (a) GM counter : conversion of current pulse into voltage pulse
(b) GM counter with an amplifying circuit and counting arrangement

Some free electrons on collision with argon atoms merely *excite* them which, on return to the normal state, emit photons. If a photon is absorbed by another excited atom, it may get ionised releasing electrons which produce further avalanches. The avalanche thus spreads rapidly in the *entire volume* of the counter and an amplification as high as 10^8 is attained. *The total number of ions is now 'independent' of the initial number of ions formed by the incoming particle.*

In a short time ~ 1 μs, the space charge (i.e., positive ion-sheath) becomes enough dense to cancel the field round the anode, discharged and ionisation stops; positive ions are drawn to the cathode and the ionisation restarts. The time interval during which the ionisation remains suspended is known as the '*dead time*' of the counter as it is not then ready to receive another incident particle. Therefore, *some mechanism must be devised for quenching* (i.e., terminating) the *discharge after each event.*

Counting and quenching : The entry of a single particle in the counter triggers a pulse of current, independent of the energy and nature of the ionising particle. If a resistance R is connected in series in the circuit as shown in Fig. 3.9, the current pulse I produces a corresponding voltage pulse IR which is fed to a pulse amplifier $P.A$ through a capacitor C (Fig. 3.9b). The amplified pulse is finally passed on to a scalar S and a mechanical counter MC. The scaler records the arrival of each individual pulse separately, giving the exact number of particles entering the tube in a given interval.

The resistance R in the counter circuit not only provides a p.d. that can be amplified but also has another function. When a large current pulse occurs, the momentary voltage drop IR across the resistance *lowers* the tube voltage to $(V - IR)$ which is insufficient to maintain the discharge and the counter is said to be *quenched* or *dead*. This prolongs the time-interval before the counter may become ready to accept another fresh particle and pulse.

This time interval is called the '*dead time*' because the counter is unable to detect any ionising particle during this interval. The *sensitivity* of the counter depends largely on its dead time : ***the lesser the dead time, the greater is the sensitivity.*** The traces of organic vapour like ethyl alcohol present in the tube, along with inert gas such as argon, *increase the sensitivity* of the counter considerably.

3.4.1 Some terms relating to GM-counter

Operating voltage — The operation of a GM-counter should be in the proper voltage region, the region CD in Fig. 3.6, between 800-1000 V. At such voltages, the tube operates in a plateau such that even with changes in applied voltage, the pulse height is practically constant, being independent of the number of ions formed in the tube. This is called the *Geiger region* which starts at *Geiger threshold voltage C*. The Geiger region is the normal operating region of a GM-counter and if it is exceeded, the tube may go to a *continuous discharge* with breakdown of the gas within it and may be ruined.

Self-quenching of GM-counter — A typical GM-counter contains 90% Ar and 10% alcohol. The ultra-violet photons from Ar on getting absorbed by alcohol cannot reach the cathode. As positive ions move towards the cathode they collide with alcohol molecules resulting in electron-transfer from alcohol to Ar to neutralise the latter. The alcohol molecules on arrival at the cathode dissociate rather than eject electrons. The discharge thus gets quenched. Such self-quenching by dissociation of organic molecules uses up the molecules after about 10^9 discharges, when a refilling of the counter is needed.

It is also possible to use *halogen molecules* for quenching. The *advantage* is that they recombine after dissociation. If a diatomic (or polyatomic) gas such as Br is introduced in the tube, the positive Ar-ions in their *slow* motion to the cathode would have multiple collisions with Br-molecules and transfer their charge to them. Only neutral Ar-atoms would thus reach the cathode. Br-ions (*molecular*) in their turn reach the cathode, gain electrons, and move into excited states. The excited Br-molecules lose their excitation energy *not by photon emission* but *by dissociation* into Br-atoms. No spurious pulses are thus produced. In course of time, Br-atoms recombine into Br-molecules. Bromine thus quenches the discharge and the tube becomes ready to receive the next particle within 10^{-4} s.

Dead time, recovery time, resolving time — The *dead time* of a GM-counter, is the time interval between the production of the initial pulse and initiation of second Geiger discharge. It is called *dead time* because during this period the counter is insensitive (dead) to further pulses. It is usually ~ 50-100 μs and arises due to slow mobility of heavier positive ions from anode region to cathode. The presence of positive ion-sheath around the inner electrode lowers the electric field below the Geiger threshold, $V_{th}(= V_s)$.

As the ion-sheath moves towards the cathode, the field at the central electrode recovers quickly as the external resistance is usually small. ***The time for recovery to threshold is the dead time.*** The counter can record another ionising particle only after the field has been restored to a value above $V_{th}(= V_s)$. Since a finite pulse must be developed for the counter circuit to count it, the actual *resolving time* of the counter is slightly longer than the dead time.

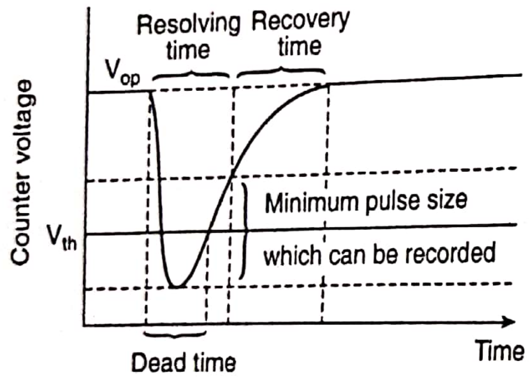

Fig. 3.10 Three time intervals associated with the operation of a GM-counter

The *recovery time* of the counter is defined as *the time interval for the counter to return to its original state to produce full sized pulses again.* Fig. 3.10 gives the three time-intervals – *dead time, resolving time* and *recovery time* – of operation of a GM-counter.

- The resolving time of a counter is often taken to be synonymous with dead time. During the resolving time, pulses are recorded but they are of smaller size. During dead time, a high flux through the counter should be avoided.

- **Expression for resolving time** — To determine the true counting rate of a GM-counter, its resolving time τ should be known. Plainly, the counter does not respond to ionising events that occur during τ. If n be the counting rate of a counter and N the actual rate of arrival of the particles in the counter,

$$N - n = Nn\tau$$

since the counter was insensitive for an interval $n\tau$ second, missing thereby $Nn\tau$ particles per second.

We, therefore, get

$$\boxed{N = \frac{n}{1 - n\tau}} \tag{3.4.1}$$

From (3.4.1), we can find the *true* counting rate N from the *observed* counting rate n, if τ is known.

Determination of τ — By measuring separately the counting rates n_1' and n_2' with two radioactive sources 1 and 2 of nearly equal strength, τ can be determined. Let n_t' denote the total counting rate when both sources are placed in the same position as before and n_b be the background rate (i.e., with no source).

$$\therefore \quad n_1 = n_1' - n_b; \quad n_2 = n_2' - n_b; \quad n_t = n_t' - n_b \tag{3.4.2}$$

where n_1, n_2, n_t are the above counting rates corrected for background.

If N_1, N_2 and N_t be the true rates of arrival of particles in the counter in the above three situations, we have, using (3.4.1)

$$N_1 = \frac{n_1}{1 - n_1\tau}; \quad N_2 = \frac{n_2}{1 - n_2\tau}; \quad N_t = \frac{n_t}{1 - n_t\tau} \tag{3.4.3}$$

$$\text{Also,} \quad N_t = N_1 + N_2 \tag{3.4.4}$$

Assuming the values of terms involving τ^2 to be negligible, we have, solving for τ

$$\boxed{\tau = \frac{n_1 + n_2 - n_t}{2n_1 n_2}} \tag{3.4.5}$$

• **Usefulness and limitations** — This counter is *very simple* to construct and is *very sensitive* to the passage of charged particles. In fact, with a suitable counting circuit, it is one of the most *versatile detecting instruments.*

Two GM-counters are said to be *in coincidence* if they are so arranged that there is no response unless the radiation passes through both. Such an arrangement of GM-counters has been widely used in cosmic ray researches to scan the sky for studying the directional variation in the cosmic ray intensity at a given place. It is called a *cosmic ray telescope.*

Another method of connecting GM-counters is known as *anti-coincidence.* In this case, two counters are connected in such a way that the counts would be registered only when a ray goes through one counter or another but not through both. This arrangement has also been widely used in cosmic ray studies.

The counter however *does not distinguish between the types of particles, nor does it measure their energies,* because the magnitude of the pulse is independent of the nature or energy of the incoming particle. A proportional counter however does it. It is usually designed to count α-particles, β-particles, x-rays and γ-rays. The particles, however, could be distinguished by finding what absorber placed in their path can stop them to enter the tube.

3.5 Neutron detection

Neutrons are *uncharged particles* and cannot therefore be deflected by electric or magnetic fields. Nor can they be produced by ionisation process. They do not cause fluorescence, nor produce cloud chamber tracks or emulsion tracks, nor trigger Geiger counters. For these reasons, special techniques are needed to detect neutrons.

Methods for detecting neutrons are based on some *intermediate nuclear reactions* involving neutrons in which charged particles capable of producing ionisation are released. The usual reaction is

$$^{10}_{5}\mathrm{B} + ^{1}_{0}\mathrm{n} \rightarrow ^{4}_{2}\mathrm{He} + ^{7}_{3}\mathrm{Li}$$

Each neutron interacting with a boron nucleus produces one α-particle and a lithium nucleus. The α-particle in its turn produces an ionisation track which can be used to detect *indirectly* the presence of neutron.

Thus ***a neutron counter*** must contain some gas that ionises after neutron-collision with its molecules. This is possible with *boron-trifluoride gas*, BF_3, in which the boron atoms produce α-particles which are detected in the usual manner. Neutron counters are thus either *ionisation chambers with electrodes coated with boron* or *proportional counters with* BF_3 *gas in it.*

A typical BF_3-counter consists of a cylindrical cathode, usually made of stainless steel, with an axial anode wire of tungsten of dia $\sim$ 0.5 mm. The operating voltage ranges between 2000-2500 V at a gas pressure $\sim$ 100-600 torr (1 torr = 1 mm of Hg). For greater efficiency of detection, the gas is prepared using boron, highly enriched in ^{10}B isotope.

The efficiency of a BF_3-counter depends on the energy of the neutron.

- He-3 *proportional counters* are also used as a *neutron detector*. The pulse-producing charged particles (protons) are produced in nuclear reactions induced by thermal neutrons in the nuclei of He-3 gas filling the counter. They *can be operated at higher pressures*. The *reaction cross-section* is also *larger*. These *two factors* make the He-3 proportional counters *more efficient* than BF_3-counters.

region.

10.11. INVERSE PROCESS

(*Reciprocity Theorem*). Let us consider a reversible process $X+\alpha \rightleftharpoons Y+y$, in which X,x,Y and y occur in arbitrary numbers in a large box of volume V. We are interesting in the relation between the total cross-section $\sigma(x \to y)$, most generally $\sigma(\alpha \to \beta)$ of the reaction with entrance channel α and reaction chanal β and the total cross-section $\sigma(\beta \to \alpha)$ of the inverse reaction. For this we use the fundamental theorem of statistical mechanics (*the principle of overall balance*), which states that when the system is in dynamical equilibrium all energetically permissible states are occupied with equal probability. Here we are interested in two particular states, the reaction channels α and β. The theorem is then equivalent to stating that in a given energy range the number of possible channels in the box is proportional to the number of possible channels into the box. The latter is given by

$$N_\alpha = \frac{4\pi p_\alpha^2 \, V \, dp_\alpha}{h^3} = \frac{p_\alpha^2 \, V \, dp_\alpha}{2\pi^2 \hbar^3}.$$

Since $v = dE/dp$, hence $N_\alpha = p_\alpha^2 \, V dE_\alpha / 2\pi^2 \hbar^3 v_\alpha$. ...(59)

Similarly, we have $N_\beta = p_\beta^2 \, V dE_\beta / 2\pi^2 \hbar^3 v_\beta$. ...(60)

The energy range for the two channels must of course be the same, *i.e.* $dE_\alpha = dE_\beta$, hence

$$\frac{\text{No. of channels } \alpha \text{ in the box}}{\text{No. of channels } \beta \text{ in the box}} = \frac{N_\alpha}{N_\beta} = \frac{p_\alpha^2 \, v_\beta}{p_\beta^2 \, v_\alpha}. \quad ...(61)$$

The system is in dynamical equilibrium when the number of the transitions $\alpha \to \beta$ per second is equal to the number of transitions $\beta \to \alpha$ per second. The condition usually holds and is known as the *principle of detailed balance*. Further

No. of transitions $\alpha \to \beta$ per sec $= N_\alpha \times \omega(\alpha \to \beta)$,
where $\omega(\alpha \to \beta)$ is the transition probability for the reaction $(\alpha \to \beta)$.

Hence $p_\alpha^2 \, v_\beta \, \omega(\alpha \to \beta) = p_\beta^2 \, v_\alpha \, \omega(\beta \to \alpha)$. ...(62)

The transition probability measures the chance that one particle moving with velocity v in volume V is scattered per sec. Hence the cross-section σ which corresponds to unit incident flux is given by the relation

$$\sigma = \omega \, V / v. \quad ...(63)$$

Combining relations (62) and (63) and using $k=p/\hbar$, we have

$$k_\alpha^2\ \sigma(\alpha\to\beta)=k_\beta^2\ \sigma(\beta\to\alpha) \qquad \ldots(64)$$

or

$$\sigma(\alpha\to\beta)/\bar{\lambda}_\alpha^2=\sigma(\beta\to\alpha)/\bar{\lambda}_\beta^2. \qquad \ldots(65)$$

We have assumed zero intrinsic angular momenta for the particles so far. If I is the intrinsic angular momentum of any one of the particles, the corresponding density of states then must be multiplied by $2I+1$. Thus if there are intrinsic momenta for X, x, Y and y, we may write

$$(2I_X+1)\ (2I_x+1)k_\alpha^2\sigma(\alpha\to\beta)=(2I_Y+1)(2I_y+1)k_\beta^2\sigma(\beta\to\alpha). \qquad \ldots(66)$$

If the initial and final states have definite angular momenta then the above equation must be employed.

At high energies the cross-section approaches the classical value πR^2 and increases with decreasing energy, but less strongly than $\pi(R+\lambda\!\!\!^{-})^2$, because of the reflection at the nuclear boundary.

Similar approach can also be used to obtain an expression for the reaction cross-section of charged particles. In this case the incident beam is deviated by the Coulomb potential $V(r)=Z_1Z_2e^2/4\pi\epsilon_0 r$. The incident particles reaching the nuclear surface thus have a maximum impact parameter $R[1-(B/E)]^{1/2}$, where $B=$ Coulomb barrier height$=V(R)$. Hence the reaction cross-section can be expressed as

$$\sigma c=\pi R^2[1-B/E] \qquad E>B$$
$$=0 \qquad E<B. \qquad \ldots(86)$$

Here we see that the high energy limit of this eqn is πR^2, identical to that for neutrons.

An attempt to obtain a better fit to the continuum theory value of σc has been made by Destrovsky *et.al.* in 1959.

10.14. RESONANCE : BREIT WIGNER DISPERSION FORMULA

The concept of cross-section and level width can be applied to resonances in a quantitative way. In the particularly important case of resonance processes, a theoretical formula for the cross-section was derived by G. Breit and E.P., Wigner in the United States in 1936. In its simplest form, it gives the value of the cross-section in the neighbourhood of a single resonance level formed by an incident particle with zero angular momentum and charge zero so that spin and the Coulomb effects can be ignored. The result is analogous to the theory of optical dispersion, so that the main formula obtained is often called the *dispersion formula.*

Whether or not the level of a compound nucleus is bound, excitation by an incident particle can be treated as analogous to the excitation of the oscillations produced in an electric circuit by an electromagnetic wave. We therefore, expect the nuclear cross-section to vary with the incident energy in the same way that the energy in a forced oscillation varies with incident frequency. The classical resonant circuit absorbs energy because of resistive levels. In the nuclear case, damping arises because of the possibility of decay. Because of this possibility the nuclear state has a finite width Γ. The wave function of a decaying state of mean energy E_0 may be written as

$$\psi(r,t)=\psi(r)e^{-iE_0 t/\hbar}\, e^{-\Gamma t/2\hbar}. \qquad \ldots(87)$$

This corresponds to an exponential decrease of intensity of excitation $|\psi(r,t)|^2$ with a time constant $\tau\ (=\hbar/\Gamma)$. This wave function also shows that a decaying state is not a state of definite energy E of the form $\Psi(r)\, e^{-i(E/\hbar)t}$. Never the less, it can be

represented by a superposition of states of slightly different energies E, each with a different amplitude $A(E)$

$$\psi(r,t)=\int_{-\infty}^{+\infty} A(E)\, e^{-iEt/\hbar}\, dE. \qquad \ldots(88)$$

Using the Fourier analysis technique, we can show that the energies E are grouped about a mean energy E_0 with a spread of the order of $\Gamma=\hbar\lambda$. Equating eqns (87) and (88), we get

$$e^{-\Gamma t/2\hbar}=e^{-\lambda t/2}=\int_{-\infty}^{+\infty} A(E)e^{-i(E-E_0)t/\hbar}\, dE. \qquad \ldots(89)$$

According to the Fourier theorem any well behaved function $f(t)$ can be represented as

$$f(t)=\frac{1}{2\pi}\lim_{\Omega\to\infty}\int_{-\Omega}^{\Omega} e^{-i\omega t}\, d\omega\int_{-\infty}^{\infty} e^{i\omega t'}\, f(t')dt'. \qquad \ldots(90)$$

Applying this to the function $e^{-\lambda t/2}$, we get

$$A(E)=\frac{1}{2\pi\hbar}\int_0^{\infty} e^{[i(E-E_0)/\hbar-\lambda/2]t'}\, dt'$$
$$=\frac{i}{2\pi}\frac{1}{(E-E_0)+i\hbar\lambda/2}. \qquad \ldots(91)$$

Here we have assumed that the decaying system was prepared at the time $t=0$. The probability of finding the system with a given energy E is proportional to

$$|A(E)|^2=\frac{1}{4\pi^2}\frac{1}{(E-E_0)^2+(\hbar\lambda/2)^2}\quad\frac{1}{4\pi^2}\frac{1}{(E-E_0)^2+\Gamma^2/4} \ldots(92)$$

This gives the level shape. It is exactly as for pure radiative decay except that particle emission is now included by using the total width Γ instead of the radiative width Γ_r. The cross-section for excitation of the level by collision of particle x width nucleus X is, therefore, expected to have the form

$$\sigma_x=C/[(E-E_0)^2+\Gamma^2/4], \qquad \ldots(93)$$

where C is constant. For the determination of C, let us suppose that the compound nucleus formation and decay processes take place in a box of volume V which contains one nucleus X and one particle x. If the states are quantised, the no. of states of motion of particles with momentum between p and $p+dp=(4\pi p^2dpV)/h^3$.

The probability of formation of the compound level per unit time = No. of possible states of motion × probability that the nucleus X is contained within the small volume $\sigma_x v$ swept out by the effective collision area per sec., i.e.

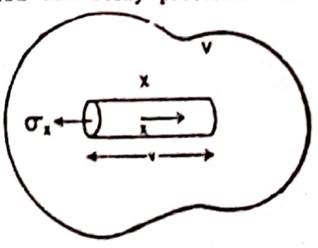

Fig. 10.1. Formation and decay of a compound nucleus in a single channel.

$$dP=\frac{4\pi p^2 dp}{h^3}V.\frac{\sigma_x v}{V}=\frac{4\pi}{h^3}v\sigma_x p^2 dp.$$

Substituting the value of σ_x from eqn (93) in the above eqn and integrating over the energy spectrum, we get

$$P=\int_{-\infty}^{+\infty}\frac{4\pi}{h^3}v.p^2.\frac{C}{(E-E_0)^2+\Gamma^2/4}\,d;$$

$$=\int_{-\infty}^{+\infty}\frac{4\pi C}{h^3}.\frac{1}{(E-E_0)^2+\Gamma^2/4}\,dE.$$

If we assume that the variation of the channel wavelength λ of the particle over the level width Γ may be neglected, then the probability of formation per sec

$$=\frac{4\pi C}{h\lambda^2}.\frac{2}{\Gamma}\left[\tan^{-1}\frac{2(E-E_0)}{\Gamma}\right]_{-\infty}^{+\infty}$$

$$=\frac{4\pi C}{h\lambda^2}.\frac{2}{\Gamma}.\pi=\frac{C}{\hbar\pi\bar{\lambda}^2\Gamma}. \qquad \text{...(94)}$$

Probability of decay per sec $=\Gamma_x/\hbar$,

where Γ_x is the partial width of the compound level for the emission of x. In the equilibrium state the probability of formation per sec would equal to the probability of decay per sec of the excited state back into the system $X+x$. Hence

$$C/\pi\hbar\bar{\lambda}^2\Gamma=\Gamma_x/\hbar \text{ or } C=\pi\bar{\lambda}^2\Gamma\Gamma_x, \qquad \text{...(95)}$$

Substituting this value in eqn. (93), the cross-section for the formation of the level becomes

$$\sigma_x(E)=\frac{\pi\bar{\lambda}^2\Gamma\Gamma_x}{(E-E_0)^2+\Gamma^2/4} \qquad \text{...(96)}$$

For the process $X\,(x, y)\,Y$, we obtain reaction cross-section as

$$\sigma_r=\sigma_{xy}(E)=\frac{\sigma_x\Gamma_y}{\Gamma}=\pi\bar{\lambda}^2\frac{\Gamma_x\Gamma_y}{(E-E_0)^2+\Gamma^2/4}. \qquad \text{...(97)}$$

Here Γ_x and Γ_y are partial level widths defined as

$$\Gamma_x\tau_x=\hbar \text{ and } \Gamma_y\tau_y=\hbar.$$

where τ_x and τ_y are the main life times that the compound nucleus would have if elastic scattering of x or the emission of y were the only possible modes of decay.

If spin is considered, the right hand side of eqn (97) must be multiplied by the factor

$$g_c=(2I_c+1)/(2I_x+1)\,(2I_X+1), \qquad \text{...(98)}$$

where I_x is the total angular momentum of the incident particle, I_X is that of target nucleus and I_c is of the compound state, which is

formed only by those orbital angular momentum l_x which satisfy the conditions

$$I_c=I_X+I_x+l_x \text{ and } \Pi_X\Pi_x(-1)^{l_x}=\Pi_c. \qquad \text{...(99)}$$

Hence for the nuclear reaction in which particles have definite spins, the relation (97) can be written as

$$\sigma_r=\pi\bar{\lambda}^2\frac{(2I_c+1)}{(2I_x+1)\;(2I_X+1)}\frac{\Gamma_x\Gamma_y}{(E-E_0)^2+\Gamma^2/4}. \qquad \text{...(100)}$$

This is known as the *Breit Wigner resonance formula*. For the (n, γ) reaction in particular

$$\sigma(n,\gamma)=\pi\bar{\lambda}^2\frac{(2I_c+1).\quad\Gamma_n\Gamma_\gamma}{2(2I_X+1)(E-E_0)^2+\Gamma^2/4.} \qquad \text{...(101)}$$

This is maximum when $E=E_0$ and is equal to

$$\sigma_{max}\,(n,\gamma)=4\pi\bar{\lambda}^2 g_c\Gamma_n\Gamma_\gamma/\Gamma^2. \qquad \text{...(102)}$$

For $E=E_0\pm\Gamma/2$, $\sigma=\frac{1}{2}\sigma_{max}$ and hence Γ is the full width at half maximum. A sharp resonance corresponds to a narrow width

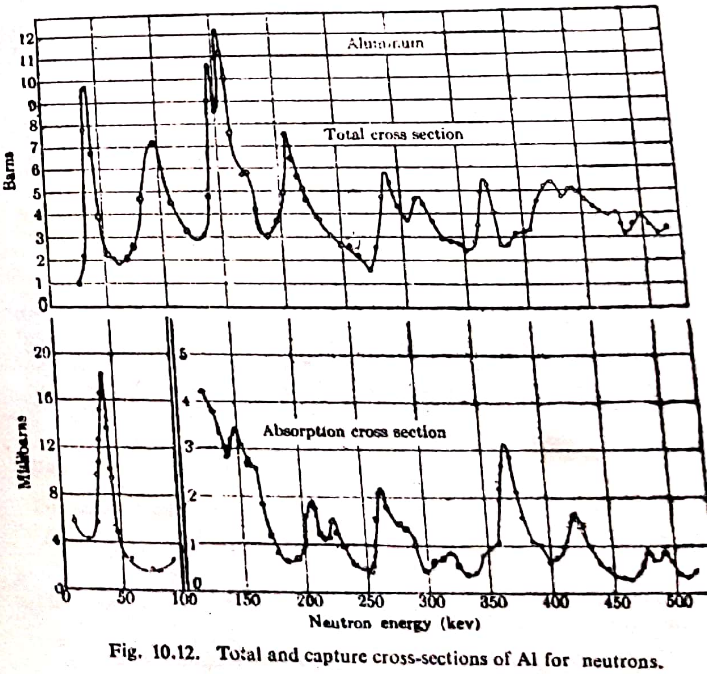

Fig. 10.12. Total and capture cross-sections of Al for neutrons.

Γ and thus to an excited state of long life. A largest possible capture cross-section will occur when $\Gamma_n=\Gamma_\gamma=\Gamma/2$. Its maximum possible value $\sigma_{max}=\pi g c\bar{\lambda}^2$. The width of the resonance peak affects the cross-section. In a general way, if the peak is broad, covering a large energy range, the cross-sections are likely to be somewhat decreased as compared with the case of sharp and narrow peak. The width of the peak is inversely related with the life of the excited state of the compound nucleus.

The total cross-section σ_t and the radioactive capture cross-section $\sigma(n, \gamma)$ have been measured as functions of the incident neutron energy. Some of the results are shown in fig. 10.12 in which these cross-sections are plotted as functions of energy in the intermediate range (10−500 keV). In this energy range total cross-section for Al^{27} is practically equal to the elastic scattering cross-section as only reactions in this case are the elastic scattering and radioactive capture.

Equation (100) applies to all resonance cross-sections except for the elastic re-emission of the incident particle $\sigma(x, x)$, *i.e. elastic resonance scattering*. Besides compound nucleus scattering (i.e. absorption and re-emission of neutron of the same energy), the incident particle wave is scattered by the nucleus as if it were an impenetrable sphere. This type of scattering is known as *potential* or *shape-elastic scattering*. The elastic-scattering cross-section σ_{el} is given by

$$\sigma_{el}=4\pi\bar{\lambda}^2\left[gc\left|\frac{\Gamma_n/2}{(E-E_0)+i\Gamma/2}+e^{i\phi_l}\sin\phi_l\right|^2+(1-gc)\sin^2\phi_l\right]. \qquad ...(103)$$

where ϕ_l is an energy dependence quantity known as the hard sphere phase shift. For $l=0$ or S-wave neutrons $\phi=R/\bar{\lambda}=Rk$. Hence for S-wave neutrons on a spinless target

$$\sigma_{el}=4\pi\bar{\lambda}^2\left|\frac{\Gamma_n/2}{(E-E_0)+i(\Gamma/2)}+e^{ikR}\sin kR\right|^2. \qquad ...(104)$$

Here the coefficient $4\pi\bar{\lambda}^2$ is the maximum possible S-wave scattering cross-section. The first term between bars is called the resonance scattering amplitude, which if present alone would lead to eqn (97). The second term is called the *potential scattering amplitude*, which if present alone would lead to

$$\sigma_{el}=4\pi\bar{\lambda}^2\sin^2 kR. \qquad ...(105)$$

This term varies smoothly with energy. For small energies $kR \ll 1$. As $E\rightarrow 0$, we get

$$\sigma_{el} \simeq 4\pi R^2, \qquad ...(106)$$

which is the potential scattering cross-section for an impenetrable sphere when $R \ll \bar{\lambda}$.

The resonance term rises to large values near $E=E_0$, but is small elsewhere. For $E<E_0$ the two terms interfere destructively

yielding a low value of σ_{el}. For $E>E_0$ the interference is constructive. For charged particles, resonance scattering involves coherence between Coulomb potential scattering, nuclear potential scattering and resonance scattering.

Let us consider the lowest energy resonance of the compound nucleus. For $E \ll E_0$, the denominator of eqn (101) does not change much with E and Γ_γ is independent of E but Γ_n does depend on E. Hence $\sigma(n, \gamma) \propto \bar{\lambda}^2\Gamma_n$. The probability of elastic emission of a neutron of energy E (momentum p) is proportional to the density of states in momentum space around p. Hence

$$\Gamma_n \propto p^2 dp/dE \left\{\begin{array}{l} E=p^2/2m \\ dE=(p/m)dp \end{array}\right\}$$
$$\propto p$$

Thus we have

$$\sigma(n, \gamma) \propto \bar{\lambda}^2 p$$
$$\propto 1/p \qquad (\because \bar{\lambda}=\hbar/p)$$
or $$\propto 1/v, \qquad ...(107)$$

where v is the velocity of neutron. *It is known as 1/v-law.* Thus Breit-Wigner formula leads to the conclusion that at low neutron energies the cross-section should be inversely proportional to the neutron speed. Following ***1/v region*** there occurs the *resonance region* in which the cross-sections rise sharply to high values. The cross-sections are low with neutrons of very high energy.

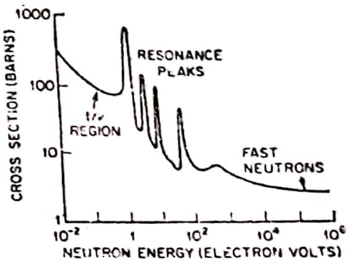

Fig. 10.13. Curve of neutron cross-sections showing 1/v, resonance, and fast neutron regions.

10.15. OPTICAL MODEL

The continuum theory does not stand upto experimental tests satisfactorily. Barschall plotted the measured total neutron cross-sections in a three dimensional graph against the neutron energy E and the mass number A, and found that the cross-sections did not decrease smoothly with increasing E, as predicted by the theory, and that the trend of those maxima and minima with energy was a smooth function of A. He showed that the disagreement with the theory was not due to unexpected resonances in individual nuclides, but to a general flow in our theory. The widely spaced shallow maxima and minima were expected from scattering by a potential well, as in the shell model. Thus we see that *our compound nucleus theory must be modified in the light of shell model idea.*

A mathematical mode, known as *optical model*, pictures the interaction among the nucleus as being intermediate to that predicted by the continuum and shell models of the nucleus. It is the model of a complex nuclear potential, the real part produces a potential scattering like the scattering by a hard sphere and imaginary part corresponds to the cross-section for compound nucleus formation. The nucleus can thus be viewed as a *cloudy crystal ball,* The Fermi gas model is not useful for the prediction of the detailed properties of low lying states of nuclei observed in the radioactive decay processes. Though the model suggests that nucleon collisions will not often transfer small amount of momentum to the nucleus, because the nucleon momentum states near the origin are filled. A nucleon in an excited state is no longer embedded in the Fermi gas. Its interactions with the remaining nucleons become more and more important with increasing excitaion energy. Hence highly excited states of nuclei are many body states in which the energy is shared by many particles. An exciteo nucleus is more like a normal condensed material than a nucleus in the ground state. For a nucleus composed of many particles, the only practical way of describing nuclear excitation is in the statistical approach. This statistical approach is applicable even to unbound states for medium and heavy nuclei.

9.3. LIQUID DROP MODEL

A nuclear model usually associated with the semi-empirical mass formula was suggested by Bohr in 1937. In this model the finer features of nuclear forces are ignored but the strong internucleon attraction is stressed. The essential assumptions are ; (1) The nucleus consists of incompressible matter so that $R=R_0A^{1/3}$; (2) The nuclear force is identical for every nucleon ; (3) The nuclear force saturates. Thus one might inquire whether a nucleus can be represented as a crystalline aggregate of nucleons. But it gives that the zero point vibrations of the nucleons about their mean rest positions would be too voilent for stability. Hence the individual nucleons must be able to move about within the nucleus much as does an atom of a liquid and one might, therefore, think of a nucleus as being like a *small drop of liquid*. Such a model is thus known as *liquid drop model*.

The idea that the molecules in the drop of liquid correspond to the nucleons in the nucleus is confirmed due to following similarities : (1) The nuclear forces are analogous to the surface tension force of a liquid ; (2) The nucleons behave in a manner similar to that of molecules in a liquid ; (3) The fact that the density of nuclear matter is almost independent of A shows resemblance to liquid drop where the density of a liquid is independent of the size of the drop ; (4) The constant binding energy per nucleon is analogous to the latent heat of vaporisation ; (5) The disintegration of nuclei by the emission of particles is analogous to the evaporisation of molecules from the surface of liquid ; (6) The energy of nuclei corresponds to internal thermal vibrations of drop molecules ; (7) The formation of compound nucleus and absorption of bombarding particles are correspond to the condensation of drops.

Inspite of these similarities we see following differences : (1) Molecules attract one another at distances larger than the dimensions of the electron shells and repel strongly when the distance is smaller than the size of the electron orbits. Nuclear forces are attractive within the smaller range, *the range of nuclear forces*. (2) The average K. E. of the molecules in the liquid is of the order of 0·1, eV, the corresponding de Broglie wavelength is 5×10^{-11} m which is very much smaller than the intermolecular distances. The average K. E. of nucleons in nuclei is of the order of 10 MeV, the corresponding $\lambda\simeq6\times10^{-15}$ m, which is of the order of inter-nucleon distances. Hence the motion of the molecules in the liquid is of classical character whereas in nuclei the motion of the nucleons is of quantum character.

Semi-empirical formula gives no information about any other properties of nuclei than their energies and the Z/A ratio. In estimating the properties of the excited states of nuclei, one has to consider deformation of a spherical drop giving rise to periodic oscillations of the surface.

A spherical drop (a nucleus) of radius R_0 is deformed. If $R(\theta, \phi)$ be the distance of the deformed surface from the centre at an angle θ, ϕ, the difference can be expressed as

$$q(\theta, \phi)=R(\theta, \phi)-R_0=\sum_{l=0}^{\infty}\sum_{m=-l}^{l} q_{lm}\, Y_{lm}(\theta, \phi). \quad ...(5)$$

To make the problem simpler, let us consider cylindrically symmetric deformations for which $m=0$ and $q_{l\,0}$ oscillate harmonically in time as

$$q_{l,0}=q_l \cos(\omega_l t). \quad ...(6)$$

The characteristic frequency ω_l is determined by the dynamics of the vibration. The surface tension opposes the surface deformation. Since the liquid is incompressible, the waves at the surface implies motion within the liquid. The wavelength of surface vibrations of a liquid drop is given by the relation $\bar{\lambda}=R/l$. The mass μ participating in the vibration is equal to the mass of the outer shell of thickness $\bar{\lambda}$, given by

$$\mu\simeq M(3\bar{\lambda}/R). \quad ...(7)$$

The kinetic energy in the vibration $T=\frac{1}{2}\mu\dot{q}_l^2$. ...(8)

Due to the wave of amplitude q_l and wavelength $\bar{\lambda}$, the plane surface S increases by an amount

$$\Delta S\simeq\tfrac{1}{2}(q_l/\bar{\lambda})^2\, S. \quad ...(9)$$

The change in surface energy of the drop $\Delta S\alpha$ is equal to the potential energy. Hence we get

$$\Delta E_s=\tfrac{1}{2}(q_l/\bar{\lambda})^2\, S\alpha=\tfrac{1}{2}K\, q_l^2. \quad ...(10)$$

From relations (8) and (10), we get the frequency

$$\omega_l=(K/\mu)^{1/2}=(4\pi\alpha l^3/3M)^{1/2}. \quad ...(11)$$

The specific properties of the spherical surface change the l^3 into $l(l-1)(l+2)$. The surface tension coefficient α can be calculated in terms of surface energy $E_s=a_s A^{2/3}$ as

$$4\pi R^2\alpha = E_s = a_s A^{2/3} \quad \text{or} \quad \alpha = a_s/4\pi R_0^2. \qquad \ldots(12)$$

Hence relation (11) becomes

$$\omega_l \simeq [\, l(l-1)\,(l+2)\,(a_s/3R_0^2\, MA)]^{1/2}. \qquad \ldots(13)$$

This gives us too high value of the excitation energy. The frequency ω_l is reduced by the Coulomb effect, as

$$\omega_l = \left[\, l\,(l-1)\left\{(l+2) - \frac{10\gamma}{2l+1}\right\}\frac{a_s}{3r_0^2 MA}\right]^{1/2}, \qquad (14)$$

where γ is the ratio between the Coulomb energy $E_c = \frac{3}{5}Z^2e^2/4\pi\epsilon_0 R$ and the surface tension energy $E_s = 4\pi\alpha R^2 = a_s A^{2/3}$. This equation leads to somewhat smaller frequencies for heavier nuclei, but is insufficient to represent the actual level distances.

Relation (14) shows that the frequency becomes imaginary when γ is larger than a certain limiting value γ_c. Its smallest value is 2 for $l=2$. Hence condition for stability against surface deformation is

$$\gamma_c(=E_c/E_s = 0.0474\, Z^2/A) < 2 \quad \text{or} \quad Z^2/A < 42.2. \qquad \ldots(15)$$

We, therefore, expect in this model that the nuclei near the limit of Z^2/A split into two parts by the additional supply of small amounts of energy.

We summarise the results : The liquid drop model not only gives atomic masses and binding energies accurately, but also predicts α-and β emission properties. The binding energy formula does not include closed shell effects, but it can be used to provide a base line from which shell effects can be calculated. This model is able to explain certain features of nuclear fission, but is not very successful in describing the actual excited states as it gives too large level distances. *This model is the forerunner of the collective model of nuclear structure.* It forms the basis of Bohr's theory of the compound nucleus formation in nuclear reactions.

9.4. SHELL MODEL

In the liquid drop model we have emphasized the properties of nuclear matter and have said nothing about single nucleons. This is a great departure from the atomic model where the emphasis is on the motion of the electrons in the field provided by the nucleus. Now questions are : Can be nucleons exist in well ordered quantum controlled nuclear shells ? Is there any evidence for the grouping of nucleons into shells ? Can quantum numbers similar to n, l, s, j be applied to the nucleus ? For certain numbers of neutrons or protons, *called magic numbers*, nuclei exhibit special characteristics of stability reminiscent of the properties shown by noble gases among the atoms. Nuclei in which either N or Z is equal to one of these magic numbers (2, 8, 20, 28, 50, 82, 126) show certain paticulars that are not understandable in terms of the liquid drop model. We will see that the magic numbers of the nucleons can be explained with a shell model of the nucleus. Evidently protons and neutrons in the nucleus are not all equivalent as had been assumed in introducing the liquid drop model. We will see that this model is capable of explaining not only the magic numbers but also many other nuclear properties such as spin, magnetic moment and energy levels.

1. Evidence for the existence of Magic numbers—(1) Mayer in 1948 suggested that nuclei with a magic number of nucleons are especially abundant in nature.

(2) $_2He^4$, and $_8O^{16}$ are particularly stable, can be seen from the binding energy curve. Thus we see that numbers 2, 8, indicate stability.

(3) Above $Z=28$, the only nuclides of even Z which have isotopic abundances exceeding 60% are Sr^{88} ($N=50$), Ba^{138} ($N=82$) and Ce^{140} ($N=82$).

(4) No more than five isotones occur in nature for any N except $N=50$, where there are six and $N=82$, where there are seven. Neutron numbers of 82, 50, therefore, indicate particular stability.

(5) Sn ($Z=50$) has ten stable isotopes, more than any other element, while Ca ($Z=20$) has six isotopes. This indicates that elements with $Z=50$ and $Z=20$ are more than usually stable.

(6) Alpha decay energies are rather smooth functions of A for a given Z but show striking discontinuities at $N=126$. This represents the magic character of the number 126 for neutrons.

(7) Very similar relations exist among the energies of beta-ray emissions. These energies are abnormally large when the neutron or proton number of the final nucleus assumes a magic value

(8) The particularly weak binding of the first nucleon outside a closed shell is shown by the unusually low probabilities for the capture of neutrons by nuclides having $N=50$, 80 and 126.

(9) It is found that some isotopes are spontaneous neutron emitters when excited above the nucleon binding energy by a preceding β-decay. These are : O($N=9$), Kr ($N=51$) and Xe($N=83$)

(10) Nuclei with the magic proton numbers 50 (Sn) and 82 (Pb) have much smaller capture cross-sections than their neighbours.

(11) The doubly magic nuclei (Z and N both magic numbers) $_2He^4$, $_8O^{16}$, $_{20}Ca^{40}$ and $_{82}Bb^{208}$ are particularly tightly bound.

(12) The binding energy of the next neutron or proton after a magic number is very small.

(13) The asymmetry of the fission of uranium could involve the sub-structure of nuclei, which is expressed in the existence of the magic numbers.

(14) The Schmidt theory of magnetic moments for odd A nuclides shows that the ground states of these nuclides change from even parity to odd parity or vice versa at the numbers $A=4$, 16, 40, when the nucleon numbers are 2, 8 and 20 respectively.

(15) The electric quadrupole moments of nuclei show sharp minima at the closed shell numbers, indicating that such nuclei are nearly spherical.

2. Extreme Single Particle Model. In this model it is assumed that the nucleons in the nucleus move independently in a common (mean) potential, determined by the average motion of all the other nucleons. Most of the nucleons are paired so that a pair of nucleons contributes zero spin and zero magnetic moment. The paired nucleons thus form an inert core. The properties of odd A nuclei are characterized by the unpaired nucleon and of odd-odd nuclei by the unpaired proton and neutron. In order to understand some of the properties of nuclei including the magic numbers two cases, *infinite square well* and *harmonic oscillator potentials* are considered. In these cases we can obtain an exact solution. They provide two contrasting view points. The square well has an infinitely sharp edge where as the harmonic oscillator potential diminishes steadily at the edge. The addition of the spin orbit potential eliminates some of the difficulties experienced with the above two potentials.

The starting point of all shell models is the solution of the Schrodinger equation for a particle moving in a spherically symmetrical central field of force. The eigenstates available to a nucleon of mass M moving in a (mean) spherically symmetrical potential $V(r)$ are determined by the solutions of the equation

$$\left(\nabla^2+\frac{2M}{\hbar^2}\{E-V(r)\}\right)\psi(r)=0, \qquad \ldots(16)$$

where E is the energy eigenvalue. In such a relation reduced mass m is replaced by M, as in a heavy nucleus m is practically equal to the nucleon mass M. The general solution of this equation can be written as

$$\psi_{nlm}(r,\theta,\phi)=u_{nl}(r)\,Y_{lm}(\theta,\phi), \qquad \ldots(17)$$

where $u_{nl}(r)$ is the radial function and Y_{lm} (θ,ϕ) are the spherical harmonics. The set of quantum numbers n, l, m determines an eigenstate corresponding to an eigen-value E_{nl}. The radial wave-function $u_{nl}(r)$ is a solution of the equation

$$\frac{1}{r^2}\frac{d}{dr}\left(r^2\frac{du_{nl}}{dr}\right)+\frac{2M}{\hbar^2}\left[E_{nl}-V(r)-\frac{l(l+1)\hbar^2}{2Mr^2}\right]u_{nl}=0 \qquad \ldots(18)$$

(*a*) *Square-well of Infinite Depth*. We will here first treat the manageable problem of calculating the position of the various energy levels in an infinitely deep square well of radius R. For simplicity let us assume that the potential is zero inside the well and infinite outside. Outside and at the boundary of the well the radialwavefunction u_{nl} (r) vanishes. The radial solutions are regular at the origin and inside the well are the spherical Bessel functions $j_l(k_{nl}r)$.

$$\therefore\quad u_{nl}(r)=j_l(k_{nl}r)=\frac{A}{\sqrt{(k_{nl}r)}}\,J_{l+1/2}(k_{nl}r)\,, \qquad \ldots(19)$$

where A is a constant, $J_{l+1/2}(k_{nl}r)$ is a Bessel function and k_{nl} is the wave number can be defined by the equation

$$k_{nl}^2=\frac{2M}{\hbar^2}\Big[E_{nl}-V(r)\Big]. \qquad \ldots(20)$$

where E_{nl} is the total $-$ve energy and V($=-$U) is the well depth. It is better to measure energies from the bottom of the well and then we have

$$k_{nl}^2=(2M/\hbar^2)E'_{nl}, \qquad \ldots(21)$$

where E'_{nl} is positive, measured from the bottom of the well.

The permitted values of k_{nl} are selected by the boundary condition. In the simple case of a well of infinite depth, the wave function has to vanish at the nuclear boundary. Thus at $r=R$

$$u_{nl}(R)=j_l(k_{nl}R)=0.$$

Each l-value has a set of zeros and each of them corresponds to a value of k_{nl} given by $k_{nl}R=x$. Thus the eigen-value $k_{nl}R$ is the n^{th} zero of the l^{th} spherical Bessel function. The number n, giving the number of zeros of the radial part of the wavefunction (not counting the origin), is known as the *radial quantum number*. It differs from the principal quantum number of atomic spectroscopy, since the latter counts all the total wavefunction, angular as well as radial and is of major importance for specifying the energy of the corresponding state.

Fig. 9.2. is a graph of spherical Bessel function for $l=0$, 1 and 2. There is succession of zeros at $k_{nl}R=x$, numbered serially $n=1, 2\ldots$and these values differ for different l. The order of levels in a spherical square well of infinite depth is given by the order of the zeros in the Bessel functions. We indicate such levels in order of increa ing energy. The level energies are given by the relation

$$E'_{nl}=k^2_{nl}\hbar^2/2M=(\hbar^2/2MR^2)x^2. \qquad \ldots(22)$$

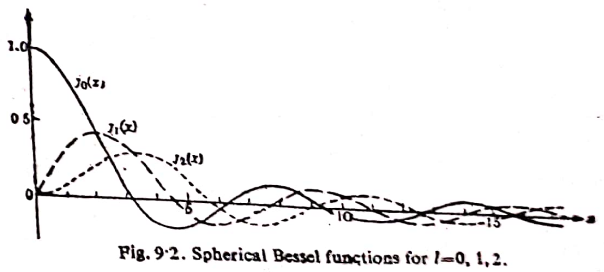

Fig. 9·2. Spherical Bessel functions for $l=0, 1, 2$.

above results that the closure of a shell for the harmonic oscillator potential occurs corresponding to neutron or proton numbers 2, 8, 20, 40, 70, 112 and 168, whereas the square well potential suggests magic numbers at 2, 8, 18, 20, 34, 40, 58, 68, 70, 92, 106, 112, 138 and 156. Experimentally observed values are 2, 8, 20, 50, 82 and 126. Thus the truth may lie in between these two potentials.

(C) *Spin-Orbit Potential.* Several attempts have been made to modify the potentials to yield the observed magic numbers. Mayer and Haxel, Jensen and Suess in 1949, suggested that a non-central component should be included in the force acting on a nucleon in a nucleus. It is corresponding to the interaction between the orbital angular momentum and the intrinsic angular momentum (spin) of a particle. The magnetic moment is associated with the spin angular momentum and the magnetic field is induced due to the orbital angular momentum. This magnetic field has an effect on the magnetic moment. The interaction energy

$$W=-\vec{\mu}_s.\vec{B}=-f(r)\,\mathbf{s}.\mathbf{l}, \qquad \ldots(28)$$

where **s** and **l** denote the spin and orbital angular momentum vectors respectively and $f(r)$ is a potential function. Thus the potential which determines the single particle wave function will be $V(r)-f(r)$ s.l. where $V(r)$ and $f(r)$ depend only on the radial distance and the size

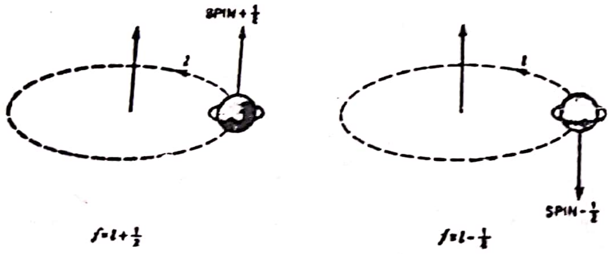

Fig. 9.4. Coupling of orbital and spin angular momenta of a nucleon.

of the nucleus. Because of the strong coupling, the two vectors combine to a total angular momentum **j** for this particle. Since $s=\frac{1}{2}$, there are only two possible ways of combining s and l, resulting in the *stretch case* $j=l+s$ and the *jacknife case* $j=l-s$. We can find the product s.l by the cosine rule applied to the triangle formed by the vectors **s**, **l** and **j**, as follows—

$$\mathbf{l}=\tfrac{1}{2}[\mathbf{j}^2-\mathbf{l}^2-\mathbf{s}^2]=\tfrac{1}{2}[j(j+1)-l(l+1)-s(s+1)]$$
$$=\tfrac{1}{2}l \qquad \text{for} \qquad j=l+\tfrac{1}{2}$$
$$=-\tfrac{1}{2}(l+1) \qquad \text{for} \qquad j=l-\tfrac{1}{2}. \qquad \ldots(29)$$

The energy shifts from the central value are

$$\Delta E_{nl}=-\tfrac{1}{2}l\int dr|\psi_{nl}(r)|^2 f(r) \qquad \text{for } j=l+\tfrac{1}{2}$$
$$=\tfrac{1}{2}(l+1)\int dr|\psi_{nl}(r)|^2 f(r) \qquad \text{for } j=l-\tfrac{1}{2} \qquad \ldots(30)$$

and the total spin-orbit energy splitting is

$$\Delta(\Delta E_{nl})=\Delta E_{nl}(j=l-\tfrac{1}{2})-\Delta E_{nl}(j=l+\tfrac{1}{2}),$$
$$=(l+\tfrac{1}{2})\int dr|\psi_{nl}(r)|^2 f(r). \qquad \ldots(31)$$

Thus we see that the spin orbit interaction splits each of the higher single particle levels. The term with $j=l+\frac{1}{2}$ lies lower in energy and is thus more tightly bound, than the term with $j=l-\frac{1}{2}$. The splitting increases with l and can become so large that for a given n the term with the largest l value and $j=l+\frac{1}{2}$ can slide down to energies as low as those of the multiplet with quantum number $(n-1)$. The effect of such an spin-orbit coupling is analogous to the effect of the magnetic coupling that causes the fine structure splitting in atomic physics, but such effects are much too weak to give necessary splitting. There is an evidence for the existence of a strong spin-orbit force between nucleons from high energy polarisation experiments. Sequence of energy levels is like that shown in figure 9.5. Spectroscopic notation is used here to denote the terms. The letters (s, p, d,... etc.) determine l and the subscripts the j, the total angular momentum quantum number. The number in front of the letter is 1 if the symbol following appears for the first time, 2 if it appears for the second time and so on. Spin-orbit level scheme also shows that the odd-parity $1h_{11/2}$-level is grouped with the even-parity $3s_{1/2}$ level, although the energy difference between these is small and they are markedly different in their spins. Similarly $1g_{9/2}$ and $2p_{1/2}$; $1i_{13/2}$ and $3p_{1/2}$ are bounded together.

The lowest state $1s_{1/2}$ holds two nucleons. There is thus a closed shell at 2. In the next state the interaction is not yet strong enough to separate the $1p_{3/2}$, and $1p_{1/2}$ levels by an amount comparable with well spacing so the next closed shell occurs, when all the $6p$ states are filled, at 2+6=8. The state $1d_{5/2}$ is definitely lower than $1d_{3/2}$, but it still forms part of the same shell. The states $1d_{5/2}$, $1d_{3/2}$ and $2s_{1/2}$ are sufficiently close to constitute a single shell. The next shell therefore, closes at 8+12=20.

For the state $1f_{7/2}$, the l value $l=3$, is high enough to lower the state below all the other $N=3$ states, but not enough to make it join the group from $N=2$. Thus this shell closes at 20+8=28. The next shell comprises $1f_{5/2}$, $2p_{3/2}$, $2p_{1/2}$ and $1g_{9/2}$. The last coming down because of spin-orbit coupling from the next higher group of levels. As it contains 22 sub-levels, this shell closes at 28+22=50.

Similarly the next shell is made up of the 32 sub-levels of $1g_{7/2}$, $2d_{5/2}$, $2d_{3/2}$, $3s_{1/2}$ and $1h_{11/2}$, closes at 50+32=82 and the one after that with 44 sub-shells of $1h_{9/2}$, $2f_{7/2}$, $2f_{5/2}$, $3p_{3/2}$, $3p_{1/2}$ and $1i_{13/2}$ at $82+44=126$.

In this way we see that the shell closures occur at particle numbers 2, 8, 20, 28, 50, 82, 128 exactly as required by experiments.

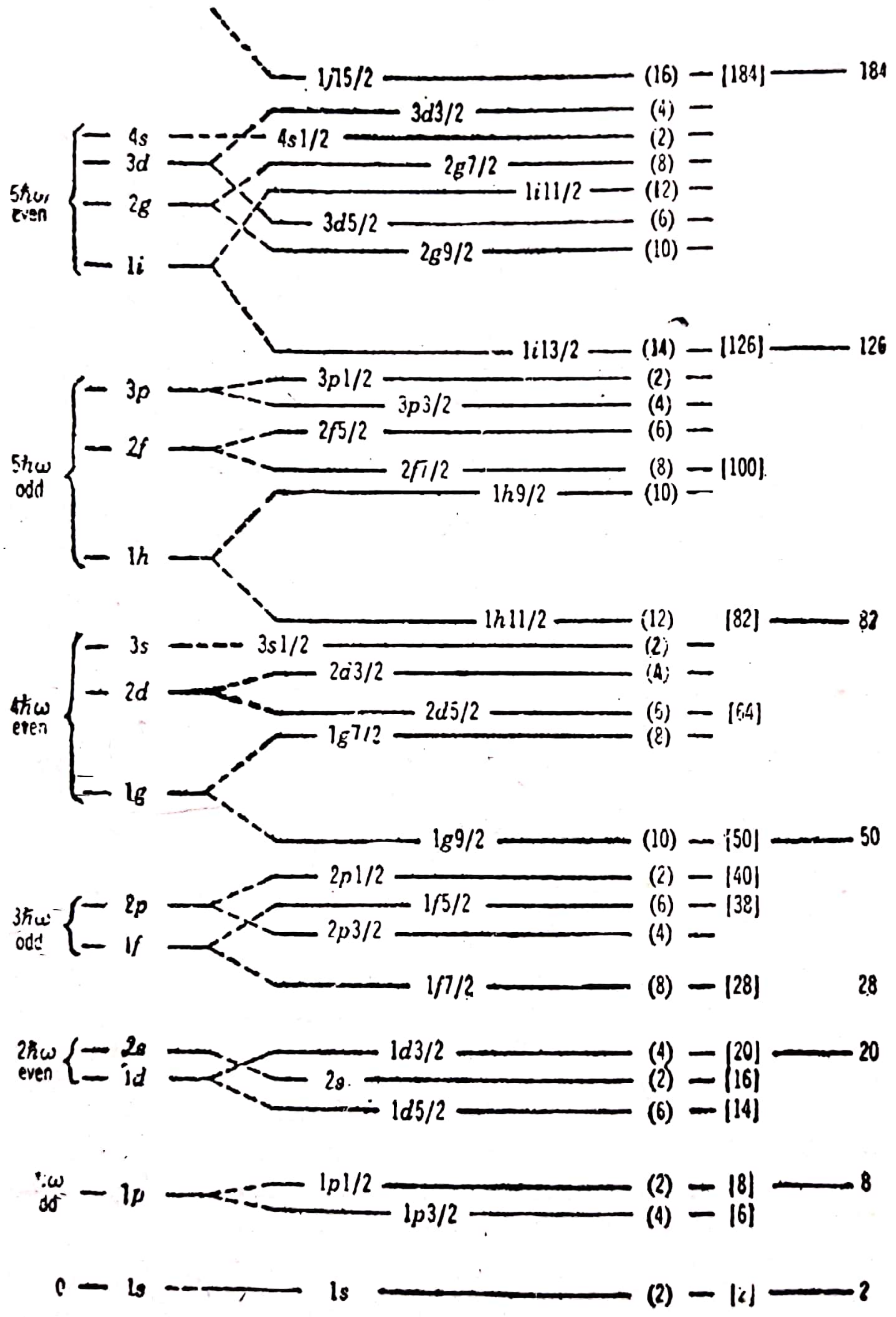

Fig. 9.5 Effect of spin-orbit coupling on the level system of a well of a shape intermediate between the square and oscillator wells. The magic numbers are given on the far right (Mayer and Jensen).

spins and parities of these states, of the unstable nuclei which decay by β-emission. Hence β-decay study is the most powerful method of getting the detailed order of orbital momenta with in the shells.

(7) *Stripping Reactions*. Stripping reactions can be explained by single particle model (See Art. 10.18).

9.5. COLLECTIVE NUCLEAR MODEL

The shell model has been most successful in explaining a number of nuclear features. The deviations of magnetic moments from the Schmidt curve make this model less acceptable. The measured quadrupole moments are several times larger than can be attributed to the odd nucleon even in nuclei with just one nucleon more or less than a closed shell, where the single particle model should be at its best. Related to it is the observation that $E2$ transitions are often much faster than would be expected for transition between single particle states.

J. Rainwater, the American physicist, in 1950, suggested that these discrepancies might be overcome in odd-A nuclei by considering the polarization of the even-even core by the motion of the odd nucleon. The nuclear core, consisting even nucleons, thus have a spheroidal rather than a spherical shape. This distortion would make an additional contribution to the quadrupole moment and to quadrupolar transition rate. The idea of the deformed nuclear core has been developed by A. Bohr and B. Mottelson. The individual nucleons are imagined to move in orbits as before in a potential distribution determined by the remaining nucleons. It is now suggested that the entire shell configuration can undergo periodic oscillations in shape. This collective motion of the nucleons influences the individual particle orbits because it changes the potential of the region in which these particles move. Because of the stability of the core, the collective motion is small and the independent particle characteristics are prominent, for the nuclei consisting of almost closed shells.

The scheme of nuclear energy levels which results from the collective motion of the nucleons in the core and interplay between the motion of losely bound surface nucleons depends upon the strength of the coupling between them. When the coupling is strong the energy states resemble with the linear molecules. Corresponding to the *rotation, vibration and electronic energy* states of a molecule, we have *rotational, vibrational and nucleonic energy* states in the nuclei. The rotations and vibrations arise from the motion of the nuclear core and the nucleonic states arise due to the motion of the loosely bound nucleons. The total energy is expressed as :

$$W = L_{rot} + E_{vib} + E_n \qquad \ldots(51)$$

Mathematically this means that the Hamiltonian is composed of three additive parts containing, (1) rotational co-ordinates, (2) vibrational co-ordinates and (3) nucleonic co-ordinates. The wave function is then the product of three wave functions each containing the respective co-ordinates.

The vibrational states of nuclei are formed by flexings of the nuclear surface and are of complex nature. Nuclear rotational motion is also some what more complex in that it is not rigid body rotation but a rotation of the shape of the deformed surface enclosing A free particles. The collective motion now becomes a vibration about the equilibrium shape, and a rotation of the nuclear orientation which maintains the deformed shape. Let us now discuss these states one by one.

1. *Vibrational States*. The nucleus is considered as an incompressible liquid drop and is described in terms of the radius vector specifying the nuclear surface. The general shape of the nuclear surface can be written as

$$R(\theta, \phi) = R_0\left[1 + \sum_{\lambda,\mu} \alpha_{\lambda\mu} Y_{\lambda\mu}^*(\theta, \phi)\right] \qquad \ldots(52)$$

where R_0 is the nuclear radius if it was spherical, $Y_{\lambda\mu}$ are the spherical harmonics representing successive modes of surface standing waves produced by surface disturbances, $\alpha_{\lambda\mu}$ are deformation parameters determining the nuclear shape, and θ and ϕ are polar angles. The subscript μ takes the values $-\lambda$ to $+\lambda$, hence there are $2\lambda+1$ modes of deformation of order λ. The mode with $\mu=0$ (for all λ values) represents an axially symmetric nuclear shape.

Any collective motions are expressed by letting $\alpha_{\lambda\mu}$ vary in time. The kinetic energy of the nuclear mass is of the form

$$T = \frac{1}{2} \sum_{\lambda,\mu} B_\lambda \,|\dot{\alpha}_{\lambda\mu}|^2 \qquad \ldots(53)$$

In the case of the irrotational flow of a constant density fluid, Rayleigh's method gives

$$B_\lambda = \rho R_0^5/\lambda, \qquad \ldots(54)$$

where ρ is the density of nuclear matter. The potential energy for collective motion is

$$V = \frac{1}{2} \sum_{\lambda,\mu} C_\lambda \,|\alpha_{\lambda\mu}|^2, \qquad \ldots(55)$$

where C_λ are the deformability coefficient, given as

$$C_\lambda = (\lambda-1)(\lambda+2)\, S\, R_0^2 - \frac{3}{2\pi}\frac{Z^2e^2}{R_0}\frac{\lambda-1}{2\lambda+1}. \qquad \ldots(56)$$

where S is the surface tension.

Eqns (53) and (55) show that the total Hamiltonian H is given by

$$H = E_0 + \sum_{\lambda,\mu} \left[\frac{1}{2} B_\lambda |\dot{\alpha}_{\lambda\mu}|^2 + \frac{1}{2} C_\lambda |\alpha_{\lambda\mu}|^2\right]. \qquad \ldots(57)$$

Hence the classical frequency of oscillation

$$\omega_\lambda = (C_\lambda/B_\lambda)^{1/2}. \qquad \ldots(58)$$

This shows that the frequency $\omega_\lambda=0$ for $\lambda=0$ and $\lambda=1$. The $\lambda=0$ motion implies change of density and is not an oscillator. The $\lambda=1$ motion implies translational motion of the whole system only. The energy eigenvalues corresponding to Hamiltonian H are the harmonic oscillator energies, given by

$$E=E_0+\sum_{\lambda\mu}(n_{\lambda\mu}+\tfrac{1}{2})\,\hbar\,\omega_\lambda\,, \qquad \text{...(59)}$$

where $n_{\lambda\mu}$ is the number of oscillators or phonons in the $\lambda\mu$-mode of oscillation. The phonon of type $\lambda\mu$ carries angular momentum quantum number λ, with Z-component μ and parity $(-1)^\lambda$.

According to the collective model, the electromagnetic radiation field produced during a transition from the first excited vibrational state to the ground state results from a rearrangement of the nuclear charge from a spheroidal to a spherical distribution. Under this process the angular momentum changes ($\Delta\lambda=2$) and the electromagnetic radiation emitted has the characteristics of $E\,2$ transition. Since pairing forces depress the energy of the ground state of even-even nuclei relative to the levels predicted by shell model, no low energy individual particle states exist and states formed by collective motions can more easily be observed. The first excited level of most even-even nuclei is formed by the $\lambda=2$ quadrupole surface vibrational state and is generally known as a one phonon state. The next excited state always appears to have +ve parity and even angular momentum. Level scheme of Cd^{114} shows that the third, fourth and fifth levels (0^+, 2^+ and 4^+) are formed by the coupling of two quadrupole surface vibrations each with $\lambda=2$. This triplet set of levels is known as two phonon state. Even three phonon states have also been identified experimentally. For the octupole oscillations begin with 0^+, 3^-, since the phonons would have $\lambda=3$. The 3^- state is expected to occur very close to the second excited state of the quadrupole oscillation.

For odd nuclei a certain amount of insight can be gained by considering the odd nucleon (in ground state) coupled to the one or

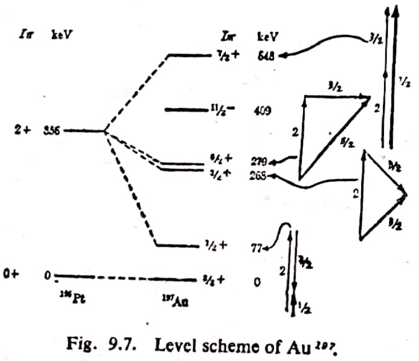

Fig. 9.7. Level scheme of Au^{197}.

more vibrational collective excitations of the even-even core. The shell model predicts a $d_{3/2}$ ground state for the 79th proton. Experimental observations have found a level at 77 keV ($\frac{1}{2}^+$ level) and a level at 409 keV ($\frac{11}{2}^-$ level). But there are three other observed levels at 268, 279 and 548 keV, that are explained easily by the shell model. Braunstein and deShalit have proposed that these are core excited vibrational states formed by the coupling of the angular momentum of the 2^+ vibrational level of the core (Pt^{196}) to the angular momentum of the ground state of Au^{197}.

Let us confine attention to quadrupole shape $\lambda=2$. The eqn of the nuclear surface is

$$R(\theta',\phi')=R_0\left[1+\sum_{\mu=-2}^{2}\alpha^*_{2\mu}\,Y_{2\mu}(\theta',\phi')\right]. \qquad \text{...(60)}$$

where the deformation parameters $\alpha_{2\mu}$ and the polar co-ordinates θ', ϕ' are in lab system. Since $\delta R=R(\theta',\phi')-R_0$ is real, hence

$$\alpha_{2,-\mu}=(-1)^\mu\,(\alpha_{2\mu})^*. \qquad \text{...(61)}$$

In the rotation from one set of co-ordinates to another by Euler angles $\Theta\ \Phi\ \Psi$, the spherical harmonics transform according to

$$Y_{\lambda\mu}(\theta,\phi)=\sum_\nu Y_{\lambda\nu}(\theta',\phi')\,D^\lambda_{\mu\nu}(\Theta,\Phi,\Psi). \qquad \text{...(62)}$$

The function D^λ constitute a unitary matrix, and are found in the study of angular momentum.

$$\therefore\quad \alpha_{2\mu}=\sum_\nu a_{2\nu}D^{2*}_{\mu\nu}(\Theta,\Phi,\Psi). \qquad \text{...(63)}$$

Since the body axes are principal axes, the products of inertia are zero, which implies that

$$a_{20}=\beta\cos\gamma,\ a_{21}=a_{2,-1}=0 \text{ and}$$

$$a_{22}=a_{2,-2}=\sqrt{\tfrac{1}{2}}\,\beta\sin\gamma,$$

where β and γ are new parameters. The deformations δR along the principal axes j=1, 2, 3 are obtained as

$$\delta R_1(\pi/2,0)=(5/4\pi)^{1/2}\,\beta R_0\cos(\gamma-2\pi/3)$$

$$\delta R_2(\pi/2,\pi/2)=(5/4\pi)^{1/2}\,\beta R_0\cos(\gamma-4\pi/3)$$

$$\delta R_3(0,\phi)=(5/4\pi)^{1/2}\,\beta R_0\cos\gamma$$

or in general

$$\delta R_j=(5/4\pi)^{1/2}\,\beta R_0\cos(\gamma-2\pi j/3)\,. \qquad \text{...(69)}$$

For $\gamma=0$, the nucleus would be prolate (cigar shaped) spheroid with the 3 axis as its symmetry axis. For $\gamma=2\pi/3$ and $4\pi/3$, the nuclei would be prolate spheroids with 1-and 2-axes as symmetry axes. For $\gamma=\pi$, $\pi/3$, $5\pi/3$, the nuclei are oblate spheroids. If $\gamma\neq n\pi/3$, the nuclear shape is that of an ellipsoid with three unequal axes. The kinetic energy for collective oscillations, eqn (53), can be written in terms of β and γ as

$$T=\frac{1}{2}B_2\,(\dot{\beta}^2+\beta^2\dot{\gamma}^2)+\frac{1}{2}\sum_{j=1}^{3}\mathcal{J}_j\,\omega_j^2, \qquad ...(65)$$

where B_2 is the mass parameter for collective quadrupole oscillations, ω_j is the angular velocity of the principal axes with respect to the space fixed axes and $\mathcal{J}_j$ are effective moments of inertia, given by

$$\mathcal{J}_j=4B_2\beta^2\sin^2\left(\gamma-\frac{2\pi j}{3}\right)=\frac{15}{4\pi}\mathcal{J}_{rigid}\,\beta^2\sin^2\left(\gamma-\frac{2\pi j}{3}\right), \qquad ...(66)$$

where $\mathcal{J}_{rigid}$ is the moment of enertia of a rigid sphere of radius R_o and is having value $(16\pi/15)\,B_2$. Above eqn shows that the moment of inertia for collective rotation about the symmetry axis is zero, *i.e.* for $\gamma=0$ or π, $\mathcal{J}_3=0$. For the other axes, its values are equal, *i.e.*

$$\mathcal{J}_1=\mathcal{J}_2=\mathcal{J}=3B_2\beta^2=(45/16\pi)\,\mathcal{J}_{rigid}\,\beta^2. \qquad ...(67)$$

Since β is small, very little of the nuclear matter is actually taking part in the effective rotation.

2. **Rotational States** —The observable rotational motion is possible if the nucleus is pictured to be a fluid drop or to have any form with a definite surface. This rotational effect can be either *rigid* in which case particles actually move in circles around the axis of rotation, or *wavelike* in which case particles perform oscillatory motions and only the geometrical shape of the drop changes. If we retain the shell model as a reasonably good picture of the independent motions of individual nucleons, within a nucleus, it is difficult to picture the nucleus as a rigid body rotating around an axis. Thus a wave like rotation seems to be a more logical explanation, but such

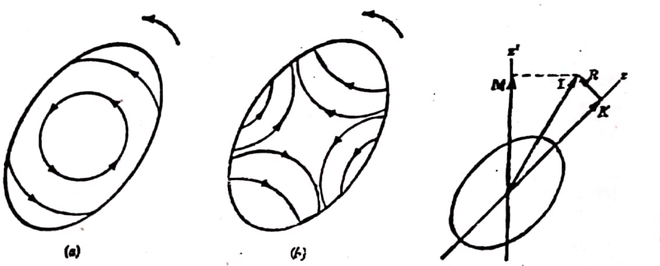

Fig. 9.8. (*a*) Rigid and (*b*) Wave like rotational motion of a deformed nucleus. (c) Coupling scheme in the collective motion model.

wave like rotations can be observed only in deformed nuclei because the apparent motion must then be solely a surface phenomenon.

If the rotating nuclear system were a rigid structure, the energy associated with rotation would be purely kinetic and would have value $\frac{1}{2}\mathcal{J}_0\omega^2$. Here $\mathcal{J}_0$ is the moment of inertia which for a rigid system is given by the relation

$$\mathcal{J}_0=\sum_p m_p r_p^2, \qquad ...(68)$$

The observed moments of inertia for deformed nuclei are smaller than those for rigid rotors. They are, however, larger than expected for purely wave like surface motion. Thus we see that the apparent rotational motion is of a form intermediate between rigid rotation and wave like surface motion of the constituent particles.

According to the collective model, moments of inertia of nuclei can be determined from the energies of their rotational states. Rotational energy levels of an axially symmetric nucleus can be described by the three constants of motion : I, the total angular momentum ; K, the projection of I on the nuclear symmetry axis (z-axis) ; and M, the projection of I on a space fixed axis (z'-axis). The collective rotational angular momentum R is perpendicular to the symmetry axis. For a wave like rotation there can be no rotation about the symmetry axis. The quantum number K is, therefore, a constant for each set of rotational levels and represents an intrinsic angular momentum for that band.

If $\mathcal{J}_3$ and $\mathcal{J}$ are the moments of inertia for rotations about symmetry axis 3 (*i.e.* z-axis) and about an axis $\perp$ to it, and I_1, I_2 and I_3 are the components of the total angular momentum operator along the body fixed axes, the Hamiltonian is given by

$$H=\sum_{i=1}\frac{\hbar^2}{2\mathcal{J}_i}I_i^2=\frac{\hbar^2}{2\mathcal{J}}(I_1^2+I_2^2)+\frac{\hbar^2}{\mathcal{J}_3}I_3^2$$

$$=\frac{\hbar^2}{2\mathcal{J}}(I^2-I_3^2)+\frac{\hbar^2}{2\mathcal{J}_3}I_3^2. \qquad ...(69)$$

For such an Hamiltonian eigen functions are the D-functions, which are the transformation functions for the spherical harmonics under finite rotations. We thus have

$$I^2 D^I_{MK}=I(I+1)D^I_{MK}$$
$$I_3 D^I_{MK}=K\,D^I_{MK}$$
$$I_z' D^I_{MK}=M\,D^I_{MK} \qquad ...(70)$$

and
$$H\,D^I_{MK}=\left\{\frac{\hbar^2}{2\mathcal{J}}[I\,(I+1)-K^2]+\frac{\hbar^2}{2\mathcal{J}_3}K^2\right\}D^I_{MK}$$

and the energy eigen values are

$$E=\frac{\hbar^2}{2\mathcal{J}}[I\,(I+1)-K^2]+\frac{\hbar^2}{2\mathcal{J}_3}K^2. \qquad ...(71)$$

In the case of symmetry both the model and experimental facts indicate that $\mathcal{J}_3$ is quite small. This leads to low lying rotational states for which $K=0$, and the energy expression thus becomes

$$E=\frac{\hbar^2}{2\mathcal{J}}I\,(I+I). \qquad ...(72)$$

States with $K\neq0$, other rotational states may occur if one or more of the nucleons are excited to a higher shell model state so that the intrinsic angular momenta no longer cancel by pairs. For non-zero K, I takes all the values K, $K+1$, $K+2$, etc.

Thus we see that these low lying rotational levels be characterized by the sequence of states with $I=0^+, 2^+, 4^+$, etc. with even parity throughout and with energies proportional to $I(I+1)$. It may be seen that the ratio of excitation of successive states is

$$\frac{E_4}{E_2}=\frac{10}{3},\ \frac{E_6}{E_2}=7,\ \frac{E_8}{E_2}=12, \text{ etc.,}$$

aad these characteristic values are verified for many even-even nuclei. As an example, fig. 9.9 shows the energy level diagram of $_{72}Hf^{180}$. The excitation energies are measured with great precision with a bent crystal spectrometer. Substituting experimental value of energy for the 2^+ level in equation (72), we obtain $\hbar^2/2\mathcal{I}=15.55$. Using this value of $\hbar^2/2\mathcal{I}$ the energies of other levels are calculated and are listed to the extreme right of each level in the diagram. The agreement is quite good, but there is a symmetric difference which increases with increasing excitation energy. This difference may be explained as resulting from an increase in the moment of inertia with increasing I because of the actions of the centrifugal force. When a correction for this effect is included, the equation (72) then becomes

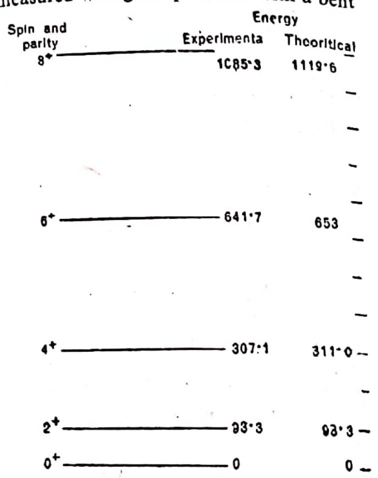

Fig. 9.9. Energy level diagram of Hf 180

$$E=\frac{\hbar^2}{2\mathcal{I}}\,I(I+1)-BI^2(I+1)^2. \qquad \ldots(73)$$

The agreement with experimental value is now extremely good.

Thus we see that collective model is quite successful in interpreting the pattern of exited states of even-even nuclei. For odd-even nuclei, the situation is complicated by the fact that the motion of the core and the motion of the odd nucleon must be coupled and thus the motion of the odd nucleon is no longer adequately described by the shell model states which correspond to a static spherical core.

Furthermore, the excitation energy of the first rotational state of the deformed nuclei shows a smooth variation with A, whereas magic and near magic nuclei show no rotational spectra. From

these data and with the help of eqn. (73) we can obtain effective moment of inertia of the various nuclei. The values of moments of inertia help us to understand the kind of rotational motion that occurs. If R be the mean radius and $\triangle R$ the difference between the major and minor semiaxes of the deformed well, then we can define deformation parameter by using the relation $R=R_0\,[1+\beta\,(5/4\pi)^{1/2}\,(\frac{3}{2}\cos^2\theta-\frac{1}{2})]$ as

$$\beta=\tfrac{4}{3}\,(\pi/5)^{1/2}\,\triangle R/R=1.06\,\triangle R/R_0. \qquad \ldots(74)$$

The nuclear deformation is connected with the electric quadrupole moment as

$$Q_0=\frac{3}{\sqrt{(5\pi)}}\,ZeR_0^2\,\beta\,[1+0.36\,\beta+\ldots]. \qquad \ldots(75)$$

To find the value of Q, multiply intrinsic quadrupole moment Q_0 by a projection factor, which is a function of I and K By using the coupling scheme, a complicated calculation gives

$$Q=Q_0\,\frac{3K^2-I\,(I+1)}{(I+1)\,(2I+3)}$$

which in the ground state ($K=I$) reduces to

$$Q=Q_0\,\frac{I\,(2I-1)}{(I+1)\,(2I+3)}. \qquad \ldots(76)$$

The collective model has its most convincing successes, ascribing the Q values to a surface deformation of the nuclear core. This model goes a long way to explain the individual deviations from the Schmidt curves. Prof. Rainwater, Prof. A. Bohr and Prof. Mottelson shared the Noble prize in Physics for 1975 for their work on collective model of nuclei

9.6. UNIFIED MODEL

Bohr and Mottelson have described a single model, known as unified model. According to this model, nucleons move very nearly independently of each other, as in the shell model, but in a potential energy field that is constantly changing. This change is always slow compared to the motions of the individual nucleons. The rotational and vibrational energy states are on account of this slow collective motion of the entire nucleus. The nucleus, as a whole, looks something like a liquid drop such that its surface motions can be described by analogy to hydrodynamic phenomena. The individual nucleons move so fast in their shell model states that they cause very little interference with the hydrodynamic type motion. According to this model, nuclei are deformed away from a spherical shape because the nucleus is not rigid structure and nucleons outside closed shells can set up tensions in the closed shell core and thereby establishing polarization of the nucleus. If the forces between the external nucleons and the core are repuilsve, the prolate spheroid is formed. On the other hand, oblate spheroid is formed when the forces are attractive. Although small effects of polarization of the core can be observed with only one or two nucleons outside closed shell.

13

Nuclear Fission and Fusion

13.1. NUCLEAR FISSION

When uranium was bombarded with neutrons it was found that a β-active product resulted, followed by a whole chain of β-active products such as

$$_{92}U^{238}+{}_0n^1\rightarrow{}_{92}U^{239}\rightarrow{}_{93}X^{239}\rightarrow{}_{94}Y^{239}\rightarrow\text{etc.}$$

It was recognised that more than one neutron was produced. Hahn and Strassman in 1939 proved that the product might be consisted of two large fragments, which they identified as barium and krypton. Frisch and Meitner in 1939 used the *word fission to describe the process which takes place when a heavy nucleus is caused to break down into two roughly equal parts, known as fission fragments.* In this process neutrons are also emitted with the release of considerable energy. This process has been also observed to occur when heavy nuclides are bombarded with protons, deuterons, α-particles and even electrons and gamma rays. Further work showed that lighter elements could also be fissioned by high energy particles, as for example in the case of copper

$$_{29}Cu^{63}+{}_1p^1\rightarrow{}_{11}Na^{24}+{}_{19}K^{39}+{}_0n^1. \qquad ...(1)$$

A. TYPES OF FISSION

(a) *Thermal fission.* Since a thermal neutron adds negligible energy to the fissionable nucleus, it is clear from semi-empirical mass formula that the fission of the nuclei in which the compound nuclei are of even-even structure take place even with the thermal neutrons. Fission of U^{235} and Pu^{239} by thermal neutrons are the most important reactions.

(b) *Fast Fission.* Other isotopes of Uranium and other elements which form compound nuclei of even-odd structure enter into (n, f) reactions with fast neutrons ($\geqslant$1MeV). The example is U^{238}

(c) *Charged-particle Fission.* Elements with Z> 90 show fission process with protons, deuterons and α-particles. High energy charged particles induce fission in elements even in the middle of the periodic table.

(d) *Photo fission.* High energy photons induce fission in the heavier elements. 5.1 MeV γ-rays can produce fission with U^{238}.

In all cases very large disintegration energies were released and fast neutrons are emitted. Meitner and Frisch indicated that, because of their exceptionally high neutrons to protons ratio, the fission fragments should be unstable, undergoing a chain of β^- distintegrations. For example

$$_{92}U^{235}+{}_0n^1\rightarrow{}_{92}U^{236}\begin{cases}{}_{40}Zr^{98}\rightarrow{}_{41}Cb^{98}\rightarrow{}_{42}Mo^{98}\\ {}_{52}Te^{136}\rightarrow{}_{53}I^{136}\rightarrow{}_{54}Xe^{136}\end{cases}+2{}_0n^1 \qquad ...(2)$$

A typical beta decay chain is

$$_{54}Xe^{140}\rightarrow{}_{55}Cs^{140}\rightarrow{}_{56}Ba^{140}\rightarrow{}_{57}La^{140}\rightarrow{}_{58}Ce^{140}\text{ (Stable)} \qquad ...(3)$$

For the nuclei near the middle of the periodic table (E_B=8.5 MeV/nucleon), the fission process is expected to release a large amount of energy. Assuming fission of a ucleus of mass number 240, for which $E_B\simeq7.6$, into two similar fragments with A$\sim$ 120, the energy released in fission is $2\times120\times8.5-240\times7.6=216$ MeV. Assuming their separation equal to the sum of their nuclear radii, the Coulomb repulsion energy is given by

$$E_c=\frac{Z_1Z_2e^2}{4\pi\epsilon_0 d}=\frac{52\times40\times(1.6\times10^{-19})^2\times9\times10^9}{1.5\times10^{-14}\times1.6\times10^{-13}}\text{ MeV.}$$

$$\sim200\text{ MeV.}$$

Thus we see that the Coulomb repulsion energy is nearly equal to the energy released in fission process. We can, therefore, regard this fission process as a result of Coulomb repulsion. The Q value of fission reaction (2) is also calculated from the exact mass difference of the two sides of the equation. The combined isotopic masses before and after fission are $\Sigma m_i=m(U^{235})+m({}_0n^1)=235.0439+1.0087=236.0526$ mu. and $\Sigma m_f=m(Mo^{98})+m(Xe^{136})+m(2{}_0n^1)=97{\cdot}9054+135{\cdot}9072+2.0154=235.83$ mu.

Hence $Q=\Delta mc^2=(\Sigma m_i-\Sigma m_f)c^2=210$ MeV, which is comparable with the value calculated by the binding energy method.

B. Distribution of Fission Products. We have seen that a fissionable nucleus gives only two fission fragments which decay by β^--emission to a *stable end product.* Although the sum of two large fragments always adds up to 234, there is a wide distribution in possible products. The mass distribution of the fission products is shown most conveniently in the form of a *fission yield curve*, in which the percentage yields (*in log scale*) of the different products are plotted against mass number. There is a tendency for masses to concentrate respectively round 90 and round 140. Actually about 97% of the total fission products fall within the narrow range 85—104 for the lighter fragments and 130-149 for the heavier. In the case of U^{235} the maxima lie near mass numbers 95 and 140 ; fission produced by slow neutrons is highly asymmetric process and division into two equal fragments occurs in only about 0.01% of the fissions. Symmetric fission becomes increasingly more probable with increasing neutron energy. Single peak appears for high energy neutrons. The trough in the curve also tends to fill, when the nuclei are fissioned by the particles other than neutrons. A comparison of the U^{233} and Pu^{239}

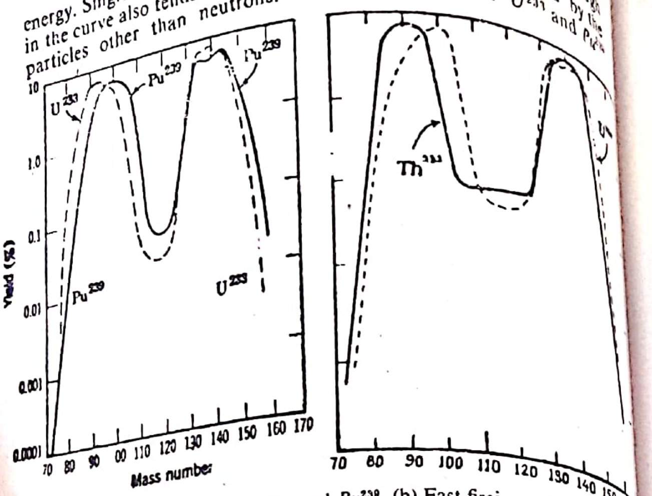

Fig. 13.1. (a) Thermal fission of U^{233} and Pu^{239}, (b) Fast fission of Th^{232} and U^{238}.

fission yield curves shows that the distribution of the heavier products are practically the same, whereas the portions of the curves for the lighter fragment yields are displaced by six mass units with respect to other.

The mass distribution of the fission fragments can also be obtained from the distribution of their kinetic energies. The nucleus undergoing fission can be considered to be at rest initially and, if the neutrons emitted are neglected, the law of conservation of momentum gives $M_1V_1=M_2V_2$.

$$\therefore \quad \frac{E_1}{E_2}=\frac{\frac{1}{2}M_1V_1^2}{\frac{1}{2}M_2V_2^2}=\frac{M_2}{M_1}. \qquad \ldots(4)$$

Thus we see that the masses are inversely proportional to the kinetic energies. W. Jentschke and F. Prankl in Germany and Booth, Dunning and Slack in U. S. A. showed that there were two distinct groups, each group were found to have mean energies about 70 and 100 MeV. Later studies, based on measurement of ionization and velocities of the fission fragments, indicate that the K.E. of these fragments is 167 MeV in the fission of U^{235} by slow neutrons (Fig. 13.2). There are two groups of energies, with maxima about 68 and 99 MeV. The difference between this quantity and the quantity released in fission process (200 MeV) is carried out by the gamma rays (11 MeV), neutrons (5 MeV), beta particles (7 MeV) and neutrinos (11 MeV). From equation (4), it is clear that $M_1/M_2=E_2/E_1=99/68\simeq 1.5$, which is in close agreement with the ratio 140/95. Such measure-

ment on the fission fragment energies gives us a clear evidence for the asymmetry of the fission process.

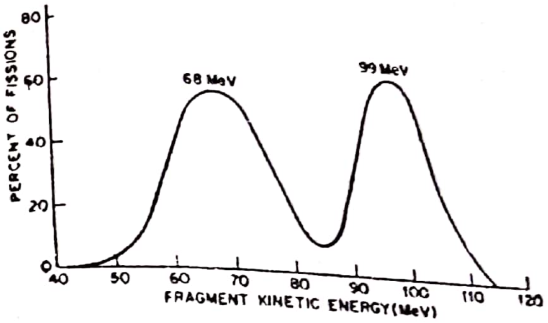

Fig. 13.2. Kinetic energy distribution of fission fragments in U^{235}

C. Neutron Emission in Fission—An accurate knowledge of the average number of neutrons emitted per second is of great importance to the scientists. Actually the number of neutrons released in any one fission is an integer, but averege value, ν_{av}, of the number of neutrons in one fission is not an integer, because the fissionable nucleus can divide in at least 30 different ways, and can be obtained by the relation

$$\nu_{av}=\Sigma\nu_0\, n\, \nu_0/\Sigma\, n\, \nu_0. \qquad \ldots(5)$$

Most of these neutrons are emitted within possibly 10^{-13} sec. and are called *prompt neutrons*. A smaller number of neutrons is also emitted with a time lag of several seconds to more than a minute after the fission. These neutrons are called *delayed neutrons*.

For sufficiently large piece of fissionable substance, the neutrons that are released in a first fission process will be absorbed by the other nuclei and produce new processes which in turn emit new neutrons. Actually some of the compound nuclei decay to the ground state by gamma emission, rather than fission. The ratio of the radiative capture cross-section to the fission cross-section is usually denoted by α. given by

$$\alpha=\sigma_r/\sigma_f \qquad \ldots(6)$$

and the number of fission neutrons released per neutron absorbed in the fissionable nuclide is denoted by η and is given by

$$\eta=\nu_{av}/(1+\alpha). \qquad \ldots(7)$$

The relative probability that a compound nucleus decays by fission is thus be $(1+\alpha)^{-1}$. Values of ν_{av}, α and η for thermal neutron are listed in the table 13·1.

Table 13·1

	U^{233}	U^{235}	Natural uranium	Pu^{239}
σ_f	525±4	577±5	4.18±0.06	742±4
σ_r	53±2	101±5	3.50	286±4
ν_{av}	2.51±0.02	2.44±0.02	2.47	2.89±0.03
α	0.101±0.004	0.18±0.01	0.83	0.39±0.03
η	2.28±0.02	2.07±0.01	1.34±0.02	2.08±0.02

D Fissile and Fertile Materials. For a number of reasons, isotopes such as U^{238}, which only fission with energetic neutrons, can not alone be used to fuel nuclear reactors. The only neutrally occurring nuclide that can be fissioned with thermal neutrons is U^{235}, which is 0.71% of the naturally occuring uranium. The only other nuclides that can undergo fission with thermal neutrons are U^{233} and Pu^{239}. These do not occur in nature but can be produced by the interaction of neutrons with Th^{232} and U^{238} respectively and are called *fissile materials*. Th^{232} and U^{238} are not *fissile* materials but can be used as raw material for the production of fissile isotopes and are called *fertile or fissionable materials*. The nuclear reactions which convert these fertile materials into fissile materials are called *breeding reactions*. They are neutrons capture processes with subsequent β-decay.

$$
\begin{aligned}
{}_{92}U^{238}+{}_0n^1 &\rightarrow {}_{92}U^{239}+\gamma\\
{}_{92}U^{239} &\rightarrow {}_{93}Np^{239}+{}_{-1}e^0\\
{}_{93}Np^{239} &\rightarrow {}_{94}Pu^{239}+{}_{-1}e^0.
\end{aligned}
\qquad ...(8)
$$

Similarly

$$
\begin{aligned}
{}_{90}Th^{232}+{}_0n^1 &\rightarrow {}_{90}Th^{233}+\gamma\\
{}_{90}Th^{233} &\rightarrow {}_{91}Pa^{233}+{}_{-1}e^0\\
{}_{91}Pa^{233} &\rightarrow {}_{92}U^{233}+{}_{-1}e^0
\end{aligned}
\qquad ...(9)
$$

E. Spontaneous Fission Most heavy nuclides undergo spontaneous fission in competition with the α-emission. Spontaneous fission is predicted by the empirical nuclear mass equation. Consider the special case, when the nucleus splits into equal parts. Neglecting the pairing term δ, we have the Q-value for the fission reaction

$$E_f=[zM^A-2\ (z_{/2}M^{A/2})]c^2. \qquad ...(10)$$

Consider Weizsaker's semi empirical binding energy equation

$$M\ (Z,\ A)=ZM_P+(A-Z)\ M_n-a_vA+a_sA^{2/3}+a_cZ^2A^{-1/3}$$
$$+a_a\ (A-2Z)^2A^{-1} \qquad ...(11)$$

$$M(\tfrac{1}{2}Z,\ \tfrac{1}{2}A)=\tfrac{1}{2}ZM_P-\tfrac{1}{2}(A-Z)M_n-a_v(\tfrac{1}{2}A)+a_s(\tfrac{1}{2}A)^{2/3}$$
$$+a_c(\tfrac{1}{2}Z)^2(\tfrac{1}{2}A)^{-1/3}+\tfrac{1}{2}a_a(A-2Z)^2\ A^{-1} \qquad ...(12)$$

Substituting value of zM^A and $z_{/2}M^{A/2}$ in eqn. (10), we have

$$E_f=[a_s\{A^{2/3}-2(\tfrac{1}{2}A)^{2/3}\}+a_c\{Z^2/A^{1/3}-2(\tfrac{1}{2}Z)^2/(\tfrac{1}{2}A)^{1/3}\}\ ]\ c^2$$
$$=-3.42\ A^{2/3}+0.22\ Z^2/A^{1/3}\ \text{MeV} \qquad ...(13)$$

This eqn shows that the splitting of a nucleus affects Coulomb energy and surface energy in such a way that the change in one and that in other tend to cancel one another partially. This is reasonable and to be expected, since the division of the nucleus increases (1) the separation between proton groups, thus reducing their Coulomb potential energy, (2) the total nuclear surface which increases the surface energy. Thus for spontaneous fission

$$-3.42A^{2/3}+0.22Z^2/A^{1/3}\geqslant 0 \quad \text{or} \quad Z^2/A\geqslant 15. \qquad ...(14)$$

This relation shows that the fission should be energetically possible for nuclei with mass number $A\geqslant 85$. However, the slow neutron fission does not take place even with many of the heavy nuclei. In order to explain this discrepancy Bohr and Wheeler considered the Coulomb's potential barrier of the two fragments at the instant of separation. The existence of this barrier prevents the immediate breaking of these two. If we denote the height of the Coulomb barrier by E_b, we can say that the nucleus will be unstable and break apart into two fragments if $E_f > E_b$. The barrier height corresponding to the Coulomb potential between the two symmetric fragments when they are just in contact with each other is given by

$$E_b=(\tfrac{1}{2}Z)^2e^2/4\pi\epsilon_0(2R)=Z^2e^2/32\pi\epsilon_0R_0(\tfrac{1}{2}A)^{1/3}$$
$$=0.15\ Z^2/A^{1/3}\ \text{MeV}. \qquad ...(15)$$

$$\therefore\ E_b-E_f=0.15\ Z^2/A^{1/3}-[-3.42\ A^{2/3}+0.22\ Z^2/A^{1/3}]$$
$$=3.42\ A^{2/3}-0.07\ Z^2/A^{1/3}. \qquad ...(16)$$

Thus the condition for stability gives

$$E_b-E_f\geqslant 0 \quad \text{or} \quad Z^2/A\leqslant 49. \qquad ...(17)$$

For a particular nucleus, the closer the value of Z^2/A to 50, the shorter should be the half life for spontaneous fission. It is

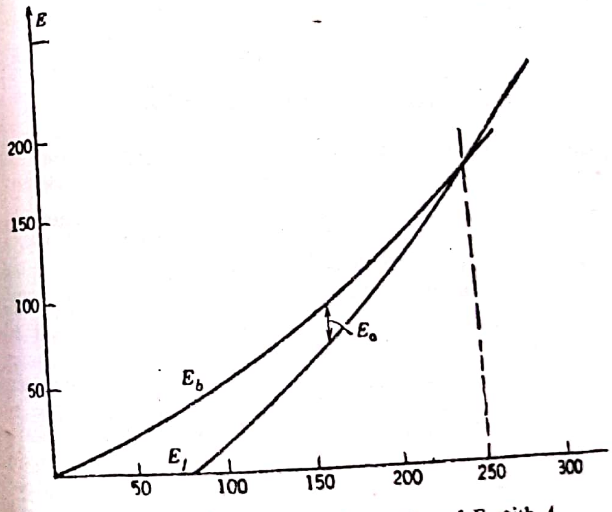

Fig. 13.3. Variation of E_b and E_f with A.

clear that Z^2/A may have value 50 for a nucleus of mass number 250, hence a nuclide ($A>250$) would be too unstable to exist for more than 10^{-12} sec or less.

Computing E_b and E_f for various values of A for symmetric fission and plotting on the same graph, we get fig. 13.3. The graph shows that for $A \simeq 250$, E_b becomes equal to E_f and $E_f > E_b$ for nuclei with $A>250$. This indicates that we do not expect nuclei with $A>250$ to be found in nature. This graph also shows that fission begins to become exoergic in the neighbourhood of $A \simeq 85$ in agreement with the earlier occurring result.

F. **Deformation of liquid drop.** The fission process can be explained with the help of liquid drop model. The incident neutron combines with the nucleus to form highly energetic compound nucleus. Its extra energy is partly the kinetic energy of the neutron but largely the added binding energy of the incident neutron. This energy appears to initiate a series of rapid oscillations in the drop which tend to distort the spherical shape so that the drop may become ellipsoidal in shape. *The surface tension forces tend to make the drop return to its original spherical shape, while excitation energy tends to distort the shape still further.* If the excitation energy is sufficiently large, the drop may attain the shape of a *dumb-bell*. If the oscillations become so violent that stage fourth is reached then the final fission into stage fifth is inevitable. Thus there is a *threshold energy* or a *critical energy* required to produce stage fourth after which the nucleus can not return to stage first. When the distortion produced is not pronounced enough to get the nucleus beyond the critical point, the ellipsoid will return to

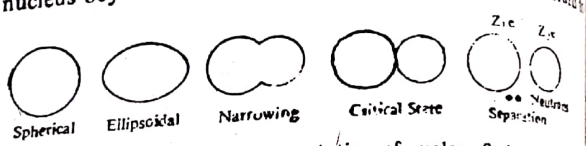

Fig. 13.4. Schematic representation of nuclear fission.

the spherical shape with the excitation energy being liberated in the form of γ-rays and we have a *radiative capture* rather than fission.

The potential energy of the drop in the different stages can be calculated as a function of the degree of deformation of the drop. It is plotted against r, the separation of the centres of two fission fragments. The curve is supposed to be divided into three regions.

In region I the fragments are completely separated and the potential energy E is simply the electrostatic Coulomb energy resulting from the mutual repulsion of the two positively charged nuclear fragments. If distance $r=2R$, when the drops just touch each other, energy E at that point is less than the corresponding Coulomb potential by an amount CD. This amount is equal to the potential of the surface forces which are just beginning to come into play at this point. As we pass through region II we reach the critical

distance r_c, where the potential energy curve has a maximum value E_b. This corresponds to barrier height and explains why fission does not take place spontaneously in all cases where $E_f > 0$. An additional amount of energy $E_a = E_b - E_f$, the *activation energy* is required

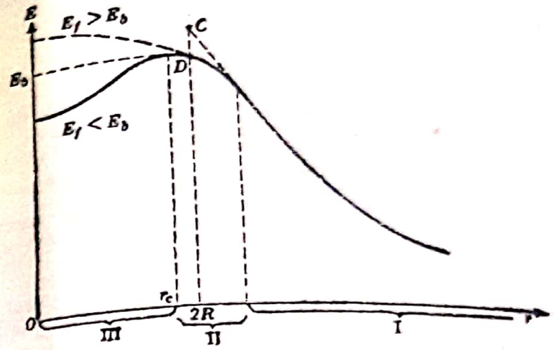

Fig. 13.5 Potential energy curve for fission.

by the nuclear system before the potential barrier can be surmounted and fission can take place. In the *III* region, the fragments have coalesced and the short range nuclear forces have become predominant.

Bohr and Wheeler's Theory of Nuclear Fission—The first thorough theoretical treatment of this process was carried out by Bohr and Wheeler in 1939. They applied a simple form of analysis (Legendre polynomial expansion) to express the radius r making angle θ with the axis of maximum deformation

$$r = R\left[1 + \sum_{l=0}^{\infty} \alpha_l P_l (\cos\theta)\right]$$

$$= R\,[1 + \alpha_2 P_2 (\cos\theta) + \alpha_3 P_3 (\cos\theta) + \ldots], \qquad \ldots(18)$$

where R is the radius of the spherical nucleus and α_2, α_3, are the deformation parameters. Here $\alpha_0 = \alpha_1 = 0$, as the centre of mass of the drop is assumed to remain unchanged.

The surface energy of a spherical drop $E_s^{sphere} = 4\pi R^2 T$, where T is the surface tension. Hence surface energy of the deformed drop

$$E_s = 4\pi R_0^2 A^{2/3}\, T\,[1 + \alpha_2(\tfrac{3}{2}\cos^2\theta - \tfrac{1}{2}) + \ldots]^2.$$

$$= 4\pi R_0^2 A^{2/3}\, T\,[1 + \tfrac{2}{5}\alpha_2^2 + \ldots].$$

$$\therefore\ \Delta E_s = E_s^{sphere}\,[\tfrac{2}{5}\alpha_2^2 + \ldots]. \qquad \ldots(19)$$

The Coulomb energy of a spherical drop $E_c^{sphere}=\frac{3}{5}Z^2e^2/4\pi\epsilon_0 R$, hence that of the deformed drop

$$E_c=\frac{3}{5}\frac{Z^2e^2}{4\pi\epsilon_0 A^{1/3}R_0}\left[1+\alpha_2\left(\frac{3}{2}\cos^2\theta-\frac{1}{2}\right)+\ldots\right]^{-1}$$

$$\therefore \quad \Delta E_c=E_c^{sphere}\left[-\tfrac{1}{5}\alpha_2^2-\ldots\right]=-E_c^{sphere}\left[\tfrac{1}{5}\alpha_2^2+\ldots\right] \qquad \ldots(20)$$

Thus the total energy variation

$$\Delta E=\Delta E_s+\Delta E_c=\tfrac{1}{5}\alpha_2^2\left[2E_s^{sphere}-E_c^{sphere}\right]. \qquad \ldots(21)$$

If it is +ve, *i.e.*, $2E_s^{sphere}>E_c^{sphere}$, the drop is stable to small distortions. Fissions may occur spontaneously if $\Delta E=-$ve or $E_s^{sphere}<\frac{1}{2}E_c^{sphere}$.

$$\therefore \quad 4\pi R_0^2 A^{2/3}\, T<3Z^2e^2/40\pi\epsilon_0 A^{1/3} R_0 \text{ or } Z^2/A>45.$$

The ratio $E_c^{sphere}/2E_s^{sphere}$ is known as *critical parameter*, represented by χ. Thus when $\chi<1$, the nuclear is stable against spontaneous fission. It is possible to estimate the degree of distortion of a nucleus in the critical state by equating the *critical* or *threshold energy* E_{th} to the total energy variation ΔE. From semi-empirical data $4\pi R_0^2 T=13$ MeV, hence for U^{238}, $E_s^{sphere}=520$ MeV and $E_c^{sphere}=830$ MeV and thus $\alpha_2^2=1/7$.

The energy that has to be imparted to the nucleus in order to reach this critical shape, the threshold energy is given as

$$E_{th}=4\pi R^2 T f(\chi)=4\pi R_0^2 A^{2/3}\, T f(\chi)=17.8\, A^{2/3} f(\chi) \text{ MeV} \qquad \ldots(22)$$

This energy can be calculated by neglecting the second order change in energy due to the neck joining the two fragments

$$E_{th}=2\,(4\pi R_0^2)\,T\,(\tfrac{1}{2}A)^{2/3}-4\pi R_0^2 A^{2/3}\,T+2\times\tfrac{3}{5}\times(\tfrac{1}{2}Ze)^2/4\pi\epsilon_0 R_0(\tfrac{1}{2}A)^{1/3}$$
$$+(\tfrac{1}{2}Ze)^2/8\pi\epsilon_0 R_0(\tfrac{1}{2}A)^{1/3}-\tfrac{3}{5}(Ze)^2/4\pi\epsilon_0 R_0 A^{1/3}.$$

or $$E_{th}/4\pi R_0^2 T A^{2/3}=f(\chi)=0.260-0.215\,\chi. \qquad \ldots(23)$$

For an uncharged droplet $\chi=0$ and $f(0)=0.260$, hence the critical energy is just the work done against surface tension in separating into two drops. For $\chi\approx 1$, a small deformation from the spherical shape causes the drop to reach the critical shape and separate.

If the critical energy is compared with the excitation energy, it becomes possible to predict fission probability. The excitation energy E_e, contributed to the resultant compound nucleus by the capture of a neutron, is equal to the binding energy of neutron in the compound nucleus and can be calculated by the relation.

$$E_e=B(A+1, Z)-B(A, Z)=zM^A+M_n-zM^{A+1}.$$

The values of the excitation energy calculated in this way for a number of heavy nuclei are listed in the table 13.2 and compared with the corresponding values of the critical energy. In reviewing the results, it is seen that for uranium—238 a critical deformation energy of 6.5 MeV is necessary for fission, but it acquires only 5.9 MeV when it takes up a neutron of zero K. E. Thus no fission is

Table 13.2

Compound Nucleus	E_e (MeV)	E_{th} (MeV)	E_e-E_{th} (MeV)
Pa^{232}	5.4	5.0	0.4
Th^{233}	5.1	6.5	−1.4
U^{236}	6.6	5.5	1.1
Np^{238}	6.0	4.2	1.8
U^{239}	5.9	6.5	−0.6
Pu^{240}	6.4	4.0	2.4

possible with thermal neutrons with 0.03 eV energy. If the neutrons have a K. E. of 0.6 MeV fission becomes possible. Experiments indicate that neutrons of about 1 MeV energy are required. The fission cross section increases rapidly with neutron energy. The situation is quite different with U^{235}. Here the excitation energy or the energy available by the capture of a slow neutron is greater than the threshold energy. It is evident that in this case thermal neutrons should be capable of causing fission of U^{235} nucleus. The reason for the difference in the excitation energy for U^{236} and U^{239} lies in the pairing term which appears in the semi-empirical mass formula. The term makes a positive contribution of about 0.5 MeV to the binding energy of U^{236} but it is zero for U^{235} On the other hand the contribution is zero for U^{239} but is abont 0.5 MeV for the U^{238}. Thus the odd-even effect is responsible for approximately 1 MeV of the difference in the energies gained by these isotopes upon the addition of a neutron.

A general review of the changes in various types of nuclei, after neutron capture, shows that the liberation of energy is greater or the nuclei are likely to undergo fission with slow neutrons if the original nucleus contains an even number of protons and an odd number of neutrons or an odd numbers of both. Whereas fast neutrons would be required for the nuclei containing odd-even or even-even numbers in the same mass region.

Quantum Effects—The values shown in table 13.2 do not agree well with measured values. This disagreement may be the result of two quantum mechanical effects.

(1) The fission may take place for excitation energies below the threshold due to the tunneling effect.

(2) The vibration of the drop in the distorted mode will have a zero point energy.

The tunneling effect is the origin of spontaneous fission. The fission problem is more difficult than the α-decay problem as it is very difficult to have a clear picture of the exact shape of the fission potential barrier. The fission barrier penetration probability

$$P\propto\exp\left[-\frac{2}{\hbar}\int_0^b\left\{2M(V-E)\right\}^{1/2}dr\right], \qquad \ldots(24)$$

where M is the reduced mass of the two fragment system, $(V-E)$ is the $-$ve K. E. in the barrier of width b. For simplicity, let the barrier be of a parabolic form, given as

$$V=\frac{1}{2}K(r-R)^2, \quad \cdots(25)$$

where r is the separation of the two fission fragments and R is the separation at the top of the barrier. The width of the barrier b is given by the relation

$$E=\frac{1}{2}K(b-\frac{1}{2}b)^2 \text{ or } \frac{1}{2}b=\sqrt{(2E/K)}. \quad \cdots(26)$$

Thus using parabolic function, we get

$$P \propto \exp[-(2\pi/\hbar)(M/K)^{1/2}E]$$
$$\propto \exp[-(b\pi/2\hbar)(2ME)^{1/2}]. \quad \cdots(27)$$

For U^{238}, $E \sim 6$ MeV, $b=1.5\times10^{-14}$ m and $M=240/4=60$ mu

$$\therefore \quad P \propto \exp(-100). \quad \cdots(28)$$

Frankel and Metropolis obtained an expression for the life time for spontaneous fission using the idea of barrier penetration as

$$t=10^{-21}\times10^{7.85E_{th}} \text{ sec.} \quad \cdots(29)$$

Seaborg calculated E_{th} for various heavy elements and found that the fission rate could be determined by the formula

$$t=10^{-21}\times10^{178-3.75(Z^2/A)} \text{ sec.} \quad \cdots(30)$$

After comparing with eqn (29), he obtained the relation

$$E_{th}=19.0-0.36\,Z^2/A, \quad \cdots(31)$$

which is in close agreement with experiment.

13.2. NUCLEAR FUSION AND THERMONUCLEAR REACTIONS

Power from nuclear fission is now a reality both on land and sea and in those countries where coal or oil is costly. An alternative to the fission reaction as a source of energy is its reverse process known as *fusion process*, in which the lighter nuclei fuse together and produce a heavier nucleus. The sum of the masses of the individual light nuclei is more than would be the mass of the nucleus formed by their fusion, and thus the fusion process should result in a liberation of energy.

Some indication of how this might be achieved can be obtained by considering the source of energy produced continuously in the stars, including the sun. It has been calculated that the sun (our nearest star) emits electromagnetic energy at a rate of about 10^{26} joules per second. Astronomical and geological evidences show that the sun has been radiating energy at about its present rate for several billion years. Chemical reactions cannot possibly be the source of this energy, because even if the sun is supposed to be consisted of pure carbon, its complete combustion would supply energy to maintain these radiations only for few thousand years. Now question arises how can the sun have maintained this energy output for

so long and what is the source of all *stellar energy*? Helmholtz, in 1853, suggested that the contraction was taking place and thus the gravitational energy was being converted into heat energy in sun. This conversion is analogous to the production of electricity from the falling of water. It has been shown that if contraction were taking place it could supply not more than 1% of the total energy output needed and it led to an estimate of the age of the sun which was much too short.

With the discovery of radioactivity at the end of the 19th century, it appeared possible that atomic energy might be contributing to the sun's energy. In 1904, J.H. Jeans suggested that the energy of the sun might be resulted from the mutual annihilation of +ve and $-$ve charges. Eddington in 1920, suggested that the stellar energy was liberated in the formation of helium from hydrogen. This theory received wide support, although there was no satisfactory mechanism to account for the formation of helium from hydrogen, because large amounts of hydrogen and helium exist in the sun. In 1929, Atkinson and Houtermans, in Germany, considered that energy might be liberated in the very high stellar temperatures. Such processes are called *thermonuclear reactions.*

In order to interact two nuclei, that must have enough kinetic energy to permit them to overcome the electrostatic repulsion barrier which tends to keep them apart. It can be shown from calculations that the energy required to make the nuclear reactions occur at a detectable rate is about 0.1 MeV for nuclei of the lowest atomic number (*e g*, isotopes of hydrogen), the larger energies are needed for nuclei of higher atomic number. This energy can be resulted from a sufficient increase in temperature (1000×10^6 °K if the average energy of the particles is to be 0.1 MeV). Such temperatures are considerably higher than those existing in stars. In stars, like sun where the central temperatures are less than 50×10^6 °K, the fusion reaction takes place with a finite rate and releases enough energy to keep up the heat and light of the star.

H.A. Bethe in the United States suggested in 1939 that *the production of stellar energy is by thermonuclear reactions* in which helium-4 nuclei are synthesized from four protons (the nucleus of hydrogen, the most abundant element in the universe). A few years ago, it was held that the major portion of the sun's energy was derived from the *carbon nitrogen cycle*. Recent modification of the estimates of the central temperature of the sun now favour the *proton-proton chain*. In the *carbon-nitrogen* cycle carbon acts as a short of catalyst in facilitating the combination of four protons to form a helium nucleus. In this cycle a proton first interacts with a C^{12} nucleus with a release of fusion energy. The product nucleus N^{13} decays in a very short time. The stable nucleus of C^{13}, thus formed, then reacts with another proton. The more energy being liberated by this process. The stable nucleus of N^{14} combines with a third proton. The product nucleus O^{15} is a positive β emitter, which decays into N^{15}. This nucleus finally interacts with a fourth proton and regenerates C^{12} nucleus. These reactions can be written as :

$$
\begin{aligned}
{}_6C^{12} + {}_1H^1 &\rightarrow ({}_7N^{13}) \rightarrow {}_7N^{13} + 1.94 \text{ MeV } (10^6\ y)\\
{}_7N^{13} &\rightarrow ({}_6C^{13}) + {}_{+1}e^0 + \nu + 1.20 + 1.02 \text{ MeV } (10\ m)\\
{}_6C^{13} + {}_1H^1 &\rightarrow ({}_7N^{14}) \rightarrow {}_7N^{14} + 7.55 \text{ MeV } (2\times10^5\ y)\\
{}_7N^{14} + {}_1H^1 &\rightarrow ({}_8O^{15}) \rightarrow {}_8O^{15} + 7.29 \text{ MeV } (3\times10^7\ y)\\
{}_8O^{15} &\rightarrow {}_7N^{15} + {}_{+1}e^0 + \nu + 1.74 + 1.02 \text{ MeV } (2\ m)\\
{}_7N^{15} + {}_1H^1 &\rightarrow ({}_8O^{16}) \rightarrow {}_6C^{12} + {}_2He^4 + 4.96 \text{ MeV } (10^4\ y)\\
\hline
4\,{}_1H^1 &\rightarrow {}_2He^4 + 2\,{}_{+1}e^0 + 2\nu + 26.7 \text{ MeV.}
\end{aligned}
$$

It will be noted this this chain of reactions can start with either carbon or nitrogen, since each one is reproduced in the reaction. The four protons are associated with four electrons to maintain electrical neutrality, whereas only two are required for the helium nucleus, and rest two electrons combine readily with positrons resulting in the formation of γ-rays.

The mass difference released as energy in this chain of reactions is simply the difference between the masses of four protons and one helium nucleus. A small amount of this energy is carried away by the neutrons that are emitted during the e^+-decay. Bethe estimates this to be about 1.84 MeV leaving rest for each α-particle formed.

In the *p-p* chain, two protons first fuse to produce a deuterium nucleus which combines with an another proton to yield He^3. Two He^3 nuclei interact and form He^4 and two protons. These reactions can be represented by the equations

$$
\begin{aligned}
{}_1H^1 + {}_1H^1 &\rightarrow ({}_2He^2) \rightarrow {}_1H^2 + {}_{+1}e^0 + \nu + 0.42 \text{ MeV } (7\times10^9\ y)\\
{}_1H^2 + {}_1H^1 &\rightarrow ({}_2He^3) \rightarrow {}_2He^3 + \gamma + 5.5 \text{ MeV (10 sec.)}\\
{}_2He^3 + {}_2He^3 &\rightarrow ({}_4Be^6) \rightarrow {}_2He^4 + {}_1H^1 + {}_1H^1 + 12.8 \text{ MeV } (3\times10^5\ y)\\
\hline
4\,{}_1H^1 &\rightarrow {}_2He^4 + 2\,{}_{+1}e^0 + 2\nu + 2\gamma + 26.7 \text{ MeV}
\end{aligned}
$$

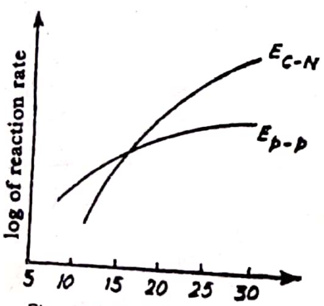

Fig. 13.6. Variation in the rate of energy produced with the central temperature.

The positrons emitted are annihilated by free electrons with the production of gamma rays. The energy released in *p-p* chain is the same as in the *C-N* cycle (26.7 MeV for each helium nucleus).

Which of the two hydrogen-helium fusion processes plays the major role in energy production in star? The answer is based on our knowledge of the stellar temperature. H. Bondi and E.E. Salpeter (1952) developed empirical equations for the rate at which energy is liberated in each of the above chains of reaction. The *p-p* chain reaction rate varies more slowly with temperature, roughly as T^4 and is much more important at lower temperatures. The carbon cycle rate predominates as the temperature is in the vicinity of 18×10^6 °K.

For the case of the sun, they estimated that the rate of generation of energy in the *p p* chain was about the same as that in the carbon cycle. Actually the *p-p* chain predominates (96%) because the interior temperature of the sun is about 15×10^6 °K.

Solar Future. When all the hydrogen is used up in the above thermonuclear reactions, the star will consist mostly of helium. At this stage gravitational contraction will occur once again until a temperature of about 10^8 °K is reached and the density of the star is about 10^7 kg/m³. Under these conditions three helium nuclei combine and form a C^{12} nucleus with the release of about 7.3 MeV. Hoyle estimates that such processes provide energy for an additional 10^7 years. Further gravitational contraction of the star will occur, when all the helium is used up, and will produce a further rise in the temperature of the star. The atoms formed in this way are most stable. Any appreciable combination of these atoms to form heavier ones will lead to endothermic rather than exothermic reactions. Bondi and Salpeter suggested that the endothermic reactions might account for the sudden collapse of a star identified as the sudden appearance of a *supernova*.

13.3 CONTROLLED THERMONUCLEAR REACTIONS

In stars, nuclear fusion reactions release great amounts of energy. The rate depends upon the density and temperature of the gas and upon the cross sections or lifetimes of the reactions involved. Bearing in mind the masses of materials available on earth, it is certain that the reactions of the carbon cycle and the *p-p* chain would occur extremely slowly. There are thermonuclear reactions which occur much more rapidly and depend on an most abundant material. Among the nuclei of the hydrogen isotopes, ${}_1H^2$ and ${}_1H^3$ reactions are :

$$
\left.
\begin{aligned}
{}_1H^2 + {}_1H^2 &\rightarrow {}_1H^3 + {}_1H^1 + 4.0 \ MeV\\
{}_1H^2 + {}_1H^2 &\rightarrow {}_2He^3 + {}_0n^1 + 3.2 \ MeV
\end{aligned}
\right\}\quad \text{D-D reactions}
$$

$$
{}_1H^3 + {}_1H^3 \rightarrow {}_2He^4 + {}_0n^1 + 17.6 \ MeV. \quad \text{D-T reaction}
$$

The D-D reaction can go in two equally probable ways, the first of which produces ${}_1H^3$ while the second produces ${}_2He^3$. When reactions take place in a chamber the deuterium can react with ${}_1H^3$ to give an α-particle and a neutron. 14.1 *MeV* energies are carried off by the neutron and 3.5 *MeV* by the α-particles. In these fusion reactions, the energy released is much less than that released in fission reaction but the energy yield per unit mass of material is greater slightly. Deuterium occurs in nature with an abundance of about one part in 6500 hydrogen and can be separated from the lighter isotope quite cheaply It has been calculated that the energy equivalent of the deuterium in one gallon of water is the same as that obtained from the combustion of 300 gallons of gasoline. The more than 10^{20} gallons of water present in the oceans could thus supply the world's power requirement for several million years, if all the deuterium could be utilized to provide energy by fusion processes.

Thermonuclear (hydrogen) bomb—Even before the achievement of atomic bomb, it was realized by J. Robert Oppenheimer and others that the explosion of an atomic bomb might create the high temperature needed to start a thermonuclear reaction and thus an atomic bomb might serve as the *fuse or trigger* to set off a hydrogen bomb. Hydrogen bomb can be made with deuteron or tritium or the combination. It is possible to produce tritium (as it occurs in nature only in infinitesimal amounts) by the neutron bombardment of lithium in a nuclear reactor. Calculations show that a given weight of tritium would release 7 times as much energy as an equal weight of *Pu*. One kg of tritium would release as much energy as 140,000 tons of *T. N. T.* (the recognized abbreviation for the common chemical explosive 2, 4, 6-trinitrotoluene, assuming that the explosive energy of 1 ton of *T. N. T.* is 10^9 calories).

The energy produced in a hydrogen bomb is in an uncontrolled manner. To control thermonuclear reactions some of the essential conditions must be satisfied. The process must be self sustaining and the balance must be obtained between the energy released in fusion and the amount lost by radiation. The temperature corresponding to this condition of balance is known as *critical ignition temperature*. The relation $E=kT$ implies that it is of the order of 10^8 °K. At very high temperatures the atoms are fully ionized and these ions and the free electrons are moving about very rapidly. The result is a completely ionized gas, called a *plasma*. The plasma is electrically neutral so that in the absence of electric or magnetic fields, there are no external forces acting on it except gravity. Because of the internal pressure, the plasma would expand in a vacuum to fill the container in which it is kept. When it comes in contact with the walls, it heats up the walls.

The power produced in fusion reactor will depend on the plasma density and temperature. Because of the very low density of the plasma, used in controlled thermonuclear reactions, and the relatively small volume of the system, it does not behave as a black body. The radiation should consist mainly of bremsstrahlung accompanying the deflection of the rapidly moving electrons in the plasma by the electrostatic fields of the positively charged nuclei. The amounts of energies released per unit time per unit volume in the D-D reactions and in the D-T reactions and of energy lost as radiation at various temperatures are shown in Fig. 13.7. In common practice the temperatures are expressed in *keV*, which is equivalent to 1.16×10^7 °K It is clear from the figure that the bremsstrahlung

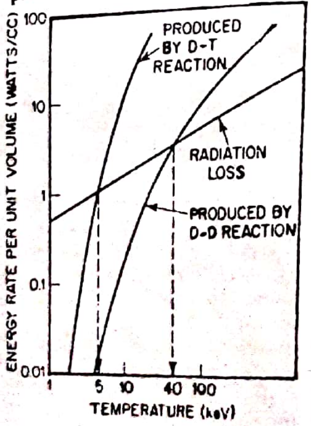

Fig. 13.7. Critical ignition temperature for the D-T and D-D reactions.

loss equals to power produced at plasma temperature about 5 *keV* for a D-T and about 40 *keV* for D-D reactions This does not necessarily mean that the plasma temperature for a D-D reactor has to be higher than 40 *keV* to produce a net power gain. The reason is that the bremsstrahlung is not lost but absorbed by the walls of the plasma container and converted therefore into heat in the way similar to the *K. E.* of the reaction products. The minimum operating temperature for a given reactor will therefore depend on the efficiency with which heat can be converted into other forms of energy. A part of this energy should be taken back by the plasma again to keep it at the operating voltage.

J. D. Lawson in England in 1957 pointed out another necessary condition, known as the *Lawson Criterion*, for a self-sustaining thermonuclear system. According to this criterion for a fusion reactor the total useful recoverable energy shall be at least sufficient to maintain the temperature of the reacting species. It can be expressed in terms of the product nt, where n is the number of reacting nuclei per unit volume and t is the time in seconds during which thermonuclear reaction takes place or the time during which the high temperature plasma can be confined. 6×10^{19} and 2×10^{21} are the calculated minimum values for nt for D-T system and D-D system respectively. Thus we see that critical ignition temperature and this criterion are very much favourable for D-T reactor than for D-D reactor.

Several equipments were constructed in an attempt to produce fusion reactions in a controlled manner. These are described as given below.

(a) Pinched Discharge—In principle the simplest way of heating and containing the plasma is to make use of a phenomenon called the *pinch*, utilized in U.S.A., U.K., and in the U.S.S.R. simultaneously and independently in the early 1950. In it a very strong electric current amounting to a million amperes is passed through a deuterium like gas at low pressure. This current heats the gas and ionizes it, thus converting it into a *plasma*. At the same time the current flow produces a magnetic field with its lines of force encircling the plasma. The pressure of this field then pinches the plasma into a narrow region in the centre of the containing vessel which may be a torus or a straight tube. In this manner the plasma is not only kept away from the walls but heated also by the current itself and by the compression produced by the magnetic field, the current generates.

Several experimental machines have been built, some on quite a large scale. Two machines name *Zeta* and *Sceptre* were designed by Harwell group and by associated electrical industries respectively. An entirely different approach to the confinement and heating of plasmas is by the method of *fast magnitude compression* also called the *theta pinch*, originated in 1957 at the Los Alamos scientific laboratory. The apparatus consists of an open ended tube containing deuterium gas at low pressure surrounded by a single turn coil. An oscillating current of several million amperes is passed through the coil for a very short time by the discharge of a large bank of capacitors. The first half cycle of the oscillating magnetic field produces an ionized sheath of plasma which is rapidly compressed and partially heated. In the second half cycle the direction of the magnetic field is reversed and the mutual annihilation of the oppositely directed fields releases a large amount of energy that heats the deuterium plasma. Scientists at Los Alamos were able to obtain plasmas with temperatures in excess of 5 keV and densities of about 4×10^{22} deuterons per m^3 by fast magnetic compression of low density preionized deuterium.

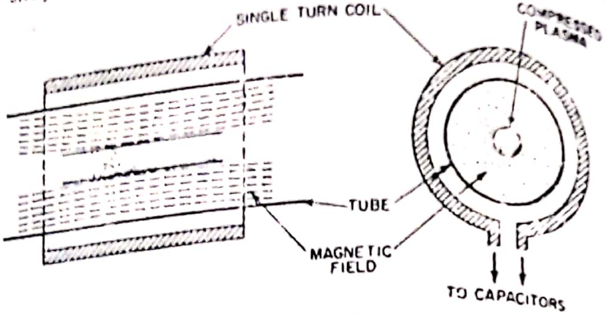

Fig. 13.8. Schematic diagram of theta pinch apparatus.

(b) **Stellarator**—In 1951, the astrophysicist L. Spitzer at Princeton University described a principle of stellarator as an another approach to plasma confinement. This name is used because controlled fusion reactions are similar to those in stars (*stella* is Latin). Stellarators are the modified torous type machines. Here a plasma is confined in a closed ring shaped tube. The magnetic field with the lines of force parallel to the circumference of the ring is produced by winding a coil of wire around the tube and passing an electric current through it. The magnetic field is stronger at the inner perimeter of the torus than at the outer perimeter, thus causes the plasma as a whole to move to the outer walls. The confinement is thus impossible.

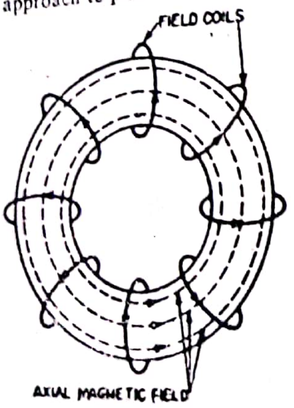

Fig. 13.9. Axial magnetic field in a toroidal tube.

Spitzer suggested to twist the toroidal tube into a space like a figure of 8. The difficulty of instability which causes a escape fo particles towards the walls is removed in this shape. The tendency of the plasma to drift in a particular direction in one bend of the tube is compensated by the opposite tendency in the other bend. In each circuit of the stellarator tube, a line of force is somewhat displaced from its original position. A magnetic field of this type is said to possess a *rotational transform*. The earliest stellarators were of the figure of eight type. The most recent stellarator is the Model *C* stellarator, which was completed in 1961 at Princeton. It is a large and complex but has a flexible facility for the study of plasma confinement and heating. The maximum strength of the axial magnetic field is about 5 tesla which is held constant for periods upto 1 sec. or so.

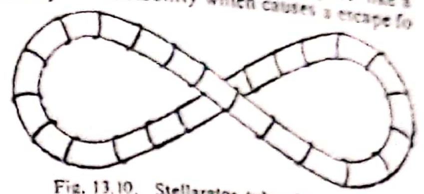

Fig. 13.10. Stellarator tube of figure eight.

(c) **Magnetic Mirror Systems**—In the stellarator and other systems using closed containing tubes, the plasma can escape in the axial direction and so confinement is required only in radial direction. In magnetic mirror systems the plasma is confined in a *bottle shaped magnetic field*. This system consists of a straight tube with magnetic coils wound around it in such a way as to provide a field that is considerably stronger at the ends than in the middle. The ions move in spiral orbits with radii of curvature inversely proportional to the field strength and under certain conditions are reflected when move into regions of higher field strengths. In this way the magnetic mirrors inhibit but do not prevent entirely the escape of plasma from the ends of the tube. For a particle to be reflected it must have a significant component of velocity perpendicular to the magnetic field lines in the central region between the mirrors. The greater the value of B_{max}/B_{min}, the smaller the value of $v_{\perp}$ relative to actual velocity v for which reflection is possible. The heating of the plasma in this system is accomplished by increasing the magnetic field relatively slowly such that the plasma is compressed. This compression can be carried out in several stages and the compressed plasma is transferred after each stage from one magnetic bottle to a smaller one in which it is further compressed.

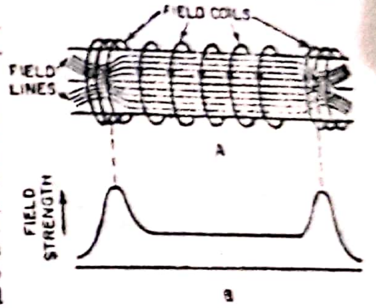

Fig. 13.11. (A) Field coils and lines of force in a magnetic mirror system ; (B) Variation in the magnetic field strength.

(d) **Beam-injection Method**—The injection of charged particles with a significant velocity component along the radial direction, directly across the magnetic field presents a difficulty. To solve this problem, the use of electrically neutral atoms of high energy was suggested, but it was very difficult to accelerate neutron atoms to a very high energy. Indirect process is the use of deuterium ions (~20 kV) which are allowed to pass into a chamber containing neutral deuterium gas. In this chamber a charge exchange occurs and the stream of high energy neutral deuterium atoms are produced, which then enter the magnetic field where they are ionized. Similar injection process used at the Oak Ridge National Laboratory starts with a high energy beam of molecular deuterium ions (D_2^+). These ions dissociate as $D_2^+ \rightarrow D^+ + D^\circ$. Since the mass of deuterium is half that of the molecular ions, hence the resulting D^+ ions can be trapped but the undissociated D_2^+ ions are not. The neutral atoms are not affected by the magnetic field and hence escape. As a result of collisions, the trapped deuterons acquire random motion equivalent to a high temperature.

EXERCISES

Example 1. *Calculate the fission rate for U^{235} required to produce 2 watt and the amount of energy that is released in the complete fissioning of ½ kg of U^{235}.*

As we know that 200 MeV energy is released per fission of U^{235}.

$\therefore$ Fission rate=2 watt/200 MeV per fission

$=6.25 \times 10^{10}$ fission/sec.

No. of U^{235} nuclei in ½ kg. of $U^{235} = (0.5/235) \times 6.0247 \times 10^{26}$.

On fissioning this number of U^{235} nuclei, the energy release will be

$= (0.5/235) \times 6.0247 \times 10^{26} \times 200$ MeV

$= 2.57 \times 10^{26}$ MeV$=10^{10}$ kilocalories.

Example 2. *Calculate η for thermal neutron induced fission of a uranium mixture containing U^{235} and U^{238} isotopes in a 1 : 20 ratio. Given $\nu=2.43$, $\sigma_a(U^{235})=683$ b, $\sigma_a(U^{238})=2.73b$, $\sigma_f(U^{235})=583b$.*

Average number of fission neutrons released per absorption

$$\eta=\nu(\sigma_f/\sigma_a).$$

For a mixture

$$\sigma_a = \frac{N_0(235)\ \sigma_a(235)+N_0(238)\ \sigma_a(238)}{N_0(235)+N_0(238)} = \frac{683+20\times 2.73}{1+20}$$

$=35.1$ barns.

and $$\sigma_f = \frac{N_0(235)\ \sigma_f(235)}{N_0(235)+N_0(238)} = \frac{583}{1+20} = 27.8 \text{ barns.}$$

Hence $\eta = 2.43 \times (27.8/35.1) = 1.924$.

Example 3. *Calculate ... and for*

7.22 Nuclear reactor

A *nuclear reactor* is a device wherein a neutron-induced self-sustained chain reaction involving fission of heavy elements takes place. The purpose of the reactor is to (i) *initiate nuclear fission reaction,* (ii) *control these reactions,* and (iii) *extract the energy produced* by fission. The **control of neutrons** is the key to the functioning of a reactor.

The first nuclear reactor came into operation in 1941 at the Columbia University under the leadership of Fermi and it was then called a *uranium-carbon pile.* The design, construction and operation of a nuclear reactor however are now parts of a huge and expanding field of nuclear engineering. Naturally, we cannot delve deep into the various features of a reactor. For instance, the detailed calculation of the critical size or mass of a nuclear reactor is beyond our scope. We shall study here only its basic elements, its different types etc. A schematic diagram of a reactor is shown in Fig. 7.13a.

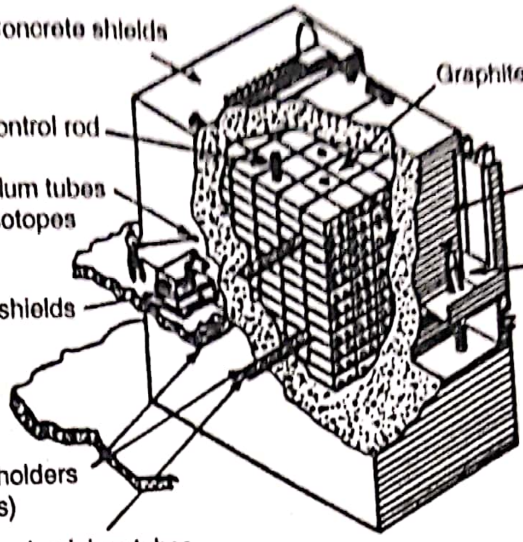

Fig. 7.13a Schematic diagram of a reactor

Basic elements of a reactor — All types of nuclear reactors contain the following essential *basic* elements :

(a) the *fuel*, a material that undergoes fissions and thereby supplies neutrons for inducing further fissions;

(b) the *moderator* for slowing down the speed of the fast neutrons (this however is not needed in case of fast nuclear reactors);

(c) the *neutron reflector* to prevent neutrons from escaping from the core;

(d) the *cooling system* to control the temperature of fuel elements and transport the generated heat to heat engine, and

(e) the *control and safety arrangements* to control the chain reaction against, 'running away' and protect the surroundings.

We shall now spend hereunder few lines on each of the above aspects.

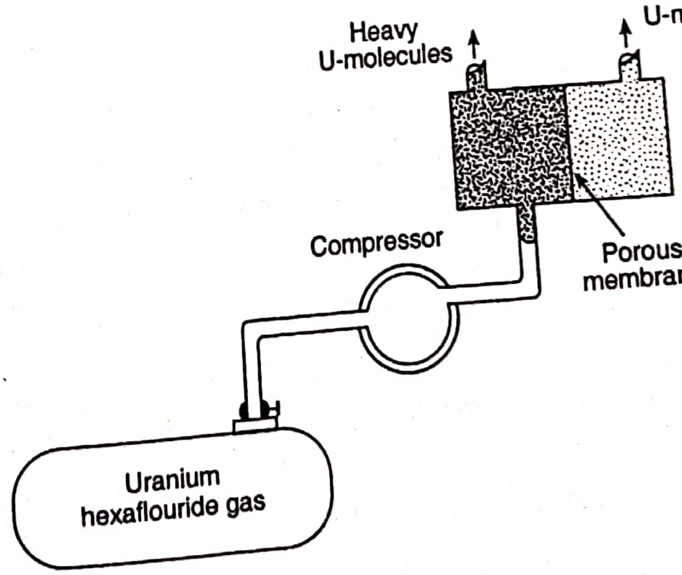

Fig. 7.13b Schematic arrangement of separating ^{235}U from ^{238}U by gas diffusion

The commonly used ***fissionable materials*** are the uranium isotopes : U-233, U-235, U-238; the thorium isotope Th-232 and the plutonium isotopes: Pu-239, Pu-240 and Pu-241. In natural uranium, the two isotopes ^{238}U and ^{235}U are in the ratio 140 : 1. One of the common methods to *enrich* natural uranium with isotope ^{235}U is the *gaseous diffusion through a porous barrier* and is schematically illustrated (only one stage, out of many) in Fig. 7.13b. In many reactors, natural uranium enriched with isotope ^{235}U, is also used.

The materials to be used as ***moderators*** should have a large inelastic scattering cross-section and small neutron capture (absorption) cross-section. The usual moderators are : graphite, heavy water (D_2O), beryllium oxide, hydrides of metals and organic liquids. The nuclei of these materials hardly absorb neutrons.

A ***reflector*** is a material placed around the reactor core (that contains the fuel and the moderator) to *prevent neutrons from escaping from the core. Good moderators* are usually *good reflectors* and the efficiency of a reflector increases rapidly with its thickness.

The ***cooling system*** in a reactor *helps to control the temperature of the fuel element and transports the heat generated by fission to the heat engine.* There are four types of possible coollants. These are (i) *gases* : air, CO_2, He or steam, (ii) *water type liquids* : water or heavy water, (iii) *molten metals* : Hg, Na, K, Na-K eutectic, Pb, Bi or Pb-Bi eutectic and (iv) *fused salts.* Each type has its own merits and demerits.

The ***control and safety system*** is intended to *control the chain reaction against its 'running away' spontaneously* and also for *protecting the surroundings against the intense neutron flux and dangerous γ-radiation inside* the core. While the first is achieved by pushing *control rods* of a material having *large neutron absorption cross-section* (e.g. boron, cadmium) into the core, the second one is accomplished by surrounding the reactor with massive layers of concrete and lead and by providing completely *closed* coolant circuits.

• The power level at which a reactor operates depends on the rate of fission and hence on the number of neutrons in it. By controlling the number of neutrons, therefore, the power level can be controlled. For this cadmium rods or steel rods with boron are used. Both cadmium and boron have high absorption cross-section for thermal neutrons and can change the reproduction factor k. To control the *criticality* of a reactor, control rods are *inserted into* the reactor. In the process, so many neutrons are absorbed that the reactor *shuts down.* Rods are then *moved out* until enough neutrons are present for the reactor to start toward *supercriticality* and then they are re-inserted until it is *critical* and the reactor operates at a constant power level. Needless to mention, *the process of reactor control is made automatic to eliminate any possible human error.*

7.23 Types of reactor

Reactors are broadly classified according to the type of fuel, moderator and the heat-transfer agents used.

With respect to the arrangements of the fuel and the moderator, the reactors are classed as (i) **homogeneous** and (ii) **heterogeneous.** In homogeneous reactors, the fuel and the moderator are finely divided and uniformly mixed together, while in heterogeneous reactors these two substances are in separate elements as blocks.

Depending on the energy of neutrons, the reactors may be **thermal, intermediate** and **fast.** In fast reactors, the fission-neutrons are directly used and as such the *moderator* is completely *dispensed with.*

Purpose-based division of the reactors is : **power reactor, test and research reactor, breeder reactor, isotope producing reactor** etc. In a *power reactor*, the energy available from the chain reaction is transformed into useful power form such as electricity. The *test and research reactors* are designed for a number of different testing purposes such as dimensional stability or instability of materials under irradiation and other radiation damage phenomena. In a *breeder reactor*, the fissionable materials are bred and in an *isotope producing reactors*, radioactive isotopes are produced for use in various sectors e.g. industry, agriculture, medicine etc.

Taking into account all the above features, the nuclear reactors can be classed as : *uranium-graphite, water-cooled, water-moderated, boiling* etc.

7.24 Homogeneous reactor

A *homogeneous reactor*, as already stated, is the one where the fuel and the moderator are uniformly mixed so that each U-nucleus has the same chance of capturing a neutron. We have already mentioned that with natural uranium, a homogeneous reactor can attain criticality only with heavy waer (D_2O) as moderator. Ordinary water (H_2O) may instead be used provided the fuel is enriched with ^{235}U.

A common type of such reactors uses a solution of uranyl nitrate in water with highly enriched fuel ($^{235}U : {}^{238}U \simeq 1 : 6$). The critical mass of ^{235}U in this case is nearly 0.8 kg, when the container is *spherical* with walls surrounded by graphite — a *neutron-reflector.* With no reflector, however, the critical mass is about 2 kg.

If the nuclear fuel is ^{235}U, the critical mass is about 0.6 kg and if the fuel is ^{239}Pu, it is 0.5 kg nearly.

7.25 Heterogeneous reactor

A *heterogeneous reactor* is one in which lumps of nuclear fuel are embedded in the moderator. It was suggested by Fermi and Szilard in the context of the fact that both enriched uranium and heavy water are highly expensive, and that in natural uranium the resonance escape probability is low for a sustained chain reaction. When uranium is used in lumps, the chance of capturing a neutron, unlike in a homogeneous reactor, is not the same for each U-nucleus. The neutrons with energies corresponding to resonant states of $(^{239}_{92}U)^*$ are mostly absorbed *on the surface only*, and once they are inside, the energies do not change much and thus escape the resonant absorption. The probability of neutron absorption inside uranium being much less than on the surface, it acts itself as *self-shielding* of uranium against neutron absorption.

Once the neutron is out of the lump, it enters a *uranium-free zone* of moderator only, where it colides with moderator nuclei losing much of its energy. Neutron can thus skip over several resonance, absorption levels before being with the next uranium lump where the same story is repeated.

What then are the **effects of lumping fuel in a moderator**? These are :

1. *Increase in fast fission factor* by about 10% ($\varepsilon \sim 1.1$), since the probability of fast neutron fission increases.

2. *Better moderation in uranium-free region*, for resonance absorption of neutrons by ^{238}U is very strong.

3. Resonance absorption in uranium is a *surface phenomenon* and the *resonance escape probability* ν *is not lowered inside a lump*. It implies that compared to the total volume, the surface layer volume in large lumps is small.

4. Large lumps however *lower the thermal utilisation factor a*, since the neutron-density in or near the lumps tends to be less than in the moderator—a condition favouring *unwanted neutron absorption in moderator*.

Factors (3) and (4) are mutually antagonistic and obvously therefore a compromise between them is to be struck.

Elementary Particles

16.1. INTRODUCTION

The problems concerning the elementary particles are to-day undoubtly the focus of interest and of research for the experimental as well as the theoretical physicists. Experimental investigations of elementary particles all involve some source of particles to study and some way of detecting those particles and measuring their behaviour. Many of the practical problems of such investigations are caused by the fact that many elementary particles are unstable. The classical elementary particle, the individual atom was nothing but the mass point of classical machanics. The investigation of electromagnetic phenomena suggested that the atom had an internal structure. At that time the typical photo-type of the elementary particle was the electron. The problem of the dualistic nature of matter was resolved by the quantum theory of fields : *the elementary particles are nothing but the quanta of a corresponding field.* The study of elementary particles is basis to the understanding of radiation phenomena, or one may regard any kind of radiation as a flux of elementary particles.

In 1932, when Chadwick identified the neutron and Heisenberg suggested that atomic nuclei consisted of neutrons and protons, it seemed as if p, n and e^- were sufficient to account for the structure of matter. Besides these there was the photon, *the intermediary or field particle for electromagnetic forces*, such as exist between the nucleus and electrons in the atom. If anti-matter exists it would then be made up of anti-electrons, *i.e.* positions, anti-protons and anti-neutrons. Thus we see that seven particles could explain both matter and anti-matter. In 1935, Yukawa postulated the existence of another particle, with a mass $m \simeq 200\ m_e$ *as the field particle for the strong nuclear forces*. Recently the extensive studies made partly on high energycosmic ray particles and even more, with the help of high energy accelerators have revealed the existence of numerous new nuclear particles. Apart from a dozen or so, the particles have very short lifetimes, very much less than 10^{-8} sec. They cannot therefore be regarded as normal constituents of matter. They are characterised by the parameters, mass, spin, electric charge and magnetic moment. They have been described by such adjectives, as *fundamental*, *strange* and *elementary*, but none of these is quite appropriate. The word fundamental implies that the particles are the basic building blocks of matter, but unstability of most of the particles indicates that the great majority are certainly not. It is true that their behaviour was strange in the early 1950, but it is much less now. For the want of better one the term elementary particles is now commonly used. These particles are elementary in much the same sense as are the chemical elements.

16.2. CLASSIFICATION OF ELEMENTARY PARTICLES

The elementary particles are separated into two general groups, called *bosons* and *fermions*. These two groups have different types of spin and their behaviour is controlled respectively by a different kind of statistic (*i.e.* the Bose statistic or the Fermi statistic, hence the names). Bosons are particles with intrinsic angular momentum equal to an integral multiple of $\hbar$. Fermions are all those particles in which the spin is half integral. The most important difference between the two classes of particles is that *there is no conservation law controlling the total number of bosons in the Universe, whereas the total number of fermions is strictly conserved*.

Boson is a term, which not only includes material particles but also includes those quanta and photons which arise from interactions. Thus in the case of the simple electromagnetic field the bosons are merely the light photons or the X-ray photons. The photon has a mass of zero and a spin of unity and is consequently described as a massless boson. A massless boson, called a *graviton* with a probable spin of two units has been postulated as a field particle for gravity. These bosons, created by the electromagnetic field, are essentially of one kind, while the bosons formed in the strong interaction are of two distinct kinds. First there are those which are known as *pions or π-mesons* (π^+, π^- and π°). The second group of bosons are much heavier than that of pions, and are known as *kaons or K-mesons* (K^+, K^- and $\overline{K^\circ}$).

The fermions fall in two main classes, according to whether they are lighter than mesons, or heavier. Those in the lighter group are often called *leptons* (*after the Greek word meaning light in weight*), whilst those in the heavier group are called *baryons* (*after the Greek word for heavy*). The leptons are the *electrons*, *muons* and *neutrinos* and *their anti-particles*. These are all with masses less than the pions and with spin half. Leptons interact weakly with other particles. The total number of leptons minus the total number of anti-leptons remains unchanged in all reactions and decay processes involving leptons and anti-leptons. The baryons consist of the *two nucleons* with their *anti-particles* (n°, $\overline{n^\circ}$; p^+, p^-) and the *hyperons*. Hyperons are the extremely unstable somewhat heavier particles and can be divided into four sub-groups, Λ°-particle (a neutral particle of mass about 2180 m_e), the Σ-particles (Σ^-, Σ° and Σ^+ with masses in the range

2320 to 2340 m_e), the Ξ-particles (Ξ^- and Ξ° with masses near 2580 m_e) and the Ω^--particle (of mass about 3284 m_e). There is no reason to doubt the existence of the anti-particles of these fermions. **The total number of baryons minus the total number of anti-baryons is absolutely conserved in all interactions.**

The kaons and pions together with the baryons are placed into a group of strongly interacting particles, called *hadrons*.

Table 16.1 ***Classification of Elementary Particles***

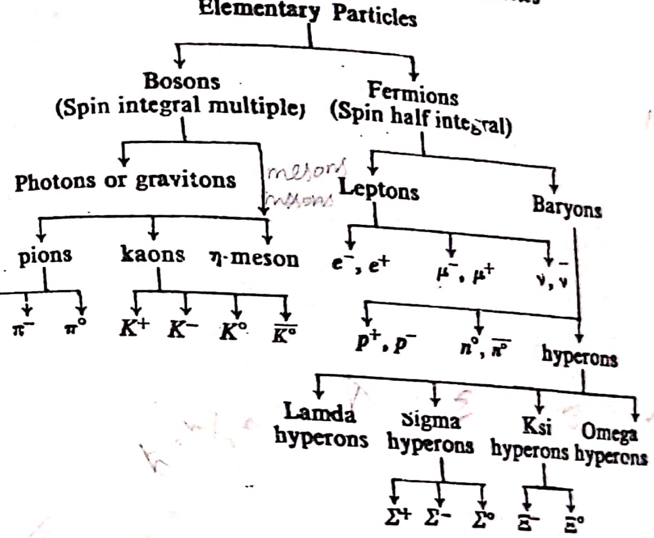

16.3. PARTICLE INTERACTIONS

The interactions among elementary particles can be classified into following four types :

(*a*) **The Gravitational Interaction.** The first force that any of us discover is gravity. It holds the moon and earth together, keeping the planets in their solar orbits and binds stars to form our galaxy. Newton gave a formula $F=Gm_1m_2/r^2$ for the interaction between two masses. The gravitational effect does not depend on the colour, size, charge, velocities, spin and angular orientation but depends on the *magnitude of the inertia*. The gravitational force between two nucleons separated by a nucleon diameter is

$$F=G\frac{m_1m_2}{r^2}=6.7\times10^{-11}\,\frac{(1.7\times10^{-27})^2}{(10^{-15})^2}\approx2\times10^{-34}\text{ newton} \quad ...(1)$$

and the gravitational attraction is only about 2×10^{-49} joule. Hence we see that it plays no role in particle reactions. In the nineteenth century the forces were thought to be propagated by fields, space warped for particular effects. In the twentieth century these fields are explained in terms of agents or messengers which actually propagate the effect. Gravitation can thus be explained in terms of the interactions of *gravitons*. Their mass must be zero and therefore, their velocity must be that of light. *As the gravitational field is extremely weak, the gravitons cannot be detected in laboratory.*

(*b*) **Electromagnetic Interactions.** All of the ordinary chemical and biological effects are due to the interaction of electric charges and the fields they produce. The term electromagnetism is because the electricity and magnetism are both part of the same phenomenon. The appropriate law for the interaction of point charges bears the name of Coulomb ($F=q_1q_2/4\pi\epsilon_0r^2$). For two protons, 10^{-15} metre apart, the repulsion force will be $9\times10^9\times(1.6\times10^{-19})^2/(10^{-15})^2\approx30$ newtons. It is about 10^{38} times greater than the gravitational attraction caused by the mass. The energy released by the complete separation of these protons would be 3×10^{-14} joules.

If the particles are not at rest but are moving, the field will not only be an electric field but would be new one depending on the velocity and magnitude of the charge. When the charge is accelerated, the energy is radiated out in the form of an electric and magnetic pulses. This energy comes from the agent which accelerates the charge. The pulse is called a *photon* and travels with the velocity of light. If the source charge is accelerating in an oscillating fashion, the propagated signal will consist of successive waves of electric and magnetic fields or the *radio-photons*. Thus we see that the photons are emitted and reabsorbed by a charge. *Interaction between two charged particles consists of an exchange of these photons.* The strength of the electromagnetic interaction is given by the dimensionless fine structure constant $\alpha\,(=e^2/\epsilon_0\hbar c=1/137)$, and is due to photon exchanges.

The electromagnetic interaction is charge dependent. In terms of isobaric spin, the interaction depends on T_3 and is governed by the isospin rule $\Delta T=0,\pm1$. All other quantities such as charge, baryon number, lepton number, hypercharge, parity, strangeness number are conserved.

The capture of photon can effect the production of mesons or hyperons by an electromagnetic interaction

$$\gamma+p\begin{matrix}\nearrow\pi^0+p\\ \searrow\Lambda^0+K^+\end{matrix}$$

An example of a radiative capture reaction is

$$\pi^-+p\rightarrow n+\gamma.$$

The neutral particles such as

$$\pi^0\rightarrow\gamma+\gamma,\ \Sigma^0\rightarrow\Lambda^0+\gamma,$$

$$\eta^0\rightarrow\pi^++\pi^-+\pi^0\qquad\eta^0\rightarrow\gamma+\gamma,$$

decay electromagnetically since these processes involve no change of strangeness. The decay processes such as $\Sigma^+\rightarrow p^++\gamma$ are forbidden because the change $\Delta S=1$ is required. The paradox that the decay

of neutral particle is by electromagnetic interaction is resolved by introducing as an intermediate step in the overall reaction. The virtual production of a *nucleon-anti-nucleon* (*or electron-positron*) pair. Thus we have

$$\pi^0\xrightarrow[\text{strong}]{}(N+\bar{N})\xrightarrow[\text{virtual}]{}\xrightarrow[\text{electromagnetic}]{}\gamma+\gamma.$$

The process of mutual annihilation of particles and anti-particles is an example of electromagnetic interaction.

(*c*) **Strong Interaction.** The strong nuclear interaction is independent of the electric charge. The force is same between *p-p* and *n-n*. For this purpose the proton and neutron are one but in different electric charge states. Strong interactions involve mesons and baryons. The range is very much shorter than that of gravitational or electromagnetic interaction. Strong interaction energy falls off rapidly when the distance between two particles increases. Yukawa in 1935 predicted the existence of heavy quanta, which played the same role in nuclear forces (or strong forces) as photons in electromagnetic ones. From estimates of the range of nuclear forces, Yukawa predicted that the new particles, called mesons, should have a mass of the order of 200 to 300 electron masses. In the chapter of nuclear forces, we outlined an elementary theory of pion-nucleon interaction and introduced the concept of a nucleon charge *g* analogous to the electric charge *e*. The strength of the nuclear interaction is represented by the magnitude of the dimensional coupling constant $g^2/4\pi\hbar c$ (≈14). It is about a thousand times the electromagnetic coupling constant α.

Strong interactions between elementary particles are responsible for the total cross sections as a function of energy. The strong interaction is a short range force ($\approx10^{-15}m$), conserves baryon number B, charge Q, hypercharge Y, parity π, isospin T and its component T_3. It is responsible for kaon production, however the decay of mesons, nucleons and hyperons proceeds by an electromagnetic or weak interactions.

(*d*) **Weak Interaction.** The weak interaction is responsible for the decay of strange and non-strange particles and for non-leptonic decays of strange particles. The numerical constant, which is characteristic of the weak interactions, is obtained from Fermi's theory of β-decay. Its value is $g_F=1.41\times10^{-62}\ Jm^3$. In analogy with the expression for the other interactions, the dimensionless weak interaction coupling constant is of magnitude

$$[g_F^2/(\hbar c)^2]\,[m_\pi c/\hbar]^4\simeq5\times10^{-14}.$$

Consider the reactions which do not involve a change of strangeness and yet which must be due to weak interaction. The neutron decay is the proto-type of all the β-decays:

$$n\rightarrow p+e^-+\bar{\nu}_e.$$

The nature of such an eqn is that the reaction can go in either direction so long as energy is conserved and that any participant can be replaced on opposite side by its anti-particle, *i.e.* $p \to n + e^+ + \nu_e$. Another variation of this four fermion interaction is the proton capture of an anti-neutrino ($\bar{\nu}_e + p \to n + e^+$). Another example of the four-fermion interaction is the muon decay ($\mu^- \to e^- + \nu_\mu + \bar{\nu}_e$). There is also a coupling among muons, nucleons and neutrinos, thus

$$\mu^- + p \to n + \nu_\mu .$$

There are however other types of weak interactions which require coupling between other pairs of fermions.

$$\Lambda^\circ\ (S=-1) \to \pi^-\ (S=0) + p\ (S=0).$$

There is no neutrino involved here, strangeness changes by +1 and only two fermions are involved. For four fermions one can assume this decay as through a virtual stage ($\Lambda^\circ \to \bar{p} + n^\circ + p^+$). In the first vitual step, four fermions are involved. In the next stage, the strong nuclear forces come into play. There are restrictions whether one transition is forbidden or allowed : *In a weak interaction involving change in strangeness of baryons or mesons, the change in strangeness must be equal to the change in charge.* The change in isospin T and its component T_Z may be nonzero. The strangeness and isospin are not meaningful for leptons, and are useful when hadrons are involved in the weak interactions. The lepton number is conserved in these interactions. The parity is not conserved, but CP and CPT are conserved.

Similar to the graviton for gravity, photon for elecromagnetism and mesons for the strong nuclear force there is one agent for the weak interaction. It would also be a boson of mass above 800 MeV and is named as the *intermediate charged vector-Boson* and given the symbol W. Its half life against decay into electron neutrino or muon-neutrino would be less than 10^{-17} sec.

One associates neutrino and anti-neutrino exclusively with the weak interaction, just as one associates photons with *em*-interaction. One particle may respond to the different types of interaction: *e.g.*, pion scattering is effected by a strong force, pion radioactive capture by an electromagnetic interaction and decay by a weak interaction.

We can thus write these interactions as :

Table 16.2 *Comparison of the four basic interactions*

Field	Relative magnitude	Associated particles	Characteristic time
Strong interaction	1	Pion, kaon	10^{-23} sec.
Electromagnetic	10^{-2}	Photon	10^{-20} sec.
Weak interaction	10^{-12}	Intermediate boson	10^{-10} sec.
Gravitational	10^{-39}	Graviton	10^{16} sec.

16.4. CONSERVATION LAWS

The behaviour of the elementary particles is restricted by a number of conservation laws or invariance principles. That is to say, certain properties of representative physical quantities must remain unchanged in any process. The most familiar quantities in large scale experiments that are conserved in all (strong, electromagnetic and weak) interactions are :

(1) *Conservation of linear momentum*

(2) *Conservation of angular momentum.* The conservation of angular momentum includes both types (orbital and spin) of angular momentum together. The first is given by the motion of the object as a whole about any chosen external axis of rotation. The second is the intrinsic angular momentum of each object about an axis through its own centre of mass. Strongly interacting fermions have a half integer spin ($s=\frac{1}{2}$ for Ξ, Σ, Λ, n and p ; $s=\frac{3}{2}$ for Ω), strongly interacting bosons (η, K, π) have $s=0$, weakly interacting fermions (leptons μ, e, ν_e, ν_μ) have $s=\frac{1}{2}$, massless bosons (electromagnetic interacting γ-rays) have $s=1$ and gravitions have $s=2$.

(3) *Conservation of energy.* Conservation of energy on other hand seems more complicated with elementary particles because a large fraction of the total energy is oftenly interchanged between rest energy associated with mass and kinetic or potential energy. The sum of these three, the total energy is always conserved in any reaction. For example the decay reaction $K^\circ \not\to \pi^+ + \pi^- + \pi^\circ + \pi^\circ$ is forbidden because the rest energy of the K° is not great enough to make four pions even if they all could be make at rest. However, the reaction $K^\circ \to \pi^+ + \pi^- + \pi^\circ$ is allowed.

(4) *Conservation of charge.* The most familiar of the conservation laws is the conservation of *electric charge*. The charge is conserved in all processes and no exceptions are known. We note that all elementary charges are 0, or -1 ; multiple charges are not found.

(5) *Conservation of baryon number.* The number of baryons minus the number of anti-baryons is conserved. In other words *the net baryon number in any process always remains unchanged.* All normal baryons such as p^+, n^0, Λ°, Σ^+, Σ^-, Σ^0, Ξ^-, Ξ^0 and Ω^- have a baryon number of $+1$, the corresponding anti-particles known as anti-baryons have a baryon number of -1. *All the mesons have a baryon number of zero.* For example, the reaction $\Lambda^0 \to p^+ + \pi^-$ is *allowed* because the baryon Λ^0 is replaced by the baryon p^+, keeping the total number of baryons constant. The reaction $\Lambda^0 \not\to \bar{p} + \pi^+$ is *forbidden* because one baryon is replaced by one anti-baryon changing the baryon number by -2.

(6) *Conservation of lepton number.* The number of leptons minus the number of anti-leptons is conserved. In other words *the net leptons number in any process always remains conserved.* The ordinary electron, negative muon and neutrinos all have a lepton number $+1$, the corresponding anti-particles known as antileptons have a lepton number of -1. The reaction $\mu^+ \to e^+ + \nu + \bar{\nu}$ is allowed

because a lepton number of -1 is replaced by a lepton number $(-1)+(+1)+(-1)=-1$.

The reaction $n \rightarrow p+e^{-}+\bar{\nu}$ is allowed by both conservation of baryons and conservation of leptons. No exception to the rules of conservations of baryons and leptons has been found in the many elementary particle reactions so far studied one by one. Conservation of leptons has a significance for strong interactions. There are other conservation laws which are not applicable to weak interactions. The property that is conserved in strong interactions only is known as isospin. Other properties which are not conserved for all the three interactions, but are conserved in one or two interactions only, are hypercharge, *strangeness*, *parity*, invariance under charge conjugation and invariance under *CP* conjugation.

1. *Conservation of Isospin*. According to the ordinary idea of isotopic spin, each nuclear particle posseses a certain total isotopic spin T and each possible projection of this isotopic spin along a certain axis T_3 appears to us as a different charge state of the corresponding particle. In the case of nucleons, $T=\frac{1}{2}$ and the $2T+1=2$, possible values of T_3 are $+\frac{1}{2}$ (for the proton state) and $-\frac{1}{2}$ (for the neutron state). For the pions, $T=1$ and so there are $2T+1=3$ charge states. The triplet consists of π^{+}, π^{0} and π^{-} particles and the values of T_3 are $+1, 0, -1$, respectively.

B is $+1$ for the proton, neutron and hyperons and is zero for the pions. Inserting the value of T_3 and B, one obtains :

$$Q_p=+\tfrac{1}{2}+\tfrac{1}{2}=+1,\ Q_n=-\tfrac{1}{2}+\tfrac{1}{2}=0,$$

$$Q_{\pi^{+}}=+1+0=1,\ Q_{\pi^{0}}=0+0=0,\ Q_{\pi^{-}}=-1+0=-1.$$

Analytically, if B is the baryon number, T the isotopic spin quantum number, T_3 the component of T and Q the charge in units of the electron charge, the relation between these quantities is

$$Q=T_3+B/2. \qquad \text{...(2)}$$

Isospin numbers are associated with *hadrons* (particles that can exhibit strong interactions) but not with leptons. The isospin component T_3 is conserved in both strong and electromagnetic interactions but not in weak interaction.

2. *Conservation of Hypercharge*. A quantity called *hypercharge* (the twice the average charge of the members of the group), is also conserved in strong and electromagnetic interactions. For example, for the triplet π^{+}, π^{0}, π^{-}, average charge is zero and hence all these three mesons have a hypercharge of zero. The hypercharge of the pair of the particles K^{+} hnd K^{0} is $+1$ and that of the pair of anti-particles K^{-} and $\bar{K}^{0}$ is -1. Thus the alternative definition is that it is twice the difference between the actual charge Q and the isospin component T_3 of a particle. Thus hypercharge

$$Y=2(Q-T_3). \qquad \text{...(3)}$$

3. *Conservation of Strangeness*. The concept of strangeness has found wide application in particle physics. It is an additional quantum number which describes the interactions of elementary

particles. It has been chosen in such a manner that it becomes zero for all the well known particles (non-strange particles). Rochester and Butler, in 1947, at the Univeriity of Manchester arranged a magnetic cloud chamber and after about a year of operation reported certain new types of forked or V shaped tracks in cloud chamber photographs of cosmic rays. These new V-particles were also investigated intensively by cloud chamber groups from various institutions for several years. By 1953, at an International Conference on Elementary particles at Bagneres a decision was taken to name those particles of mass greater than π-mesons, but smaller than protons, *K-particles*, while those particles whose masses were greater than protons were to be termed *hyperons*.

One of the most common V-particles (Λ°) was neutral and decayed ($\Lambda^{\circ} \rightarrow p+\pi^{-}$) in time 2.5×10^{-10} seconds. The question arised if the Λ° could interact strongly, why did not its decay go via strong interactions with a life time of $\sim 10^{-23}$ sec instead of the observed 10^{-10} sec ? To explain this, Pais suggested the hypothesis of *associated production. The V-particles can interact strongly and, therefore, are produced only in pairs, once separated each number can decay into ordinary particles only through the weak interaction.* A typical example is

$$\pi^{-}+p^{+} \rightarrow \Lambda^{\circ}+K^{\circ}$$

$$\Lambda^{\circ} \rightarrow p^{+}+\pi^{-} \qquad K^{\circ} \rightarrow \pi^{+}+\pi^{-}.$$

Both the associated creation of the strange particles and their individual stability against immediately decay were the features that earned them the title *strange*. Both features can be explained by insisting that the total *strangeness* must remain constant in fast particle reaction.

If the baryons are arranged in columns accordingto their electric charge (plus under plus, minus under minus, neutral under neutral) The electric charge centres do not thus occur in the same vertical line. The electric charge centre of the nucleon is at $+\frac{1}{2}$, half way between p and n. The charge centre of Λ° is at 0. The triplet sigma is centred at 0, but the doublet xi is centred at $-\frac{1}{2}$. The Ω^{-} singlet is at charge -1. If we take the charge centre of the nucleon doublet arbitrarily to be reference origin, then we have

For Λ°...$\Delta Q=Q_{\Lambda}-Q_{N}=-\frac{1}{2}$; for Σ-hyperons...$\Delta Q=Q_{\Sigma}-Q_{N}=-\frac{1}{2}$: for Ξ-doublet...$\Delta Q=-1$ for Ω^{-}...$\Delta Q=-\frac{3}{2}$.

By defining strangeness quantum number as

$$S=2\Delta Q. \qquad \text{...(4)}$$

We obtain $S=0$ for the nucleons and non-zero for hyperons ($S=-1$, for Λ° and Σ's, -2 for Ξ's and -3 for Ω^{-}). Once a hyperon or K-meson is produced and gets beyond the influence of the collision, it can decay. As the decay products have strangeness zero hence the strangeness remains conserved in fast nuclear processes. Once produced and separated from each other, they must wait for some weaker interaction to allow them to decay. Strangeness conservation governs only the strong interactions and not the weak. Even the weak interactions have some respect for strangeness. It is found experimentally that weak decays change strangeness as little as possible.

$\Delta S=\pm 1$. No example with $\Delta S=\pm 2$ has been seen.

The examples are :

$\Sigma^+ \rightarrow \Lambda^\circ + e^+ + \nu_e$, $\quad \Delta S=0$

$\Sigma^- \rightarrow n + e^- + \bar{\nu}_e$, $\quad \Delta S=1$

$\Lambda^\circ \rightarrow p + e^- + \bar{\nu}_e$, $\quad \Delta S=1$.

M. Gell Mann in U. S. A. and T. Nakano and K. Nishijima in Japan independently suggested this strangeness quantum number. They suggested a scheme, known as Gell-Mann and Nishijima scheme after their names, for this quantum number. In this relation (2) is replaced by

$$Q=T_3+\tfrac{1}{2}Y = T_3+\tfrac{1}{2}(B+S), \quad ...(5)$$

where

$$Y=S+B \quad ...(6)$$

Since B is conserved always, the strangeness like the hypercharge is conserved in strong and electromagnetic interactions.

To cover a whole range of strongly interacting particles, the formalism has also been extended to mesons. Since the hyperons all have negative strangeness, they can be produced only in association with K-mesons of positive strangeness. On the assumption that strangeness is a conserved quantity in a reaction such as

$$p^+ + p^+ \rightarrow p^+ + \Lambda^\circ + K^+$$

$$S: \quad 0+0 \rightarrow 0+(-1)+S_k,$$

strangeness $S_k=+1$. Similar argument gives strangeness $S=1$ for neutral kaon. From the associated production reaction

$$\pi^- + p \rightarrow \Lambda^\circ + K^\circ$$

$$S: \quad S_\pi + 0 = -1 + 1,$$

it follows that $S_\pi=0$. It also applies to π^+, π° and η° mesons. Since for mesons the baryon number $B=0$, hence strangeness S=hypercharge Y.

Thus we see that strangeness is not an independent new quantity, but is related to a combination of Q, T_3 and B, each of which is regulated by conservation laws.

Let us now see what kinds of particle type can be formed by various choices of T, B and S. *If $S=0$, there are three possibilities,*

(a) $B=0$, $T=0$ yields $Q=0$ (*natural meson*), η° *meson*.

(b) $B=0$, $T=1$ yields $Q=+1, 0, -1$ (*pions*).

(c) $B=1$, $T=\tfrac{1}{2}$ yields $Q=+1, 0$ (*nucleons*).

If $S=1$, the multiple charge can be avoided only when

(a) $B=1$, $T=0$ and $Q=+1$ (*Baryon singlet*).

(b) $B=0$, $T=\tfrac{1}{2}$ and $Q=+1, 0$ (K^+, K°).

If $S=-1$, the multiple charges can be avoided only when

(a) $B=0$, $T=\tfrac{1}{2}$ and $Q=0, -1$ ($\bar{K}^\circ$ and K^-).

(b) $B=1$, $T=0$ and $Q=0$, (singlet baryon Λ°).

(c) $B=1$, $T=1$ and $Q=+1, 0, -1$ (Σ^+, Σ° and Σ^-).

If $S=-2$, the multiple charges can be avoided only when

(a) $B=1$, $T=\tfrac{1}{2}$ and $Q=0, -1$ (hyperons Ξ°, Ξ^-).

If $S=-3$, the multiple charges can be avoided only when

(1) $B=1$, $T=0$ and $Q=-1$ (Ω-hyperon).

All these results are summarised in the followidg table :

Table 16.3

S	B	T	T_3	Q	Particle
0	0	0	0	0	η°
	1	$\tfrac{1}{2}$	$\tfrac{1}{2}$	+1	p
			$-\tfrac{1}{2}$	0	n
	0	1	+1	+1	π^+
			0	0	π°
			−1	−1	π^-
1	1	0	0	1	Baryon (Not detected)
	0	$\tfrac{1}{2}$	$+\tfrac{1}{2}$	1	K^+
			$-\tfrac{1}{2}$	0	K°
−1	0	$\tfrac{1}{2}$	$+\tfrac{1}{2}$	0	$\bar{K}^\circ$
			$-\tfrac{1}{2}$	−1	K^-
	1	0	0	0	Λ°
	1	1	+1	+1	Σ^+
			0	0	Σ°
			−1	−1	Σ^-
−2	1	$\tfrac{1}{2}$	$\tfrac{1}{2}$	0	Ξ°
			$-\tfrac{1}{2}$	−1	Ξ^-
−3	1	0	0	−1	Ω^-

In the case of hadrons, the strangeness must be conserved($\Delta S=0$) for fast reactions. The decays of kaons and hyperons are very slow because they involve a breakdown of strangeness conservation. The decays $\Xi^- \rightarrow n+\pi^-$ and $\Xi^\circ \rightarrow p+\pi^-$ which involve $\Delta S=2$ would be expected to be exceptionally slow, and the decays $\Xi^- \rightarrow \Lambda^\circ + \pi^-$ and $\Xi^\circ \rightarrow \Lambda^\circ + \pi^\circ$ with $\Delta S=1$ to be slow. Since charge and baryon number are always conserved hence for weak decay processes, eqn (5) gives

$$|\Delta S| = 2|\Delta T_3| \quad ...(7)$$

or

$$|\Delta T_3| = \tfrac{1}{2}.$$

As T_3 is the component of total isospin along a particular direction, hence the general form of eqn (7) for weak decays is ...(8)

$$|\Delta T| = \tfrac{1}{2}.$$

Let us apply conservation laws to high energy pion-nucleon collisions which often give large quantities of kaons. Examples of possible equations are

$$\pi^{+}+n^{\circ}\rightarrow\Lambda^{\circ}+K^{+}$$

$$\rightarrow K^{\circ}+K^{+}.$$

Using the conservation of baryons and strangeness, we see that the second reaction violates baryon conservation and, therefore, can not occur. Similarly equation $\pi^{-}+p^{+}\rightarrow\Lambda^{\circ}+K^{\circ}$ is possible whereas $\pi^{-}+p^{+}\rightarrow\Lambda^{\circ}+\pi^{\circ}$ is not possible by strangeness violation.

Let us consider equation $p^{-}+p^{+}\rightarrow 2\pi^{+}2\pi^{-}+\pi^{\circ}$. Applying various conservation laws and remembering that the pairs of pions are ejected with opposite isospins, we have

$$Q=-1+1\rightarrow 2-2+0, \quad \therefore \quad \delta Q=0$$
$$B=-1+1\rightarrow 0+0+0, \quad \therefore \quad \delta B=0$$
$$T=\tfrac{1}{2}+\tfrac{1}{2} \rightarrow 0+0+1, \quad \therefore \quad \delta T=0$$
$$Y=-1+1\rightarrow 0+0+0, \quad \therefore \quad \delta Y=0$$
$$S=0+0 \rightarrow 0+0+0, \quad \therefore \quad \delta S=0.$$

4. Charge Conjugation. Charge conjugation is defined as the interchange of particles and anti-particles. It does not simply mean a change over the opposite electric charge or magnetic moment, the sign of other charge quantum numbers [hypercharge Y, baryon number B, lepton numbers (l_e, l_μ)] is also reversed without changing mass M and spin s. Thus a unitary operator, also known as charge conjugation operator **C**, satisfies the following relations :

$$\mathbf{C}Q\mathbf{C}^{-1}=-Q,\ \mathbf{C}Y\mathbf{C}^{-1}=Y,\ \mathbf{C}B\mathbf{C}^{-1}=-B,\ \mathbf{C}l_e\mathbf{C}^{-1}=-l_e$$

and

$$\mathbf{C}l_\mu\mathbf{C}^{-1}=l_\mu.$$

Some elementary particles *e.g.*, γ, π°- mesons and the positronium atom $(e^{-}+e^{+})$ are transformed into themselves by charge conjugation. They are their own anti-particles. These are known as *self-conjugate or true neutral particles*. The neutron $(B=1, Y=1)$ and K°-mesons $(Y=1, B=0)$ are not invariant under **C**.

A system is said to possess charge conjugation symmetry or to be invariant under charge conjugation if the system (or the process) is such that it is impossible to know that it has undergone charge conjugation. For example, the operation **C** converts the negative pion decay $(\pi^{-}\rightarrow\mu^{-}+\bar{\nu}_\mu)$ into the positive pion decay $(\pi^{+}\rightarrow\mu^{+}+\nu_\mu)$, since the π^{+} is the anti-particle of π^{-}. Until about two decades ago it was believed that the entire universe is invariant under **C**. In the end of 1956, experiments revealed that weak interactions violated it. It turned out that the μ^{+} and μ^{-} decay electrons have angular distributions of opposite asymmetry : that the π^{+} and π^{-} decay muons have opposite polarizations and that while a free neutrino is left handed an anti-neutrino is right handed. Charge conjugation applied to a free moving neutrino then results in a process which does not exist in nature.

The charge conjugate of the Dirac equation, which corresponds to the wave functions of positrons, has the form

$$\mathbf{C}=i.e^{i\phi}\begin{pmatrix}0 & \sigma_y\\ \sigma_y & 0\end{pmatrix}=e^{i\phi}\, i\,\alpha_y.$$

The phase ϕ is arbitrary. For zero phase ...(9)

$$\mathbf{C}=i\alpha_y,$$

where α_y is a square matrix and σ_y is the Pauli spin matrix having value ...(10)

$$\sigma_y=\begin{vmatrix}0 & -i\\ i & 0\end{vmatrix}$$

For a single photon state ...(11)

$$\mathbf{C}\,|\,\gamma>=-|\gamma>.$$

A state vector for n-photons ...(12)

$$\mathbf{C}\,|\,n\gamma>=(-1)^{n}\,|n\gamma>.$$

Thus for n-quanta the eigenvalue of **C** is $(-1)^n$. Since π°mesons decay through electro magnetic interaction into two photons $\pi^{\circ}\rightarrow 2\gamma$, it follows that the π°-meson is in eignstate of **C** with eignvalue $+1$, *i e.* ...(13)

$$\mathbf{C}\,\pi^{\circ}>=|\,\pi^{\circ}>$$

On the other hand $|\,\pi^{+}>$ and $|\,\pi^{-}>$ and not eignstates of **C** as

$$\mathbf{C}\,|\,\pi^{+}>=-|\pi^{-}>\text{ and }\mathbf{C}\,|\,\pi^{-}>=-|\,\pi^{+}>.$$

As the triplet spin state is symmetrical and the singlet spin state anti-symmetrical, hence to exchange an electron with a positron we must induce factor $(-1)^{s+1}$ as well as a factor $(-1)^{l}$. Thus we have

$$(-1)^{l+s+1}\,\mathbf{C}=-1 \qquad \text{or } \mathbf{C}=(-1)^{l+s}.$$

This relation gives that the singlet ground state $(l=0)$ decays into two photons $(\mathbf{C}=1)$ and the triplet ground state decays into three photons.

5. Space-inversion Invariance (parity). The parity principle says that there is a symmetry between the world and its mirror image. This may be defined as reflection of every point in space through the origin of a co-ordinate system $x\rightarrow -x, y\rightarrow -y$ and $z\rightarrow -z$. If a system or process is such that its mirror image is *impossible to obtain in nature*, the system of process is said to violate the law of parity conservation.

Human body is a good example of mirror symmetry. The body of a car is symmetric except for the position of the steering wheel. If we were looking at the mirror image of a normal car, it seems to violate the symmetry but it is not the case as it is also possible to design a car with the steering wheel on the other side. The min view of a printed page looks wrong. But there is nothing impossible about it. A printer could design inverted type and produced a page. One can read the page from right to left. The type of printing is not unnatural but is unconventional and unfamiliar.

All phenomena involving strong and electromagnetic interactions alone do conserve parity. In these cases the systems can be classified by the eigen values of the parity operator **P**. For a single particle Schrodinger wave function ψ, the result of the parity operation is

$$\mathbf{P} \mid \psi(x) > = e^{i\alpha} \mid \psi(+x) > , \quad \ldots(14)$$

As α is an arbitrary real phase, hence can be set equal to zero.

$$\mathbf{P} \mid \psi(x) > = \mid \psi(-x) > \quad \ldots(15)$$

and

$$\mathbf{P}^2 \mid \psi(x) > = \mid \psi(x) > . \quad \ldots(16)$$

It shows eignvalues of **P** as +1 or −1.

The parity of the photon depends upon the mode of transition, it is due to the change of the sign of electromagnetic current **j** under the parity operation. The nucleons and electrons are assigned *positive* or *even* intrinsic parity. The pions have ***negative or odd*** parity as they involve in strong interactions with nucleons. *K*-mesons and η°-meson have negative parity. $\Lambda^\circ - \Xi^-$ -, Σ-, Ω-hyperons have positive intrinsic parity. All anti-particles of spin $\frac{1}{2}$ are of opposite parity to the corresponding particle, while the bosons and their anti-particles have the same parity.

The conservation of parity requires that the Hamiltonian of a free system commute with the parity operator.

$$(\mathbf{PH} - \mathbf{HP}) = 0. \quad \ldots(17)$$

The transition probability must be scalar it may contain pseudoscalar operator (**I**.**p**). The conservation of parity prevents the mixing of even and odd operators in the amplitude. Thus for the non-conservation of pairty in β-decay, the transition probability must contain both scalar and pseudoscalar terms, *or the number of electrons emitted parallel and anti-parallel to the spin of the source should be different.*

The weak decay of the *K*-mesons, which was difficult to reconcile with parity conservation and known as the τ-θ puzzle, was explained by Lee and Yang. They suggested that *the weak interaction was not invariant to space reflection.* In 1956, Wu and others, using polarized Co^{60}-nuclei, found that the direction of emission of electrons in the transformation to Ni^{60} was preferentially opposite to the spin direction. The value of the pseudoscalar **I**. **p**, where **I** is the nuclear spin and **p** the electron momentum, was measured and found to be different from 0.

(6) *Combined Inversion* (**CP**). Landu (1956) advanced a hypothesis to the effect that any physical interaction must be invariant under simultaneous reversal of position coordinates and change over from particles to anti-particles. For example a neutrino has a definite helicity and its parity conjugate has opposite helicity. The charge conjugate of the neutrino also has opposite helicity. *Thus under the combined operation* **PC** (*or* **CP**) *the neutrino changes to anti-neutrino.* The combined operation also known as *combined parity* (charge and space) *is conserved in most of the known physical processes.* Let us consider the decay of the positive pion,

$$\pi^+ \rightarrow \mu_L^+ + \nu_{\mu L}.$$

Here subscript *L* indicates that neutrino and +ve muon fly apart with left handed spin. As the **C**-inversion changes particles into anti-particles and vice-versa, whereas the **P**-inverson converts left handed motion to right handed motion. Hence

C-inversion	: $\pi^- \rightarrow \mu_L^- + \nu_{\mu L}$	Impossible process
P-inversion	: $\pi^+ \rightarrow \mu_R^+ + \nu_{\mu R}$	"
CP-inversion	: $\pi^- \rightarrow \mu_R^- + \nu_{\mu R}$	possible "

Let us consider the case of the β-decay of polarized nuclei (*e.g.* Co^{60}). The interpretation of the parity non-conservation, charge non-conservation and conservation under the combined operation is shown in fig. 16.1. In this figure *B* shows the direction of a magnetic field due to current loop, used for polarizing the nuclei. It represents the nuclear spin and thus known as *polarization vector*. The upper diagrams represent the result of the reflection of the process

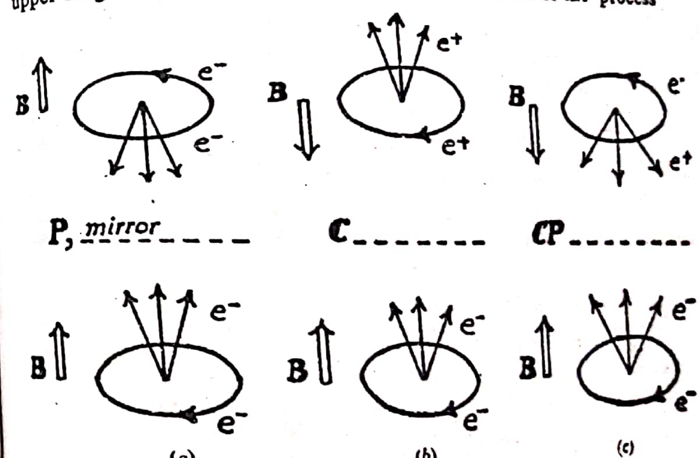

Fig. 16·1. (*a*) Parity mirror, (*b*) charge conjugation mirror and (*c*) *CP*-mirror

shown in the lower diagrams of Fig. 16.1. Fig. 16.1 (*a*) shows that the space reflection creates a different system, as it changes the direction of decay arrows but not the direction of B. Fig. 16.1 (*b*) represents the charge conjugation only. This process leaves the direction of the decay unchanged, although electrons are replaced by positrons and the polarization direction is reversed. Fig. 16.1 (*c*) shows the combined effect of **CP** operation. This shows that under **CP** reflection, we obtain the process of decay of the anti-nucleus. From the above results we conclude that the reflection type of symmetry can be obtained by the combined operation of **C** and **P** only in weak interactions. Number of other examples show that the weak interactions do not grossly violate the combined **CP**-invariance. Unfortunately the decay of K-meson is not invariant under the combined operation **CP**.

(7) Time Reversal. The time reversal operator is defined as that operator which reverses the direction of time, or the direction of all motions. Under this operation displacement, acceleration and electric fields remain invariant but momenta, angular momenta and magnetic fields invert their signs. If the time reversed process is impossible to occur in nature we can say that the process violates time reversal symmetry. In order to imagine a process under time reversal, it is convenient to imagine that a film of the process is being non-backwards.

Time reversal invariance finds its simplest application in the world of particles, where it appears to govern the strong and electromagnetic interactions and possibly also the weak. It also shows that a particle possessing time reversal symmetry cannot have electric and magnetic dipole moments simultaneously. The time reversal process is the creation of an electron-positron pair by the collision of two photons.

Time reversal invariance is satisfied in quantum mechanics if the Hamiltonian H is time independent and real. In this case $\psi^*(\mathbf{x}, -t)$ is the time reversal wave function of $\psi(\mathbf{x}, t)$. Thus time reversal operation **T** changes ψ as

$$\mathbf{T}\,\psi(\mathbf{x}, t)=\psi^*(\mathbf{x}, -t). \qquad ...(11)$$

The motion of a particle in an external fixed magnetic field is not invariant under inversion of time. The relativistic treatment of time reversal shows that the inversion of time axis inverts the sign of the electrostatic potential. The (π°-) mesic field, like the magnetostatic potential, is odd under time reversal in order to ensure that the interaction is time reversible.

(8) Combined Inversion of CPT. The strong and the electromagnetic interactions are invariant under the separate operations of **C**, **P**, and **T**. The weak interaction does not conserve parity and also is not invariant under charge conjugation. All the interactions are invariant under the combined *strong reflection* operation **CPT**, irrespective of the order of the operations. No example of a violation of the **CPT** theorem is known. It follows that if **T** invariance is satisfied for all interactions, then these interactions will also be invariant under the combined operation of **CP**. The existence of **CP** violating interactions means that the analysis is not quite accurate.

The quantities conserved have the quantum numbers, which behave in two different ways, when one considers a system formed by the combination of two other systems. The quantum numbers, such as *angular momentum*, *isospin*, *strangeness*, *baryon number*, *lepton number*, *electric charge* are called *additive*. On the other hand, quantum numbers, such as *parity*, *invariance under charge conjugation*, *invariance under time reversal* are called *multiplicative*.

16.19. ELEMENTARY PARTICLE SYMMETRIES

Mendelyeev was able to predict correctly the atomic weights and other properties of then unknown elements by means of his periodic system. Similarly, the classification of the elementary particles has also met with success in predicting new particles. The method developed for the arrangement is based on a branch of advanced mathematics, known as *group theory*. It has been found that, in general, *the conservation law represents an invariance which corresponds to an appropriate symmetry operation.* The set of operators that represents the symmetry constitutes the group from which the theory gets its name. The irreducible representations of a group consist of a number of states, quantities or objects to which the symmetry operations are applicable. Thus the appropriate group operation can transform any one of these states into another in the same representation. The fundamental representation is the one containing the smallest number of states for the particular group.

If the system is invariant with respect to displacement in space linear momentum is conserved. Angular momentum is conserved if invariance is *w.r.t.* angular displacement and energy is conserved if it is *w.r.t.* time.

The simplest unitary group $U(1)$ contains transformations which add a phase factor only to particle wave functions. The invariance under such transformations gives conservations of charge Q, baryon B, lepton L and hypercharge Y.

Unitary Symmetry [SU (2) Symmetry]. We know that proton and neutron are identical as far as the nuclear force is concerned, but differ in their electromagnetic interactions. Thus, it is possible to imagine a group of symmetry operators which could transform a neutron into a proton (or proton into a neutron) in the absence of an electromagnetic field. The proton and neutron would then form the fundamental representations of the group. The existence of such a symmetry implies that something remains constant under the strong interaction. This is known as *isospin* and is $\frac{1}{2}$ for proton as well as for neutron. The component of the isospin, T_3 is $+\frac{1}{2}$ for the proton and $-\frac{1}{2}$ for the neutron. The operators of the symmetry group thus change the co-ordinates of isospin in such a way as to reverse the sign of T_3. It can also be expressed as: *the strong interactions are assumed to be invariant under rotations in the isotopic spin space.*

The particular symmetry group applicable to isospin conservation is a form of *unitary symmetry known as a* $U(2)$, which can be expressed by a set of 2×2 matrices. This group may be reduced to a *special unitary group* $SU(2)$, which is also written as SU_2. It is *special* because a restriction reduces by unity the number of operators in the group. *The two dimensions* refer to the two basic states which make up the fundamental representatation in this case. The restriction of special reduces the number of operators $2\times2=4$ to three. The group is then said to have *three generators.*

By the use of the algebra of the $SU(2)$ group it can be shown that all irreducible representations of the symmetry group consist of a multiplet of $2T+1$ states. All the members of the multiplet have the same isospin T and are essentially identical except for charge. If the symmetry was exact, *i.e.* isospin is strictly conserved, the components of a multiplet would differ in charge and T_3. The SU (2) symmetry is violated by the *electromagnetic interaction for which conservation of isospin is not applicable.*

The nucleon states $|p>$, $|n>$ have anti-nucleon states $|\bar{p}>$, $|\bar{n}>$. Omitting $|>$ brackets for clarity and separating the trace from traceless part, the combination of nucleon with an anti-nucleon may be represented as

$$\begin{pmatrix} p \\ n \end{pmatrix} \times (\bar{p}\ \bar{n}) \rightarrow \frac{p\bar{p}+n\bar{n}}{\sqrt{2}}\begin{pmatrix} 1 & 0 \\ 0 & 1 \end{pmatrix} + \begin{pmatrix} (p\bar{p}-n\bar{n})\frac{1}{2} & (p\bar{n}) \\ n\bar{p} & (p\bar{p}-n\bar{n})\frac{1}{2} \end{pmatrix}$$

The first term of *r h.s.* represents singlet (η meson, $T=0$, $I=0^-$) and the second term represents the triplet array (pions $T=1$, $I=0^-$). The second term can be written as

$$\begin{pmatrix} \pi^\circ/\sqrt{2} & \pi^+ \\ \pi^- & \pi^\circ/\sqrt{2} \end{pmatrix}$$

Eightfold Way [SU (3) Symmetry]. The $SU(3)$ theory is a generalization of the theory of isospin. This stands for *special unitary group in three dimensions.* The term, *three dimensions* refers to the three basic states which make up the fundamental representaton in this case. In a three dimension unitary group there are, in general $3\times3=9$ operators, but the restriction of "special" reduces the number in eight. The group is then said to have *eight generators.* Gell-Mann has referred to the resulting group of symmetry operators as the *eightfold way, named for Buddha's Eightfold Path to Nirvana, comprising eight right actions.* Three of the generators apply to *three components of isospin, as in SU* (2) and *a fourth is associated with hypercharge. The remaining four also involve hypercharge in a different way.*

Application of the group algebra showed that the SU (3) symmetry should give rise to six supermultiplets, containing 1, 8, 8, 10, $\overline{10}$ and 27 members. The $\overline{10}$ multiplet is equivalent to the 10 but with hypercharges of opposite signs. In each of these supermultiplets the parity and intrinsic spin of members are the same, while the hypercharge and the isotopic spin are not same. Among above mentioned groups, 8 and 10 member groups are of particular interest.

In the case for $B=0$ we may form particle anti-particle states to fill a 3×3 array :

$$\begin{pmatrix} p \\ n \\ \Lambda \end{pmatrix} \times (\bar{p}\ \bar{n}\ \bar{\Lambda}) \rightarrow \begin{Bmatrix} \frac{1}{3}(2p\bar{p}-n\bar{n}-\Lambda\bar{\Lambda}) & p\bar{n} & p\bar{\Lambda} \\ n\bar{p} & \frac{1}{3}(-p\bar{p}+2n\bar{p}+\Lambda\bar{\Lambda}) & n\bar{\Lambda} \\ \Lambda\bar{p} & \Lambda\bar{n} & \frac{1}{3}(-p\bar{p}-n\bar{n}+2\Lambda\bar{\Lambda}) \end{Bmatrix}$$

It can be identified with known spin zero mesons

$$\begin{Bmatrix} (\pi^\circ/\sqrt{2})+(\eta/\sqrt{6}) & \pi^+ & K^+ \\ \pi^- & (-\pi^\circ/\sqrt{2})+(\eta/\sqrt{6}) & K^\circ \\ K^- & \bar{K}^\circ & -2\eta/\sqrt{6} \end{Bmatrix}$$

The neutral η meson is now written as

$$\eta=(p\bar{p}+n\bar{n}+2\Lambda\bar{\Lambda})/\sqrt{6}.$$

There is in addition the symmetrical neutral combination or singlet

$$\eta'=p\bar{p}+n\,n+\Lambda\bar{\Lambda}/\sqrt{3}$$

Since these mesons are formed from fermion particle-antiparticle pairs, hence have odd parity. These eight particles with $B=0$, and $J^p=0^-$ should be arranged as :

one triplet with $Y=0$, $T=1$
one doublet with $Y=1$, $T=\frac{1}{2}$
one doublet with $Y=-1$, $T=\frac{1}{2}$
one singlet with $Y=0$, $T=0$
} 8 members

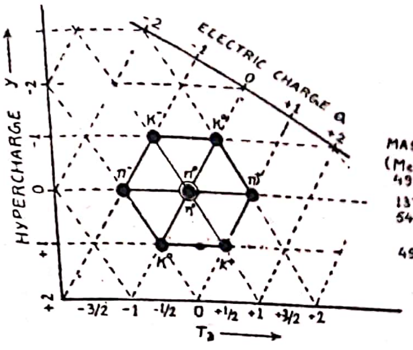

Fig. 16.11. Boson Octet ($J^P=0^-$)

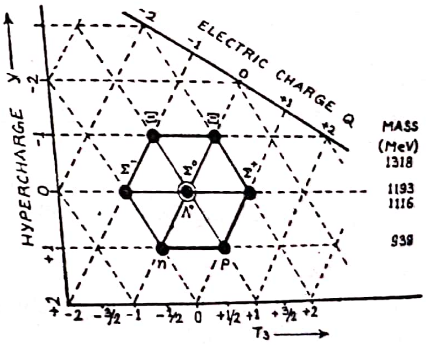

Fig. 16.12. Baryon Octet ($J^P=\frac{1}{2}^+$)

When this was first postulated there were seven ground state mesons. The missing meson was expected to have $Q=0$, $Y=0$, $T=0$

and was predicted both by Gell-Mann and by Ne'eman. This eighth meson was named η-meson. Octects of metastable mesons (zero intrinsic spin) is shown in fig. 16.11.

In 1962, Gell-Mann and Ne'eman pointed out that the baryon also formed an octet array. For $B=1$, the octet representation of $SU(3)$ gives an octet array

$$\begin{Bmatrix} & & \Sigma^{+} & & p \\ (\Sigma^{\circ}/\sqrt{2})+(\Lambda/\sqrt{6}) & & (-\Sigma^{\circ}/\sqrt{2})+(\Lambda)/\sqrt{6}) & & n \\ \Sigma^{-} & & \Xi^{\circ} & & -2\Lambda/\sqrt{6} \\ \Xi^{-} & & & & \end{Bmatrix}$$

These are eight in number ($p, n, \Lambda, \Sigma^{+}, \Sigma^{-}, \Sigma^{\circ}\ \Xi^{-}, \Xi^{\circ}$). For these $I^{p}=\frac{1}{2}^{+}$, $B=1$, $Y=1$ and $T=\frac{1}{2}$ or 0. The eightfold way arrangement of this baryon octet is shown in fig. 16.12.

For the octet mesons, Gell-Mann suggested a relationship among the average masses of the components, $\eta(M_0)$, π (M_1) and K $(M_{1/2})$, as

$$3M_0^2+M_1^2=4M_{1/2}^2 \qquad \ldots(48)$$

Another interesting case is that of the boson octet with $I^{p}=1^{-}$. The particles are :

$K^{*\circ}$ $(T_3=-\frac{1}{2}, Y=1)$, K^{*+} $(T_3=\frac{1}{2}, Y=1)$, $\rho^{-}(T_3=-1, Y=0)$, $\phi^{\circ}\&\rho^{\circ}$ $(T_3=0, Y=0)$, K^{*-} $(T_3=-\frac{1}{2}, Y=-1)$, $\overline{K}^{*\circ}$ $(T_3=\frac{1}{2}, Y=-1)$.

For $I^{P}=1^{-}$, a boson singlet ω° $(T=0, Y=0)$ has also been suggested. Neither the mass of ϕ° nor ω° fits with the expected value of M_0 in above relation. The masses of ω and ϕ^{0} are found approximately equally distant from the expected value (M_0=930 Me of mass. Gell-Mann and later Sakurai explained this by assuming ω^{0} and ϕ^{0} approximately the following mixtures of the octet and singlet states

$$\text{Real } \omega=\sqrt{(1/3)}\ \phi-\sqrt{(2/3)}\ \omega$$
$$\text{Real } \phi=\sqrt{(2/3)}\ \phi+\sqrt{(1/3)}\ \omega. \qquad \ldots(49)$$

Without really knowing which particle belongs in the octet state and which in the singlet, the ϕ^{0} has been arbitrarily placed in the octet.

Gell Mann derived a relationship among the average masses of the components of the four baryon multiplets in the intrinsic spin half octet, given as

$$2\,(M_N+M_{\Xi})=3\ M_{\Lambda}+M_{\Sigma}, \qquad \ldots(50)$$

where M_N is the average nucleon mass and the average masses of the hyperons are indicated by the respective subscripts.

The relations (49) and (50) are special cases of the general formula, given by Okubo,

$$M\,(T, Y)=M_0\,[1+aY+b\,\{T\,(T+1)-\tfrac{1}{4}Y^2\}], \qquad \ldots(51)$$

where a and b are constants for a particular multiplet.

The baryon octet for intrinsic spin $\frac{3}{2}^{-}$ consists of one doblet ($Y=+1$; resonance states N^{*0} with $T_3=-\frac{1}{2}$ and N^{*+} with $T_3=\frac{1}{2}$) ; one doublet ($Y=-1$; resonance states Ξ^{*-} with $T_3=-\frac{1}{2}$; and Ξ^{*0} with $T_3=\frac{1}{2}$) ; one triplet ($Y=0$; resonance states Y^{*-} with $T_3=-1$, Y^{*0} with $T_3=0$ and Y^{*+} with $T_3=+1$.) and one singlet ($Y=0$, $T_3=0$ and member is $Y^{*(0)}$).

A more remarkable prediction was the case of the ten-fold baryon group with intrinsic spin $\frac{3}{2}$. Theory predicted that there should be a group of ten members : $Y=1$, $T=\frac{3}{2}$, quartet (nucleon resonance denoted by N and exists in four charge states), $Y=0$, $T=1$, triplet (hyperon resonance Y_1^{*} which is containing excited Σ particles), $Y=-1$, $T=\frac{1}{2}$, doublet (hyperon resonance which is equivalent to excited cascade particles Ξ), $Y=-2$, $T=0$, singlet (a particle with charge -1).

In 1962, when the proposal was made to incorporate the N, Y_1, and Ξ resonances in a decuplet, the tenth particle was unknown. The existence of such a particle was predicted by Gell Mann and was named omega (Ω). The baryon decuplet for intrinsic spin $\frac{3}{2}$ is shown in fig. 16.13.

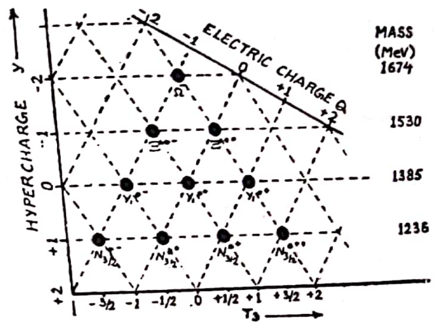

Fig. 16.13. Baryon decuplet for intrinsic spin 3/2+.

Before the Ω^{-} had been discovered, the values of a and b (eqn. 51) could be found in order to fit the $Y=1, 0$ and -1. Thus the mass of the $Y=-2$ member was predicted as 1676 MeV, while the measured value is 1675 MeV.

Although all the other members of the baryon decuplet for intrinsic spin $\frac{3}{2}$ are resonant states, decaying by the strong interaction, Gell-Mann noted that the Ω^{-} particle should decay by the weak interaction. Possible decay modes are

$$\Omega^{-} \rightarrow \Xi^{-}+\pi^{0}$$
$$\rightarrow \Xi^{0}+\pi^{-}$$
$$\rightarrow K^{-}+\Lambda^{0}$$

It is clear that in these modes baryon number is conserved while isospin, hypercharge and strangeness are not conserved. These conservations only hold for strong interactions, hence the decay of Ω^- is by weak interaction.

In a recent development attempts have been made to combine ordinary spin with T and Y. The new group is described as SU (6).

16.20. QUARK THEORY

It is obviously desirable to find whether or not the multiplicity of particles can be built up from other similar units. Analysis has shown the possible existence of three basic units which could be the really *fundamental particles*. Zweing called the three particles *aces*, but the name *quark*, proposed by Gell-Mann, has become widely accepted. The elementary particles can be conceived (as far as isospin and hypercharge are concerned) as being built out of combinations of *quarks*. The quarks (a, b, c) are the basic states, which are represented as the basic three component column matrices.

$$a=\begin{pmatrix}1\\0\\0\end{pmatrix}, \quad b=\begin{pmatrix}0\\1\\0\end{pmatrix}, \quad c=\begin{pmatrix}0\\0\\1\end{pmatrix}.$$

The quarks a and b form a isospin doublet with $T=\frac{1}{2}$ and $T_3=\frac{1}{2}$ and $-\frac{1}{2}$, whereas the c quark is an isosinglet with $T_3=0$. The quarks can be interchanged with the unitary matrix, as

$$q_i=\sum_{j=1}^{3} U_{ij}\, q_j.$$

The unitary matrices U can be expressed in terms of Hermitian generators F_j as

$$U=\exp\left[\, i\sum_{j=1}^{8} \alpha_j F_j \right],$$

where $\alpha_1, \alpha_2, \ldots \alpha_8$ are parameters, and $F_1, F_2 \ldots$ are F_8 eight independent traceless hermitian 3×3 matrices. The quantum numbers of the quarks, are given in the table 16.5.

Table 16.5.

Quark	Q	T	T_3	B	Y	S
a	+2/3	1/2	1/2	1/3	1/3	0
b	−1/3	1/2	−1/2	1/3	1/3	0
c	−1/3	0	0	1/3	−2/3	−1

For the corresponding antiquarks, the numerical values are the same but the signs of Q, B, T_3, Y and S, are changed. The antiquarks are represented as row matrices

$$\bar{a}=(1,0,0), \quad \bar{b}=(0,1,0), \quad \bar{c}=(0,0,1),$$

Which transform as

$$\bar{q}_j=\sum \bar{q}_i \left(U^+\right)_{ij}$$

In associating particles with SU (3) representation, the baryons with integer baryon number must be associated with states formed from three quarks. Thus for baryons $a\times b\times c$ indicates 27 states (a singlet, two octets and a decuplet). The mesons with zero baryon number must be form from one quark and one antiquark. Thus for mesons $a\times\bar{b}$ gives 9 states (a singlet and an octet). Examples of meson formation are as follows :

$\pi^+ (a\bar{b})$, $\pi^0 (\bar{a}a)$, $\pi^- (\bar{a}b)$, $K^+ (a\bar{c})$, $K^0 (b\bar{c})$, $K^- (\bar{a}c)$, etc.

Table 16.6

Quarks	Q	T	M	Y	B	S	Particle
$a\,a\,a$	2	1/2	2	1	1	0	—
		3/2	4	1	1	0	Δ^{++}
$o\,b\,b$	−1	1/2	2	1	1	0	—
		3/2	4	1	1	0	Δ^-
$a\,a\,b$	1	1/2	2	1	1	0	$p^+(N^+)$
		3/2	4	1	1	0	Δ^+
$a\,b\,b$	0	1/2	2	1	1	0	$n^0(N^0)$
		3/2	4	1	1	0	Δ^0
$a\,a\,c$	1	0	1	0	1	−1	—
		1	3	0	1	−1	Σ^+
$a\,b\,c$	0	0	1	0	1	−1	Λ^0
		1	3	0	1	−1	Σ^0
$b\,b\,c$	−1	0	1	0	1	−1	—
		1	3	0	1	−1	Σ^-
$a\,c\,c$	0	1/2	2	−1	1	−2	Ξ^0
$b\,c\,c$	−1	1/2	2	−1	1	−2	Ξ^-
$c\,c\,c$	−1	0	1	−2	1	−3	Ω^-

The baryons are each constructed from three quarks, no antiquarks. This permits both octet and decuplet representations, as observed actually. All the possible combinations of three quarks for baryons only are set out in the table 16.6.

The quarks and antiquarks are assumed to be the interacting particles of spin $\frac{1}{2}$ carrying the quantum numbers shown in table 16.5. The fact that the quarks have not been detected in nuclear collisions, either in cosmic radiation or in high energy laboratories, suggests that the quark must have very high mass. The quarks have no independent existence outside the hadrons like the phonons of solid state physics. If the mesons are composed of one quark interacting with one antiquark through a scalar potential, the total spin must be either 1 or 0. For the angular momentum L, the total parity P of the meson must be $(-1)^{L+1}$. The baryon states formed from three quarks must have total spin 3/2 or $\frac{1}{2}$.

No evidence had been obtained that the quarks can exist. Attempts are now being made to find quarks in the fields of cosmic ray and large accelerator research but the difficulties are great. It has been suggested that meteorities might have collected quarks during their lifetimes in the planetary system of 4.5×10^9 years. Such bits of cosmic material which have arrived on earth would perhaps contain charges less than the electronic charge. Attempts to detect these sub-electronic charges are now being tried but have get to be found.